Universidad del País Vasco Euskal Herriko Unibertsitatea

NAZIOARTEKO BIKAINTASUN CAMPUSA
CAMPUS DE EXCELENCIA INTERNACIONAL

Osteopontin role in lipid metabolism: involvement in age-related hepatosteatosis

PhD Thesis

Beatriz Gomez Santos

June, 2019

Universidad del País Vasco
Euskal Herriko Unibertsitatea
NAZIOARTEKO BIKAINTASUN CAMPUSA
CAMPUS DE EXCELENCIA INTERNACIONAL

Faculty of Medicine and Nursing

Physiology Department

Molecular Biology and Biomedicine PhD Program

Osteopontin role in lipid metabolism: involvement in age-related hepatosteatosis

Beatriz Gómez Santos
Doctoral Thesis, June 2019

PhD Thesis supervised by Dr. Patricia Aspichueta Celaá & Dr. Mª Luz Martínez Chantar

I have been recipient of a predoctoral fellowship from the Basque Government, from January 2015 to December 2018.

I have also received a predoctoral EGONLABUR fellowship from the Basque Government for a 3-month stay.

INDEX

ABBREVIATIONS

ACAT	Acyl-CoA:cholesterol aciltransferase
ACC	Acetyl-CoA carboxylase
FPLC	Fast protein liquid chromatography
ALT	Alanine aminotransferace
AMPK	5'-AMP-activated protein kinase
ANOVA	Analysis of variance
AST	Aspartate aminotransferace
BA	Bile acid
BCA	Bicinchoninic Acid
BMI	Body mass index
BSA	Bovine serum albumin
CA	Cholic acid
CDCA	Chenodeoxycholic acid
CEH	Cholesteryl ester hydrolase
Chol	Cholesterol
Cln	Cardiolipin
CoA	Coenzyme A
CV	Central vein
CYP7A1	Cholesterol 7-alpha-hydroxylase
DCA	Deoxycholic acid
DG	Diglyceride
DGAT	Acyl-CoA:diacylglycerol acyltransferase

DMEM	Dubbelco's modified Eagle's medium
DPX	A mix of Distrene, Plasticizer and Xylene mounting media
dH2O	Distilled water
EDTA	Ethylenediaminetetraacetic acid
EGTA	Ethyleneglycoltetraacetic acid
ER	Endoplasmic reticulum
FA	Fatty acid
FAS	Fatty acid synthase
FBS	Fetal bovine serum
FC	Free cholesterol
GAPDH	Glyceraldehyde-3-phosphate dehydrogenase
GCA	Glycocholic acid
GCDCA	Glycochenodeoxycholic acid
GDCA	Glycodeoxycholic acid
GPL	Glycerophospholipid
GRP78	Glucose-Regulated Protein, 78kDa
GUDCA	Glycoursodeoxycholic acid
HDL	High-density lipoprotein
HBV	Hepatitis B virus
HCC	Hepatocellular carcinome
HCV	Hepatitis C virus
HDCA	Hyodeoxycholic acid
HFD	High fat diet
HMG-CoA	Hydroxy-3-methyl-glutaryl-CoA
HMGCR	HMG-CoA reductase

HOMA-IR	Homeostasis model assessment of insulin resistance
HPBCD	Hydroxypropyl beta-cyclodextrin
HPLC-MS/MS	High performance liquid chromatography-tandem mass Spectrometry
HSP90	Heat shock protein 90
H&E	Hematoxilin and eosin
IFC	Integrated Fluidic Circuits
IOD	Integrated optic density
IR	Insulin resistance
KH	Krebs-Henseleit perfusion medium
LCA	Lithocholic acid
LC/MS	Liquid chromatography/tandem mass spectrometry
LD	Lipid droplet
LDL	Low-density lipoprotein
LPL	Lipoprotein lipase
MRM	Multiple reaction monitoring
MTTP	Microsomal triacylglyceride transfer protein
MUFA	Monounsaturated fatty acid
m	Month-old
NAD	Nicotinamide adenine dicucleotide oxydized
NADH	Nicotinamide adenine dicucleotide reduced
NADP	Nicotinamide adenine dicucleotide phosphate oxydized
NADPH	Nicotinamide adenine dicucleotide phosphate reduced
NAFLD	Non-alcoholic fatty liver disease
NASH	Non-alcoholic steatohepatitis
NL	Normal liver
OPN	Osteopontin

OPN-KO	Osteopontin knock out
PBS	Phosphate-buffered saline
PC	Phosphatidylcholine
PE	Phosphatidylethanolamine
PEMT	Phosphatidylethanolamine N-methyltransferase
PH	Partial hepatectomy
rOPN	Recombinant osteopontin
ROS	Reactive oxygen species
RT-qPCR	Real time-quantitative polymerase chain reaction
SDS	Sodic dodecyl sulphate
SDS-PAGE	Sodium dodecyl sulphate-polyacrylamide gel electrophoresis
SEM	Standard error of the mean
SPP1	Secreted phosphoprotein 1
SREBP	Sterol regulatory element binding protein
TAE	Tris-acetate buffer with EDTA
TBS	Tris-buffered saline
TCA	Taurocholic acid
TCDCA	Taurochenodeoxycholic acid
TDCA	Taurodeoxycholic acid
TE	Tris-EDTA buffer
TEMED	N,N,N',N'-tetrametiletilendiamina
TG	Triglyceride
TGH	Triglyceride hydrolase
THCA	Taurohyocholic acid
THDCA	Taurohyodeoxycholic acid
TLC	Thin layer chromatography

TLCA	Taurolithocholic acid
TMC	Tauromuricholic acid
TUDCA	Tauroursodeoxycholic acid
TαMCA	Tauro-alpha-muricholic acid
TβMCA	Tauro-beta-muricholic acid
T2DM	Type 2 diabetes mellitus
UDCA	Ursodeoxycholic acid
UPLC	Ultra performance liquid chromatography
VLDL	Very-low-density lipoprotein
WT	Wild type
αMCA	Alpha-muricholic acid
βMCA	Beta-muricholic acid

A. SUMMARY/RESUMEN

SUMMARY/RESUMEN

1. Background and aims

Osteopontin (OPN) is a multifunctional protein that is expressed in different cell types and in a variety of tissues including liver. It is a key regulator of many metabolic and inflammatory diseases. OPN has been associated with different liver disorders; in fact, its expression is increased in different stages of non-alcoholic fatty liver disease (NAFLD). Regarding the progression of the disease, several mice and human studies show a role for OPN in the pathogenesis and progression of NAFLD and liver fibrosis.

OPN is a modulator of liver lipid metabolism. It modulates the fate of acetyl-CoA in liver and it regulates the cross-talk between phosphatidylcholine (PC) and cholesterol metabolism. OPN is also involved in the regulation of the expression of some nuclear factors related to biliary metabolism, which are altered in NAFLD progression. Hence, we **propose** that OPN might modulate the cross-talk between cholesterol and PC metabolism via CYP7A1 regulation in hepatocytes, consequently modulating the conversion of free cholesterol (FC) into bile acids (BA). Thus, the altered conversion of FC into bile acids will also induce changes in biliary PC secretion. Regarding liver regeneration, deficiency of OPN leads to a remodeling in lipid metabolism that allows the correct regeneration after partial hepatectomy (PH). The liver has the capacity for regeneration after cellular damage or surgery resection. During regeneration, liver cells need to acquire sufficient energy and metabolic precursors. PC, cholesterol and bile acids play an important role in liver regeneration, and since OPN can modulate these lipids, we **suggest** that OPN might have an important role orchestrating lipid metabolism in liver regeneration.

OPN is involved in diseases in which metabolic dysregulation is key, and taking into account that the prevalence of metabolic diseases increases with age, we considered the fact that OPN could be involved in the aging of the liver. Indeed, OPN expression is increased in many diseases in which aging in the primary risk factor and it has also been described as a senescence-associated secretory phenotype (SASP) factor. There are several studies linking OPN and aging but the available data does not give conclusive results about the role of OPN in the aging process.

Aging of the liver is associated with several hepatic alterations; these changes can negatively affect the morphology, physiology and oxidative capacity of the liver. During aging there is a loss of hepatic volume of 1/3 approximately, a reduction of the blood perfusion as well as a decrease in the capacity to metabolize certain compounds. There are also changes in the expression of a variety of proteins and diminished hepatobiliary functions. In addition, it has been reported a loss of capacity to fight against oxidative stress. In old age, fat is redistributed outside the usual fat deposits, and

lipids can accumulate in non-adipose tissues like skeletal muscle, heart and liver. Thus, aging is associated with an increase in the lipid accumulation within the liver that may compromise the normal function due to lipotoxicity. These changes in liver during aging can reduce hepatic function and promote liver injury. Aging is associated with high morbidity and a poor prognosis in patients with various liver diseases, including NAFLD, hepatitis C and liver cancer, as well as with surgeries such as liver transplantation. In addition, epidemiological studies have demonstrated that NAFDL and non-alcoholic steatohepatitis (NASH) are common among the elderly.

The number of senescent hepatocytes in the liver increases with age. Indeed, a significant fraction of hepatocytes develops a senescent phenotype during the life course. Several studies have shown that cellular senescence drives age-dependent hepatic steatosis and that elimination of senescent cells may be a novel therapeutic strategy to reduce steatosis. Interestingly, senescent cells have been found in the livers of NAFLD, cirrhotic patients and in the liver of high fat diet fed and genetically obese mice. Thus, based on the evidence that OPN is linked with liver disorders, which prevalence increases with age; and that OPN plays a role in liver lipid metabolism, which is dysregulated in aging, we **propose** that OPN could have a role in the susceptibility of the liver to aging-associated NAFLD progression.

In this context, we proposed the following specific aims:

Aim 1. To investigate whether OPN regulates PC and cholesterol metabolism via CYP7A1 in hepatocytes, and, if so, to analyze the pathways involved.

Aim 2. To elucidate which metabolic pathways are involved in OPN-KO mice liver lipid remodeling during regeneration after PH.

Aim 3. To investigate the role of OPN in the metabolic disorders of aging:

Aim 3.1 To investigate whether OPN is involved in the aging of the liver, and in that case, to identify the mechanisms involved.

Aim 3.2 To find out whether during aging OPN modifies the vulnerability of the liver to the development of NAFLD; and if so, to identify the mechanisms involved.

Aim 3.3 To define if OPN is involved in the generation of metabolic syndrome during aging.

2. Methods

To investigate the changes that OPN induces in liver lipid metabolism in quiescent and regenerating livers 10-12-week-old female OPN deficient (OPN-KO) mice and their WT (C57BL/6J) littermates were used. To study regeneration, 2/3 PH was performed, and mice were sacrificed 24 and 48 hours (h) after PH.

For the aging studies, a cohort of individuals with normal liver (NL)(n=34) and another with NAFLD (n=123) was analyzed. For the animal model studies male and female WT mice of 3, 6, 10, 14 and 20 months-old (m) were used. In addition, for the study of the effect of OPN in the liver lipid metabolism and hepatosteatosis development during aging, 3, 10 and 20 m WT and OPN-KO female mice were analyzed. Besides, a group of 16 m mice was fed a high fat diet (HFD) prior to their sacrifice at 20 m. For the in-vitro studies HepG2 and Hep3B hepatic cell lines were used.

To identify the disruption of lipid metabolism, body parameters, serum and liver lipid concentration and metabolic fluxes were analyzed. Among the metabolic fluxes analyzed, *de novo* lipogenesis, oleate esterification, fatty acid beta oxidation and several enzyme activities involved in synthesis and hydrolysis processes were evaluated. In addition, for the study of signaling pathways western blot analysis were performed. Additionally, to evaluate the state of the liver, different histochemical analysis were performed. For the in-vitro studies, in order to induce senescence to HepG2 and Hep3B cells palbociclib or H_2O_2 were used after knockdown of OPN.

3. Results

Osteopontin controls bile acid metabolism by regulating CYP7A1 levels in liver and hepatocytes

Regarding the role of OPN regulating PC and cholesterol metabolism via CYP7A1, we found that treating hepatocytes with recombinant OPN (rOPN) reduced CYP7A1 levels together with a trend toward decreased 7a-hydroxi-4-cholesteren-3-one (C4) levels, an indirect biomarker of CYP7A1 activity, while it was increased in OPN-KO mice livers. To determine the mechanism by which OPN downregulates CYP7A1, we took into account that several reports have involved AKT and/or ERK and JNK, in CYP7A1 transcription. In WT mice treated with rOPN, phosphorylation and activation of FAK was increased, while in OPN-KO animals FAK phosphorylation was reduced. In rOPN treated WT mice, together with the increased FAK phosphorylation there was an increased free cholesterol (FC) concentration. This supports the fact that rOPN downregulates CYP7A1 levels, which in turn decreases the conversion of cholesterol into BA, increasing the cholesterol levels in liver. In order to assure the involvement of this pathway in CYP7A1 regulation we used the PI3K and FAK inhibitors LY294002 and Y15, respectively. When inhibiting the FAK-AKT signaling pathway, CYP7A1 levels increased in rOPN treated hepatocytes. Thus, demonstrating a mechanism by which rOPN decreases CYP7A1 levels in hepatocytes. Taking all together, we propose that OPN will induce though FAK-AKT

signaling activation, the upregulation of CYP7A1 protein levels, and thus the conversion of cholesterol into BA. OPN will decrease the synthesis and secretion of BA. This decreased secretion will also reduce PC secretion, which will contribute to higher liver levels of PC.

Rewiring of lipid metabolism modulates liver regeneration after partial hepatectomy in OPN-KO mice

In regeneration, we analyzed the lipid metabolic pathways that are controlled by OPN. While OPN-KO mice are capable of regenerating correctly, they undergo a lipid remodeling. Since OPN-KO hepatocytes show decreased de novo lipogenesis, and assuring that the prevision of sufficient metabolites is key for an adequate regeneration, we analyzed the contribution of dietary fatty acids in the OPN-KO mice liver. For this, we evaluated if TG and PC species containing the essential linoleic acid (18:2) were altered, and we observed that most of the TG species that were increased in OPN-KO quiescent livers were enriched in linoleic acid. We also observed that PC species containing the linoleic acid were reduced in the quiescent OPN-KO liver compared to the WT. This suggests that the decreased *de novo* TG synthesis observed in the OPN-KO mice liver is compensated by increased dietary FA uptake. Thus, there is a shift of linoleic towards TG. However, this compensation does not occur with PC loss. Given that the big changes in liver lipid content during regeneration occur mainly 24 h after PH, we investigated whether the increased TG storage was associated with the increase in linoleic acid. The results showed that 24 h after PH the TG species containing linoleic acid were increased in WT compared with OPN-KO mice liver. The decrease in TG containing linoleic acid can be explained by the increased FA oxidation in OPN-KO mice livers 24 h after PH. Regarding FA oxidation, 24 h post PH, lipid oxidation was increased in OPN-KO mice when compared to WT mice. Moreover, despite the increased fatty acid oxidation and increased levels of ROS production, lipid peroxidation levels remained unaltered in OPN deficient mice along liver regeneration. Taken together, these results show that, the decrease in the PC liver concentration and the *de novo* synthesis is not compensated with the dietary essential FA linoleic, unlike what happens with TGs. The increased dietary-lipid uptake in OPN-KO mice provides the metabolic precursors required for regeneration 24 h and 48 h after PH.

Atorvastatin treatment did not induce changes in the accumulation of lipid droplets or in the liver TG content 24 h after PH in the OPN-KO or WT mice. In addition, atorvastatin recovered PC levels just in OPN-KO. In addition, the results showed that differences between WT and OPN-KO in DHE disappeared after atorvastatin treatment. Thus, atorvastatin induces changes in the liver lipidome during regeneration only in OPN-KO mice. In which, as shown in previous work, atorvastatin improves early regeneration.

Osteopontin plays a role in the age-associated NAFLD progression

Regarding OPN involvement in liver aging, the results showed that in individuals with NL there was a positive correlation between serum OPN levels and age while this correlation was lost in patients with NAFLD, in which serum levels of OPN were higher than in NL subjects. In WT mice, this positive correlation was also observed. In addition, liver levels of OPN were increased at 10 m and remained elevated at 20 m. Senescence is one of the key features of aging, and when senescence was induced to HepG2 cells, intra and extracellular OPN levels increased. Besides, when treating cells with recombinant OPN, the effect of the senescence inducing agent palbociclib was reduced, suggesting that OPN is involved in aging and senescence.

The lost age-OPN correlation in NAFLD patients, suggests that OPN might play a role in the age-associated liver vulnerability to NAFLD progression. Here, we wanted to analyze if the increased OPN expression during aging is protective or detrimental for the age-associated hepatosteatosis development. Liver β-Galactosidase and p21 levels together with hepatic concentration of triglycerides (TG) and cholesterol esters and their de novo synthesis were increased in 10 m OPN-KO mice when compared to their WTs. This phenotype was associated with the decrease of the chaperone GRP78, the activation of ER stress and the increase in fatty acid synthase (FAS) levels. The generation of senescence in OPN-knockdown HepG2 cells led to a decrease in GRP78. Although 20 m OPN-KO mice did not show ER stress symptoms, the activation of caspase 12 together with gamma-H2AX reinforces the existence of further tissue damage. In addition, in 20 m OPN-KO mice, evaluation of the liver fibrosis and inflammation showed a worse progression of the disease, especially in the HFD fed mice.

p53 controls several metabolic and cellular functions and modulates cellular adaptations to stress. It is one of the most important tumor suppressor genes, and some studies have linked p53 to OPN regulation in fibroblasts. Here, we wanted to evaluate whether p53 could modulate OPN levels. Knockdown of p53 in HepG2 cells reduced OPN levels in cells and media. Moreover, Hep3B cells, in which p53 is absent were unable to generate OPN when senescence was induced with palbociclib or H_2O_2. In vivo, p53 is involved in hepatosteatosis since p53-KO mice develop steatosis and its overexpression improves steatosis and ER stress . It is known that feeding a HFD increases OPN levels; however, p53-KO mice did not show increased liver OPN levels when fed a HFD. Thus, p53 might regulate OPN levels when inducing senescence and when feeding a HFD.

Taken together, these results show that OPN deficiency leads to an early age-associated hepatosteatosis, accompanied by an ER stress and increased senescence. This phenotype leads in old age to a worse progression of the disease as reflected by increased fibrosis, inflammation, damage and apoptosis markers. In addition, p53 might be necessary for OPN induction in response to senescence or HFD. Thus, during aging OPN might be regulated to maintain liver health.

4. Conclusions

1. Osteopontin (OPN) regulates the cross-talk between cholesterol and PC metabolism through modulation of CYP7A1 levels in hepatocytes. The FAK-AKT signaling pathway is involved in the regulation of CYP7A1 by OPN in liver.

2. OPN modulates metabolic pathways involved in TG and cholesterol metabolism during liver regeneration.

2.1. OPN deficient (OPN-KO) mice show increased fatty acid catabolism when facing regeneration. The increased metabolic demands and the decreased *de novo* synthesis of TG are compensated with dietary fatty acids.

2.2. Inhibition of cholesterogenesis using atorvastatin provides a new metabolic scenario linked to improvement of early regeneration in OPN-KO mice.

3. OPN is required to maintain the whole body metabolic homeostasis during aging.

3.1 OPN is involved in liver aging. Serum OPN positively correlates with age in individuals and animal models with normal liver. In the animal model, the increased OPN levels in serum are linked to increased levels in liver. The induction of senescence in HepG2 cells, through modulation of p53, increases cellular OPN levels and its secretion.

3.2 OPN is regulated to maintain the liver lipid metabolism balance during aging. OPN deficiency in mice makes the liver more vulnerable to age-associated hepatosteatosis, being the underlying mechanism the increased *de novo* lipogenesis linked with induced senescence and an impaired ER stress response due to the GRP78 decreased levels.

3.3 In old HFD-fed mice, deficiency in OPN does not induce body weight changes. However, it induces hypertriglyceridemia and a mild insulin resistance.

1. Antecedentes y objetivos

La osteopontina (OPN) es una proteína multifuncional que se expresa en diferentes tipos celulares y tejidos, incluido el hígado, y es también un regulador clave de muchas enfermedades metabólicas e inflamatorias. OPN se ha asociado a diferentes trastornos hepáticos, de hecho, su expresión se encuentra incrementada en diferentes etapas de la enfermedad del hígado graso no alcohólico (EHGNA). En cuanto a la progresión de la enfermedad, varios estudios en modelos de ratón y humanos muestran que la OPN tiene un papel en la patogénesis y progresión de la EHGNA y en la fibrosis hepática.

La OPN modula el metabolismo de lípidos hepáticos, ya que modula el destino del acetil-CoA en el hígado y regula la interacción entre el metabolismo de la fosfatidilcolina (PC) y del colesterol. La OPN está involucrada en la modulación de la expresión algunos factores nucleares relacionados con el metabolismo biliar, que se encuentran alterados en la progresión de la EHGNA. Por lo tanto, **proponemos** que OPN modula el metabolismo del colesterol y la PC a través de CYP7A1 en hepatocitos, controlando así la conversión de colesterol libre (FC) en ácidos biliares. En cuanto a la regeneración hepática, la deficiencia de OPN conduce a una remodelación del metabolismo lipídico que permite la correcta regeneración tras una hepatectomía parcial (PH). El hígado posee capacidad de regeneración tras un daño celular o resección quirúrgica. Durante la regeneración, las células hepáticas necesitan adquirir suficiente energía y precursores metabólicos para una regeneración adecuada. La PC, el colesterol y los ácidos biliares juegan un papel importante en la regeneración del hígado. Dado que OPN puede modular estos lípidos **sugerimos** que podría desempeñar un papel importante orquestando el metabolismo lipídico durante regeneración hepática.

La OPN está implicada en enfermedades en las que la desregulación metabólica es clave, y teniendo en cuenta que la prevalencia de las enfermedades metabólicas aumenta con la edad, consideramos que OPN podría estar implicada en el envejecimiento hepático. La expresión de OPN aumenta en muchas enfermedades en las que el envejecimiento es el principal factor de riesgo, además también se ha descrito a OPN como un factor de fenotipo secretor asociado a senescencia (SASP). Existen varios estudios que vinculan OPN con el envejecimiento, pero los datos disponibles no ofrecen resultados concluyentes sobre el papel de OPN en el proceso de envejecimiento.

El envejecimiento del hígado está asociado a una serie de alteraciones; estos cambios pueden afectar negativamente la morfología, la fisiología y la capacidad oxidativa del hígado. Durante el envejecimiento hay una pérdida de volumen hepático de 1/3 aproximadamente, una reducción de la perfusión sanguínea, así como una disminución de la capacidad para metabolizar ciertos compuestos. También hay cambios en la expresión de una variedad de proteínas y disminución de las funciones hepatobiliares. Además, de la disminución de la capacidad para luchar contra el estrés oxidativo. Durante el envejecimiento, la grasa se redistribuye fuera de los depósitos de grasa

habituales, y los lípidos pueden acumularse en tejidos no adiposos como el músculo esquelético, el corazón y el hígado. Por lo tanto, el envejecimiento se asocia con un aumento de la acumulación de lípidos hepática que puede comprometer la función normal debido a la lipotoxicidad. Por tanto, estos cambios en el hígado durante el envejecimiento pueden reducir la función y promover daño hepático. El envejecimiento está asociado con una alta morbilidad y un mal pronóstico en pacientes con enfermedades hepáticas, incluyendo EHGNA, hepatitis C y cáncer de hígado, así como en cirugías como el trasplante de hígado. Estudios epidemiológicos han demostrado que la EHGNA y la esteatohepatitis no alcohólica son comunes entre la población anciana.

El número de hepatocitos senescentes en el hígado aumenta con la edad. Una fracción significativa de hepatocitos desarrolla un fenotipo senescente a medida que se envejece. Varios estudios han demostrado que la senescencia promueve la esteatosis hepática asociada a la edad y que la eliminación de las células senescentes puede ser una nueva estrategia terapéutica para reducir la esteatosis. Relacionado con esto, se han encontrado células senescentes en los hígados de pacientes cirróticos y en el hígado de ratones alimentados con una dieta rica grasa y en ratones genéticamente obesos. Por lo tanto, en base a la evidencia de que OPN está relacionada con trastornos hepáticos, cuya prevalencia aumenta con la edad; y que OPN desempeña un papel en el metabolismo de lípidos hepáticos, que se encuentra desregulado en el envejecimiento, **proponemos** que OPN podría tener un papel en la susceptibilidad del hígado a la progresión del EHGNA asociada al envejecimiento.

En este contexto, proponemos los siguientes objetivos concretos:

Objetivo 1. Investigar si OPN regula el metabolismo de la PC y del colesterol a través del CYP7A1 en hepatocitos y, en caso afirmativo, analizar las vías implicadas.

Objetivo 2. Definir qué vías metabólicas están involucradas en la remodelación lipídica del hígado durante la regeneración tras hepatectomía parcial en ratones OPN-KO

Objetivo 3. Investigar el papel de OPN en los trastornos metabólicos del envejecimiento:

- **Objetivo 3.1** Investigar si la OPN está implicada en el envejecimiento del hígado y, en tal caso, identificar los mecanismos implicados.
- **Objetivo 3.2** Averiguar si durante el envejecimiento OPN modifica la vulnerabilidad del hígado al desarrollo de EHGNA y, en caso afirmativo, identificar los mecanismos implicados.
- **Objetivo 3.3** Definir si la OPN está implicada en la generación del síndrome metabólico durante el envejecimiento.

2. Métodos

Para investigar los cambios que induce OPN en el metabolismo de lípidos hepáticos en hígados quiescentes y regenerantes se utilizaron ratones de entre 10-12 semanas de edad deficientes en OPN (OPN-KO) y sus controles WT (C57BL/6J). Para estudiar la regeneración, se realizó el procedimiento de hepatectomía parcial (PH) 2/3, y los animales se sacrificaron 24 y 48 horas post PH.

Para los estudios de envejecimiento se analizó una cohorte de individuos con hígado normal (NL)(n=34) y otra con EHGNA (n=123). Para el estudio en el modelo animal se utilizaron ratones WT de 3, 6, 10, 14 y 20 meses de edad. Además, para el estudio del papel de OPN en el metabolismo de los lípidos hepáticos y el desarrollo de EHGNA durante el envejecimiento, se utilizaron ratones hembra de 3, 10 y 20 meses de edad WT y OPN-KO. Un grupo de cada genotipo fue alimentado con dieta rica en grasa desde los 16 meses hasta los 20, cuando se sacrificaron. Para los estudios in vitro se utilizaron las líneas celulares hepáticas HepG2 y Hep3B.

Para identificar la desregulación del metabolismo lipídico se analizaron los parámetros corporales, la concentración de lípidos en el suero y el hígado y los principales flujos metabólicos. Entre los flujos metabólicos estudiados se evaluaron la lipogénesis de novo, la esterificación de oleato, la beta oxidación de ácidos grasos y actividades enzimáticas implicadas en la síntesis e hidrólisis de los principales lípidos. Además, para el estudio de las vías de señalización se realizaron análisis mediante western blot. Asimismo, para evaluar el estado del hígado, se realizaron diferentes análisis histoquímicos. En los estudios in vitro, para inducir senescencia se utilizó palbociclib o H_2O_2 tras el silenciamiento de OPN.

3. Resultados

La osteopontina controla el metabolismo de ácidos biliares regulando los niveles de CYP7A1 en el hígado y en hepatocitos

En cuanto a los resultados sobre el papel de OPN en la regulación del metabolismo de PC y del colesterol, observamos que el tratamiento de los hepatocitos con OPN recombinante (rOPN) redujo los niveles de CYP7A1 junto con una tendencia hacia la disminución de los niveles de 7a-hydroxi-4-cholesteren-3-one (C4), que es un marcador indirecto de la actividad de CYP7A1. Para determinar el mecanismo mediante el cual OPN reduce CYP7A1, tuvimos en cuenta que en varios estudios han descrito que AKT y/o ERK y JNK participan en la transcripción de CYP7A1. En los ratones WT tratados con rOPN la fosforilación de FAK se incrementó, y por tanto su actividad, mientras que en los animales OPN-KO se redujo la fosforilación de FAK. Además, en ratones WT tratados con rOPN, junto con el aumento de la fosforilación FAK, se produjo un aumento de la concentración de colesterol libre (FC). Esto muestra que la rOPN disminuye los niveles de CYP7A1, lo que a su vez disminuye la conversión de colesterol en ácidos biliares, aumentando los niveles de colesterol hepático. Para

asegurar la participación de esta vía en la regulación CYP7A1 se utilizaron los inhibidores de PI3K y FAK LY294002 e Y15, respectivamente. Cuando se inhibió la vía de señalización FAK-AKT, los niveles de CYP7A1 aumentaron en hepatocitos tratados con rOPN. Demostrando así, un mecanismo por el cual la rOPN disminuye los niveles de CYP7A1 en hepatocitos. Por lo tanto, proponemos que OPN inducirá, a través de la activación de la señalización FAK-AKT, el descenso de los niveles proteicos CYP7A1, y por lo tanto la conversión de colesterol en ácidos biliares. El efecto de OPN disminuirá la síntesis y secreción de ácidos biliares. Este descenso de la secreción también fomentará la menor secreción de PC, lo que contribuirá a una mayor concentración hepática de PC.

La reorganización del metabolismo lipídico modula la regeneración hepática tras una hepatectomía parcial en ratones OPN-KO.

En la regeneración hepática, analizamos las vías metabólicas de lípidos que controla OPN. Aunque los ratones OPN-KO son capaces de regenerar correctamente, sufren una remodelación lipídica. Dado que los hepatocitos OPN-KO muestran una disminución de la lipogénesis *de novo*, y dado que asegurar la previsión de suficientes metabolitos es clave para una adecuada regeneración, analizamos la contribución de los ácidos grasos provenientes de la dieta en el hígado de los ratones OPN-KO. Para ello, se evaluó si las especies de TG y PC que contienen el ácido graso esencial linoleico (18:2) estaban alteradas, y se observó que la mayoría de las especies de TG que estaban aumentadas en los hígados OPN-KO quiescentes estaban enriquecidas en ácido linoleico. También observamos que las especies de PC que contenían ácido linoleico estaban reducidas en el hígado quiescente de los animales OPN-KO en comparación con los WT. Esto sugiere que la disminución de la síntesis *de novo* de TG observada en el hígado de los ratones OPN-KO se compensa con una mayor absorción de FA en la dieta. Por lo tanto, el linoleico de la dieta se direcciona hacia TG. Sin embargo, esta compensación no se produce en caso de la PC. Dado que los grandes cambios en el contenido de lípidos hepáticos durante la regeneración ocurren principalmente 24 horas después de la HP, se investigó si el aumento del almacén de TG estaba asociado con el aumento del ácido linoleico. Los resultados mostraron que 24 horas tras la PH, las especies de TG que contenían ácido linoleico estaban incrementadas en el WT en comparación con los OPN-KO. Esta disminución de los TG que contienen ácido linoleico puede explicarse por el aumento de la oxidación de FA en los animales OPN-KO 24 horas post PH. En cuanto a la oxidación de los FA 24 horas post PH, la beta oxidación aumentó en los ratones OPN-KO en comparación con los ratones WT. Además, a pesar del aumento de la oxidación de los ácidos grasos y de los niveles de producción de ROS, los niveles de peroxidación lipídica permanecieron inalterados en ratones con deficiencia de OPN durante la regeneración hepática. En conjunto, estos resultados muestran que la disminución de la concentración de PC en el hígado y la síntesis *de novo* no se compensan con el ácido esencial de la dieta linoleico, a diferencia de lo que sucede con los TGs. El aumento de la absorción de lípidos en la dieta de los ratones OPN-

KO proporciona los precursores metabólicos necesarios para la regeneración 24 h y 48 h después de la PH.

El tratamiento con atorvastatina no indujo cambios en la acumulación de gotas lipídicas o en el contenido de TG hepático 24 horas post PH en los ratones OPN-KO o WT. Además, la atorvastatina recuperó los niveles de PC sólo en OPN-KO. Asimismo, los resultados mostraron que las diferencias entre el WT y el OPN-KO en DHE desaparecieron tras el tratamiento con atorvastatina. Por tanto, la atorvastatina induce cambios en el lipidoma hepático durante la regeneración sólo en ratones OPN-KO. En los que, como se ha demostrado en trabajos anteriores, la atorvastatina mejora la regeneración temprana.

La osteopontina juega un papel en la EHGNA asociada a la edad

En cuanto al papel de la OPN en el envejecimiento, los resultados mostraron que en personas con NL había una correlación positiva entre los niveles séricos de OPN y la edad, mientras que esta correlación se perdía en los pacientes con EHGNA, en los cuales los niveles de OPN son más altos que en sujetos con NL. Además, en ratones WT también se observó esta correlación positiva. Conjuntamente, los niveles hepáticos de OPN aumentaron a los 10 meses y permanecieron elevados a los 20 meses. La senescencia es una de las características clave del envejecimiento, cuando se indujo senescencia en células HepG2, los niveles intra y extracelulares de OPN aumentaron. Además, al tratar las células con OPN recombinante, el efecto del agente inductor de la senescencia palbociclib se redujo.

Los resultados anteriores sugieren que la OPN está involucrada en el envejecimiento, y podría jugar un papel en la vulnerabilidad al desarrollo de EHGNA asociado al envejecimiento. Quisimos analizar si el aumento de la expresión de OPN durante el envejecimiento es protector o perjudicial para el desarrollo de la hepatoteatosis asociada a la edad. Los niveles hepáticos de β-galactosidasa y p21 junto con la concentración hepática de TG y ésteres de colesterol y su síntesis de novo se encontraban incrementados en ratones OPN-KO de 10 meses en comparación con sus WTs. Este fenotipo estaba asociado con la disminución de la chaperona GRP78, la activación del estrés de retículo y el aumento de los niveles de FAS. La generación de senescencia en las células con OPN silenciada llevó a una disminución del GRP78. En ratones OPN-KO de 20 meses, la evaluación de la fibrosis hepática y la inflamación mostraron una peor progresión de la enfermedad y aunque los ratones OPN-KO de 20 meses no mostraron síntomas de estrés de retículo, la activación de la caspasa-12 junto con la gamma-H2AX refuerza la existencia daño hepático mayor en los animales OPN-KO.

p53 controla varias funciones metabólicas y celulares y modula las adaptaciones celulares al estrés. Es uno de los genes supresores de tumores más importantes, y algunos estudios han

relacionado p53 con la regulación del OPN en fibroblastos. Quisimos evaluar si p53 podía modular los niveles de OPN. El silenciamiento de p53 en células HepG2 redujo los niveles de OPN intracelular y en el medio. Además, las células Hep3B, en las que no hay p53, no eran capaces de generar OPN cuando se indujo senescencia con palbociclib o H_2O_2. In vivo, p53 está implicado en la hepatoteatosis, ya que los ratones p53-KO desarrollan esteatosis. Se sabe que al alimentar con HFD aumentan los niveles de OPN; sin embargo, los ratones p53-KO no mostraron un aumento en los niveles de OPN en el hígado cuando fueron alimentados con una HFD. Por lo tanto, p53 podría regular los niveles de OPN al inducir senescencia y en respuesta a una HFD.

En conjunto, estos resultados muestran que la deficiencia de OPN conduce a una hepatoteatosis temprana asociada a la edad, acompañada de un estrés de retículo y un aumento de la senescencia. Este fenotipo conduce a una peor progresión de la enfermedad en la vejez, reflejado por el aumento de la fibrosis, la inflamación y los marcadores de apoptosis. Además, p53 podría ser necesario para la inducción del OPN en respuesta a senescencia o HFD. Por lo tanto, durante el envejecimiento, OPN podría estar regulada para mantener la salud hepática.

4. Conclusiones

1. La osteopontina (OPN) regula la interacción entre el colesterol y el metabolismo de la PC modulando de los niveles de CYP7A1 en hepatocitos. La vía de señalización FAK-AKT está implicada en la regulación de CYP7A1 por parte de OPN en el hígado.

2. La OPN modula las vías metabólicas que intervienen en el metabolismo del TG y del colesterol durante la regeneración hepática.

2.1. Los ratones deficientes en OPN muestran un aumento del catabolismo de ácidos grasos cuando hacen frente a la regeneración. El aumento de las demandas metabólicas y la disminución de la síntesis de *novo de* TG se compensan con los ácidos grasos de la dieta.

2.2. La inhibición de la colesterogénesis mediante atorvastatina proporciona un nuevo escenario metabólico relacionado con la mejora de la regeneración temprana en ratones OPN-KO.

3. La OPN es necesaria para mantener la homeostasis metabólica del organismo durante el envejecimiento.

3.1 La OPN está implicada en el envejecimiento del hígado. En suero OPN se correlaciona positivamente con la edad en individuos y modelos animales con hígado normal. En los modelos animales, el aumento de los niveles de OPN en suero está relacionado con el aumento de los niveles en el hígado. La inducción de senescencia en células HepG2, mediante la modulación de p53, aumenta los niveles de OPN celular y su secreción.

3.2 OPN está regulada para mantener el equilibrio del metabolismo lipídico del hígado durante el envejecimiento. La deficiencia de OPN en ratones hace que el hígado sea más vulnerable a la hepatoteatosis asociada a la edad, siendo el mecanismo subyacente el aumento de la lipogénesis *de novo* asociada a la senescencia y a una alteración de la respuesta al estrés de retículo debido a la disminución de los niveles de GRP78.

3.3 En ratones viejos alimentados con HFD, la deficiencia de OPN no provoca cambios en el peso corporal. Sin embargo, induce hipertrigliceridemia y una leve resistencia a la insulina.

B. INTRODUCTION

1. Aging

1.1 Definition and features

Aging is a multidimensional process characterized by a progressive loss of physiological integrity that leads to impaired function of the organism. At a biological level, aging is associated with the gradual accumulation of a wide variety of molecular and cellular damage. Over time, this damage leads to a decrease in physiological function, an increased risk of many diseases, and a general decline in the capacity of the individual to maintain homeostasis, which ultimately results in death. The deterioration of the organism function is the primary risk factor for major human diseases (World Health Organization, 2015).

There are many theories about what causes aging, and the debate is still ongoing. Despite the variety of theories, most of them can be classified into two categories; programmed or damage theories. Those that assume that aging would be predetermined are commonly known as program theories; and those that claim that the aging process would be the result of the sum of alterations and damage that occur randomly and accumulate over time, damage theories (da Costa et al., 2016).

Programmed aging theories, which are also referred to as active or adaptive aging theories, suggest that there is a deliberate deterioration with age because a limited life span results in evolutionary benefits. Moreover, this plan could be the result of aging genes. Genes undoubtedly contribute to longevity, although the extent of genetic versus non-genetic factor contributions to aging remains uncertain. If aging is indeed programmed, the purposes of such program remain unclear. Some have suggested that aging may constitute an altruistic plan (Longo, Mitteldorf, & Skulachev, 2005), by eliminating post-reproductive age individuals, who would compete for resources, by avoiding overpopulation and by promoting adaptation through a succession of generations.

Regarding damage theories, evolutionary biologists argue that aging occurs due to the absence of natural selection at the post-reproductive stage of life. Hence, aging is not programmed; instead, it is the absence of selection for maintenance. The accumulation of damage is a spontaneous entropy-driven process. It can be genetically and environmentally modulated, resulting in the wide range of life spans we observe. In damage theories, one of the fundamental contributors for the causing aging is genome instability (López-Otín, Blasco, Partridge, Serrano, & Kroemer, 2013). Both stability and integrity of DNA and other macromolecules are challenged on a continuous basis by numerous endogenous and exogenous factors, including DNA replication errors and physical, chemical and biological agents (da Costa et al., 2016)(Ogrodnik, Salmonowicz, & Gladyshev, 2018).

Lopez-Otín et al., divided the hallmarks that represent the aging process into 3 groups (López-Otín et al., 2013); primary hallmarks, antagonistic hallmarks and integrative hallmarks (Fig. B.1).

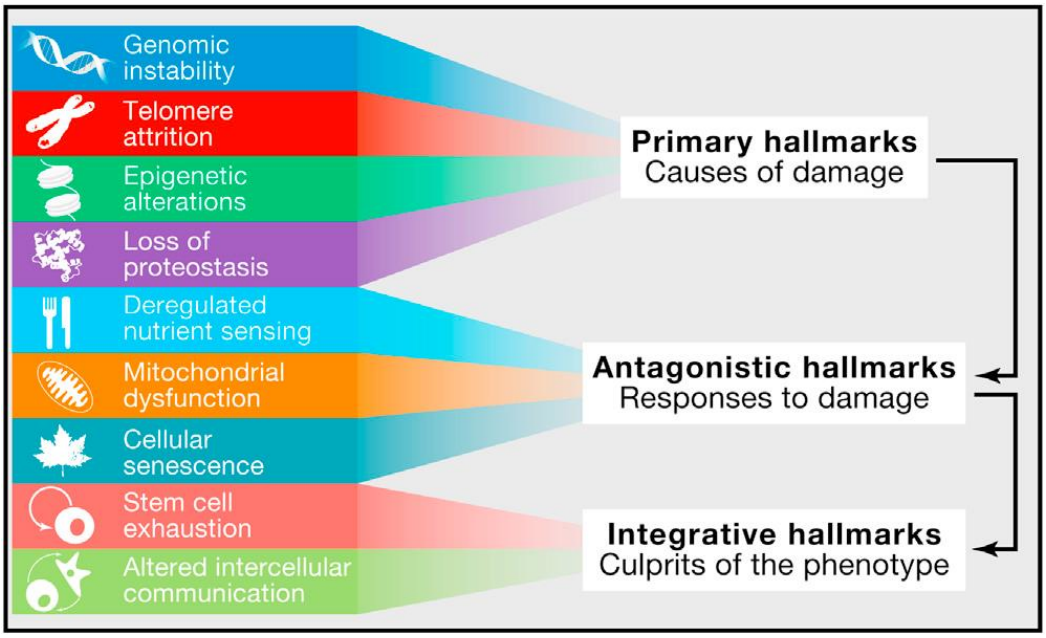

Figure B.1 Interconnections between the Hallmarks of Aging. The nine hallmarks of aging are grouped into three categories. Primary Hallmarks, those hallmarks considered the primary causes of cellular damage. Antagonistic Hallmarks, those considered part of compensatory or antagonistic responses to the damage. These responses initially mitigate the damage, but eventually, if chronic or exacerbated, they become deleterious. Finally, integrative hallmarks that are the result of the previous two groups of hallmarks and are ultimately responsible for the functional decline associated with aging (López-Otín et al., 2013).

1.1.1 Primary hallmarks of aging

Genomic instability, telomere attrition, epigenetic alterations and loss of proteostasis are considered the primary hallmarks of aging. These are considered the cause of cellular damage. One of the most common and accepted denominators of aging is the accumulation of genetic damage.

Genomic instability: The genetic lesions caused by extrinsic or intrinsic damages are very diverse and include point mutations, translocations, chromosomal gains and losses, telomere shortening, and gene disruption caused by the integration of viruses or transposons. All the organisms have evolved a complex network of DNA repair mechanisms that are collectively capable of dealing with most of the damages inflicted to nuclear DNA. This machinery for genomic stability also include specific mechanisms for maintaining the appropriate length and functionality of telomeres.

Telomere attrition: The telomeres are a region of repetitive nucleotide sequences at each end of a chromosome, which protects the end of the chromosome from deterioration and from fusion with

neighboring chromosomes. Telomeres are particularly susceptible to age-related deterioration, where the general chromosomal DNA replication machinery cannot completely copy the DNA out to the extreme ends of the linear chromosomes. Over the course of cell divisions, this leads to attrition of chromosome ends. This deficiency can be resolved in eukaryotes by the cellular ribonucleoprotein enzyme telomerase, which can add telomeric repeat sequences to the ends of chromosomes, hence elongating them to compensate for their attrition (Blackburn, Greider, & Szostak, 2006). On the other hand, even mildly over-activating telomere maintenance promotes risks of subsets of cancers (Blackburn, Epel, & Lin, 2015).

Epigenetic alterations involve alterations in DNA methylation patterns, posttranslational modification of histones, and chromatin remodeling. Studies of chromatin changes suggests that there is a global upregulation of activating marks and downregulation of repressive marks and that there are gene-specific changes in chromatin states regulating expression of key longevity genes Histone demethylases, for example, modulate lifespan by targeting components of key longevity routes such as the insulin/ insulin and insulin-like growth factor-1 (IGF-1) signaling pathway. In addition, inhibitors of histone deacetylases (HDACs) have been proposed, among other drugs, as a promising anti-aging therapy (López-Otín et al., 2013; Sen, Shah, Nativio, & Berger, 2016).

Proteostasis is the concept that refers to the competing and integrated biological pathways within cells that control the biogenesis, folding, trafficking and degradation of proteins present within and outside the cell (Balch, Morimoto, Dillin, & Kelly, 2008). Not just the damaged genetic material contributes to aging, but also damage in other macromolecules such as proteins. The proteostasis network can be divided into several processes: protein synthesis, folding and conformational maintenance, protein degradation and posttranslational modifications (PTM) (Klaips, Jayaraj, & Hartl, 2018).

Protein synthesis: Although the production of individual proteins is regulated by specific factors and pathways, the levels of bulk protein synthesis must be adjusted to the protein folding capacity of the cell to avoid the accumulation of misfolded proteins. Translation attenuation is also critical in relieving proteostasis network overload in conditions of stress. This is typically mediated by inhibition of translation initiation factor 2α (eIF2α). For example, on activation of the unfolded protein response (UPR) to the accumulation of misfolded proteins in the endoplasmic reticulum (ER), protein kinase RNA-like ER kinase (PERK) in the ER membrane, phosphorylates eIF2α attenuating its function in translation (Harding et al., 2001).

Protein folding: Proteins often face significant challenges during folding, because partially folded states with exposed hydrophobic amino acids residues are in danger of misfolding and aggregating. Aberrant folding may occur during de novo synthesis or in conditions of conformational stress, where preexisting proteins may fail to maintain their folded states. To be able to deal with protein folding, cells have evolved chaperones. These proteins assist in the folding, assembly, conformational

maintenance and regulation of another protein without becoming part of its final structure. Accumulation of protein aggregates and loss of the balance is often observed in aging. One feature affecting protein damage in cellular senescence is the downregulation of cellular chaperones mainly Hsp90 and Hsp70 (Ogrodnik et al., 2018). Thus, a healthy chaperone network is required to maintain a stable proteome and to prevent the accumulation of toxic aggregate proteins.

Degradation: When proteins are not able to properly fold, they must be disposed to avoid the formation of toxic aggregates. Like other proteostasis pathways, the ability of the cell to maintain spatial quality control also declines with age (Klaips et al., 2018). Misfolded proteins usually undergo disposal by the ubiquitin-proteasome system or by chaperone mediated lysosomal degradation (C. Zhang & Cuervo, 2008). If these degradation systems do not work properly, misfolded and aggregated proteins can accumulate. Chronic expression of unfolded, misfolded, or aggregated proteins contributes to the development of some age-related pathologies, such as Alzheimer's disease, Parkinson's disease, and cataracts.

The protein network ensures that most proteins fold to a stable native state. When these proteins are no longer needed or errors in folding occur, they are efficiently targeted for degradation, primarily via the ubiquitin-proteasome system (UPS). If cells undergo transient stress, healthy cells activate a stress response. Chaperone bind to misfolded species and trigger the appropriate transcriptional program leading to a general increase in protein-folding capacity, increase in protein turnover, and decrease in the production of additional substrates via attenuation of general protein translation. In cases of chronic stress, such as during aging or disease, sequestration of key protein network components by aggregates can lead to aberrant transcriptional programs, a deficit in folding capacity due to a lack of functionally available chaperones, and a buildup of misfolded species due to a decline in proteasome capacity. This can lead to an inability to restore the balance and further accumulation of misfolded species (Fig B.2)(Klaips et al., 2018).

Protein posttranslational modifications (PTMs) occur as a consequence of either modifying enzymes related to posttranslational processing or signaling pathway activation. In this context, both enzymatic and nonenzymatic PTMs can undergo age-related alterations. Alteration in the pattern of nonenzymatic PTMs depends mainly on the nature of the modifying substances, such as metabolites and free radicals. In contrast, changes in the nature of enzymatic PTMs rely primarily on the activities of modifying enzymes. Associated to the aging process, phosphorylation, N-Acetylation, glycosylation, sumoylation, nitrosylation, methylation and oxidation are some of the changes that proteins can undergo (Santos & Lindner, 2017).

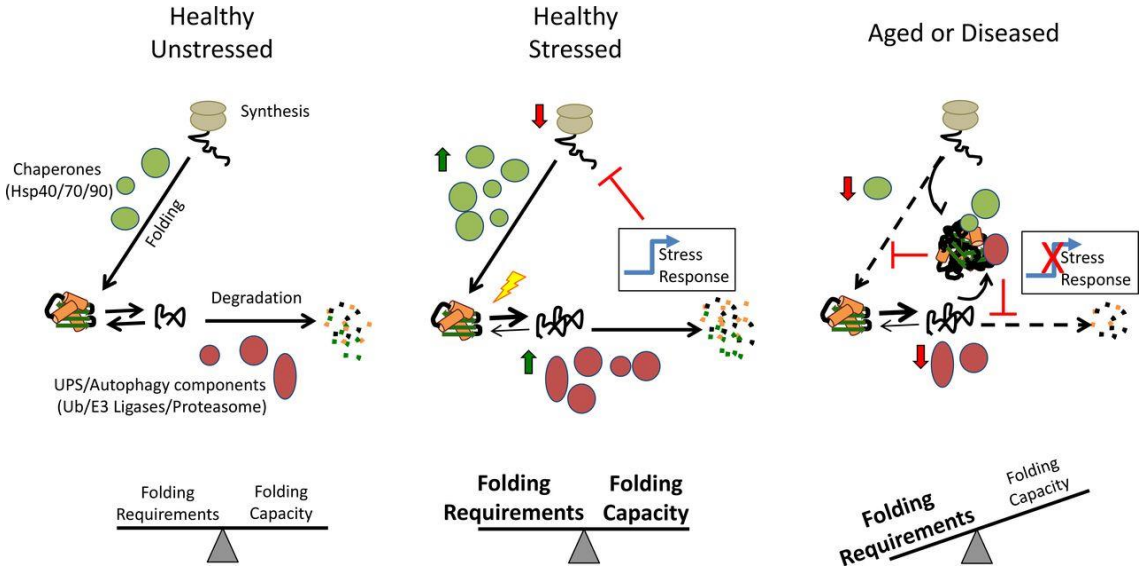

Figure B.2 Protein network in healthy and aged cells (Klaips et al., 2018)

1.1.2 Antagonistic hallmarks of aging

The antagonistic hallmarks are those considered part of compensatory or antagonistic responses to the damage. The antagonistic hallmarks are the deregulated nutrient-sensing, the mitochondrial dysfunctions and cellular senescence. These responses initially mitigate the damage, but eventually, if chronic or exacerbated, they become deleterious themselves.

Altered nutrient sensing: The correct regulation of the nutrient sensing is key for the maintenance of the cell. It has been observed that many manipulations that attenuate signaling of insulin and IGF-1 pathway at different levels are able to expand lifespan. Other nutrient sensing regulators like mTOR and AMP-activated protein kinase (AMPK) have influence on lifespan. A growing list of evidence suggests that mTOR signaling influences longevity and aging. Indeed, inhibition of the mTOR complex 1 (mTORC1) with rapamycin is currently one of the known pharmacological treatments that increases lifespan in many model organisms studied (Weichhart, 2018). AMPK is a fundamental regulator of energy metabolism and stress resistance. AMPK signaling controls an integrated signaling network that is involved in the regulation of lifespan and its activation mediates lifespan extension. AMPK can inhibit mTOR, IGF-1 signaling (Salminen, Kaarniranta, & Kauppinen, 2016). Evidence suggests that the anabolic signaling accelerates aging and that the decreased nutrient signaling (i.e. dietary restriction) extends longevity (Fontana, Partridge, & Longo, 2010; López-Otín et al., 2013).

Mitochondrial dysfunction is other antagonistic hallmark of aging. On one hand, the aging-associated mitochondrial dysfunction is thought to cause an increased production of radical oxygen

species (ROS), which causes further mitochondria deterioration and cellular damage. This is the basis for the mitochondrial free radical theory of aging (Harman, 1965). Apart from generating ROS, the dysfunctional mitochondria can also affect the apoptotic signaling and reduces the bioenergetics efficiency. During aging, cells present defective mitophagy (a form of macroautophagy that targets defective mitochondria for degradation), and lower mitochondrial biogenesis. These two phenomena leads to a decreased turnover of "healthy" mitochondria, which may contribute to the aging process. Thus, mitochondrial dynamics can also be important for delaying aging and extend longevity by improved mitochondrial quality control (Bratic & Larsson, 2013; R. Shi, Guberman, & Kirshenbaum, 2018).

Cellular senescence is considered one of the key hallmarks of aging. One of the main features of aged organisms is the accumulation of senescent cells. However, senescence and aging should not be considered as the same concept, although many times aging and senescence words are used indistinctly. Indeed, aging is a much broader and complex process. Senescence is the irreversible cell cycle arrest that constitutes a stress response triggered by insults such as genomic instability and telomere attrition, radiation, oncogenic stress, oxidative stress, tumor suppressor loss, oxidative stress and certain cytokines among other factors (Bolden & Lowe, 2015; López-Otín et al., 2013; McHugh & Gil, 2018). Thus, it is a mechanism to restrict the propagation of cells under stress. A cell can enter cellular senescence either by gradual accumulation of damage in replicative aging or by a sudden outburst of damage, like the damage induced by radiation or chemotherapeutics. Therefore, senescent cells often show high levels of various forms of damage and resemble chronologically aged cells observed in an old organism. While the cell stops dividing when entering senescence, it remains metabolically active and keeps accumulating damage in the process that can last months or even years ending in cell death (Ogrodnik et al., 2018). Senescence is characterized for several features like flat enlarged cytomorphology, extracellular matrix reorganization, reorganization of chromatin, p53/Rb pathway activation, senescence-associated β-Galactosidase (SA β-Galactosidase) activity, the formation of senescence-associated heterochromatic foci (SAHF), epigenetic changes and secretion of a diverse collection of soluble and insoluble factors: the senescence-associated secretory phenotype (SASP) (Bolden & Lowe, 2015).

The main outputs of senescence are beneficial as senescence imposes a potent barrier to tumorigenesis and contributes to tissue repair and embryonic development, together with a role in wound healing, tissue regeneration and immune surveillance. However, senescence can also have detrimental consequences as the SASP can enhance proliferation of neighboring tumor cells, chemoresistance, and aging (Lujambio, 2018; Malaquin, Martinez, & Rodier, 2016). The SASP is one of the key features of the senescent cells, and it can affect intercellular communication. This secretory phenotype is composed of cytokines, chemokines, growth factors, receptors and proteases

(Malaquin et al., 2016). However, the SASP can vary depending on cell type and senescent stimuli. These secreted factors function physiologically in the tissue microenvironment, in which they can propagate the stress response and communicate with neighboring cells, having thus, paracrine but also autocrine effects. Some SASP factors have important roles in the onset of stable cell-cycle arrest in senescent cells, which contributes to the tumor-suppressive function of cellular senescence. Paradoxically, many SASP factors have the potential to cause chronic inflammation and tumorigenesis, depending on the biological context (Lau & David, 2019; Rao & Jackson, 2016).

Despite the deleterious effects of SASP, it is important to keep in mind, that, primarily its effects are beneficial, since it also contributes to embryonic development, wound healing and inhibits tumorigenesis (Fig B.3). These beneficial effects of SASP happens when the presence of senescent cells in the tissue is transient (Malaquin et al., 2016). The SASP plays a critical role by removing these transient senescent cells via immune-mediated clearance, by recruiting immune cells. It is when senescent cells remain in the tissue because of defective clearance when the detrimental effects appear. Thus, depending on the biological context senescence will have a beneficial or deleterious effect. Senescence in the aging context has negative effect, since accumulation of senescent cells contributes to tissue dysfunction.

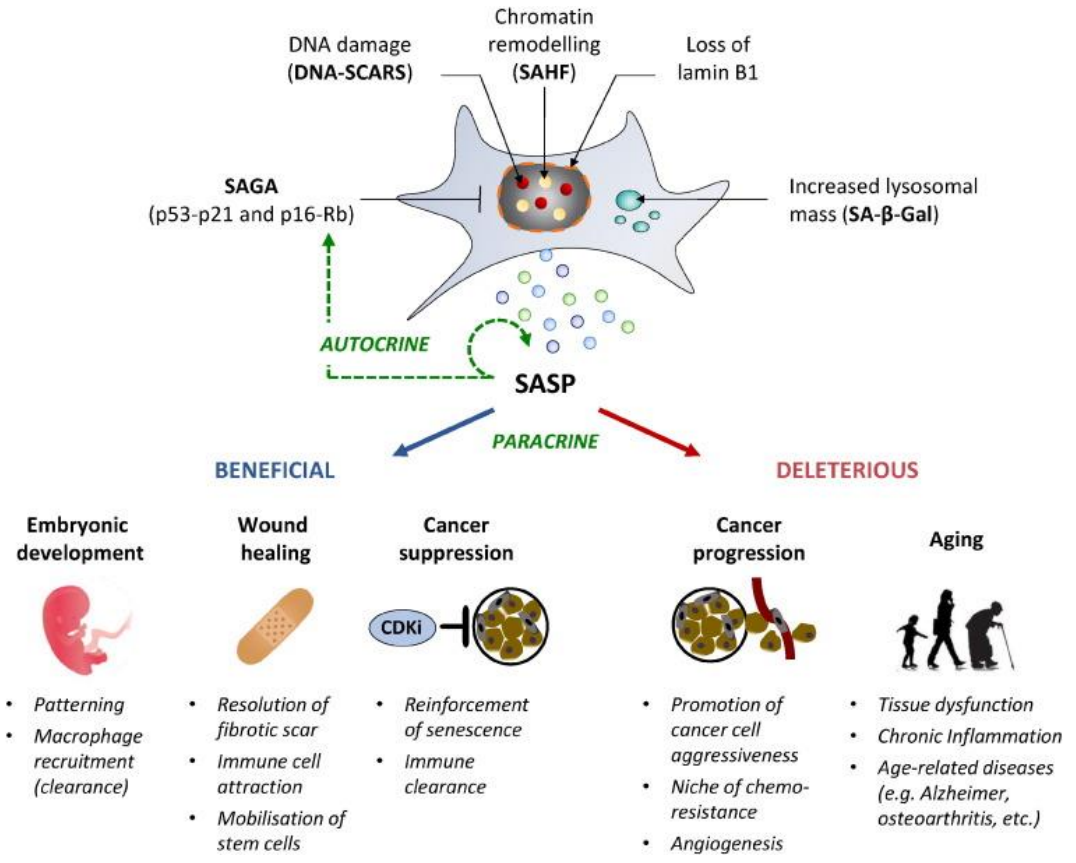

Figure B.3 Cell senescence and SASP effects. (Malaquin et al., 2016).

The mechanisms by which senescence is induced can be diverse, many of which involve p53 activation. Most senescence inducers activate the tumor suppressor pathways TP53/CDKN1A and/or pRb/CDKN2A. All the mechanism meet in the activation of the cyclin-dependent kinase (CDK) inhibitors such as p16, p15, p21 and p27. The inhibition of CDK-cyclin complexes results in proliferative arrest. Being its feature the hypo-phosphorylation of Rb. The senescence-inducing pathways may vary from a cell type to others (Munoz-Espin & Serrano, 2014).

1.1.3 Integrative hallmarks of aging

Finally, the integrative hallmarks are the consequence of the primary and antagonistic hallmarks, and are ultimately responsible for the functional decline associated with aging. These hallmarks are stem cell exhaustion and altered intracellular communication (López-Otín et al., 2013).

Stem cell exhaustion: the decline in the regenerative potential of tissues is one of the most obvious characteristics of aging. The life-long persistence of stem cells in the body makes them particularly susceptible to the accumulation of cellular damage. Interestingly, recent promising studies suggest that stem cell rejuvenation may reverse the aging phenotype at the organismal level (Rando & Chang, 2012). Stem cells in many tissues have been found to undergo profound changes with age, exhibiting reduced responsiveness to tissue injury, dysregulation of proliferative activities and declining functional capacities. Exhaustion of the stem cell pool with age can occur because these cells lose self-renewal activity and terminally differentiate, thereby exiting the stem cell pool, or because they undergo apoptosis or senescence induced by exposure to cellular stress. These changes translate into reduced effectiveness of cell replacement and tissue regeneration in aged organisms (Oh, Lee, & Wagers, 2014).

Intercellular communication is another integrative hallmark of aging. Intercellular communication is key for cells to grow and work normally. Cells signal each other by direct contact with each other or by the release of a substance from one cell that is taken up by another cell. Intercellular communication is fundamental to the immune response. Several studies have highlighted that aging is characterized by a state of low-grade persistent inflammation that leads to a global loss of efficiency, being the biological background for many aging-related diseases and may be the underlying mechanism responsible for the decline in physical function with age. The so-called “Inflammaging”, which may result from multiple causes. Various data suggest that besides persistent viral and bacterial infections, cell debris, misplaced self-molecules and misfolded and oxidized proteins are major contributors to inflammaging (Franceschi, Garagnani, Parini, Giuliani, & Santoro, 2018). Linked to this, a major characteristic of inflammaging is the chronic activation of the innate immune system. The deregulated production of inflammatory cytokines promotes an altered

response in the elderly (Bruunsgaard, Pedersen, Schroll, Skinhøj, & Pedersen, 2000; Fagiolo et al., 1993).

Senescent cells secrete proteins, such as inflammatory cytokines, chemokines, extracellular matrix remodeling factors, and growth factors. These secreted proteins function physiologically in the tissue microenvironment, in which they could propagate the stress response and communicate with neighboring cells. As previously mentioned, this is known as the SASP. Interestingly, inflammaging and metaflammation (a specific situation of chronic inflammation caused by nutrient excess) largely share the same molecular mechanisms (Franceschi et al., 2018).

1.1.4 Perspectives and consequences

Aging is emerging as a key policy issue because both the proportion and absolute number of older people in populations around the world are increasing dramatically (Fig. B.4). There are two key drivers of population aging, increased life expectancy and decreased fertility rates. Regarding the increasing life expectancy, on average, people around the world are living longer. Part of this global increase is due to the improved survival of people at older ages, the other part is explained by improved survival at younger ages. The second reason is that populations are aging because of falling fertility rates (World Health Organization, 2015).

The aging of the population is expected to have a severe socio-economic impact especially in the developing countries, which account for over 60% of the older population (World Health Organization, 2015). Because the health dynamics of older age are related to increased needs for health care, it might be expected that increasing age would be associated with increased health-care utilization. This predicted increase in the life expectancy over the next years demands better healthcare services and disease prevention measures. Research in the aging field has gained a great relevance lately because age-related issues involve a large part of the population, not only the elderly, but also the mayor part of society because of the medical and economic impact. Therefore, it is essential to have a better understanding of the mechanisms of the progression of organ dysfunction with aging, to be able to find markers, targets and treatments to help to reduce or avoid the severity of diseases associated or aggravated with age and improve as much as possible the health span and quality of life of the elderly.

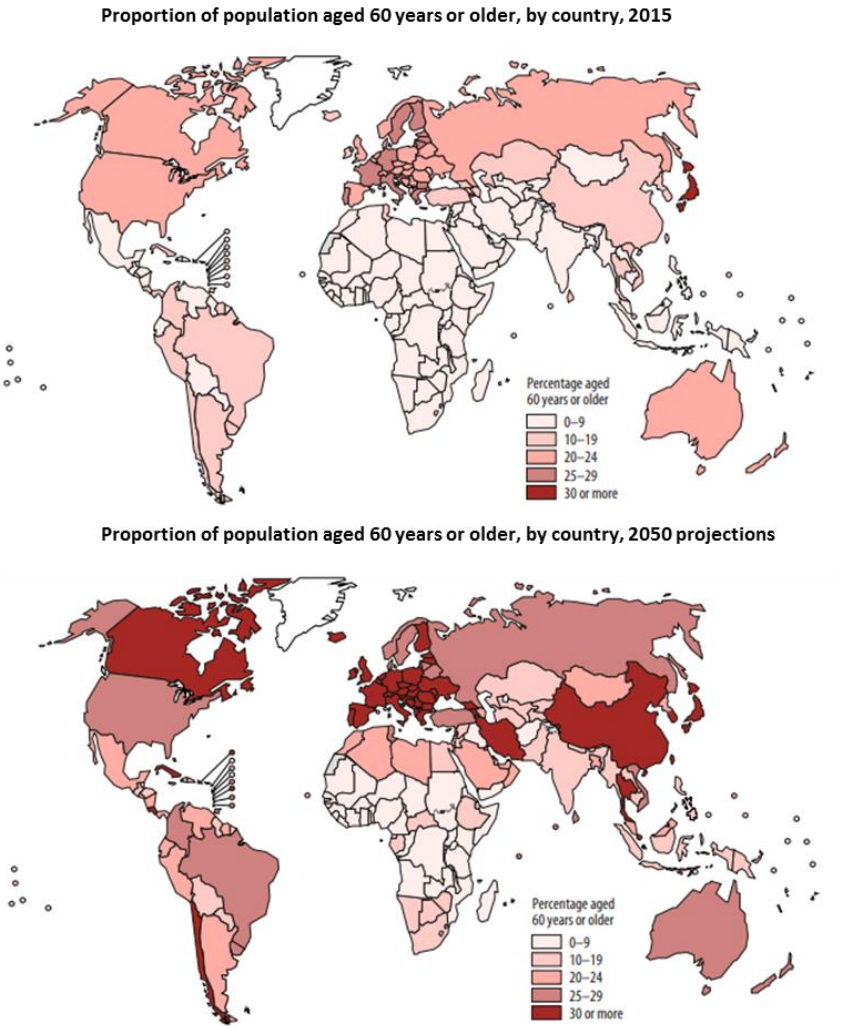

Figure B.4 Proportion of aged people in 2015 and predictions for 2050. (WHO, 2015)

1.2 Aging and disease

The aging of a large part of the population, especially in Western societies, is a quite recent phenomenon that is consequence of the rise in the human life expectancy and low fertility. However, longer lifespan does not mean the maintenance of the health span, usually the number of chronic diseases in the elderly population is very high, especially of metabolic and cardiovascular diseases (Ferrucci, Giallauria, & Guralnik, 2008). Several underlying changes tend to occur to some degree in all humans as they age. Although there is marked diversity in how these changes are experienced at an individual level, general trends are seen when the population as a whole is considered. All the following features are considered a manifestation of the aging process: sarcopenia, decline in vision and hearing, decrease of cognitive function, decreased immune function and frailty (World Health Organization, 2015)

The deterioration that accompanies aging is the primary risk factor for major human pathologies, including cancer, diabetes, cardiovascular disorders, and neurodegenerative disorders. An important aspect of disease status that distinguishes the older population from the younger population is the high rate of co-occurrence of multiple chronic conditions, termed *comorbidity.* The concept of comorbidity is useful in considering the burden of disease in older people. The reason for the increased prevalence of diseases in the elderly is, as mentioned above, the accumulation of damage that leads to the tissue malfunction and deterioration, and the inability to repair this damage leads to disease, often, chronic disease. Among them, the prevalence of metabolic diseases is high as shown in the table (Table B.1).

Table B.1. Prevalence of the main health problems in the population over 64 years, rate for every 1,000 people assigned to the primary care of the National Health System, sorted by gender. Spain, 2012

Health problem	Both genders	Males	Females
Hypertension	503,3	473,6	525
Lipid metabolism disorders	341,6	310,6	365
Athrosis (except back bone)	220	146,6	275,6
Diabetes mellitus	197	218	181
Acute infection of the respiratory apparatus	165,7	160,9	169,4
Backbone syndromes	127,3	105	144,2
Other locomotor system problems	106,9	69,5	135,2
Cataracts	101,5	89,9	110,3
Arrithmia	95,2	105,1	87,7
Obesity and overweight	95,2	79,2	107,2
Teeth / gums diseases	94,2	100,1	89,8
Other cardiovascular diseases	89,1	61	93,6
Skin disorders	88,4	81,7	53,7
Isquemic cardiopathy	85,7	127,9	53,7

The most common metabolic disorders associated with aging are:

Hypertension: Hypertension, a major contributor to atherosclerosis, is the most common chronic disease of older adults. Atherosclerosis and hypertension are the major factors responsible for the myocardial infarction and stroke. Isolated systolic hypertension is particularly common among older adults and is associated with mortality at advanced ages (Belikov, 2018; Jaul & Barron, 2017).

Cardiovascular Disease: Cardiovascular disease remains the most common cause of death of older adults, although death rates have dropped in the last 20 years. This category includes chronic ischemic heart disease, congestive heart failure, and arrhythmia. Normal aging includes vascular remodeling and vascular stiffness (J. C. Wang & Bennett, 2012). Atherosclerosis causes inflammation and further vascular changes increasing risk for cardiac events, stroke, peripheral vascular disease, cognitive impairment, and other organ damage (Collerton et al., 2009; Jaul & Barron, 2017).

Diabetes Mellitus: Diabetes rates have been increasing as populations age and become more overweight. The prevalence of diabetes among American older adults may increase more than 400% by 2050. Diabetes mellitus is the group of metabolic diseases characterized by increased blood glucose levels. Diabetes is considered a strong risk factor for cardiovascular disease; it is also associated with peripheral arterial disease and peripheral neuropathy, contributing to diabetic foot ulcers and amputation. There many other complications associated to diabetes. These would include skin conditions, fatty liver disease, infections, polycystic ovarian syndromes, Alzheimer's disease and cancer (Jaul & Barron, 2017).

Cancer: Cancer is the second leading cause of death in older adults. However, by age 85, the death rate from cancer begins to fall (Gorina, Goulding, Hoyert, & Lentzner, 2005). Slow-growing tumors seem to be common in old population. Usually, response to cancer treatment depends on functional status rather than age. At any age, life expectancy when suffering from cancer is quite variable in older adults, based on comorbidities and other factors (Jaul & Barron, 2017).

1.3 Aging and metabolic changes in whole body metabolism

The prevalence of metabolic syndrome (MS) is increasing worldwide, especially among the elderly. Indeed, the prevalence of MS is increased with aging (Bertolotti et al., 2014a). Due to multiple age-related physiologic mechanisms, MS is a term that describes a cluster of independent risk factors that increase the likelihood of cardiovascular disease and type 2 diabetes. These factors include central obesity, insulin resistance, dyslipidemia (elevated levels of triglycerides and low density lipoproteins (LDL) and decreased levels of high density lipoprotein (HDL)), and high blood pressure. In addition, there are other factors such as proinflammatory and prothrombotic states that have been associated with MS (Hutcheson & Rocic, 2012).

Aging complicates the maintenance of cellular and organic metabolic homeostasis, hence favoring an imbalance in metabolism that self-amplifies and eventually becomes clinically manifest. Several metabolic alterations accumulate over time along with a reduction in biological fitness, suggesting the existence of a "metabolic clock" that controls aging. It has been demonstrated that some metabolic interventions can increase longevity, such as caloric restriction, selective limitations of specific nutrients and physical exercise (López-Otín, Galluzzi, Freije, Madeo, & Kroemer, 2016). Multiple defects in metabolism accelerate aging, whereas genetic loci linked to exceptional longevity influence metabolism. Lipids are crucial for a variety of biological processes, including aging and longevity. Interestingly, it has been demonstrated that lipid metabolism can regulate chromatin modifications. Signaling pathways that regulate longevity, such as the insulin pathway and the mTOR pathway can also affect lipid metabolism. These longevity pathways mostly act by influencing the

activity of transcription factors that in turn modulate enzymes involved in lipid metabolism (Papsdorf & Brunet, 2018).

Major metabolic impairments associated to aging include unrestrained hepatic gluconeogenesis, adipose lipogenesis, defective glycogen synthesis and defective glucose uptake in skeletal muscle (Barzilai, Huffman, Muzumdar, & Bartke, 2012). Energy expenditure regulation is key for the maintenance of the metabolic state. Dysregulation of energy intake occurs in old age even in apparently healthy individuals and increase the risk of energy imbalance. Interestingly, when examined relative to the energy needs of the metabolically active tissues, the release of free fatty acids is actually greater in older compared to younger individuals (Toth & Tchernof, 2000). Thus, there is data suggesting the existing dysregulation of body energy expenditure and substrate oxidation in old age. The extent to which body weight and fat increases or decreases in response to age-related energy dysregulation will depend on the prevailing environmental circumstances and health of the individual (Roberts & Rosenberg, 2006).

2. Liver disease

2.1 Liver

2.1.1 Liver features and function

The liver is the largest organ of the human body, it represents between 2 to 5% of the body weight in adults. It is located in the abdominal cavity inferior to the diaphragm. It is the organ that most irrigation receives, accounting the 27% of the cardiac output in rest. The human liver structure is composed of four lobes: right, left, squared and caudate lobe. Its basic structure is the liver lobule, which is hexagonal in shape. The lobule consists of many cellular plates that radiate from the central vein, and each plate consists of liver specialized cells, the hepatocytes. The liver functional unit is the hepatic acinus, a mass of liver parenchyma that is supplied by terminal branches of the portal vein and hepatic artery, and drained by branches that form the hepatic vein (Fig B.5).

The liver is composed of several cell populations (Fig B.6). These cells are classified into two principal groups: parenchymal cells or hepatocytes and non-parenchymal or sinusoidal cells such as endothelial cells, Kupffer cells, stellate cells, lymphoid cells or Pit cells and the biliary epithelium.

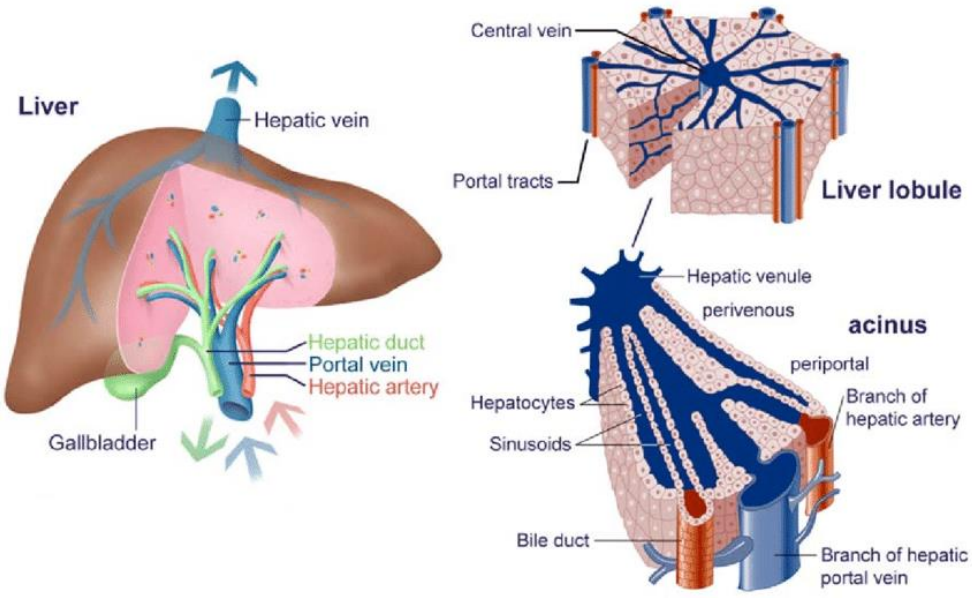

Figure B.5 Representation of the liver, liver lobule and acinus structure (Cunningham & Van Horn, 2003).

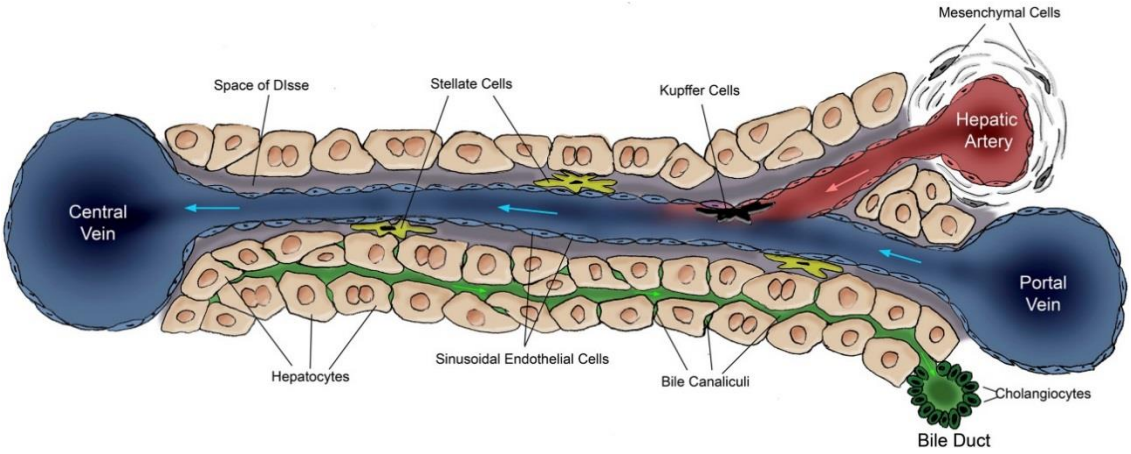

Figure B.6 Representation of liver cell types.(Fanti et al., 2017)

Hepatocytes represent about 60% of the liver population, and roughly, 80% of the mass of the liver is contributed by hepatocytes. The cells are polygonal in shape, and can have a single nucleus or more nuclei. Hepatocytes present acidic cytoplasm with basophil bodies and have abundant organelles. They can store intracellular lipids and glycogen. The hepatocytes are polarized with a basolateral membrane facing the blood and an apical membrane facing the bile canaliculus. The canaliculus is defined by two adjoining cells, which are connected by junctional complexes. In the liver, endothelial cells lack basement membranes, and this facilitates transfer of materials into the space of Disse between endothelial cells and hepatocytes and allows the hepatocytes to contribute to blood proteins and lipoproteins.

Liver sinusoidal endothelial cells (LSECs) line the low shear, sinusoidal capillary channels of the liver and are the most abundant non-parenchymal hepatic cell population. LSECs do not simply form a barrier within the hepatic sinusoids but have vital physiological and immunological functions, including filtration, endocytosis, antigen presentation and leukocyte recruitment. Reflecting these multifunctional properties, LSECs display unique structural and phenotypic features that differentiate them from the capillary endothelium present within other organs. It is now clear that LSECs have a critical role in maintaining immune homeostasis within the liver and in mediating the immune response during acute and chronic liver injury (Shetty, Lalor, & Adams, 2018).

Kupffer cells, the resident macrophage in the liver, comprise the largest population of resident tissue macrophages in the body. Kupffer cells play a critical role in the innate immune response; their localization in the hepatic sinusoid allows them to efficiently phagocytize pathogens entering from the portal or arterial circulation. Kupffer cells also serve as a first line of defence against particulates and immunoreactive material. Dysregulation in the precise control of inflammatory responses in Kupffer cells can contribute to chronic inflammation in the liver.

Hepatic stellate cells (also known as perisinusoidal cells or Ito cells) are located between the hepatocytes and small blood vessels in the liver, also known as the space of Disse. They are characterized by the presence of lipid droplets and thin protrusions extending around the blood vessels. Their activation in damaged liver leads to secretion of collagen and formation of scar tissue, leading to chronic fibrosis or cirrhosis.

Pit cells are one type of hepatic sinusoidal cells, defined morphologically as large granular lymphocytes (LGLs) and functionally as liver-associated natural killer (NK) cells. They are situated inside the sinusoidal lumen, adhering to the endothelial cells and Kupffer cells.

Cholangiocytes are the epithelial cells of the bile duct. They are a heterogeneous, highly dynamic population of epithelial cells that line a three-dimensional network of bile ducts known as the biliary tree. Their major physiologic function lies in modification of hepatic canalicular bile as it is transported along the biliary tree.

The liver has a central role regulating whole body metabolic homeostasis. It processes aminoacids, carbohydrates, lipids and vitamins coming from the digestive system for its storage, processing and/or secretion to the blood or bile. It also synthetizes essential proteins, secretes lipoproteins and takes part in defensive processes of the organism, such as the defensive humoral response as detoxifying of substances like drugs and alcohol. Most of the metabolic functions are carried out by hepatocytes.

2.1.2 Liver lipid metabolism

Lipid metabolism in hepatocytes includes processes of **acquisition of lipids**, including uptake from diet and from circulating lipoproteins, and fatty acids derived from white adipose tissue (WAT) lipolysis, as well as lipid de novo synthesis (de novo lipogenesis); **lipid storage** and formation of lipid droplets and **lipid disposal** in consumption processes and the secretion of lipids into lipoproteins (Fig B.7). Many liver diseases are accompanied by disorders in lipid metabolism.

TG and FA metabolism: Hepatocyte uptake of fatty acids (FA) can occur through passive diffusion because of the hydrophobicity of FAs. However, facilitated transport of particularly long-chain FAs is regulated by translocases and transporters. In the fasting state, a reduction in insulin levels stimulates triglycerides (TG) hydrolysis in adipose tissue releasing FAs, which will be transported to the liver.

Dietary fats are packed into chylomicrons in enterocytes. Once in circulation the endothelial lipoprotein lipase of adipose tissue and muscle will hydrolyze the chylomicrons and TGs and FAs will be released. This degradation of chylomicrons results in their conversion into

chylomicron remnants, which are imported into hepatocytes by remnant receptors through apoE on the surface of the remnants.

As previously mentioned FAs can also be synthesized in the hepatocyte. *De novo* lipogenesis (DNL) of FAs occurs in the cytosol. Under physiological conditions, excess glucose stimulates FA and TG synthesis in hepatocytes. SREBP1c is a key transcription factor regulating FA synthesis, which upregulates several lipogenic genes, including those encoding acetyl-CoA carboxylase (ACC) and fatty acid synthase (FAS). FAs can be used for the synthesis of TG via esterification, which will be stored into lipid droplets, or secreted into VLDL in which apolipoprotein B (apoB) is required. Regulation of VLDL assembly and secretion is a complex process. VLDLs transport FAs from the liver to adipose tissue and other peripheral tissues. TGs are synthesized primarily in the liver, adipose tissue and small intestine as a major nontoxic energy storage form. In the liver, the acyl-CoA diacylglycerol acyltransferases (DGAT) membrane-bound enzymes that catalyze the final step of TG synthesis from diacylglycerol (DAG) and fatty acyl-CoA, play a crucial role.

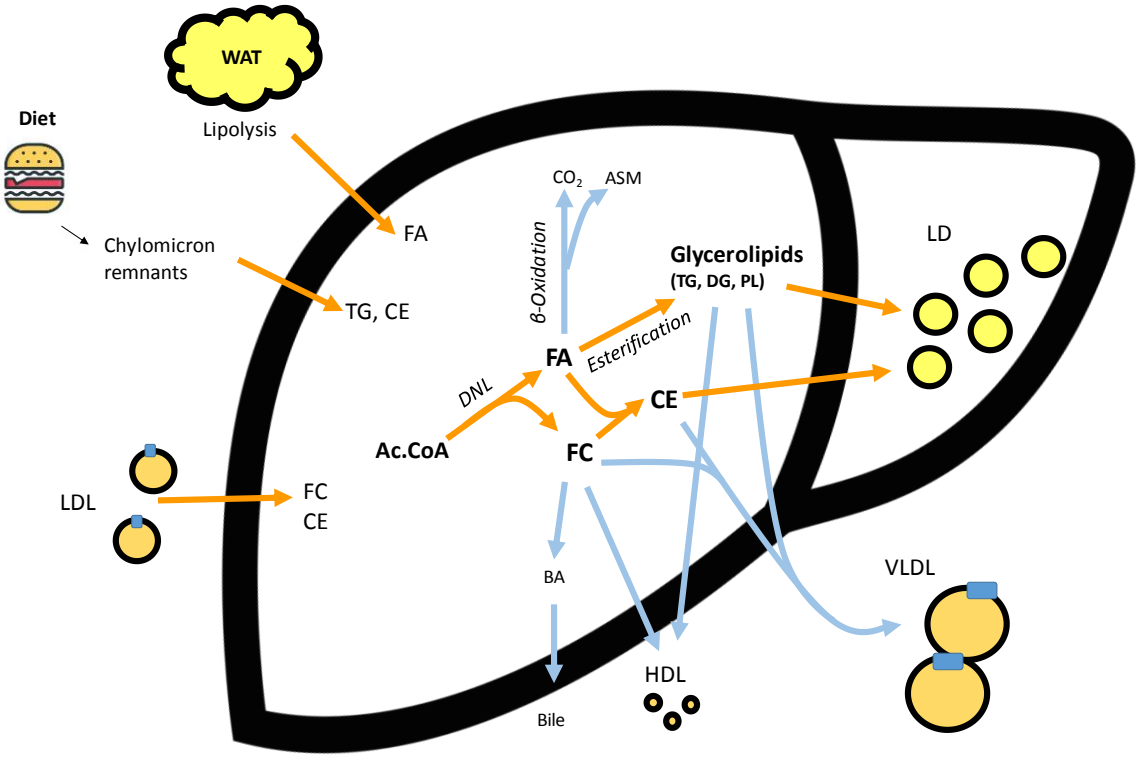

Figure B.7 Schematic representation of the main processes involved in lipid output and input in the liver. Orange arrows represent the main lipid input processes and blue arrows the main lipid output processes. Ac.Coa (Acetyl-CoA), ASM (Acid soluble metabolites), BA (bile acids), CE (cholesteryl ester), DG (diglycerides), DNL (*de novo* lipogenesis), FA (Fatty acid), FC (Free cholesterol), HDL (high density lipoprotein), LD (lipid droplet), LDL (low density lipoprotein), TG (triglycerides), VLDL (very low density lipoprotein).

In the liver, FAs derived from peripheral tissue or diet can be used for energy production via mitochondrial β-oxidation. The β-oxidation of FAs occurs within the mitochondria and peroxisomes. In general, short-, medium-, and long-chain FAs are oxidized within mitochondria, while very long-chain FAs are oxidized within peroxisomes. β-oxidation is a major metabolic pathway that is responsible for the mitochondrial breakdown of long-chain acyl-CoA to acetyl-CoA for energy production. This process involves many steps that are regulated at the transcriptional and post-transcriptional level.

Cholesterol metabolism: The liver plays an important role in the metabolism and regulation of cholesterol. There are two hepatic forms of cholesterol: free cholesterol (FC) and cholesteryl ester (CE). CE can either be stored, hydrolyzed or secreted. There are two sources of cholesterol, the diet and de novo synthesis. Both dietary cholesterol and de novo synthesized cholesterol are transported through the circulation into lipoprotein particles. The cholesterol biosynthesis pathway involves enzymes that are in the cytoplasm, endoplasmic reticulum (ER) and peroxisomes. Synthesis of cholesterol, like most biological lipids, begins from the two-carbon acetate group of acetyl-CoA. The initial steps in the pathway of cholesterol biosynthesis are collectively called the mevalonate pathway. The cholesterol synthesis is a long process with high demands of energy. Excess of FC can be converted into CE, a more inert lipid, and stored. High cholesterol concentrations can be toxic for the cells. Thus, the cholesterol output pathways include bile acid formation, bile secretion and secretion into lipoproteins. Cholesterol can be oxidized in bile acids (BA). This conversion represents the major pathway for its elimination; representing half of the daily excretion. The liver excretes FC via bile, into the digestive tract.

Phospholipid (PL) metabolism: The PLs found in most of the cell membranes are glycerophospholipids. The most abundant glycerophospholipid types are phosphatidylcholine (PC), phosphatidylethanolamine (PE), phosphatidylserine (PS) and phosphatidylinositol (PI). The structure of the phospholipid molecule generally consists of two hydrophobic fatty acid and a hydrophilic part consisting of a phosphate group. These two components are joined together by a glycerol molecule. The phosphate groups can be modified with simple organic molecules such as choline, ethanolamine or serine. The nature of the acyl groups and the type of the alcohol group decide the classification, properties, and biological functions of the PL.

PC is the most abundant PL in the liver and can be synthesized by two different pathways: the Kennedy pathway and the phosphatidylethanolamine methyltransferase (PEMT) pathway. The de novo or the CDP-choline pathway, known as the Kennedy pathway, is in charge of 70% of the PC synthesis in liver. The phosphatidylethanolamine methyltransferase (PEMT) pathway, which is mainly limited to liver cells, is in charge of 30% of the synthesis.

2.1.3 Hepatic changes with aging

In general, the liver function under normal physiological conditions is not intensely impaired with aging. However, when is stressed the aged liver will respond differently (Sheedfar, Biase, Koonen, & Vinciguerra, 2013). Changes in liver during aging can reduce hepatic function and promote liver injury. The aging liver is associated with higher morbidity, enhanced vulnerability and a poor prognosis in patients with various liver diseases, including NAFLD, hepatitis C and liver cancer. In addition, liver regeneration capacity is decreased with aging (Schmucker & Sanchez, 2011). There are hepatic changes associated with the aging process; these changes can negatively affect the morphology, physiology and oxidative capacity of the liver. During aging there is a loss of hepatic volume of 1/3 approximately, a reduction of the blood perfusion and a decrease in the capacity to metabolize certain compounds (Wynne et al., 1989). There are changes in the expression of a variety of proteins and diminished hepatobiliary functions. Aging is also accompanied by significant liver sinusoidal deregulation (Maeso-Díaz et al., 2018) and a loss of capacity to fight against oxidative stress (Schmucker, 2005). In addition, apoptosis increases with liver aging (Zhong et al., 2017).

In old age, fat is redistributed outside the usual fat deposits, and lipids can accumulate in non-adipose tissues like skeletal muscle, heart and liver. Aging is associated with an increase in the lipid accumulation within the liver that may compromise the normal function due to lipotoxicity (Slawik & Vidal-Puig, 2006). Fat may accumulate in the liver as a result of many alterations in lipid metabolism (Cohen, Horton, & Hobbs, 2011). Although there are many possible mechanisms to explain the increase of age-related liver steatosis, the mechanisms that underlie this accumulation are not clearly defined. Increased fatty acid uptake, increased de novo lipogenesis (DNL) (Kuhla, Blei, Jaster, & Vollmar, 2011), decreased FA oxidation, and/ or disrupted synthesis or secretion of VLDL (Toth & Tchernof, 2000) could be involved in the aging-associated liver lipid accumulation. Finally, the rate of liver regeneration is decreased in old animals and humans and this may enhance the progression of hepatic diseases and compromise liver transplantation in the elderly (Schmucker, 2005).

The number of senescent hepatocytes in the liver increases with age. Hepatocyte senescence is characterized by expression of SA-β-gal activity, blockage of cell proliferation, accumulation of foci of DNA damage and increased levels of cell cycle inhibitors p16, p21 and p53 (M. Wang et al., 2014). Senescence of hepatocytes can also be induced by metabolic stress, oncogene over-expression or deletion of tumor suppressing genes, either in vivo or in vitro.

Hepatocyte senescence is also involved in development and progression of other chronic liver diseases such as NAFLD (A. Aravinthan et al., 2013). It was found that the fibrosis stage of patients with chronic hepatitis C was significantly correlated with senescent cell accumulation. Interestingly,

such senescence occurs highly selectively in hepatocytes rather in hepatic stellate cells or lymphocytes, and this process is associated with progression of liver cirrhosis (Wiemann et al., 2002).

2.1.4 Liver regeneration and aging

Liver regeneration has been investigated in detail in rodents using the partial hepatectomy (PH) model, a surgical resection that removes two-thirds of the liver. The remaining liver expands in mass to compensate for the lost tissue. Therefore, the liver regeneration is, actually, a compensatory growth. Liver regeneration is a complex process regulated in young animals by the cooperation of several signal-transduction pathways. However, as mentioned above, one of the main features of the aging liver is the decreased rate of regeneration. It is well established that adult hepatocytes are characterized by a very low replicative rate; however, they can rapidly re-entry into the cell cycle following tissue loss/death (Fausto, Campbell, & Riehle, 2006; Fausto, FAU, & Riehle, 2006; Timchenko, 2009). Since aging affects the regenerative response of the liver after chronic tissue injury or following surgical resection, it represents a critical problem in aged patients with liver disease (Zhu et al., 2014).

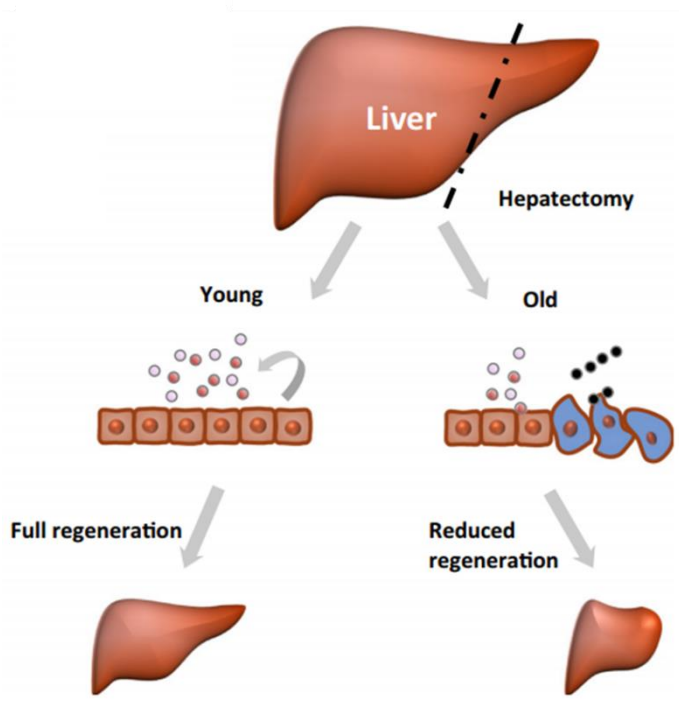

Figure B.8 Prolonged senescence may restrict tissue regeneration (Lasry & Ben-Neriah, 2015). Senescent cells are represented in blue and normal hepatocytes in brown.

The age-dependent decline of the liver regeneration capacity is the consequence of multiple factors that cooperate to affect liver mass recovery after tissue damage. The induction of hepatocyte proliferation factors and the expression of cell cycle genes is inhibited in the elderly. In addition, the repression of cell proliferation and cell cycle gene inhibitors is compromised in the elderly (Pibiri, 2018; Schmucker & Sanchez, 2011).

Regarding hepatocyte senescence, it has been observed that chronic hepatocyte damage and concomitant hepatocyte regeneration accelerate telomere shortening in hepatocytes. When hepatocytes reach the senescent stage, liver regeneration decreases but the chronic liver damage continues. At advanced stages of liver disease, other cell types, like hepatic stellate cells, which usually do not participate in the regenerative process, become activated and form fibrotic scar tissue in areas of hepatocyte loss (Wiemann et al., 2002). Senescence and SASP have an important role in tissue regeneration. As previously mentioned, SASP provides signals that induce cell plasticity and stemness, which are beneficial for tissue regeneration. However, an aberrant or prolonged exposure to the SASP can generate a cell-intrinsic senescence that blocks and obstructs the growth promoting signals (Fig. B.8). This results in a decreased regenerative capacity. In benign senescence, SASP activates the immune system to promote its own clearance and also induces plasticity in neighboring cells. This facilitates the replacement of the cleared cells and promotes tissue regeneration. However, this mechanism is defective in old livers (Fig B.8)(Ritschka et al., 2017).

2.2 Non-alcoholic fatty liver disease (NAFLD)

NAFLD is considered one of the most common cause of chronic liver disease in the Western world, and it is commonly associated with insulin resistance and obesity, which are the most prevalent risk factors for NAFLD. This disease includes a spectrum of disorders (Fig B.9). Hepatic steatosis is the earliest stage of NAFLD, and it is caused by the accumulation of fat in the hepatocytes. The aberrant accumulation of lipids in the liver can lead in some individuals to an inflammatory response that can progress to pathologies like hepatitis, cirrhosis and liver cancer. The NAFLD pathogenesis is complex, and involves a state of lipotoxicity in which insulin resistance, ER stress along with other processes related with altered lipid metabolism, may play an important role in the progression to nonalcoholic steatohepatitis (NASH). The altered processes involved in this onset are increased free FA release from the adipose tissue to the liver, an unbalance between mechanisms of lipid input (uptake and synthesis) and output (lipid secretion as lipoproteins and disposal through bile acid synthesis) (Friedman, Neuschwander-Tetri, Rinella, & Sanyal, 2018; Slawik & Vidal-Puig, 2006). NASH is characterized by steatosis with necroinflamation and eventual fibrosis, which can lead to further progression of liver disease (Cohen et al., 2011; Lomonaco, Sunny, Bril, & Cusi, 2013). Any form of persistent hepatitis, including steatohepatitis, can eventually cause scar tissue, fibrosis, to

form within the liver, and if the scarring continues the liver can develop a state called cirrhosis. The pathogenic mechanisms for NASH are being unraveled, but metabolic stress, inflammation and fibrosis are considered key processes (Fig B.10) (Diehl & Day, 2017). It is considered that 20-30% of NASH patients will develop fibrosis, which may progress to fibrosis. Cirrhosis is a condition where normal liver tissue is replaced by fibrotic tissue, and the function and structure of the liver are disrupted. Severe cases of cirrhosis can provoke liver failure, and cirrhosis patients are at high risk of developing hepatocellular carcinoma (HCC). However, HCC can also develop in the absence of liver cirrhosis. Indeed, NAFLD is also fueling the increasing incidence and prevalence of primary liver cancer in many countries. The incidence of HCC is at least 1 to 2% per year among patients with cirrhosis related to NASH; primary liver cancers can also develop in patients with non-cirrhotic NASH and NAFLD (Fig B.10)(Issa & Alkhouri, 2017)(Diehl & Day, 2017). Interestingly, NAFLD has become the most common liver disease associated with HCC development. In fact, metabolic risk factors are common among patients with HCC. Besides, HCC related mortality is increasing, with typical patients being elderly with metabolic risk factors (Fig B.11) (Dyson et al., 2014).

The disease is reversible in the early stages; simple steatosis has the best prognosis within the spectrum of NAFLD, but the treatment becomes more complicated with progression, and if not treated, it may progress to more severe stages such as cirrhosis and HCC (Angulo, 2002). NAFLD is often considered the hepatic manifestation of the MS. Presence of MS in an individual is the strongest risk factor for NAFLD and NASH. The association between NAFLD and features of MS may be bidirectional, particularly with respect to diabetes and hypertension, meaning that not only MS increases the risk of NAFLD, but also NAFLD may enhance several features and comorbidities of MS. Thus, effective treatment of NASH could have the additional benefit of improving the features of MS (Friedman et al., 2018)

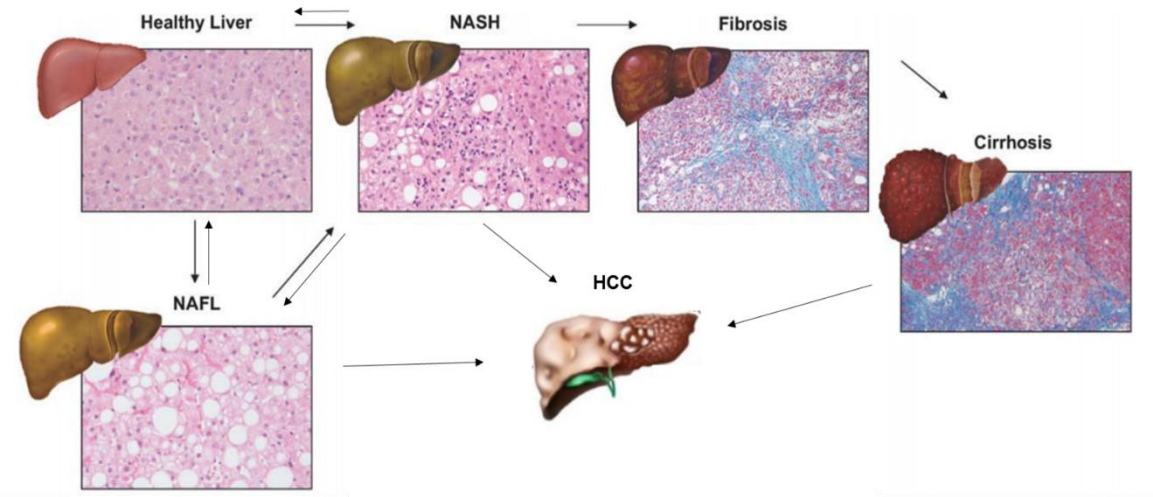

Figure B.9 The disease spectrum of nonalcoholic fatty liver disease. Schematic progression of NAFLD with histological sections illustrating the different stages. Collagen fibers are stained blue with Masson's trichrome stain. (Image adapted from (Cleveland, Bandy, & VanWagner, 2018)).

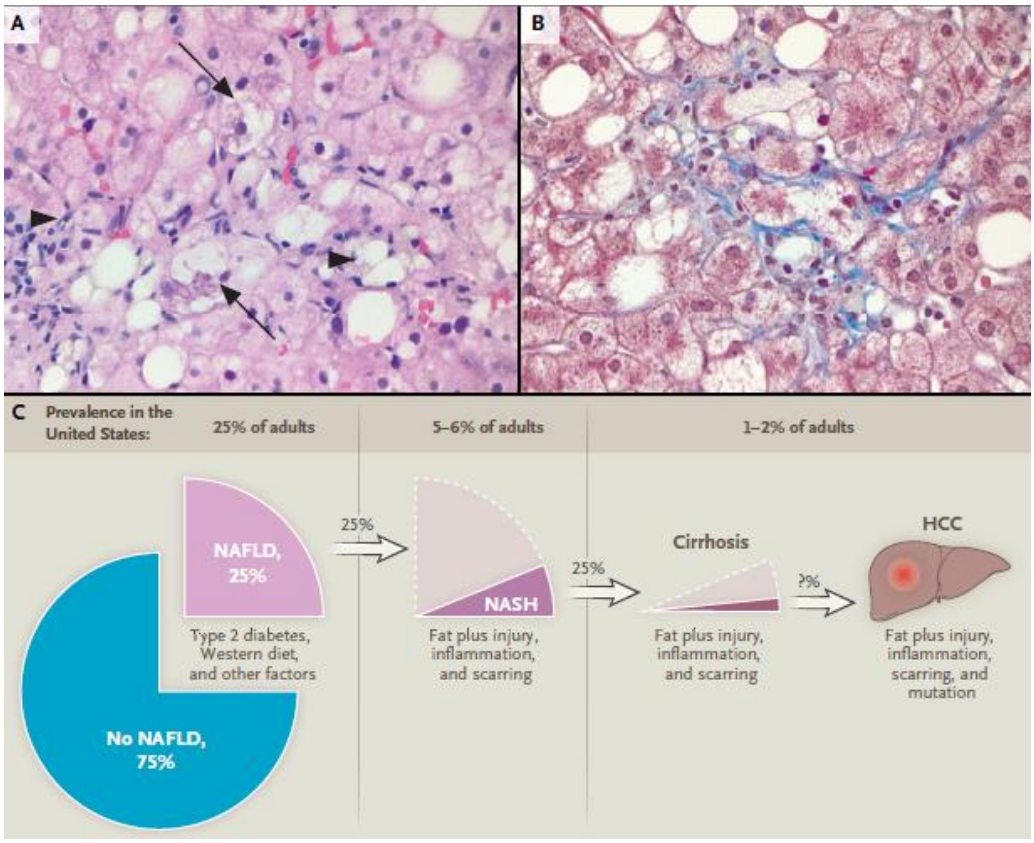

Figure B.10 Histologic features and prevalence of NAFLD. (A) NASH is a progressive type of nonalcoholic fatty liver disease (NAFLD). Histologic features of NASH in liver-biopsy specimens: ballooned hepatocytes (arrows), inflammatory infiltrate (arrowheads) and (B) fibrosis. (C) Relative distribution of NAFLD, NASH, cirrhosis, and primary liver cancer in the U.S. adult population (Diehl & Day, 2017).

2.2.1 NAFLD and aging

NAFLD is more prevalent in older populations (Fig B.12). In fact, aging is the most common cause for the progression of NAFDL. It is a disease that progresses slowly with age. However, not in all patients in the same way. Continued high rates of adult obesity and diabetes mellitus (DM) along with an aging population will increase NAFLD-related liver disease and mortality in the western countries (Estes, Razavi, Loomba, Younossi, & Sanyal, 2018).

The earliest stage of NAFLD, hepatic steatosis, is characterized by an accumulation of TGs in the cytoplasm of hepatocytes. The spontaneous steatosis observed in aging has been observed in mice from 12 months of age and in aging rhesus monkeys, in which the prevalence was increased when monkeys suffered from MS (Zheng et al., 2018). Older patients show more severe biochemical, hematological and histological changes, and the female sex is no longer protective with increasing age. In fact, estrogens have a protective role, during female fertile period; women tend to be protected from NAFLD compared to men. However, although they tend to develop the disease approximately 10 years later than men do, post-menopausal women are no longer protected from NAFLD. Elderly people have a high risk for strongly age-dependent hepatic and extra-hepatic complications. NAFLD in the elderly is expected to carry a substantial burden of NASH, cirrhosis and HCC (Bertolotti et al., 2014b; Dyson et al., 2014).

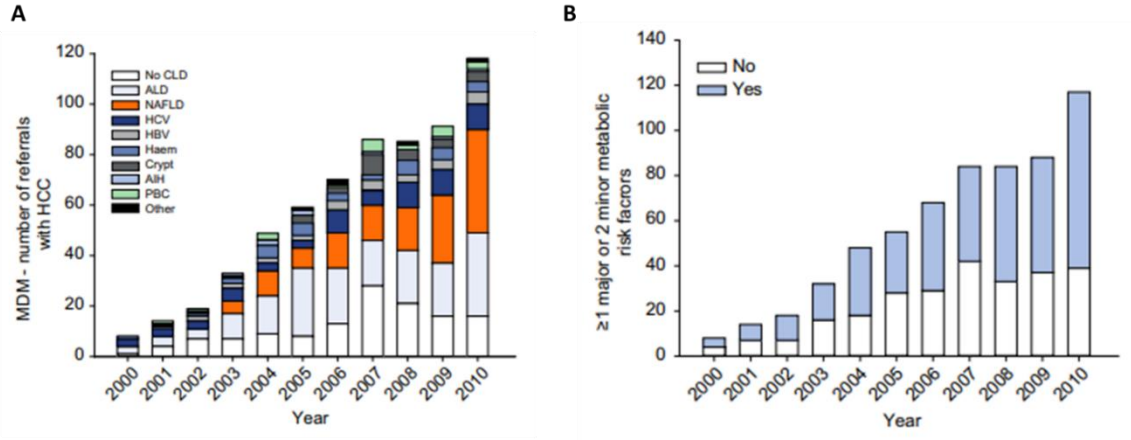

Figure B.11 Etiologies of chronic liver disease associated with HCC and prevalence of metabolic risk factors in patients with HCC. (A) Alcoholic liver disease (ALD), NAFLD and cases without chronic liver disease (CLD) account for the majority of cases. NAFLD-associated HCC increased from an unknown entity at the start of the decade to the commonest CLD associated with HCC. (B) Metabolic risk factors, defined as 1 major (obesity or type 2 diabetes), or two minor (hypertension, hypertriglyceridemia, reduced HDL cholesterol, previous cardiovascular event) were common, affecting 66.1% of individuals referred in 2010 (Dyson et al., 2014).

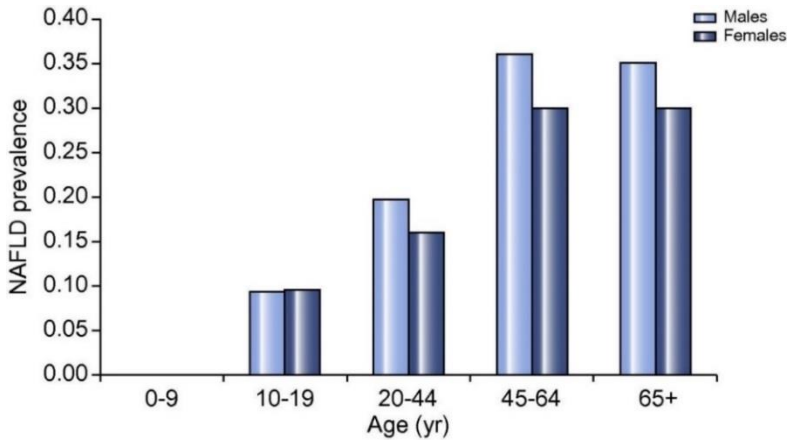

Figure B.12 Incidence of NAFLD by age group and sex.(Younossi, 2018)

The mechanisms underlying NAFLD are not completely understood nor is why its prevalence increases with aging. It has been speculated that aging process may promote NAFLD via different mechanisms, many of which are related to metabolic alteration (Fig B.13). Some of these mechanisms include altered metabolic fluxes and signaling pathways, which are explained below.

Regarding **metabolic fluxes** fat absorption and uptake, most of the studies demonstrate that the contribution of changes in dietary fat absorption to the development of hepatic steatosis is probably minimal in healthy aging (Ferramosca & Zara, 2014). However, regarding fat uptake by the liver, the reduction in FABP1 with aging and in NAFLD can have several consequences, such as impairment in β-oxidation through changes in PPARα thereby exacerbating the potential lipotoxicity of FAs, contributing to the pathogenesis and progression of NAFLD (Gong, Tas, Yakar, & Muzumdar, 2017).

Regarding TG export, aging is associated with higher levels of apoB in both men and women (Schaefer et al., 1994) which could be explained by the presence of age associated hepatic insulin resistance (Gong et al., 2017). Indeed, insulin resistance is associated with increased secretion and decreased clearance of apoB. This increase in lipoproteins increases the risk of cardiovascular disease. Besides, the age-related insulin resistance causes alterations in the post-prandial distribution of carbohydrate away from muscle to the liver, producing an increased DNL and thereby, hepatic steatosis (Gong et al., 2017). Increased hepatic lipid content may partially be attributed to the enhanced hepatic lipid uptake in the absence of growth hormone (GH) signaling.

DNL contributes to no more than 5-10% of the hepatic TG content under physiological conditions, whereas the contribution increases to more than 25% in NAFLD patients, showing that DNL may be a major determinant for NAFLD development in humans. Age- associated changes in DNL appear to be primarily modulated through changes in systemic mediators such as insulin resistance and changes in growth hormone/ insulin-like growth factor (GH/IGF) axis.

The process of FA oxidation in the liver is influenced by many factors including aging and circulating adipokines such as adiponectin and leptin. In fact, expression of genes involved in the FA oxidation in liver are decreased with aging (Houtkooper et al., 2011). Mitochondrial dysfunction can also contribute to a defective FA oxidation. Mitochondrial dysfunction and oxidative damage inevitably occur in normal aging and can lead to further progression or initiation of disease (Kudryavtseva et al., 2016).

There are some mediators of metabolism that can be altered in aging. For instance, aging is associated with decline in **GH** levels. This affects FA uptake in the liver and could be a contributor to increased hepatic lipid accumulation in aging (Gong et al., 2017). GH/IGF-1 have a key role in development and progression of NAFLD. Decrease of these two hormones is closely associated with the progression of NAFLD, while its replacement has shown to improve this disease (Takahashi, 2017). Interestingly, GH/IGF-1 axis shows a steady decline with age with a 12-15% reduction in every

decade of adult life; and changes in GH/IGF-1 axis have been linked to longevity across species (Berryman, Christiansen, Johannsson, Thorner, & Kopchick, 2008).

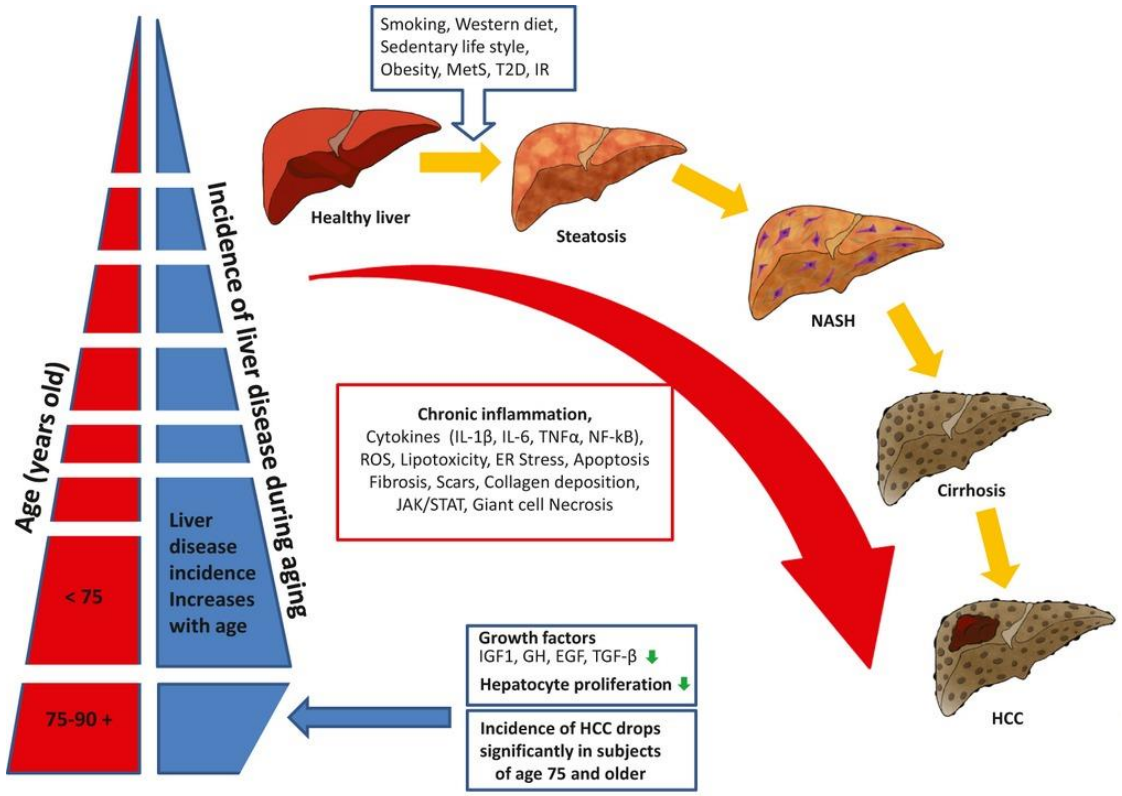

Figure B.13 NAFLD incidence and age, inflammaging, growth factors and other elements involved in the disease progression (Sheedfar et al., 2013)

Leptin is a protein produced by the adipocytes that significantly affects hepatic lipid metabolism. Secreted leptin acts primarily at the level of the hypothalamus to decrease appetite. The amount of leptin secreted by the adipocytes is proportional to fat mass. Receptors for leptin have been identified in multiple other tissues including liver, indicating direct action on target tissues. Leptin has a role in modulating liver fat levels. In fact, increased FA oxidation, increase in ketogenesis and decrease in DNL are mechanisms through which leptin decreases hepatic lipid accumulation. Thus, leptin resistance has a role in the development of hepatic steatosis. The age-associated increase in hepatic fat accumulation is a leptin-resistant state. Serum leptin levels are increased, along with a lack of effects on body intake and energy expenditure to infused leptin. Age-associated leptin resistance, along with age-related changes in body composition and insulin resistance contribute to increased hepatic lipid accumulation with age. In addition to its role in hepatic lipid metabolism, leptin plays a role in hepatic inflammation and fibrosis (Gong et al., 2017).

Insulin is the master regulator of glucose utilization by liver and extrahepatic tissues. Through suppression of lipolysis, insulin decreases the circulating FA levels, thereby reducing the availability of FA to the liver. In liver, insulin inhibits gluconeogenesis, and promotes glycogen synthesis and DNL. In addition, insulin, through the phosphoinositide-3-kinase (PI3K) pathway, controls DNL via

activating nuclear transcription factor SREBP-1c, which induces ACC and FAS expression, two key enzymes in fatty acid synthesis. As mentioned above, insulin also controls TG export by decreasing post-prandial VLDL secretion via restricting apoB synthesis and increasing its degradation. Aging is often considered an insulin resistant state. Many factors contribute to insulin resistance in aging including changes in body adiposity, increase in visceral fat, alterations in biology of fat including increased adipose tissue inflammation, age associated increase in circulating cytokines, decrease in activity, sedentary life style and changes in the GH-IGF axis. Indeed, caloric restriction has been shown to decrease body weight, visceral fat, thereby improving insulin resistance as well as improve NAFLD.

Apart from the mechanism explained above, there are other processes that are important for the pathogenesis of NAFLD progression related to aging such as adipose tissue dysfunction (Duval et al., 2010), impaired autophagy (González-Rodríguez et al., 2014) and oxidative stress (Kumar et al., 2013).

Regarding the role of **senescent cells** in NAFLD progression, a significant fraction of hepatocytes develops a senescent phenotype during the life course (C. Wang et al., 2009). Several studies have shown that cellular senescence drives age-dependent hepatic steatosis and that elimination of senescent cells may be a novel therapeutic strategy to reduce steatosis (Ogrodnik et al., 2017). Interestingly, senescent cells have been found in the livers of NAFLD, cirrhotic patients and in the liver of high fat diet (HFD) fed mice (A. D. Aravinthan & Alexander, 2016; Ogrodnik et al., 2017).

There is a relationship between NAFLD and the typical clinical features associated with aging, but this relationship is not well defined yet. For example, sarcopenia and NAFLD share a number of pathophysiological mechanisms, such as insulin resistance, decreased vitamin D concentrations and chronic low-grade inflammation. Several studies have shown an increased risk of NAFLD among patients with sarcopenia (Bertolotti et al., 2014; Tovo, Fernandes, Buss, & de Mattos, 2017). The association between fat accumulation in the liver and in the muscle has recently been established. The fat content in the paravertebral muscles may be correlated with aging and steatosis, and a reduction in muscle fat may be associated with a decrease of the liver fat content. Interestingly, insulin resistance and MS has been consistently associated with sarcopenia and NAFLD. However, the association between sarcopenia and NAFLD seems to be independent of IR, raising the possibility that the loss of muscle mass may contribute to the development of NAFLD. Other feature related to aging is dementia; NAFLD has recently been postulated to be an additional risk factor for dementia (Yilmaz & Ozdogan, 2009).

In general, there is a marked increase in mortality due to liver disease in elderly subjects in comparison to younger populations. It has been reported a 3–5-fold increases in deaths due to liver diseases in the over 65 population against those under 45 years of age (Regev & Schiff, 2001).

3. Osteopontin

3.1 Molecule and characteristics

Osteopontin (OPN) is a multifunctional protein that is expressed in different cellular types and in a variety of tissues: brain, liver, gastrointestinal tract, lung, bone, cardiac tissues, joints, and kidney; and it also appears in a variety of biologic fluids: milk, urine, blood... This protein is involved in many physiological and pathological processes. OPN is classified as a cytokine involved in bone mineralization, in kidney, cell survival, inflammation and tumoral processes. Several studies have identified that OPN expression is increased in tumorogenesis, angiogenesis and in response to inflammation, cellular stress and injury (Urtasun et al., 2012). OPN induces the expression of a wide variety of proinflammatory cytokines, such as IL-12, IL-6 and inhibits IL-10 and IL-27 (Castello et al., 2017). In addition, it plays an important role in different pathologies as arthrosclerosis and hepatic inflammation (Kiefer et al., 2011a). In addition, OPN has a role in metabolic disorders such as diabetes and obesity. OPN was primarily described as a secreted protein, but it has also been found intracellularly, thus OPN is a soluble cytokine and a matrix-bound protein that can stay intracellular or be secreted; and therefore allowing autocrine or paracrine signaling.

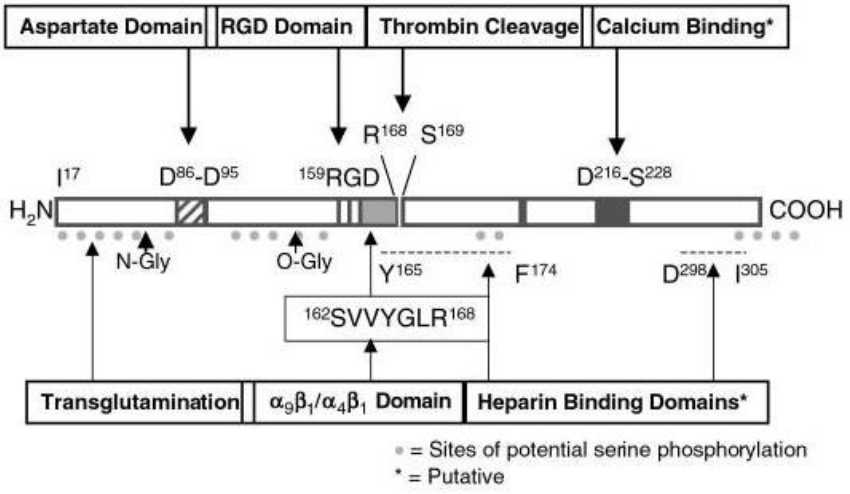

Figure B.14 Structural features of osteopontin molecule. Domains of the osteopontin molecule are represented: aspartate domain, arginine-glycine-aspartate domain (RGD), Ser-Val-Val-Tyr-Gly-Leu-Arg (SVVYGLR) domain, thrombin cleavage domain, calcium binding domain and heparin binding domain. Numbering of the amino acids is based on the human protein (Dendhart DT et al 2001).

OPN is encoded by the gene SPP1 in human, (Spp1 in mice). In humans this gene is localized in the long arm of chromosome 4, its localization is 4q13. Its gene (SPP1) contains 7 exons. The protein is composed of approximately 300 aminoacids with a molecular mass ranging 40-80 kDa due to the

alternative splicing and the variety of post transcriptional modifications. To date three splice variants have been identified: OPNa, the full-length isoform, OPNb that lacks exon 5, and OPNc that lacks exon 4. OPN has an arginine-glycine-aspartic acid (RGD) cell binding sequence, a calcium binding site and two heparin binding domains. Extracellular OPN functions through its interaction with multiple cell surface receptors. Cells may bind OPN via multiple integrin receptors including the vitronectin receptor (αvβ3) as well as various β1 and β5 integrins. Integrin binding may be RGD-dependent or -independent. OPN does not bind the standard form of CD44 but does bind various isoforms of CD44: CD44v3, CD44v6 and CD44v7. These CD44 isoforms bind OPN via multiple sites. OPN may be cleaved by thrombin, resulting in the exposure of additional binding sites, like the integrin binding motif (SVVYGLR), as well as the production of functional chemotactic fragments (Mazzali et al., 2002). A variety of phosphorylation, glycosylation and sulphation can generate different functional forms of OPN that have tissue specific and function specific versatility (Fig B.14).

OPN binding to various integrins and isoforms of CD44 lead to activation of several pathways. OPN-associated signaling pathways include PI3K/AKT (Rangaswami, Bulbule, & Kundu, 2006; Urtasun et al., 2012; Wei, Wong, & Kwok, 2017), mTOR (Ahmed & Kundu, 2010), as well as IKK-NF-κB (Castello et al., 2017; Wei et al., 2017), caspases and Bcl-2, p38/MAPK (Gimba, Brum, & Nestal De Moraes, 2019).

3.2 Ostepontin in metabolism and disease

OPN is a key regulator of many metabolic and inflammatory diseases, like diabetes, cardiovascular disease and obesity. OPN was initially identified in osteoblasts as a mineralization-modulatory matrix protein. It is well stablished that OPN has a role in bone metabolism, morphogenesis and remodeling (Morinobu et al., 2003; Standal, Borset, & Sundan, 2004; Uemura et al., 2001). Experimental evidence shows a complex cytokine and hormonal crosstalk between bone, liver and adipose tissue. Linked to this OPN may play a pivotal role in obesity-associated insulin resistance, NAFLD, and osteoporosis. (Musso, Paschetta, Gambino, Cassader, & Molinaro, 2013). Metabolically active tissue such as adipose tissue shows an increase in OPN expression under obesity (Kahles, Findeisen, & Bruemmer, 2014; Tardelli et al., 2016).

Regarding lipid metabolism, previous studies have shown that OPN plays a role in cholesterol metabolism (Ding et al., 2018; Nunez-Garcia et al., 2017). In liver, OPN regulates the fate of acetyl-CoA, towards cholesterogenesis, and liver PC concentration is regulated by circulating OPN. In fact, high levels of OPN increase liver PC concentration, while PC concentration is low in OPN-KO mice (Nunez-Garcia et al., 2017). In addition, during regeneration after partial hepatectomy (PH), circulating OPN increases the first 24 hours (h) after PH. OPN-KO mice subjected to PH undergo a lipidomic remodeling to cope with the high metabolic demands of regeneration, being thus, involved in the lipid metabolic remodeling after PH (Nuñez-Garcia et al., 2018).

Although non-manipulated OPN knockout (OPN-KO) mice exhibit a normal phenotype, they exhibit markedly abnormal responses to a variety of injurious stimuli (Mazzali et al., 2002), showing that OPN plays important biological roles *in vivo*.

3.2.1 Metabolic syndrome

OPN has shown to be involved in a variety of conditions associated with MS. Obesity constitutes the major risk factor for the development of insulin resistance, type 2 diabetes and the subsequent diabetes-related complications like cardiovascular disease. Chronic low-grade inflammation has been described as a fundamental component of adipose tissue expansion in obesity. Some studies showed that OPN expression in adipose tissue as well as circulating OPN levels are substantially elevated in obese patients compared with lean subjects, and were even more increased in obese diabetic or insulin resistant patients (Gómez-Ambrosi et al., 2007). Therefore, OPN could also be involved in the pathogenesis of type 2 diabetes. Other studies have also described OPN as a critical regulator of adipose tissue inflammation and in insulin resistance. OPN expression in macrophages is upregulated by a variety of proinflammatory mediators known to be elevated in type 2 diabetes and cardiovascular disease (Kahles et al., 2014). OPN expression has shown to be greatly upregulated in adipose tissue from diet-induced and genetically obese mice, and lack of OPN in OPN-KO mice or OPN neutralization led to decrease inflammation in adipose tissue and reduced insulin resistance, and also improved whole-body glucose tolerance (Kahles et al., 2014; Kiefer et al., 2011b).

Atherosclerosis and vascular diseases are also related with MS and obesity. OPN is upregulated in several animal models of cardiac failure and plays a promoting effect in atherosclerosis (Matsui et al., 2003; Rosenberg et al., 2008).

3.2.2 Non-alcoholic fatty liver disease (NAFLD)

OPN has been associated with different liver diseases (Nagoshi, 2014; Ramaiah & Rittling, 2007). Increased OPN expression has been found in hepatocytes and inflammatory cells in liver disease (Fig. B.15). Remarkably, OPN is markedly upregulated in the liver in obesity, and hepatic OPN levels correlate with liver TG levels (Bertola et al., 2009; Sahai, Malladi, Melin-Aldana, Green, & Whitington, 2004).

Regarding the progression of the disease, several studies in mice models and in humans demonstrate the role of OPN in the pathogenesis and progression of NAFLD and in liver fibrosis (Coombes et al., 2015; Glass et al., 2018; Syn et al., 2011). Elevated mRNA levels of SPP1 (osteopontin) are associated with increasing NASH and inflammation (Ryaboshapkina & Hammar, 2017).

Regarding fibrosis, liver OPN expression correlates with fibrosis stage (Glass et al., 2018). In

animal models, hepatic OPN expression is significantly increased in models of bile duct ligation (BDL) and carbon tetrachloride (CCl_4) (Español–Suñer et al., 2012; Lorena et al., 2006). However, the role of OPN in fibrosis is controversial. While some studies show that OPN might have a protective role, (I.e. the increase in OPN expression observed during fibrogenesis may play a protective role (Lorena et al., 2006)), others show that OPN drives the fibrogenic response and the ductular reaction (DR) contributing to scarring and liver fibrosis via TGF-β (X. Wang et al., 2014). In general, the fibrogenic role of OPN in liver diseases has been confirmed via significant research over the years. However, targeting OPN for resolution of fibrosis still remains controversial due to its opposing effects on different pathological conditions (Wen, Jeong, Xia, & Kong, 2016).

Interestingly, an OPN supplement has been released as a nutritional complement approved by the FDA in newborns and infants. In a study that analyzed liver effects of this supplement, milk osteopontin supplement diminished ethanol-mediated liver injury in OPN-KO mice. According to the authors of this study, milk OPN could be a simple effective nutritional therapeutic strategy to prevent alcohol hepatotoxicity due, among others, to gut protective, anti-inflammatory, and anti-steatotic actions (Ge, Lu, Leung, Sørensen, & Nieto, 2013; Ge et al., 2014).

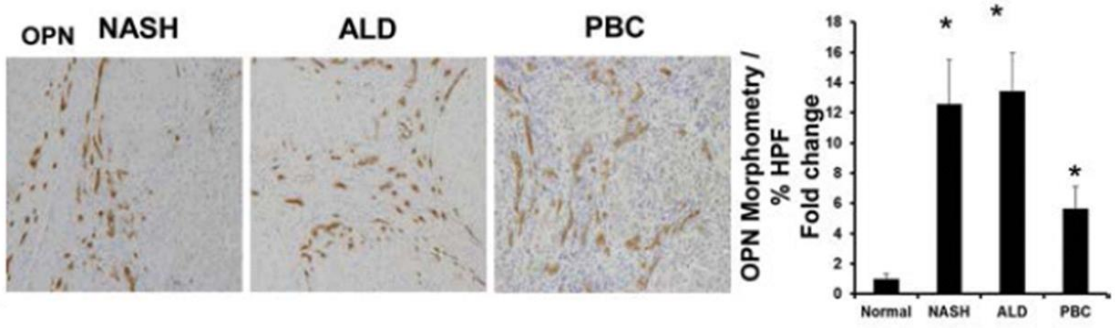

Figure B.15 Osteopontin expression is upregulated in many chronic liver diseases. Liver sections from patients with non-alcoholic hepatitis (NASH), alcoholic liver disease (ALD) and primary biliary cirrhosis stained for OPN (Coombes et al., 2015).

3.2.3 Cancer

Several studies have demonstrated the correlation between elevated OPN secretion and various malignancies, such as breast and prostate cancer, squamous cell carcinoma, melanoma, osteosarcoma and gliobastoma (Rangaswami et al., 2006). The role of OPN signaling pathways in cancer progression and metastasis is becoming increasingly recognized (Bellahcène, Castronovo, Ogbureke, Fisher, & Fedarko, 2008)(Weber, 2001).

Among these malignancies OPN has also been linked to liver cancer. In fact, in hepatocellular carcinoma (HCC), OPN has been often regarded as a biomarker. It is markedly elevated in the plasma of HCC patients, and has been identified as a diagnostic biomarker, being a good early biomarker (Cabiati et al., 2017; Shang et al., 2012; Tsuchiya et al., 2015). In addition, OPN could promote HCC metastasis (Dong et al., 2016). Even more, OPN was upregulated in cholangiocarcinoma (CCA) tumor cells and the tumor stroma, and serum levels of OPN are elevated in patients with CCA (Loosen et al., 2017).

In tumors, OPN is involved in many processes. OPN regulates tumorigenesis, tumor progression and metastasis formation (Zhao et al., 2018a) by activating cell migration, inhibiting apoptosis (Huang et al., 2017), stimulating angiogenesis (Wu et al., 2014), controlling energy metabolism (Z. Shi, Wang, Chihanga, Kennedy, & Weber, 2014) and modulating the tumor microenvironment (Malaponte et al., 2016) and the immune system (Caputo & Bellone, 2018). Notably, OPN also promotes cell survival by negatively regulating apoptosis in response to stress conditions (Štemberger et al., 2014; H. Zhang et al., 2014).

Cancer metastasis is a complex process that generally involves the detachment of cancer cells from the primary tumor, intravasation, the circulation of cancer cells, adhesion to the blood vessel wall, extravasation and the growth of the secondary tumor. Although the role of OPN regulating all of these processes is not completely understood, a meta-analysis published recently reported that overexpression of OPN is closely associated with the metastasis of colorectal cancers, lung cancers and melanomas (Weber, Lett, & Haubein, 2011; Zhao et al., 2018b). The epithelial-mesenchymal transition (EMT) has a major role in metastasis. It results in reduced epithelial cell intercellular adhesion and causes these cells to acquire fibroblastoid properties, thereby improving the ability of cells to migrate. Therefore, the EMT is important for the development, invasion and metastasis potential of cancer. Osteopontin acts as a regulator of the EM by regulating the EMT-related transcription factors (Jia et al., 2016; Kothari et al., 2016).

The role of OPN in chemoresistance is currently being investigated, with evidence suggesting that OPN is involved in mechanisms inducing chemoresistance (Gimba et al., 2019; Liu et al., 2016; Olive et al., 2018). The mechanisms by which OPN induces chemoresistance are increased autophagy (Liu et al., 2016) and anti-apoptotic effects of OPN on cancer cells (Yang et al., 2012).

3.3 Ostepontin and aging

OPN plays a role in many diseases in which aging is the primary risk factor such as MS, diabetes, cardiovascular disease, liver disease and osteoporosis, among others. Previous work have described

OPN as a SASP factor (Flanagan et al., 2017; Pazolli et al., 2009). In addition, there are several studies linking OPN and aging. However, the available data does not give conclusive results about the role of OPN in the aging process. Nevertheless, its effect seems to be tissue or cell-type dependent.

In hematopoietic stem cells, OPN is important to maintain the cell function and attenuates aging-associated phenotypes (Guidi et al., 2017; Li et al., 2018). In muscle, its neutralization improves muscle regeneration in old mice (Paliwal, Pishesha, Wijaya, & Conboy, 2012). In cardiac tissue, its deficiency protected against age-related cardiac fibrosis, but intriguingly a strong senescence induction was found in OPN-KO cardiac fibroblasts (Sawaki et al., 2018). Other studies remark that a decreased expression of OPN in old age worsens the response/ remodeling post myocardial infarction (Singh, Foster, Dalal, & Singh, 2010). In the liver, OPN deficiency contributes to enhance the severity of alcoholic liver disease in old mice (Magdaleno et al., 2018). In the retina, its deficiency is beneficial (Ruzafa, Pereiro, Aspichueta, Araiz, & Vecino, 2018).

C. OBJECTIVES

OBJECTIVES

The aging of the population is expected to have a severe socio-economic impact especially in the developing countries, which account for over 60% of the older population (World Health Organization, 2015). Aging is a complex multifunctional process (López-Otín, Blasco, Partridge, Serrano, & Kroemer, 2013). Because the health dynamics of older age are related to increased needs for health care, there will be an increased health-care utilization (World Health Organization, 2015). Therefore, it is essential to have a better understanding of the mechanisms of the progression of organ dysfunction with aging, to be able to find markers, targets and treatments to help to reduce or avoid the severity of diseases associated with age and improve as much as possible the health span and quality of life of the elderly. Indeed, with aging increases the prevalence of multiple diseases, among them diseases in which metabolic dysregulation is key, like metabolic syndrome (MS) and non-alcoholic fatty liver disease (NAFLD). In the last decades, there has been a rise in the prevalence of NAFLD, paralleling a worldwide increase in diabetes and metabolic syndrome (Friedman, Neuschwander-Tetri, Rinella, & Sanyal, 2018). These diseases can boost the development of hepatocellular carcinoma (HCC) and cardiovascular diseases. As liver ages, it undergoes several changes that can reduce hepatic function and promote liver injury, and aging liver loses its ability to respond to stressors (Sheedfar, Biase, Koonen, & Vinciguerra, 2013). In addition, with aging, the characteristic ability of the liver to regenerate is reduced (Schmucker & Sanchez, 2011). The prevalence of liver disease increases with age. Linked to this, hepatocyte senescence correlates with severity of NAFLD (Ogrodnik et al., 2017). Indeed, the accumulation of senescent hepatocytes can affect the liver function making the liver more prone to disease progression (Aravinthan et al., 2013).

Osteopontin (OPN) is a multifunctional glycoprotein that is expressed in many cell types, and it is involved in many physiologic and pathological processes. It is involved in the NAFLD pathogenesis (Kiefer et al., 2011), and its liver expression is increased in obesity and correlates with steatosis and insulin resistance, fibrosis and HCC (Gómez-Ambrosi et al., 2007; Syn et al., 2012; Zhao et al., 2018).

Previous work in our laboratory have shown that OPN plays a key role modulating liver metabolism. OPN modulates the fate of acetyl CoA in liver and regulates the cross-talk between phosphatidylcholine (PC) and cholesterol metabolism (Nuñez-Garcia et al., 2017). OPN also modulates some nuclear factors related to biliary metabolism, which are altered in NAFLD progression. CYP7A1 is the enzyme that catalyzes the rate-limiting step and the major regulator of bile acid synthesis, which is the primary mechanism for the removal of cholesterol from the body. Thus, CYP7A1 could be involved in the observed metabolic modulation. Hence, we **propose** that OPN might regulate the cross-talk between cholesterol and PC metabolism via CYP7A1 in hepatocytes. Thus, the altered conversion of FC into bile acids will also induce changes in biliary PC secretion.

In regeneration, deficiency in OPN leads to a remodeling in lipid metabolism allowing the correct regeneration after partial hepatectomy (PH) (Nuñez-Garcia et al., 2018). The liver has the capacity for regeneration after cellular damage or surgery resection. During regeneration, liver cells need to acquire sufficient energy and metabolic precursors. PC, cholesterol and bile acids play an important role in liver regeneration. Since OPN can modulate these lipids, we **suggest** that OPN might have an important role orchestrating lipid metabolism in liver regeneration.

Previous studies have described OPN as a senescent associated secretory phenotype (SASP) factor (Flanagan et al., 2017; Pazolli et al., 2009). In addition, there are several studies linking OPN and aging, but the available data does not give conclusive results about the role of OPN in the aging process. Thus, based on the evidence that OPN is linked with liver disorders and that plays a role in liver lipid metabolism; which is dysregulated in aging, we **propose** that OPN could have a role in the susceptibility of the liver to aging-associated NAFLD progression.

In this background our specific aims were:

Aim 1. To investigate whether OPN regulates PC and cholesterol metabolism via CYP7A1 in hepatocytes, and, if so, to analyze the pathways involved.

Aim 2. To elucidate which metabolic pathways are involved in OPN-KO mice liver lipid remodeling during regeneration after PH.

Aim 3. To investigate the role of OPN in the metabolic disorders of aging:

Aim 3.1 To investigate whether OPN is involved in the aging of the liver, and in that case, to identify the mechanisms involved.

Aim 3.2 To find out whether during aging OPN modifies the vulnerability of the liver to the development of NAFLD; and if so, to identify the mechanisms involved.

Aim 3.3 To define if OPN is involved in the generation of metabolic syndrome during aging.

D. METHODS

1. Materials

1.1 Media and buffers

Media:

-Krebs-Henseleit (KH) perfusion medium. NaCl 118 mM; $NaHCO_3$ 25 mM; KCl 4.7 mM; $MgSO_4$ 1.2 mM; glucose 20 mM; 4-(2-hydroxyethyl)-1- piperazineethanesulfonic acid (Hepes) 6.5 mM.

-Medium for hepatocyte adhesion. Dulbecco's Modified Eagle Medium (DMEM) 1% (w/v); $NaHCO_3$ 0.2% (w/v) ; glucose 10 mM; fatty acid (FA) free Bovine serum albumin (BSA) 0.2% (w/v) supplemented with insulin 84 nM, penicillin 10 U/ml, L-glutamine 2 mM; gentamycin 50 µg/ml and fetal bovine serum (FBS) 2% (v/v); pH 7.2.

- Hepatocyte incubation medium. DMEM 1% (w/v); $NaHCO_3$ 0.2% (w/v); glucose 10 mM; 0.2% (w/v) FA free BSA supplemented with insulin 84 nM, penicillin 10 U/ml and L-glutamine 2 mM; gentamycin 50 µg/ml; pH 7.2.

- HepG2 and Hep3B medium: Eagle's Minimum Essential Medium (EMEM) supplemented with fetal bovine serum 10% (v/v), Penicillin-Streptomycin 1%, Glutamine and Amphotericin B 1%

Buffers:

- **Sample desnaturalization buffer (5x) for SDS-PAGE.** Tris-HCl 300 mM , pH 6.8; glycerol 65% (v/v) ; SDS 10% (w/v); 72 mM DTT; bromophenol blue 0.5 (w/v).

- **Electrophoresis buffer**. Tris 25 mM; glycine 192 mM, SDS 0.1% (w/v).

- **Homogenization buffer for Western Blot**. Sucrose 250 mM ; tris(hidroximetil)aminometan hydrochloride (Tris-HCl) 10 mM, pH 7.4; NaF 1 mM; sodium orthovanadate 2 mM; EDTA 0.5 mM; β- glycerol phosphate 20 mM; protease inhibitor cocktail “Complete EDTA-Free” 1:25 (tablet/v) from Roche.

- Homogenization buffer for cellular fractionation: Sucrose 250 mM; Na_2EDTA 2 mM; Tris-HCl 10 mM; pH 7.4

- Homogenization buffer for beta-oxidation: Tris-HCl 25 mM, sucrose 500 nM, EDTA-Na_2 1 mM; pH 7.4

- Assay buffer for beta-oxidation: Sucrose 100 mM, Tris HCl 10mM, KH_2PO_4 5 mM, EDTA, 0.2 mM pH8.0 , KCl 80 Mm, $MgCl_2$ 1mM, L-Carnitine 2mM, Malate 0.1 mM, coenzyme A 0.05 mM, ATP 2 mM, DTT 1mM, fatty acid (FA) free BSA:palmitate solution 0.7% BSA/500 µM palmitate

- **Loading buffer (6x) for nucleic acid electrophoresis**. Sucrose 40% (w/v); bromophenol blue 0.25% (w/v); xylene cyanol 0.25% (w/v).

- **Transfer buffer for western blotting:** Tris-HCl 25 mM (pH 7.6), glycine 192 mM, methanol 20%.

- **Physiologic sodium chloride solution:** NaCl 0.9% (w/v).

- **Phosphate buffered saline (PBS):** Sodium phosphate buffer 10 mM, pH 7.4; NaCl 150 mM.

- Tris-buffered saline supplemented with Tween 20 0.1% (TBS-T): Tris 20 mM; NaCl 150 mM; Tween20 0.1%.

-TAE buffer: Acetic acid 0.4% (v/v); EDTA 10 mM; Tris 40 mM; pH 8.5.

- Washing buffer for subcellular fractionation: Tris-HCl 150 mM, pH 8.0; Na_2EDTA 2 mM.

- **Stripping buffer**: Tris-HCl 62.7mM, pH 6.7, SDS 2%, mercaptoethanol 100mM.

-**Buffers for enzymatic activities:**

- Acid Triglyceride hydrolase (TGH) and cholesteryl ester hydrolase (CEH) assay buffer: Acetic acid/acetate 0.1 M, pH 4.6; supplemented with 2-hydroxypropyl-β-cyclodextrin (HPBCD) 2.25% (w/v) and BSA 0.05% (w/v) .

- Extraction salts: Na_3BO_3/Na_2CO_3 50 mM.

- Neutral TGH and CEH assay buffer: Tris-HCl 0.1 M, pH 8; 2- hydroxypropyl-β-cyclodextrin (HPBCD) 2.25% (w/v).

- Diglyceride acyltransferase (DGAT) assay buffer: Tris- HCl 20 mM, pH 7.4; NaCl 150 mM, $MgCl_2$ 4 mM, NaF 20 mM, DTT 1 mM and CHAPS 0.1%.

- Acyl-CoA cholesteryl acyltransferase (ACAT) assay buffer: KH_2PO_4 0.1 M pH 7.4 cholesterol 6.25 µM in cyclodextrin 45% (w/v), BSA FA free 80 µM and GSH 2mM.

- Phosphatidylethanolamine N-methyltransferase (PEMT assay buffer): Tris-HCl 3.75 mM, pH 9.2; DTT 150 µM; 12 µl of previously prepared (3.7 mg/ml) 1,2-dioleoyl-sn-glycero-3-phosphoethanolamine-N-methyl (PMME) substrate/ ethylenediaminetetraacetic acid (EDTA) buffer; Triton X-100 0.00186 % (v/v).

- Stop solution for TGH and CEH activities: chloroform:methanol:n-heptane:oleic acid 125:140:100:0.01 (v/v/v/v).

- Buffers for histochemical staining:

- Peroxide blocking: H_2O_2 3% in PBS 1X.

- Sirius red solution: Fast Green 0.01% FCF/Sirius red 0.1% in picric acid (Sigma)

- SA-β Galactosidase staining solution: citric acid 40 mM in $Na_2HPO_4 \cdot 7H_2O$ 0.2 M pH 6.0; $C_6N_6FeK_3$ and $K_4Fe(CN)_6$ 5 mM, $MgCl_2$ 2 mM, NaCl 150 mM and X-Gal 1mg/mL.

- Fixing solution: Neutral buffered formalin (NBF) 10%.

- Fixing solution for SA-β Galactosidase: NBF 4% /Glutaraldehyde solution 0.5 %.

1.2 Equipment

Blood strips	Arkay Factory, Inc., Shiga, Japan
Centrifuges	**P selecta, Sorvall** RC6 Plus (SM-24 rotor) and RT 7 (rotor RTH-750)
Chamber for electrotransference	**Bio-Rad** Trans-Blot SD
Class II Biological Safety Cabinets	**Thermo Scientific** MSC-Advantage
Concentrator-evaporator	**Thermo Scientific** Savant SC250EXP
Densitometer	**Bio-Rad** GS-800 and Molecular Imager FX
Electrophoresis Power Supply	**Bio-Rad** Power 1000
Equipment for anesthesia	**Cibertec, S.A CA**-EAC20, CA-CIS4 and CA-MRS4m
Exposure cassette	**FUJI** EC-AWU (18 x 24 cm^2)
Hemocytometer	**Neubauer** depth of 0.100 mm and area of 0.0025 mm^2
Heater	**P Selecta** Theroven (200 °C)
Homogenizers	**Kinematica** Polytron PT 1200 C and **B.Braun Biotech International** Potter S
Horizontal electrophoresis	**Bio-Rad** Sub-Cell GT agarose Gel Electrophoresis System
Incubators of CO_2	**Jouan EG** 120 and **Thermo Scientific** HeraCell 150
Microcentrifuges	**Heraeus** Biofuge primoR, Biofuge Fresco and **Labnet** Spectrafuge™
Optic microscope	**Nikon** Eclipse 50i and **Jenoptik** ProgRes® CapturePro camera
pHmeter	**Crison** GLP 21
Scintillation counter	**LKB** Wallac 1214 Rackbeta/ **Tri-Carb**® 2810 TR

Spectophotometers	**Perkin Elmer** 550 SE, **Nanodrop** ND-1000 Spectophotometer, **Spectronic** 20 Genesys and a plate reader **Biotek** Synergy™ HT
Sterilization	Equipment of the sterilization service from de Department of Cellular Biology and Histology form the UPV/EHU
Thermocycler	**Biometra** T-Gradient Thermoblock
Thermostatic bath with shaker	**P-Selecta** Unitronic 320 OR
Tube shakers	**Velp Scientifica** 2x3
Ultracentrifuge	**Beckman Coulter** Optima™ L-100 XP
Ultracentrifuge rotors	**Beckman Coulter** 20.4 Ti
Vertical electrophoresis	**Bio-Rad** Mini Protean III
Weighing scales	**Mettler** PJ400 and **Mettler** AT231 Delta rang
Sonicator	**Soniprep 150**

2. Models of study

2.1 Human samples

This study included 157 patients; 42 were non-obese and 115 were obese. Individuals were considered non-obese when presenting a BMI lower than 30 kg/m^2 and obese when the BMI was higher than 30 kg/m^2. Inclusion criteria for patients with non-alcoholic fatty liver disease (NAFLD) was based on the absence of alcohol intake and the presence of biopsy-proven steatosis without necroinflammation and fibrosis along with negative serum tests for hepatitis B virus (HBV), hepatitis C virus (HCV) and human immunodeficiency virus (HIV). For obese patients subjected to bariatric surgery the liver biopsy was taken during this surgery. For the normal liver (NL) patients with asymptomatic cholelithiasis, the liver biopsy was taken during programmed laparoscopic cholecystectomy. All had no evidence of HBV, HCV and HIV infections. In addition, none of these individuals consumed >20 g alcohol per day. Neither NAFLD patients nor subjects with NL used potentially hepatotoxic drugs. According to Kleiner criteria, (Kleiner et al., 2005) from the obese group, 110 individuals had a clinical diagnosis of NAFLD and 5 were obese control individuals with NL. From the non-obese group 13 individuals had a clinical diagnosis of NAFLD and 29 control individuals had NL. Steatosis was assessed, as outlined by Kleiner *et al*. (Kleiner et al., 2005), grading the percentage of hepatocytes containing lipid droplets in each liver biopsy as follows: grade 0 when <5% of steatotic hepatocytes; grade 1 when 5-33% of steatotic hepatocytes; grade 2 when >33-66% of steatotic hepatocytes; and grade 3 when >66% of steatotic hepatocytes.

Human samples from non-obese patients were provided by Carmelo García-Monzón from the Liver Research Unit of the University Hospital Santa Cristina, Instituto de Investigación Sanitaria Princesa, Madrid, Spain. The NAFLD and NL obese individuals where patients subjected to a bariatric surgery. These samples were obtained in the Hospital Universitario Cruces, Barakaldo, Spain.

The study was performed in agreement with the Declaration of Helsinki and with local and national laws. The Human Ethics Committee of the University Hospital Santa Cristina and the Ethical committee of clinical research of the Basque Country approved the study procedures. Written informed consent was obtained from all patients before inclusion in the study.

2.2.1 Clinical and laboratory assessment in human samples

After a 12 h overnight fast, clinical and anthropometric data as well as venous blood samples were obtained from each patient at the time of liver biopsy. Plasma insulin was determined by a chemiluminescent microparticle immunoassay (ARCHITECT insulin; Abbot Park, Illinois, USA). Insulin resistance was calculated by the homeostasis model assessment (HOMA-IR).

2.2 Animals and treatments

For the study of the effect of osteopontin (OPN) in the modulation of liver lipid metabolism and regeneration, 10-12-week-old female OPN deficient (OPN-KO) mice (B6.Cg-Spp1tm1Blh/J) and their WT (C57BL/6) littermates were provided by Jackson´s Laboratories. They were maintained on a rodent chow diet (Teklad Global 18% Protein Rodent Diet 2018S; Harlan Laboratories INC., USA) and water ad libitum. For the study of the effect of OPN in the liver lipid metabolism and NAFLD development during aging, 3, 10 and 20 month-old WT and OPN-KO female mice were used. They were maintained on a rodent chow diet (Teklad Global 18% Protein Rodent Diet 2018S; Harlan Laboratories INC., USA) or a rodent high fat diet (Bioserv S3282, 60% Fat) and water ad libitum. For the aging studies, 10-12 week-old male and female WT mice were provided by Jackson's Laboratories, and sacrificed at 3, 6, 10, 14 and 20 months old. Mice were maintained on a rodent chow diet (Teklad Global 18% Protein Rodent Diet 2018S; Harlan Laboratories INC., USA) and water ad libitum.

Mice were housed in a temperature-controlled room with a 12 hour (h) - light/dark cycle. Animal procedures were approved by the Ethics Committee for Animal Welfare of the Basque Country, and were conducted in conformity with the EU Directives for animal experimentation.

2.2.1 Partial hepatectomy

Mice were subjected to 2/3 partial hepatectomy (2/3 PH), taking as a reference the methodogy used by Mitchell C., et al. (Mitchell & Willenbring, 2008) but with some modifications (Nuñez-Garcia et al., 2018). The surgery was performed under general anesthesia with inhaled isoflurane and they were maintained with O_2 inhalation until their recuperation.

First, the mouse was anesthetized placing into a Plexiglas chamber for induction of anesthesia with isofluorane 4% and 0.5-1 l/minute oxygen flow for 2 minutes. After anesthetization, the animal was transferred to the place where the surgery was going to be performed and the anesthesia was maintained by 1.5% of isoflurane inhalation through a suitable mouthpiece. In the midline abdominal skin and muscle an incision was made to expose the xiphoid process. The hepatectomized lobes were the left lateral and the median. They were carefully pulled out from the abdominal cavity. A 4-0 silk thread was placed on the base of the left lateral lobe, a suture was made around the lobe and it was cut above the suture. The thread was again placed for the median lobe but in this case the lobe was tied separately performing two knots (Fig D.1). They were cut leaving an ischemic stump above the knots and without taking out the gallbladder. The peritoneum and the skin were closed. Finally, after the surgery animals were sacrificed at 24 and 48 h after hepatectomy.

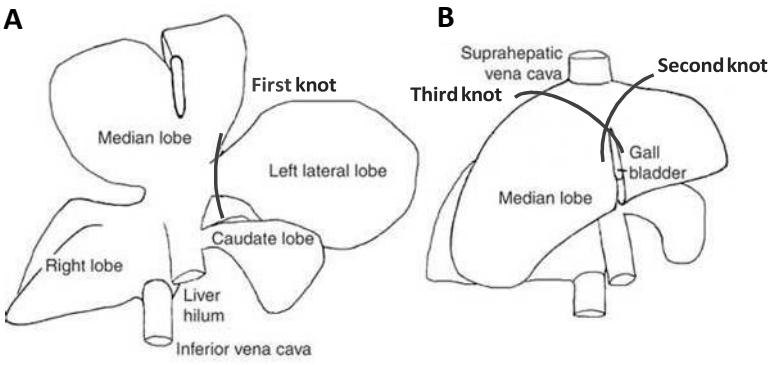

Figure D.1 Schematic drawings of mouse liver anatomy. (A) The thread for the first knot was positioned between the caudate and the left lateral lobes at the base of the latter. (B) The second and third knots were tied separating the median lobe, above the gallbladder.

2.2.2 High Fat diet treatment

Part of the animals were fed a rodent high fat diet (HFD) with 60% calories from fat (Bioserv S3282). In the case of the aging model, part of the 16 month-old OPN-KO mice (B6.Cg-Spp1tm1Blh/J) and their WT (C57BL/6) were fed a HFD ad libitum for 16 weeks prior to the sacrifice at 20 months-old.

2.2.3 Recombinant osteopontin (rOPN) treatment

Recombinant OPN (rOPN) (15 µg/mouse; R&D systems, UK) or vehicle alone (physiologic saline solution) was injected to WT mice via the tail vein in two alternate days. 24 h after the last injection the mice were sacrificed.

2.2.4 Atorvastatin treatment

For atorvastatin treatment, intragastric atorvastatin (100 mg/kg) was provided for 2 weeks in alternate days. 24 h after the last dose the mice were subjected to 70% PH and were sacrificed at different times (24 h and 48 h).

2.2.5 Tissue extraction

The liver and white adipose tissue from each mouse were collected and washed in NaCl 0.9%. The liver was weighed and immediately cut into pieces to be formaldehyde-fixed or OCT embedded for subsequent histological analysis, or to be frozen in liquid nitrogen and kept it at − 80 °C.

2.2.6 Serum collection

The blood was taken from the inferior vena cava or the submandibular vein and it was left for 30 minutes at room temperature (RT) to coagulate. To obtain the serum, blood was centrifuged at 2,000 xg for 30 minutes at 4 °C and the supernatant was centrifuged again at 10,000 xg for 10 minutes at 4 °C. After that, the serum was collected, aliquoted and frozen at – 20 °C for subsequent analysis.

2.2.7 Primary hepatocyte isolation and incubation

Hepatocytes from 3 and 10 month-old OPN-KO and WT mice were isolated. For this, perfusion with collagenase type I was used as described previously (Smedsrød & Pertoft, 1985). In brief, animals were anesthetized with sodium pentotal (150 mg/kg of body weight) intraperitoneal injection, the abdomen was opened and a catheter was inserted into the inferior vena cava while the portal vein was cut. Next, liver was washed by perfusion with Krebs-Henseleit (KH) perfusion medium equilibrated with fizzed carbogen at 37 °C. After the washing, EGTA 0.05% (w/v) from Sigma-Aldrich (USA) was added to the KH medium and the perfusion was maintained for 5 minutes. Finally, an enzymatic digestion was performed perfusing during 10-12 minutes with KH perfusion medium supplemented with $Ca^{2+,}$ 300 µg/ml collagenase from Sigma-Aldrich (USA) and 60 µg/ml tripsin inhibitor from Roche (Switzerland).

After perfusion, the liver was gently disgregated. The viable cells were purified by density centrifugation and selective adherence as described before. Isolated pure hepatocytes were seeded over collagen and fibronectin-coated culture dishes (60 mm of diameter) at a density of 1.5×10^6 cells per dish in the medium for cell adhesion. Cells were placed at 37 °C in a humidified atmosphere of 5% CO_2 -95% air.

After 2 h of attachment, the cell adhesion media was removed and replaced with the cell incubation medium supplemented with the treatments. Cultured pure hepatocytes from OPN-KO were treated with rOPN (1 µg/ml; R&D systems) for 3 h. For metabolic flux studies, pure hepatocytes were also incubated with [^{3}H]acetate for 4 h (section 3.5.1), or [^{3}H]oleate (section 3.5.2). For inhibition of the FAK-AKT pathway, hepatocytes were pre-incubated for 1 h with FAK inhibitor Y15 (30 µM); for inhibition of the PI3K-AKT pathway, downstream FAK, hepatocytes were pre-incubated with LY294002 (50 µM) for 1 h and then, hepatocytes were incubated with or without rOPN (150 nM) in the presence or absence of the inhibitors for another 3 h.

2.2.8 Glucose and insulin tolerance tests

For glucose tolerance test mice were fasted for 4 h, and then were administered a glucose solution (2 g/ kg body weight) by oral gavage. Blood glucose levels were measured before glucose

administration (time 0) and 15, 30, 60 and 120 minutes post-gavage using blood strips. For insulin sensitivity test, mice were injected intraperitoneally 1 U insulin/ kg body weight and glucose levels were measured as described above for glucose tolerance test.

2.3 HepG2 and Hep3B cell lines

Hepg2 and Hep3B cell lines were obtained from the American Type Culture Collection (ATCC). Cells were maintained in EMEM supplemented with fetal bovine serum 10% (v/v), Penicillin-Streptomycin 1%, Glutamine and Amphotericin B 1%. Cells were kept at 37 °C within a 95% humidified atmosphere containing 5% carbon dioxide in an incubator. Depending on the experiment, cells were plated in 60 mm culture dishes, 6 well plates or in 24 well culture plates.

2.3.1 siRNA transfection

For knocking down experiments, a commercial siRNA was used against osteopontin (gene SPP1) or p53 (gene TP53)(Ambion CA, USA). Negative controls were included in each assay by using SilencerTM Select Negative Control siRNA (Ambion CA, USA). Lyophilized siRNAs were resuspended in nuclease-free sterile water (Ambion, USA) at 50 mM. These stock solutions were stored at -20 °C. Work solutions were prepared for immediate use at 1 mM.

Reverse transfection was performed using RNAiMAX lipofectamine (Invitrogen Life Technologies, USA) in OptiMEM media. Briefly, Lipofectamine and siRNA were diluted separately in OptiMEM and then dilutions were mixed and incubated for 20 minutes RT. 48 h after transfection, transfection media was removed and fresh treatment media was added. Gene silencing efficiency was confirmed by RNA expression analysis.

2.3.2 Palbociclib and palmitic acid treatment

Senescence inductor palbociclib 2 µM was dissolved in 0.01% DMSO and filtered. 24h after transfection cells were exposed to palbociclib or vehicle, which was added to the regular complete media. Cells were maintained 4 days with palbocilcib treatment and collected for their study.

For the palmitic acid treatment, in order to facilitate the in-vitro incorporation, palmitic acid 200 µM was complexed with fatty acid free BSA 100 µM over-night at 4 °C. Vehicle plates were supplemented with fatty acid free BSA 100 µM. Palmitic treatment was added 24 h before collecting cells. For cell collection, for western blotting or lipid quantification, plates were washed 3 times with cold PBS 1X, and cells were scraped in 1mL PBS 1X and centrifuged at 180 xg.

2.3.3 Hydrogen peroxide treatment

Hydrogen peroxide was used for senescence induction. Cells were exposed to hydrogen peroxide (H_2O_2) 700 µM for 1h, then treatment media was removed and fresh media was added. Cells were kept in culture for 5 days and collected. For cell collection, for western blotting, plates were washed 3 times with cold PBS 1X, and cells were scraped in 1mL PBS 1X and centrifuged at 180 xg.

3. Experimental procedures

3.1 Protein quantification

For the different analysis, protein quantification was made using a commercial kit based in the bicinchoninic acid method, the *Pierce BCA Protein Assay Kit*. The assays were performed in 96 well plates by triplicate. 5 µl of SDS 20% were added to avoid turbidity and 150 µl of the reactives A and B in proportion 50:1 were added per well. The plate was incubated for 30 minutes at 37 °C in the dark and then absorbance was measured at 562 nm in a microplate reader. The protein concentration was calculated by interpolation of the absorbance value in the calibration curve made with BSA that was lineal in a range from 0 to 25 µg of protein.

3.2 Quantification of lipid parameters

Liver pieces were homogenized using a potter glass homogenizer in 5 or 10 volumes of the suitable homogenization buffer for each subsequent assay, by 20 strokes of a Teflon pestle at 700 rev./ min at 4 °C.

3.2.1 Quantification of lipids

To prepare lipid extracts from liver, the tissue was homogenized as previously described using cold PBS 1X and 1-2 mg of protein from liver homogenate. Cells were scraped and resuspended in dH_2O. Lipids were extracted by the Folch method (Folch, Lees & Sloane Stanley, 1957). For this, 1.5 ml of dH_2O and 8 ml of chloroform:methanol:HCl (2:1:0.0075, v/v) solution (Scharlau Chemicals, Spain) were added to the liver homogenate or cell extract, and tubes were vigorously shaken with a vortex for 2 minutes. Tubes were centrifuged at 1,000 xg for 15 minutes at 4 °C to separate the aqueous phase from the organic one. The lower organic phase was transferred to another extraction tube using a glass pasteur pipette. Lipids from the upper phase were reextracted. For the reextraction, 4 ml of chloroform:methanol:HCl (2:1:0.0075, v/v) were added and the tubes were vigorously shaken for 2 minutes and were centrifuged at 1,000 xg for 10 minutes at 4 °C. The organic phase was mixed with the previously obtained one. For the removal of aqueous contaminant, the

chloroform extract was washed with the third part of the total volume of KCl 0.88% solution. Each tube was shaken with a vortex for 1 minute and centrifuged for 10 minutes at 1,000 xg and the lower phase was transferred to another extraction tube. Finally, the chloroform in extract was evaporated in a concentrator- evaporator. Lipids were dissolved in an appropriate volume of toluene and were kept in glass vials at -20 °C in N_2 atmosphere until they were processed.

The lipid separation was performed by thin layer chromatography (TLC). It was done by six chromatographic developments (Ruiz & Ochoa, 1997). First, the silica-gel plates of 20 x 20 cm ("Pre-coated TLC-plates SIL-G25", Macherey-Nagel) were pre-treated with 1 mM EDTA-Na_2 (not less than 4 h). Silica-gel plates were left drying overnight and washed with chroloform:methanol:dH_2O (60:40:10, v/v/v) overnight to remove contaminants. The following day, the plates were activated at 100 °C for 30 minutes; after that, 3 µl of pure lipid mixtures (Avanti Polar Lipids, USA and Sigma-Aldrich) of known lipid concentrations and 3 or 8 µl of the lipid extracts were applied (per duplicate) at 1.5 cm from the lower edge of the plate. Lipid quantities (nmol) for calibration were the following ones: Cholesteryl ester (CE) (0.09-1.45), triglycerides (TG) (0.27-17), diglycerides (DG) (0.15-3), free cholesterol (FC) (0.36-3.6), cardiolipin (CLn) (0.02-0.3), phosphatidylethanolamine (PE) (0.33-3.91), phosphatidylinositol (PI) (0.1-1.72), phosphatidylserine (PS) (0.13-2.22) and phosphatidylcholine (PC) (0.63-7.63).

Six different chromatographic developments were consecutively carried out in solutions of decreasing polarity as presented in the Table D.1. After each chromatographic development, the plates were dried using hot air. When the chromatographic separations were performed, the plate was stained immersing in a $CuSO_4$ solution at 10% (p/v) in H_3PO_4 at 8% (v/v) for 10 seconds. After, the plates were dried with hot air until the first dots started to be visible. Then, the plates were developed for 3 minutes at 200 °C.

Table D.1 Mixtures of solvents used in the six chromatographic developments for neutral lipids and phospholipids separation by TLC.

Mobile phase composition	Proportion (v:v)	Distance of the front (cm)
Chloroform:methanol:water	60:40:10	1.8
Chloroform:methanol:water	65:40:05	2.3
Ethyl acetate:ethanol: isopropanol:methanol:chloroform: KCl at 0.25 %(v/v) in H_2O	35:20:5:15:22:9	5
Toluene:dietyl eter:ethanol	60:40:03	8
n-Heptane:dietyl eter	22:08:00	11
n-Heptane	100	12

The image of the TLC plate was digitalized with the densitometer GS-800 and quantification was performed with the Quantity One software. The integrated optic density (IOD) of each lipid spot, after subtraction of the background, was interpolated in the IOD values of the calibration curves. The results obtained were expressed in µmol per gram of liver or nmol per mg of cellular protein.

3.2.2 Lipidomic analysis

Lipid profiles were analyzed in OWL (Bizkaia Science and Technologic Park; Zamudio, Spain) as previously described (Barr J., et al, J. Proteome Res., 2012). Briefly, four UPLC®/time-of-flight mass spectrometry (TOF-MS) based platforms (Waters) analyzing methanol/dH2O and chloroform/methanol liver extracts were combined. Lipids identified in the methanol platform included: non-esterified fatty acids (FA), acylcarnitines, BAs, monoacylglycerophospholipids, monoetherglycerophospholipids, and oxidized FAs. For this, methanol was added to the frozen liver tissue (30:1, v/w) and the resulting mixture was homogenized with a Precellys 24 grinder (Precellys, France), followed by protein precipitation. The methanol used for extraction was spiked with internal standards not detected in liver tissue using the same method. After brief vortex mixing, the samples were incubated overnight at -20 ˚C. Supernatants were collected and dried after centrifugation at 16,000 xg for 15 minutes. The dried extracts were resuspended in methanol, centrifuged at 16,000 xg for 5 minutes, and finally supernatants were collected and transferred to vials for UPLC®-MS analysis.

Lipid species identified in the chloroform/methanol platform included glycerolipids, CEs, sphingolipids, DGs, and acyl-ether-glycerophospholipids profiling. For this, liver tissues were homogenized in the Precellys 24 grinder by mixing with chloroform/methanol (2:1, v/v) and sodium chloride (50 mM) (overall ratio 1:30:3, w/v/v), followed by protein precipitation. The extraction solvent was spiked with internal standards not detected using the same method. After brief vortex mixing, the samples were incubated at -20 ˚C for 1 h. After centrifugation at 16,000 xg for 15 minutes, the lower organic phase was collected and the solvent removed. The dried extracts were then resuspended in acetronitrile/isopropanol (1:1), centrifuged at 16,000 xg for 5 minutes, and finally supernatants were transferred to vials for UPLC®-MS analysis.

3.2.3 Bile acid analysis

Bile acids (BA) from liver samples were extracted using Silica-based bonded phase cartridges (Sep-Pack Plus C18, Waters-Millipore, Madrid, Spain) and analyzed in an HPLC-MS/MS (6410 Triple Quad LC/MS, Agilent Technologies, Santa Clara, CA) as previously reported (Nytofte et al., 2011) following a modification of the method described (Ye, Liu, Wang, Shao, & Ding, 2007). Chromatographic separation was carried out with gradient elution using a Zorbax Eclipse XDB-C18 column (150 mm x 4.6 mm, 5 µm) at 35 °C and a flow rate of 0.5 ml/min. Mobile phase (pH 4.6) was initially 80:20 methanol/water, and it was changed to 97:3 methanol/water over 9 minutes and then returned to 80:20 in 1 minute. Both solvents contained 5 mM ammonium acetate and 0.01% formic acid. Electrospray ionization (ESI) in negative mode was used, with the following conditions: gas temperature 350 °C, gas flow 8 l/minute, nebulizer 10 psi, capillary voltage 2500 V. MS/MS acquisition was achieved in multiple reaction monitoring (MRM) mode using the specific m/z

transitions: [M-H]- ion to 80.2 for taurine-conjugated bile acids and [M-H]- ion to 74 for glycine-conjugated bile acids. Unfortunately free BAs did not generate characteristic ion fragments, as reported before (Ye et al., 2007) and transition from unfragmented precursor molecular ions 407.1 to 407.1, 391.3 to 391.3 and 375.3 to 375.3 were selected for trihydroxylated, dihydroxylated and monohydroxylated free BAs, respectively.

3.2.4 Malondialdehyde quantification

Malondialdehyde (MDA) content is generally used as marker for lipid peroxidation. MDA content in liver samples was quantified using a commercially available kit from Sigma-Aldrich (St. QuentilFallavier, France) following manufacturer's instructions.

3.3 Subcellular fractionation of liver tissue

Lysosomal, microsomal and cytosolic fractions from mouse liver were isolated using a serial centrifugation method.

Pieces of 150-200 mg of liver were homogenized using the homogenization buffer for cellular fractionation. For this, liver pieces were homogenized in a potter homogenizer, 20 strokes and were centrifuged at 1,000 xg for 20 minutes at 4 °C to remove tissue debris and nuclei. The pellet was discarded and the supernatant was collected to be centrifuged at 20,000 xg for 10 minutes at 4 °C. After the centrifugation, the supernatant was collected and the pellet, with most of the mitochondria, was discarded. The supernatant was centrifuged at 22,000 xg for 20 minutes at 4 °C. After the centrifugation, the pellet and supernatant were separated and processed.

The pellet was used for lysosomal fraction isolation. Thus, the pellet was gently resuspended using a glass rod and 1 ml of homogenization buffer. When the pellet was properly mixed with the buffer, the last centrifugation was performed at 22,000 xg for 20 minutes. Finally, the pellet containing lysosomes was resuspended after addition of 150 µl of homogenization buffer.

The supernatant of the first 22,000 xg centrifugation was used for microsomal fraction and cytosol isolation. To perform this isolation 2 ml of homogenization buffer was added to the supernatant and was centrifuged at 105,000 xg for 1 h at 4 °C. The supernant was collected (cytosolic fraction), including the fat, and it was transferred to another centrifugation tube. The pellet (microsomal fraction) was gently homogenized using a glass rod and it was resuspended in 2.5 ml of washing buffer. The microsomal and cytosolic fractions were centrifuged again in the same conditions. From the tubes that contained the re-centrifuged microsomes, the

supernatant was discarded, the pellets were gently homogenized with the glass rod and were resuspended in 200 µl of homogenization buffer. From the cytosol tubes the supernatant was collected including the floating fat without removing the pellet.

3.4 Quantification of enzyme activities

Cholesteryl ester hydrolase (CEH), triglyceride hydrolase (TGH) diglyceride acyltransferase (DGAT), acyl-CoA cholesteryl acyltransferase (ACAT) and phosphatidylethanolamine N-methyltransferase (PEMT) enzymatic activities were measured. These enzymatic activities were quantified using radiometric assays as described by Liza et al. for ACAT (Liza, Romero, Chico, Fresnedo, & Ochoa, 1996) ; by Cristobal et al for CEH (Cristobal, Ochoa, & Fresnedo, 1999), Dolinsky et al. for TGH (Dolinsky, Douglas, Lehner, & Vance, 2004), by Dolisnky et al. for DGAT (Dolinsky et al., 2004) and by Ridgway & Vance for PEMT(Ridgway & Vance, 1992).

3.4.1 Neutral triglyceride and cholesteryl ester hydrolases

Neutral TGH activity was measured quantifying the released radioactive oleic acid (OA) as a result of the split of glycerol tri-[^{14}C]oleate (GE Healthcare, USA) by the sample. This activity was measured using 150 µg of protein from microsomal and cytosolic fractions. The substrate was prepared as mixed micelles of TG:PC:sodium taurocholate in a molar proportion 10:17:8 and glycerol tri-[^{14}C]oleate (56 mCi/mmol; 100 µCi/mL).

Neutral CEH activity was determined quantifying the released radioactive OA as a result of the split of cholesteryl [^{14}C]oleate by the sample. This activity was measured using 60 and 100 µg of protein from microsomal and cytosolic fractions, respectively. The substrate was prepared as mixed micelles of cholesteryl oleate:PC:sodium taurocholate in a molar proportion 10:47:25 and cholesteryl- [^{14}C]oleate (12 mCi/mmol; 1.25 µCi/mL). In both of the enzymatic assays the micelles were prepared following the same protocol. First, the required lipids were added into a polypropylene tube (dissolved in toluene or chloroform) containing the radiolabeled triolein (TG) for TGH activity or radiolabeled CE for CEH activity, and the organic solvent was evaporated with N_2. After the evaporation, the assay buffer was added and it was sonicated using a titanium probe of 10 mm of diameter in a sonicator at 6 microns of potency in a bath at 50 ˚C. The conditions of the sonication were 60 cycles of 30 seconds of sonication and 10 seconds of pause. Finally, the micelle preparation was centrifuged at 22,000 xg for 30 minutes to eliminate the metallic remnants of the titanium probe.

The assays were carried out in a final volume of 200 µl of assay buffer with a final concentration of TG of 750 µM for TGH and a final concentration of CE of 150 µM for CEH activity. After preincubation of the samples shaking for 10 minutes at 37 °C, both of the reactions were

started adding each substrate. Thirty minutes later, the reaction was stopped with the addition of 2.5 ml of stop solution and 500 µl of extraction salts added to make the extraction easier. The tubes were vigorously shaken for 90 seconds and were centrifuged at 1,000 xg for 10 minutes at 4 ˚C for phase separation. Afterwards, 750 µl of the upper aqueous phase, where the free radiolabeled oleate is, was transferred to vials containing 4 ml of scintillation liquid "Cocktail Biogreen 3" (Scharlau Chemicals, Spain). The radioactivity was determined in the scintillation counter. As the blank of the reaction, a mixture of the substrate and the assay buffer without enzymatic source (sample) was used. The results were determined as pmol of released FA per mg of protein and minute.

3.4.2 Acid triglyceride and cholesteryl ester hydrolase

The acid TGH and CEH activities were determined using 30 µg of protein from the lysosomal fraction. The substrate was presented as mixed micelles of TG:PC in a molar proportion 10:25 with a trace of glycerol tri-[^{14}C]oleate (56 mCi/mmol; 100 µCi/mL) for acid TGH and as mixed micelles of CHOL:PC in a molar proportion of 1:10 having cholesteryl [^{14}C]oleate (0.25 µCi/incubate) for acid CEH (section 3.5.1). Both of the micelle mixtures were dissolved in the assay buffer for acid enzymatic activities. The assay was carried out in a final volume of 200 µl of assay buffer and a final concentration of TG of 750 µM for acid TGH activity and of CE of 200 µM for acid CEH activity. After preincubate the samples shaking for 10 minutes at 37 °C, the reaction was started adding the substrate. After 5 minutes, the reaction was stopped with 2.5 ml of stop solution. Finally, 500 µl of extraction salts were added to help the extraction. All the next steps were followed as described for neutral activities determination.

3.4.3 Acyl-CoA cholesteryl acyltransferase (ACAT)

ACAT activity was used as a measure of the rate of intracellular CE formation. The ACAT activity was determined in the microsomal fraction. The substrate for the activity was prepared by adding in a tube 1 µl [^{14}C] oleil-CoA (60 mCi/mmol; 50 µCi/mL) and 120 µM of oleil-CoA to each incubate. Tubes were preincubated 10 minutes at 37 °C; and then 50 µl of substrate was added per tube and incubated for 6 minutes. The reaction was stopped by adding 5 ml of chloroform: methanol (2:1). Then 50 µl of standard [^{3}H] cholesterol oleate (48 Ci/mmol; 1000 µCi/mL) were added. Lipids were extracted using the Folch method and the radioactivity incorporated into cellular lipids were determined after TLC separation.

Table D.2 Mixture of solvents used for three chromatographic separation of lipids classes in TLC plates.

Mobile phase composition	Proportion (v:v)	Distance of the front (cm)
Chloroform:methanol:water	60:40:10	1.8
n-Heptane:diisopropyl ether:acetic acid	70:30:02	15
n-Heptane	100	16

A three chromatographic development separation was performed. This chromatographic method was able to separate the main classes of lipids: CE, TG, FC, DG, FA and PL. These developments were performed with 3 different solvents mixture (Table D.2). The plates were treated and prepared as explained before (section 3.2.1). The extracted lipids were separated using the three chromatographic developments. When the chromatographic plates were dry, they were stained with iodine vapors introducing the plates into a chromatographic tank with iodine crystals. After the scraping o f the band corresponding to cholesterol oleate, the silica gel was introduced in a vial containing 4 ml of scintillation liquid "Cocktail Biogreen 3" and the radioactivity was determined in a scintillation counter. The ACAT activity was determined as nmol of oleil-CoA released per mg of protein and per minute.

3.4.4 Diglyceride acyltransferase (DGAT)

The DGAT activity was calculated by quantifying the resultant triglyceride from the esterification of the diglyceride with the radioactive fatty acid. The substrate was prepared adding 6.2 µl of diglyceride 10 mg/ml, 69.2 µl of ^{14}C-Oleil-CoA (58.2 mCi/mmol; 20 µCi/ml) and 10 µl of Oleil-CoA 20 mg/mL. This solution was evaporated in nitrogen, and then resuspended with 2 ml of assay buffer and sonicated for 10 minutes at 37 °C.

For the assay 200 µg of microsomal sample were used. Tubes were preincubated for 5 minutes at 37 °C, and then 100 µl of substrate were added. Samples were incubated for 10 minutes. Then, reaction was stopped by adding 5 ml of chloroform/ methanol (2:1) and 1.25 ml of the extraction salts (KCl 0.88%) was added. 50 µl of a standard of ^{3}H-CE were added to each tube to normalize the extraction. Lipids were extracted and separated as explained before (section 3.4.3). The bands of TG and CE were scraped off to vials with scintillation liquid. The radioactivity of the vials was quantified with a scintillation counter. The DGAT activity was calculated as pmol of recovered triglyceride/ mg of protein/ minute.

3.4.5 Phosphatidylethanolamine N-methyltransferase (PEMT)

PEMT activity was measured quantifying the incorporation of radioactive methyl groups from S-adenosyl-L-(methyl-3H) methionine ([^{3}H]SAMe)(10 µCi/mmol; 550 µCi/mL) (Perkin Elmer, USA) into PE to give PC. This activity was measured using 50 µg of protein from liver homogenate.

First, 1,2-dioleoyl-sn-glycero-3-phosphoethanolamine-N-methyl (PMME) substrate (Avanti Polar Lipids, USA) was prepared from a PMME stock, which was dissolved in chroloform:metanol 1:2 (v/v). The PMME stock needed to have a final concentration of 3.7 mg/ml of PMME substrate was evaporated with nitrogen. EDTA buffer together with Triton X-100 0.0004% was added, mixed properly with the vortex and finally sonicated with 3 cycles of 30 seconds at no more than 6 microns using a sonicator.

The assay was carried out in a final volume of 150 µl of assay buffer with a final concentration of SAMe 1 mM (Sigma-Aldrich, USA). The substrate contained 0.66 µCi/incubate of [^{3}H]SAMe. Samples were preincubated for 15 minutes at 37 ˚C and [^{3}H]SAMe/SAMe. After 30 minutes at 37 ˚C, the reaction was stopped with 2 mL of stop solution. 2 mL of NaCl 0.5% were added and the samples were vigorously shaken for 90 seconds and finally centrifuged at 1,000 xg for 10 minutes at 4 ˚C to separate the aqueous phase from the organic one. The aqueous phase was removed and the organic one was washed 3 times with 0.5% (w/v) NaCl:metanol:chloroform 50:50:4 (v:v:v) and after the last wash all the upper phase was removed. Finally, 200 µl of the lower organic phase was transferred to vials with 4 mL of scintillation liquid "Cocktail Biogreen 3". The radioactivity was determined in the scintillation counter. As the blank of the reaction, a mixture of the substrate with the assay buffer without sample was used. The activity was expressed as total pmol of released CHs per mg of protein and minute.

3.5 Metabolic fluxes

To quantify metabolic fluxes, radioisotope incorporation experiments were performed by primary incubation of isolated hepatocytes from mice liver as described previously.

3.5.1 [^{3}H]Acetate incorporation

For *de novo* lipogenesis analysis, primary hepatocytes (1.5 x 10^6 cells/plate) were incubated with sodium [^{3}H]acetate (20 µCi/ml; 20 µM). At different times, 120 and 240 minutes, cells and mediums were collected and cells were washed 5 times with PBS. To quantify the radioactivity incorporated from [^{3}H]acetate into lipids, lipids (TG, DG, CE, FC, phospholipids (PL) and FA) were extracted and separated as explained before (section 3.4.3). After the scraping of the corresponding bands, the silica gel was introduced in a vial containing 4 ml of scintillation liquid "Cocktail Biogreen 3" and the radiactivity was determined in a LKB Wallac 1214 Rackbeta scintillation counter.

3.5.2 [^{3}H]Oleate incorporation

For fatty acid esterification analysis, primary hepatocytes (1.5 x 10^6 cells/plate) were incubated with [^{3}H]oleate (54 Ci/mmol; 2 µCi/ml; 20 µM). At different times, 120 and 240 minutes, cells and mediums were separated and cells were washed 5 times with PBS. Lipids were extracted using the Folch method and the radioactivity incorporated into cellular lipids were determined after TLC separation. A 6 chromatographic development separation was performed to quantify the radioactivity incorporated from [^{3}H]oleate into lipids. CE, TG, FC, DG, FA, PC and PE were separated as previously described. Radioactivity incorporated to each lipid was quantified as explained above in 3.4.3 section.

3.5.3 Palmitate beta oxidation rate

Beta-oxidation was assessed as described before (Gao et al., 2015; Hirschey & Verdin, 2010). Fresh liver pieces were homogenated in a Potter homogenizer (5 strokes) in cold homogenization buffer and sonicated for 10 seconds. Then, the homogenates were centrifuged at 500 xg for 10 minutes at 4 °C. Approximately 500 µg of protein from the homogenates supernatant was used for the assay in a volume of 200 µl. The reaction started by adding 400 µl assay buffer containing ^{14}C-palmitate (56 mCi; 0.4 µCi/mL; 500 µM) to the samples and was incubated for 1 h at 37 °C in eppendorf tubes with a whatman paper circle in the cap. The reaction was stopped by carefully adding 300 µl of perchloric acid 3 M and NaOH 1 M was added to impregnate the whatman cap.

After 2 h the Whatman caps were removed and the radioactivity associated was measured in a scillation counter. The eppendorf tubes were centrifuged at 21,000 xg 10 minutes at 4 °C. 400 µl from the supernatant were collected and the radioactivity was counted in a scintillation counter. The supernatant contained the acid soluble metabolites (ASM)(incomplete palmitic oxidation) and the whatman caps captured the released CO_2 (complete palmitic oxidation).

3.6 Western blotting

Electrophoresis SDS-PAGE. Liver samples were homogenated in lysis buffer and protein was quantified. Samples mixed with denaturing buffer were denaturalized for 5 minutes at 95 °C. Electrophoresis was made in polyacrylamide gels of different percentage depending on the protein of interest, using a vertical Mini Protean II electrophoresis equipment (Bio-rad, USA). 20 ug of sample were loaded in each well, and a commercial mixture of protein marker was added (*PageRuler Prestained Protein Ladder Plus*, Thermo). Electrophoresis at 150 V for an h in electrophoresis buffer.

Transfer: After running the electrophoresis, wet transfer was performed. Either nitrocellulose or PVDF membranes were used.

Wet transfer: PVDF membranes were activated by keeping them 1 minute in methanol, then 2 minutes in distilled water and 5 minutes in transfer buffer with methanol 20%. Nitrocellulose membranes were directly moisten in transfer buffer. Then, the gel and membrane were sandwiched between a sponge and the whatman paper (sponge/3 Whatman paper/gel/membrane/3 whatman paper/sponge) and all were clamped tightly. The sandwich was submerged in transfer buffer, keeping it cold with an ice plate. Then, a voltage of 100 V was applied for 2 h.

To check the efficacy of the transference the gels were washed in distilled water and stained with Gel Code from Pierce at RT for 1h and the nitrocellulose membranes were stained with Ponceau S staining.

Blocking: Membranes were incubated in TBST with a blocking agent depending on the protein of interest, BSA or milk, for 1 h under agitation at RT.

Incubation and inmunodetection: After blocking, the membranes were incubated with the primary antibody (table D.3) over night (o.n) at 4 °C with gentle agitation. The primary antibodies used and their concentrations are represented in table 4. After this incubation, membranes were washed with TBST 3 times for 10 minutes at RT with agitation. Then, membranes were incubated with the appropriate secondary antibody. All the incubations were done at RT for 1 h. Another 3 washes with TBST were made as previously described. Chemiluminiscent detection was performed by an ECL Western blotting detection kit from Amersham Biosciences, and membranes were exposed to an X-ray film (Fujifilm).

Digitalization: Images were acquired and quantified using the densitometer GS-800 of Bio-Rad.

Table D.3 Primary antibodies used for Western Blotting

Target Ab	Manufacturer	Blocking solution	Antibody dilution
ACC	CST	Milk 5% TBST	1:1000
p-ACC	CST	Milk 5% TBST	1:1000
AKT	CST	Milk 5% TBST	1:1000
p-AKT	CST	Milk 5% TBST	1:1000
AMPKα	CST	Milk 5% TBST	1:1000
p-AMPKα	CST	Milk 5% TBST	1:1000
Caspase 12	CST	Milk 5% TBST	0,736111111
CYP7A1	Santa Cruz	Milk 5% TBST	1:1000
EIF2α	CST	Milk 5% TBST	1:1000
p-EIF2α	CST	Milk 5% TBST	1:1000
ERK	CST	Milk 5% TBST	1:1000
p-ERK	CST	Milk 5% TBST	1:1000
FAK	CST	Milk 5% TBST	1:1000
p-FAK	CST	Milk 5% TBST	1:1000
GAPDH	Abcam	Milk 5% TBST	1:20000
GRP78	ENZO	Milk 5% TBST	1:1000
gamma H2A.X	Abcam	Milk 5% TBST	1:1000
Ire1a	CST	Milk 5% TBST	1:1000
p-Ire1a	CST	Milk 5% TBST	1:1000
JNK	CST	Milk 5% TBST	1:1000
p-JNK	CST	Milk 5% TBST	1:1000
mTOR	CST	Milk 5% TBST	1:1000
p-mTOR	CST	Milk 5% TBST	1:1000
OPN	Santa Cruz	Milk 5% TBST	1:1000
p21	Santa Cruz	Milk 5% TBST	1:1000
S6	CST	Milk 5% TBST	1:1000
p-S6	CST	Milk 5% TBST	1:1000
ppRB	CST	Milk 5% TBST	1:1000
Transferrin	Santa Cruz	Milk 5% TBST	1:5000

3.7 Liver histochemistry

The histological analysis were carried out in the laboratory of Dr. Mª Luz Martínez Chantar, CIC Biogune (Derio). Paraffin-embedded sections (5 µm thick) of formalin-fixed liver samples or OCT embedded samples were used. Paraffin-embedded sections were initially deparaffinized in xylene or xylene-substitute and rehydrated through graded alcohol solutions. Once hydrated, sections were subjected to the following stainings:

Hematoxylin and eosin: After the deparaffinization and rehydration process, sections were subjected to conventional hematoxylin and eosin staining. Briefly, sections were submerged for 5 minutes in Harris hematoxylin, and then sections were washed in water for 5 minutes and then stained in eosin

for 15 minutes. After this, samples were washed in water for 3 minutes and then dehydrated and cleared with Histoclear and mounted with DPX (Sigma Aldrich).

Sirius Red: Rehydrated sections were stained with Sirius red solution (0.01% Fast Green FCF/0.1% Sirius red in picric acid, Sigma Aldrich) for 30 minutes. Sections were then dehydrated directly in 100% alcohol and mounted in DPX mounting media.

SA-β Galactosidase: 10 µm thick frozen tissue sections were fixed with 4% NBF/0.5 % Glutaraldehyde solution. For the staining solution, a citric acid 40 mM was prepared in sodium phosphate heptahydrate 0.2 M pH 6.0. Potassium ferricyanide and potassium ferrocyanide was added to this solution, final concentration 5mM, MgCl2 2 mM and NaCl 150 mM. Staining solution was heated at 37 °C and 1mg/mL X-Gal was added. Samples were incubated overnight in a humid chamber. Finally, samples were counterstained with 1% Fast Red for 2 minutes, dehydrated and mounted with DPX. For the analysis, five pictures were taken and analyzed with CellProfiler.

DHE: Samples were sectioned in a cryostat (8 µm), and incubated with MnTBAP 150 µM at RT for 1 h. The samples were then incubated with DHE 5 µM for 30 minutes at 37 °C. Sections were mounted with mounting media containing DAPI.

Sudan Red: Cut liver cryostat section of 8 µm were incubated with freshly-prepared Sudan III stain (Sigma-Aldrich) and counterstained with Mayers hematoxylin. Stained area percentage of each sample were calculated using FRIDA software (Framework for Image Dataset Analysis).

Immunohistochemistry: 5 µm thick OCT embedded sections were made with the cryomicrotome for F4/80 staining. Sections were unmasked according to the primary antibody to be used and subjected to peroxide blocking, 3% H_2O_2 in PBS, 10 minutes RT. For stainings with mouse-hosted antibodies in mouse tissues, samples were blocked with goat anti-mouse FAB fragment (Jackson Immunoresearch, USA) (1:10, 1h RT) and then blocked with 5% goat serum (30 minutes, RT). Then, sections were incubated in a humid chamber with the primary antibody in DAKO antibody diluent (DAKO) followed by Envision anti-rabbit or anti-mouse (DAKO) HRP conjugated secondary antibody incubation (30 minutes, RT). Colorimetric detections was confirmed with vector VIP chromogen (Vector) and sections were counterstained with hematoxylin. Samples were mounted using DPX mounting medium. For the analysis, images were taken with an upright light microscope.

The **histopathological study** of the 20 month-old mice liver was performed by an expert pathologist from the Animal Medicine and Surgery department in the Veterinary Faculty of the Universidad Complutense, Madrid (UCM), following Kleiner criteria (Kleiner et al., 2005).

3.8 Serum analysis

3.8.1 Serum transaminases, lipids and ketone bodies quantification.

Serum transaminase alanine aminotransferase (ALT) and aspartate aminotransferase (AST) were determined using commercially available kits (Spinreact, Spain). For the quantitative serum ALT and AST 10 µl of mouse serum were mixed with 200 µl of reagent and were incubated for 1 minute at 37 °C. Absorbance was measured at 340 nm in 1 minute intervals for 30 minutes. The standard range used for the calibration curve was from 129 to 1548 µU.

Serum total cholesterol (CHOL), TG and free fatty acids (FFA) were also measured using commercially available kits (Menarini, Italy and Wako, Germany). All the measurements were made using the plate reader spectrophotometer. For serum CHOL measurement, 5 µl of mouse serum were used and 200 µl of the reagent ready to use were added, mixed and incubated for 5 minutes at 37 °C protected from direct light. Absorbance at 510 nm was measured. The standard range used for the calibration curve was from 1.4 to 27.8 µg. For serum TG 5 µl of mouse serum were used and 200 µl of the reagent ready-to-use were added, mixed and incubated for 10 minutes at 37 °C. Serum FFA were measured using 5 µl of serum. Sample was mixed with 160 µl of R1 for 3 minutes at 37 °C. Then 80 µl of R2 were added and after 8 minutes absorbance was measured at 546 nm. The calibration range was 0.5 to 12 µM.

Serum ketone bodies (KB) were determined using a commercially available kit (Wako, Germany). Serum KB were measured using 5 µl of serum. Sample was mixed with 180 µl of R1 and incubated for 5 minutes at 37 °C. Then, 60 µl of R2 were added and after 10 minutes incubation absorbance was measured at 405 nm. The calibration range was 0.5 to 12 µM.

3.8.2 Osteopontin quantification by ELISA

Serum OPN in mice was quantified using commercially available mouse OPN ELISA Kit (R&D Systems, UK) following the manufacturer's instructions. The standard range used for the calibration curve was from 39 to 2500 pg/ml. For human serum OPN determination another specific OPN ELISA Kit (R&D Systems, UK) was used following the manufacturer's instructions. The standard curve used for the calibration curve development was from 0.312 to 200 ng/ml.

3.9 White adipose tissue lipolysis

Fresh white adipose tissue (WAT) pads of 20 mg were extracted from gonadal white adipose tissue. These WAT pads were incubated in DMEM supplemented with fatty acid free BSA 4 % and (+)-Isoproterenol (+)-bitartrate salt 20 µM for the stimulation of the lipolysis. WAT pads were also

incubated in DMEM with fatty acid free BSA 4 % for the basal condition. After incubating the tissue for 4 h, culture medium was collected and the released glycerol and FAs were measured using commercially available kits.

3.10 Analysis of gene expression

3.10.1 RNA extraction

Total RNA from mouse liver tissue was extracted using Trizol Reagent (Invitrogen Life Technologies, USA) and following the commercial protocol steps. All the material was treated with RNaseZap®, an RNase decontamination solution (Thermo Fisher Scientific, USA). An additional treatment with DNase (Invitrogen Live Technologies, USA) was included in the process. The quality of the RNA was assessed by electrophoresis in an agarose gel of 1% (w/v) dissolved in TAE buffer and Sybr safe™ DNA gel stain at 1:25 (v/v) dilution from Molecular probes (Thermo Scientific, USA) using a horizontal electrophoresis equipment (Bio-rad, USA).

3.10.2 cDNA synthesis and real time-quantitative polymerase chain reaction (rt-qPCR)

The retrotranscription was performed using 1.8 µg of DNAse I pre-treated RNA extract and using the commercially available kit "SuperScript III First-Strand Synthesis System for RT-PCR" (Invitrogen Live Technologies, USA). Manufacturer instructions were followed to obtain the cDNA. A final treatment with RNAse H was performed. cDNA samples were diluted 1/10 before real time-qPCR assessment.

For real time qPCR quantification, the fluorescence dye SYBR® Green (Applied Biosystems) was used. All samples were assayed in triplicated and 40 cycles with a melting temperature of 60 °C for 1 minute and 95 °C for 15 seconds were performed. The equipment for the qPCR was the AbiPrism 7000 "Sequence Detection System" from Applied Biosystems.

Ct (cycle threshold) values were determined for each sample and extrapolated to a standard curve. The standard curve was constructed with serial dilutions of a mixture of cDNA. The expression levels are showed as arbitrary units. Expression levels were normalized using geNorm software, taking in consideration the values of glyceraldehyde-3-phosphate dehydrogenase (GAPDH), cyclophilin and TATA-box-binding protein (TBP). Primers were synthesized by Invitrogen Life Technologies. Melting curve was tested to ensure specificity of the PCR products.

3.11 Statistical analysis

The results were expressed as the arithmetical mean ± SEM (Standard error of the mean). For the statistical analysis of the data, different tests were used. For the comparison between two

groups the Student t-test was performed. For the comparison of more than two groups, a two way variance (ANOVA) analysis was used. For human samples comparison a correlation analysis between serum OPN and the age was performed. To evaluate significance of the correlation analysis a Pearson Correlation test was performed in NL, non-obese NL, NAFLD and non-obese NAFLD patients.

These statistical analyses were performed using the "GraphPad Prism" software. Differences were considered significant when the probability of the null hypothesis (p) was <0.05. The statistical significant differences are stated with different symbols as explained in each figure. The ANOVA p value is numerically described in the figures.

E.RESULTS

1. Osteopontin controls bile acid metabolism by regulating CYP7A1 levels in liver and hepatocytes

Nuñez-Garcia, M., Gomez-Santos B. *et al*. (2017) Osteopontin regulates the cross-talk between phosphatidylcholine and cholesterol metabolism in mouse liver. *J. Lipid Res.* 58, 1903-1915.

Osteopontin (OPN) is involved in different diseases in which metabolic dysruption is a hallmark. On previous work, we found that OPN regulates the glycerolipid metabolism and the liver cross-talk between phosphatidylcholine PC and cholesterol (Chol) metabolism in mouse liver. High levels of OPN increase liver PC concentration, while PC concentration is low in OPN deficient (OPN-KO) mice. We showed that in non-obese non-alcoholic fatty liver disease (NAFLD) patients, in which serum OPN is increased, serum OPN positively correlates with liver PC, phosphatidylethanolamine (PE) and CHOL concentration. We also found that when mice were treated with recombinant osteopontin (rOPN) PC, phosphatidylethanolamine (PE) and Chol levels were increased in liver. In addition, OPN deficiency resulted in an increased cholesterogenesis and reduced *de novo* lipogenesis of several lipids such as triglycerides (TG) and phospholipids (PL) in hepatocytes. This shows that OPN regulates the fate of acetyl-CoA in liver. In addition, in vivo inhibition of cholesterogenesis normalized PC content in OPN-KO mice. This demonstrates that OPN regulates the PC and Chol metabolism interplay (Nuñez-Garcia et al., 2017). Both PC and Chol are highly interconnected, both being bile lipids synthesized in the liver. On previous work, we found that several factors involved in biliary PC secretion and nuclear factors that regulate cholesterol 7α-hydroxylase (CYP7A1) expression were upregulated in OPN-KO mice, and downregulated in rOPN treated mice. CYP7A1 is the enzyme that catalyzes the initial and rate-limiting step in cholesterol catabolism and bile acid synthesis. Thus, we wanted to explore whether OPN could modulate liver metabolism by regulating CYP7A1

1.1 Osteopontin regulates CYP7A1 in hepatocytes

We wanted to elucidate whether OPN could directly modulate CYP7A1, which is the enzyme that is in charge of the conversion of Chol into bile acids (BA), in hepatocytes and to identify the mechanism involved. In order to analyze whether OPN could directly modulate CYP7A1 activity in hepatocytes, we treated hepatocytes with recombinant OPN (rOPN) for 3 hours (h). We observed that the rOPN treated hepatocytes showed reduced CYP7A1 levels together with a trend toward decreased 7a-hydroxi-4-cholesteren-3-one (C4) levels. This compound is an indirect biomarker of CYP7A1 activity (Fig E.1).

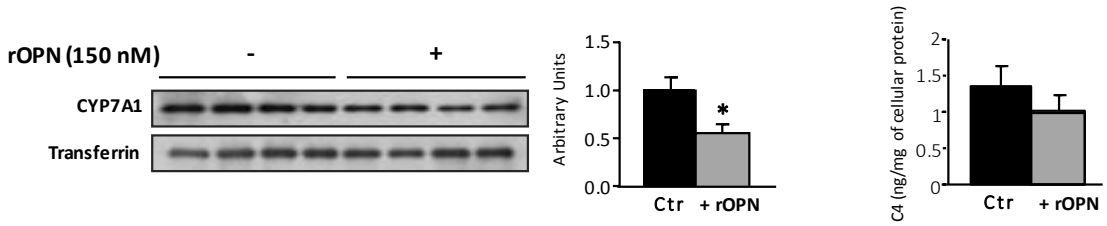

Figure E.1 OPN regulates CYP7A1 in hepatocytes. Primary hepatocytes from WT mice were incubated with recombinant OPN (rOPN) (150nM) for 3h. CYP7A1 levels in hepatocytes were assessed and transferrin was used as loading control. Analysis of 7a-hydroxi-4-cholesteren-3-one (C4) levels in hepatocytes were assessed. Values are the mean ± SEM of 4 plates per group. Significant differences between Ctrl and rOPN treated hepatocytes are denoted by *p<0.05, **p<0.01 and ***p<0.001 (Student's t test).

1.2 Osteopontin regulates FAK activation and cholesterol levels in mice liver

OPN interacts with integrins and/or CD44 at the cell surface of hepatocytes, among other cell types, thus, inducing a signaling cascade through phosphorylation/activation of FAK and AKT. To determine the mechanism by which OPN downregulates CYP7A1. We took into account that several reports have involved AKT (Li, Ma, & Chiang, 2008) and/or ERK and JNK (Henkel, Anderson, Dewey, Kavesh, & Green, 2011; Li, Jahan, & Chiang, 2006), in regulation of CYP7A1 transcription. Thus, the activation of these pathways was investigated in liver and in primary culture of hepatocytes. In WT mice treated with rOPN, phosphorylation and activation of FAK was increased, while in OPN-KO animals FAK phosphorylation was reduced (Fig E.2A). In rOPN treated WT mice, together with the increased FAK phosphorylation there was an increased free cholesterol (FC) concentration (Fig E.2B). This supports the hypotesis that rOPN downregulates CYP7A1 levels, which in turn decreases the conversion of Chol into BA, increasing the Chol levels in liver.

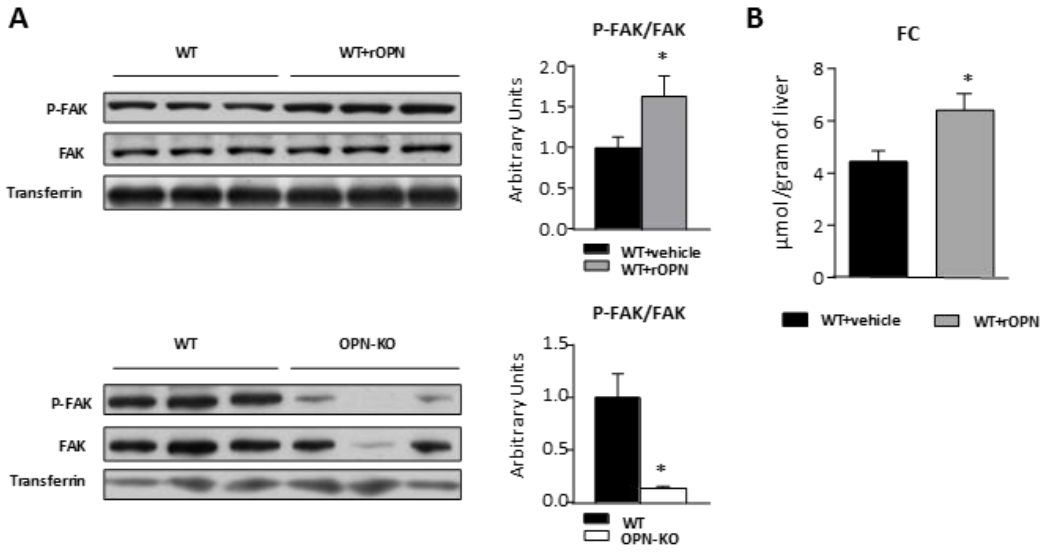

Figure E.2 OPN regulates FAK activation and free cholesterol (FC) levels in mice liver. (A) Recombinant OPN (rOPN) (15 µg/mouse) (WT+ rOPN) or vehicle treated wild-type mice (WT+ vehicle), and osteopontin knockout (OPN-KO) and their control mice (WT) were used. Liver Tyr-397 phosphorylated focal adhesion kinase (FAK) and total focal adhesion kinase (FAK) levels were assessed by immunoblotting using transferrin as the loading control. (B) Lipids were extracted from liver homogenate and free cholesterol (FC) was separated and quantified.Values are means ± SEM of 5 animals per group. Significant differences between WT+vehicle and WT+rOPN are denoted by *p <0.05 and **p <0.01 (Student's t test).

1.3 Recombinant OPN decreases CYP7A1 by activation of the FAK-AKT pathway

We wanted to know if the liver response to rOPN observed in vivo was mainly due to the hepatocyte response. Thus, we performed different assays on isolated hepatocytes. The FAK-AKT signaling pathway was induced after treatment with rOPN, as shown by the increased phosphorylation of FAK and AKT (Fig E.3A). However, the ERK and JNK phosphorylation was not affected (Fig E.3A). In order to assure the involvement of the FAK-AKT pathway in regulation of CYP7A1 expression we used the PI3K and FAK inhibitors LY294002 and Y15, respectively. When inhibiting the FAK-AKT signaling pathway, CYP7A1 levels increased in rOPN treated hepatocytes (Fig E.3B). Thus, demonstrating a mechanism by which rOPN decreases CYP7A1 levels in hepatocytes. Taking all together, we propose that OPN will induce, through activation of the FAK-AKT signaling, the downregulation of CYP7A1 protein levels, and thus will decrease the conversion of Chol into BA. OPN will decrease the synthesis and secretion of BA. This decreased secretion will also decrease PC secretion, which will contribute to the higher liver concentration of PC.

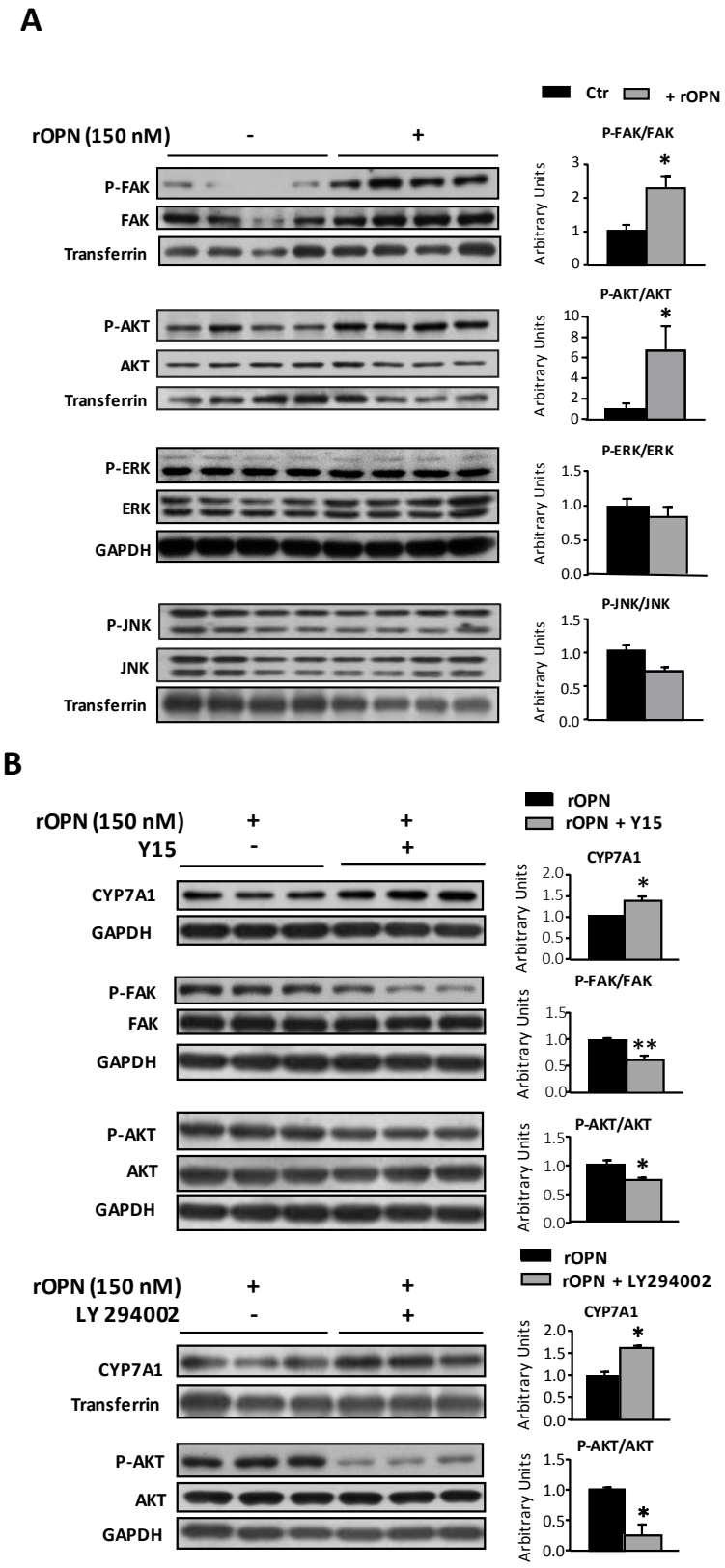

Figure E.3 Recombinant OPN (rOPN) decreases CYP7A1 by activation of FAK-AKT pathway. (A) Primary hepatocytes from WT mice were incubated with rOPN (150 nM) during 3 h and the FAK-AKT signaling pathway was analyzed. Transferrin was used as a loading control. (B) Primary hepatocytes from WT mice were incubated with rOPN (150 nM) during 3 h in the presence or absence of the FAK and PI3K inhibitors, Y15 (30 µM) or LY294002 (50 µM). Values are means ± SEM of 4 plates per group. Significant differences between control (Ctr) and rOPN-treated hepatocytes, rOPN and rOPN+LY294002 are denoted by $*P < 0.05$, $**P < 0.01$, and $***P < 0.001$ (Student's *t*-test).

2. Rewiring of lipid metabolism modulates liver regeneration after partial hepatectomy in OPN-KO mice

Nuñez-Garcia, M., **Gomez-Santos B.** *et al*.,(2018) Atorvastatin provides a new lipidome improving early regeneration after partial hepatectomy in osteopontin deficient mice. *Sci Rep.;8(1):14626.*

The liver has the capacity for regeneration after cellular damage or surgery resection. During regeneration, liver cells need to acquire sufficient energy and metabolic precursors to support the metabolic demands for rapid proliferation. Thus, a variety of metabolic pathways is switched on. Regarding phospholipid metabolism, the synthesis of PC, the mayor phospholipid in cellular membranes, is coordinated with the activation of the cell cycle and it is an essential step in cell proliferation. Changes in the hepatic PC/PE molar ratio have been linked to impaired liver regeneration (van der Veen et al., 2005). Concerning TG metabolism, hepatic TG content is widely variable and increases during liver regeneration. However, alterations in lipid metabolic pathways, has demonstrated to promote or diminish hepatic lipid content influencing hepatocyte proliferation (Newberry et al., 2008). Chol is also essential for the correct regeneration since it is a critical structural component of biological membranes that influences properties such as permeability and fluidity, while also contributing to the modulation of the membrane proteins, protein trafficking, and transmembrane signaling (Delgado-Coello, Briones-Orta, Macías-Silva, & Mas-Oliva, 2011). Related to liver Chol metabolism, the BA metabolism has also demonstrated to play a role in liver regeneration. In fact, the relative BA overload after partial liver resection causes activation of BA receptors in non-parenchymal and parenchymal cells in the liver, thus, providing signals to the regenerative process (van de Laarschot, Liyanne FM, Jansen, Schaap, & Damink, 2016). Therefore, modulation of lipid metabolism is required to ensure an adequate regeneration after partial hepatectomy (PH). The technique of PH is widely used to model liver regeneration and cell cycle dynamics in vivo, avoiding the massive necrosis observed in other regeneration models (Mitchell & Willenbring, 2008).

On previous work, we found that circulating OPN levels increases in the levels of circulating OPN during the first 24 h after PH. The OPN increase occurs at a time when hepatocytes accumulate a significant amount of lipids (mainly TGs), in the widely recognized transient regeneration-associated liver steatosis. Although deficiency in OPN does not result in changes in liver regeneration, OPN deficiency leads to remodeling of liver lipidome. OPN deficient mice exhibit changes in the enrichment of several species of TG and PC in the quiescent livers. These differences observed between quiescent OPN-KO and WT species minimize along regeneration, showing a remodeling of

PC and TG species, primarily during the first 24 h after PH. The fluctuations in several TG species along regeneration are not associated with changes in concentration of liver TG, while those of PC species are linked to decrease of PC concentration in quiescent and regenerative liver. The different liver lipidome is not associated with changes in the lipid cargo of serum lipoproteins. The inhibition of Chol synthesis restores PC levels in liver and improves liver regeneration (Nuñez-Garcia et al., 2017). The atorvastatin treatment causes an early liver regeneration in OPN-KO mice as reflected by the increased in liver to body weight ratio, percentage of ki67 positive hepatocytes and the expression of the proliferating cell nuclear antigen (Nuñez-Garcia et al., 2018).

2.1 Dietary fatty acid contribution to the liver triglycerides in OPN-KO mice

Taking into account all the previous data, we wanted to address several unsolved questions regarding lipid modulation in the OPN-KO mice livers. First, considering that PC and TG de novo synthesis are reduced in OPN-KO mice hepatocytes while TG concentration remains unaltered and PC is decreased, we wanted to analyze the contribution of dietary fatty acids (FA). For this, we evaluated if TG and PC species containing the essential linoleic acid (18:2) were altered. The linoleic acid cannot be synthesized by the cell and must be acquired from the diet. We observed that most of the TG species that were increased in OPN-KO livers were enriched in linoleic acid. We also observed that PC species containing the linoleic acid were reduced in the quiescent OPN-KO liver compared to the WT. This suggests that the decreased de novo TG synthesis observed in the OPN-KO mice liver is compensated by increased dietary FA uptake. However, this compensation does not occur with PC loss (Figure E.4A). Since the big changes in liver lipid content during regeneration occur mainly 24h after PH, we also analyzed whether the increased TG storage was associated with the increase in linoleic acid. The results showed that increase in linoleic acid-containing TG species was significantly more marked in WT than in OPN-KO mice liver (Fig. E.4B). However, changes in linoleic-acid containing PC species were less consistent, since some linoleic acid containing PC species increased while other decreased 24 h after PH (Fig E.4B).

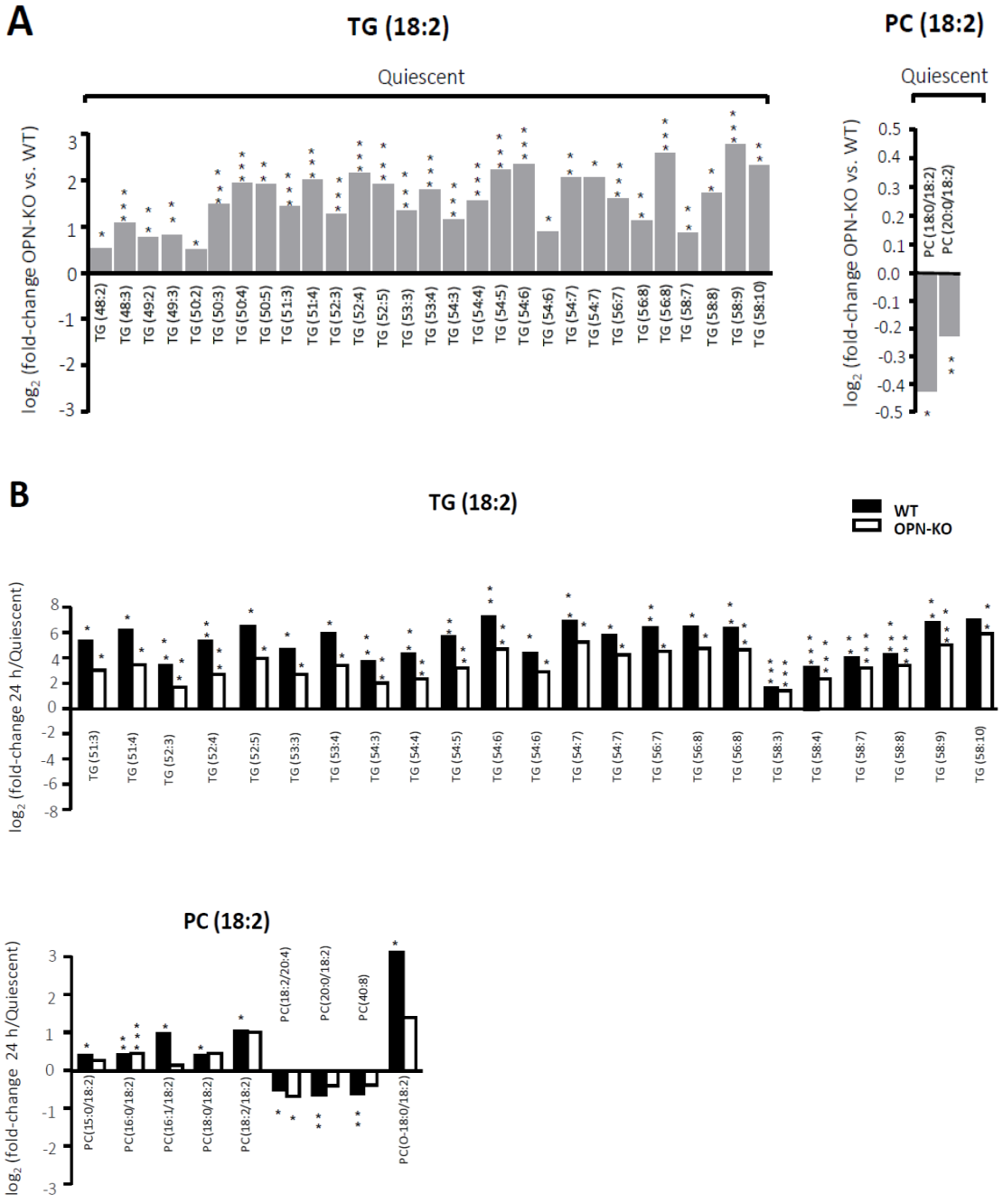

Figure E.4 Liver triglyceride is enriched in the dietary linoleic acid (18:2) in OPN-KO mice. (A) Osteopontin knockout (OPN-KO) mice and their controls (WT) were subjected to partial hepatectomy (PH), and liver was collected before and 24 h post-PH. Triglycerides (TG) and phosphatidylcholine (PC) species containing the essential linoleic acid (18:2) were analyzed comparing differences in the quiescent liver species between both genotypes. (B) Differences during the first 24 h of liver regeneration in each genotype. The results are represented as $\log_2$ of the fold-change. Values are mean of the fold change from 5 animals per group and significant differences are denoted by *p <0.05, **p <0.01 and ***p <0.001 (Student's t test).

2.2 Liver lipid oxidation rate is increased in OPN-KO mice 24 h post partial hepatectomy

Transient liver TG accumulation during PH has been correlated with changes in lipid oxidation (Newberry et al., 2008; Schofield, Sugden, Corstorphine, & Zammit, 1987). Herein, we assessed liver lipid oxidation rate by measuring the rate of conversion of ^{14}C- palmitate into acid-soluble metabolites (ASM) or CO_2 (Fig. E.5A). 24 h post PH, incomplete (ASM) and complete (CO_2) lipid oxidation was increased in OPN-KO mice when compared to WT mice (Fig. E.5A). By contrast, no differences were observed in the quiescent liver or in the regenerating liver 48 h post PH. For mitochondrial lipid oxidation to occur, FAs need to be converted into acylcarnitines by CPT-1 before being transported from the cytosol. Importantly, altered acylcarnitines content has been associated with changes in lipid oxidation. In this study, we observed that acylcarnitine levels were increased in livers of OPN-KO mice under basal (quiescent) conditions when compared to WT mice. However, although acylcarnitine levels were increased in both OPN-KO and WT mice 24 h after PH, the increase was more marked in WT mice (Fig. E.5B), in which beta oxidation was not increased (Fig. E.5A). 48 h post PH, acylcarnitines were even higher in WT mice while decreased in the KO mice (Fig.E.5B) suggesting an increased consume in beta oxidation.

Next, we found that 24 h post PH, the increased lipid oxidation in the OPN-KO was associated with increased dihydroethidium (DHE) in liver slices (Fig. E.5C), which have been used extensively to evaluate reactive oxygen species (ROS) production while no differences were observed in malondialdehyde (MDA) (Fig. E.5D), which is a natural bi-product of lipid peroxidation, or in oxidated fatty acids (FA) (Fig. E.5D). Thus, this shows that despite the increased fatty acid oxidation and increased levels of ROS production, lipid peroxidation levels remained unaltered in OPN-KO mice along liver regeneration.

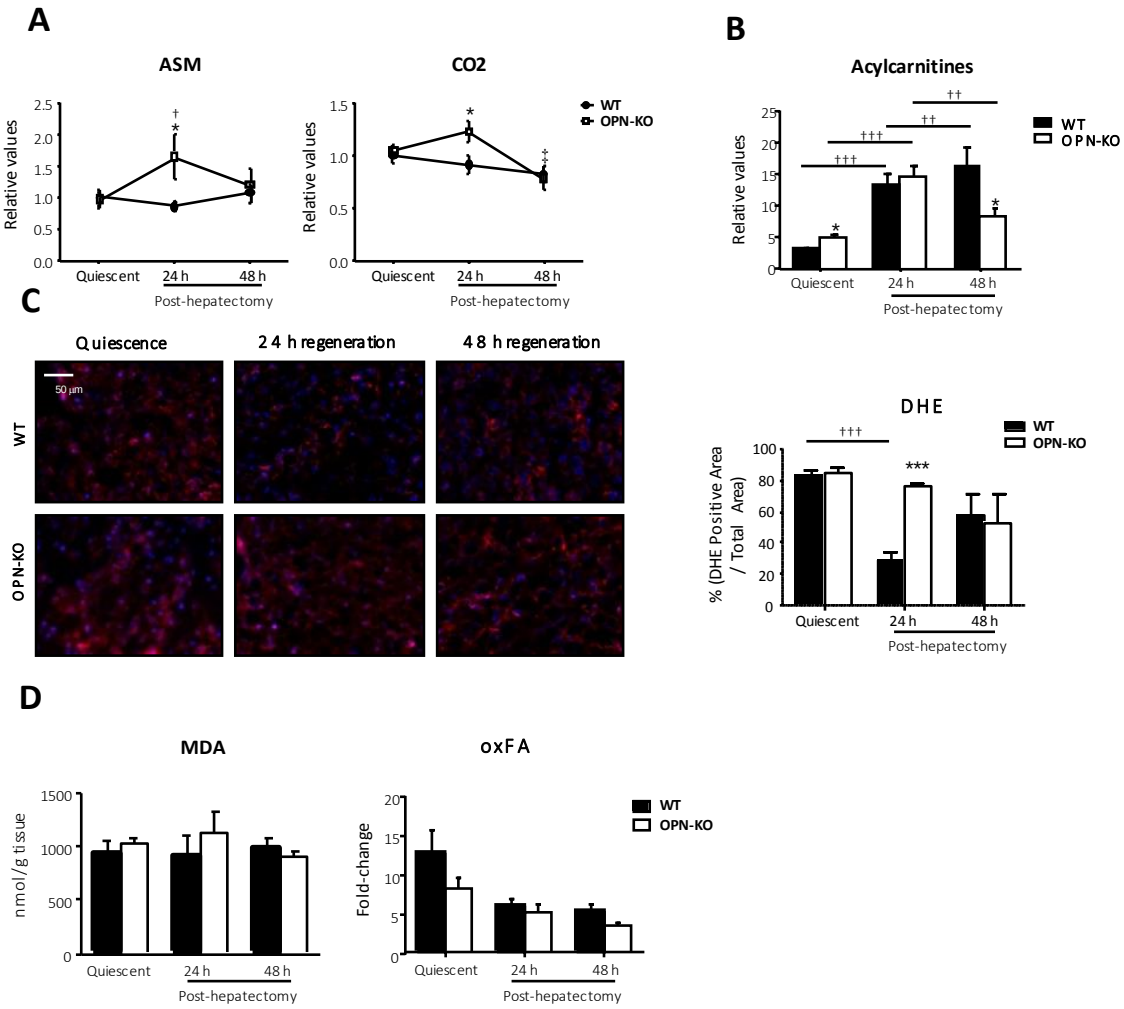

Figure E.5 Lipid oxidation is higher in OPN-KO mice than in WT mice 24 h after partial hepatectomy. Osteopontin knockout (OPN-KO) mice and their controls (WT) were subjected to partial hepatectomy (PH), and livers were collected before and 24 h and 48 h post-PH. (A) Fatty acid oxidation assay was performed and the released radioactive acid soluble metabolites (ASM) and CO_2 were quantified. (B) Total acylcarnitine content was measured. (C) Representative liver sections of DHE staining and quantification. (D) Malondialdehyde (MD) levels in liver samples represented in nmol/gram of tissue (left) and the content of oxidized fatty acids (FA) (right). Values are mean ± SEM from 4-5 animals per group. Significant differences between OPN-KO and the corresponding WTs are denoted by *p <0.05 (Student's t test); Significant differences along regeneration are indicated by †p <0.05, ††p <0.01 and †††p <0.01 (Student's t test).

2.3 Atorvastatin induces changes in the lipidome 24 h after PH only in the OPN-KO mice

As previously reported, the greatest increase in serum OPN levels occurred during the first 24 h after PH since no changes were observed between 24 and 48 h. This increase in serum OPN was linked with the peak of body weight loss (Nuñez-Garcia et al., 2018). We demonstrated that in vivo inhibition of cholesterogenesis with atorvastatin restores PC content in OPN-KO mice (Nuñez-Garcia et al., 2017). As reported, OPN modulates liver lipid metabolism (and liver lipidome) during regeneration after PH (Nuñez-Garcia et al., 2018). To provide more information to elucidate how atorvastatin improves liver regeneration in OPN-KO mice. Here we evaluated the effect of atorvastatin in the liver lipid concentration of OPN-KO mice and their WT. We found that in OPN-KO mice, treatment with atorvastatin resulted in greater body weight loss 24 h after PH, while this effect was not observed in WT mice (Fig. E.6A). Atorvastatin treatment did not alter liver FC levels in WT or KO mice (Fig. E.6B). However, 24 h after PH liver levels of cholesteryl ester (CE) (a form of Chol storage) were lower in OPN-KO than in WT mice treated with atorvastatin (Fig. E.6B). Atorvastatin also increased liver diglycerides (DG) and PC content 24 h after PH in OPN-KO mice inducing no effect in WT mice (Fig. E.6C), as we had previously observed in the quiescent livers.

Atorvastatin treatment did not induce changes in the accumulation of lipid droplets or in the liver TG content 24 h after PH in the OPN-KO or WT mice (Fig E.7A). Atorvastatin decreased liver DG content in OPN-KO mice 48 h after PH (Fig. E.7C) while it did not induce changes in body weight loss or concentration in other lipids (Fig. E.7A, B and C). Since we observed that in OPN-KO mice the increased lipid oxidation was associated with increased DHE, here we wanted to know if this increase maintained after atorvastatin treatment, that restores the lipidome. The results showed that differences between WT and OPN-KO in DHE disappeared after atorvastatin treatment (Fig. E.7B).

Taken together, these results show that, the decrease in the PC liver concentration and *de novo* synthesis is not compensated with the dietary essential FA linoleic, unlike what happens with TGs. The increased dietary-lipid uptake in OPN-KO mice provides the metabolic precursors required for regeneration 24 h and 48 h after PH. Atorvastatin induces changes in the liver lipidome in regeneration only in OPN-KO mice. In which, as shown in previous work, atorvastatin improves early regeneration.

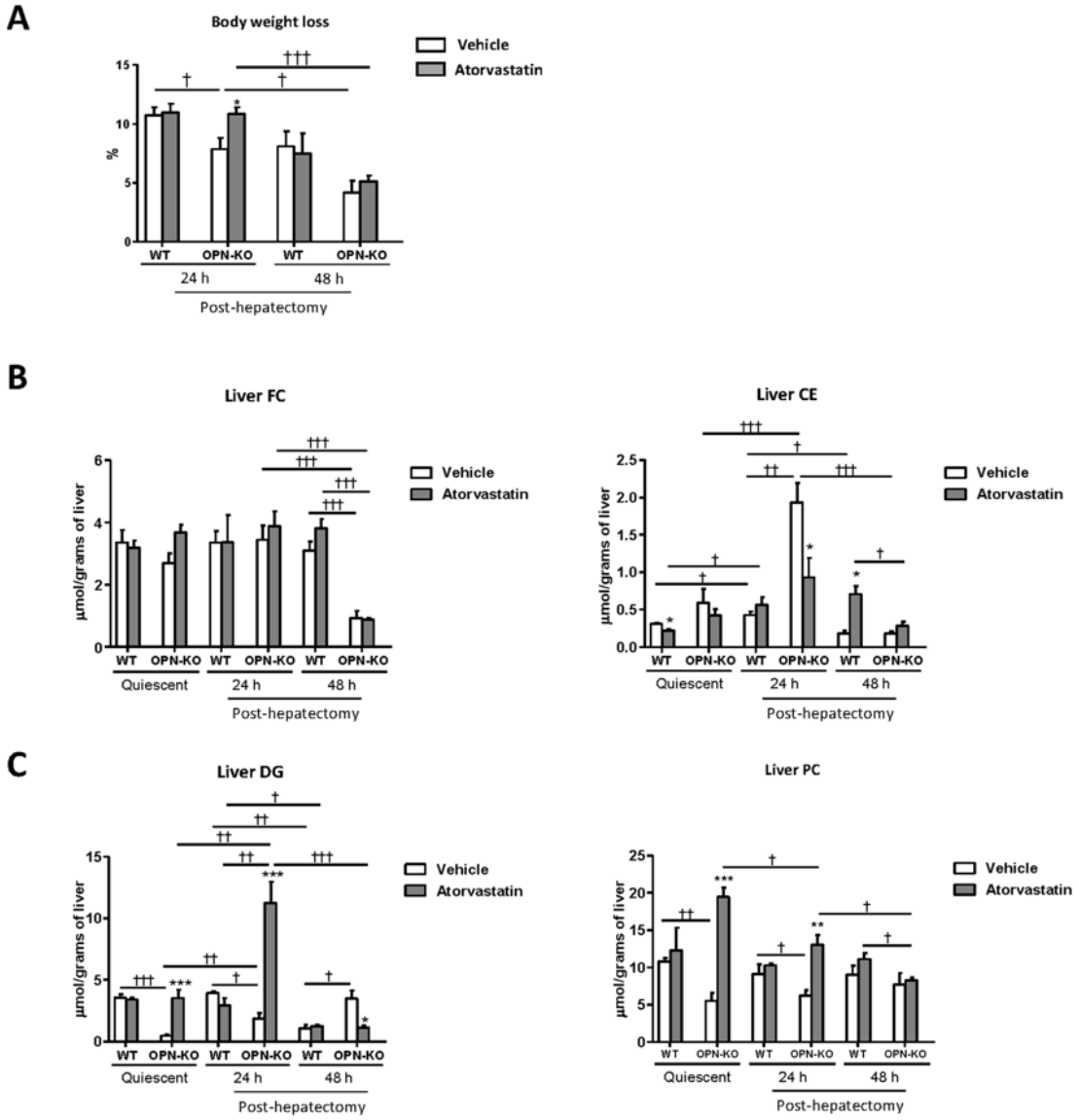

Figure E.6 In OPN-KO mice atorvastatin treatment induces changes in liver lipidome 24 h after partial hepatectomy. Osteopontin knockout (OPN-KO) mice, OPN-KO mice treated with atorvastatin (100 mg/kg), and their respective controls treated or untreated with atorvastatin (WT) were subjected to partial hepatectomy (PH) and livers were collected 0 h (quiescent), 24 h and 48 h post-hepatectomy. (A) Percentage of body weight loss. (B) Liver free cholesterol (FC), cholesteryl ester (CE). (C) Diglycerides (DG) and phosphatidylcholine (PC) content are represented in nmol/gram of liver. Values are mean ± SEM of 4-8 animals per group. Statistical differences between treated or untreated mice within one genotype are denoted by *p <0.05 (Student's t test) and differences along regeneration and between genotype are indicated by †p <0.05, ††p <0.01 and †††p <0.001 (Student's t test).

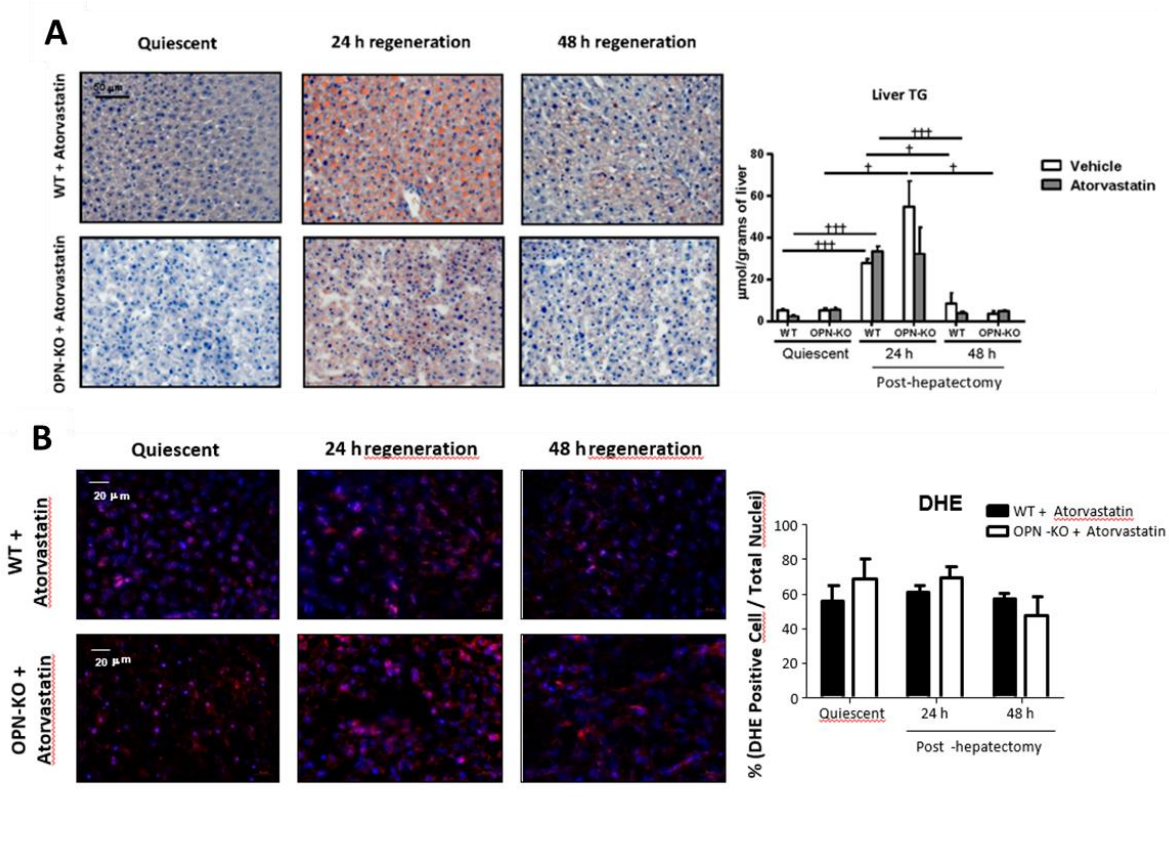

Figure E.7 Atorvastatin treatment modulation of liver TG 24 h after partial hepatectomy. (A) Representative liver sections stained with Sudan III (left) and liver triglycerides (TG) content (right) is represented in nmol/gram of liver. (B) Representative liver sections stained with DHE (left) and quantification (right). Values are mean ± SEM of 4-8 animals per group. Statistical differences between treated or untreated mice within one genotype are denoted by *p <0.05 (Student's t test) and differences along regeneration and between genotype are indicated by †p <0.05, ††p <0.01 and †††p <0.001 (Student's t test).

3. Osteopontin plays a role in the age-associated NAFLD progression

3.1 Osteopontin and aging

OPN is expressed in many organs and tissues such as the liver, brain, bone, lungs and kidney, among others. It can also be found in blood and urine. This protein is involved in many physiological and pathological processes and its expression is increased in many diseases in which aging in the primary risk factor. OPN has been linked to aging in several studies. However, the available data does not give conclusive results about the role of OPN in the aging process, but its effect seems to be tissue or cell-type dependent.

During aging, the liver undergoes a series of changes and loses its ability to respond correctly to damage. With aging, body fat undergoes redistribution, from adipose tissue to other tissues, including the liver. This results in an increased liver lipid accumulation in the liver. In addition, the prevalence of non-alcoholic fatty liver disease (NALFD) increases with age, and with aging the number of biochemical and histological alterations increases. Besides, cirrhosis has a higher prevalence among older people. Therefore, vulnerability to the development and progression of liver disease increases with age. In order to elucidate if during aging OPN is involved in the increased vulnerability of the liver to NAFLD, we analyzed if serum OPN levels increased with age in different models.

3.1.1 The positive correlation between age and serum OPN levels is lost in NAFLD patients

We analyzed circulating OPN concentration in a human cohort with normal liver (NL) (n=34) (Table E.1) and observed a positive correlation between serum OPN concentration and age (Fig E.8A). Aging is the primary risk factor for a number of diseases in which the metabolic component is key, such as cardiovascular diseases, cancer and metabolic syndrome. In fact, NAFLD has been considered the hepatic manifestation of the metabolic syndrome. We previously reported a role for OPN controlling liver lipid metabolism. Besides, we observed that circulating OPN levels were increased in NAFLD patients (Nuñez-Garcia et al., 2018; Nunez-Garcia et al., 2017). Thus, to analyze whether the positive correlation between OPN and age observed in NL individuals maintains in NAFLD patients, we analyzed a cohort of NAFLD patients (n=129) (Table E.1). We measured OPN serum concentration and observed that the correlation between circulating OPN concentration and age was lost in NAFLD patients, in which OPN levels were already high (Fig E.8A). The result indicates that variations on OPN levels might play a role in the pathogenesis of age-associated NAFLD. As mentioned earlier, NAFLD is often associated to metabolic syndrome and obesity. Since OPN levels can be altered in obesity, we wanted to discard the obesity as the cause for the observed lack of correlation. Thus, we analyzed whether the positive correlation maintained in the cohort of non-

obese patients (Table E.1). We observed that the correlation age-serum OPN concentration maintained in non-obese NL, and was lost in the non-obese NAFLD group, assuring the possible role of OPN in the liver disease associated to age (Fig E.8B).

Table E.1 Demographic, metabolic, biochemical and histological characteristics of individuals with normal liver (NL), non-alcoholic fatty liver disease (NAFLD), non-obese NL and non-obese NAFLD. Obese patients where considered when the BMI was ≥ 30.

	NL	NAFLD	non-obese NL	non-obese NAFLD
BMI (kg/m2)	28,1	41,18***	25,71	25,96
Age(Years)	48,3	49,5	48,27	52,92307692
Male gender %	32,4	31,7	34,62	46
Female gender %	67,6	68,3	65,38	54
TG (mg/dL)	104,3	145,87***	89,31	128,1*
Glucose (mg/dL)	95,4	91,3	95,38	104
CHOL (mg/dL)	188,4	166,3	188,38	201,154
CHOL-HDL (mg/dL)	49,9	38,6	49,88	53,154
ALT (IU/l)	19,2	36,53**	19,15	34,62**
AST (IU/l)	18,1	27,86**	18,13	25,69**
Insulin (mU/mL)	6,6	11,9	6,63	6,9
Steatosis %				
Grade 0	100	34,8	100	0
Grade 1		37,8		84,6
Grade 2		17,8		15,4
Grade 3		9,6		0

Data are the mean or percentage (%). ALT, alanine aminotransferase; AST, aspartate aminotransferase; CHOL, cholesterol; BMI, Body mass index; HDL, high-density lipoprotein; TG, triglyceride. Values are means of n=34 for NL, n=129 for NAFLD, n=29 for non-obese NL individuals and n=13 for non-obese NAFLD patients. Significant differences are denoted by *p<0.05, **p<0.01 and ***p<0.001 when comparing NL vs NAFLD, and when comparing non-obese NL vs non-obese NAFLD (Student's t test).

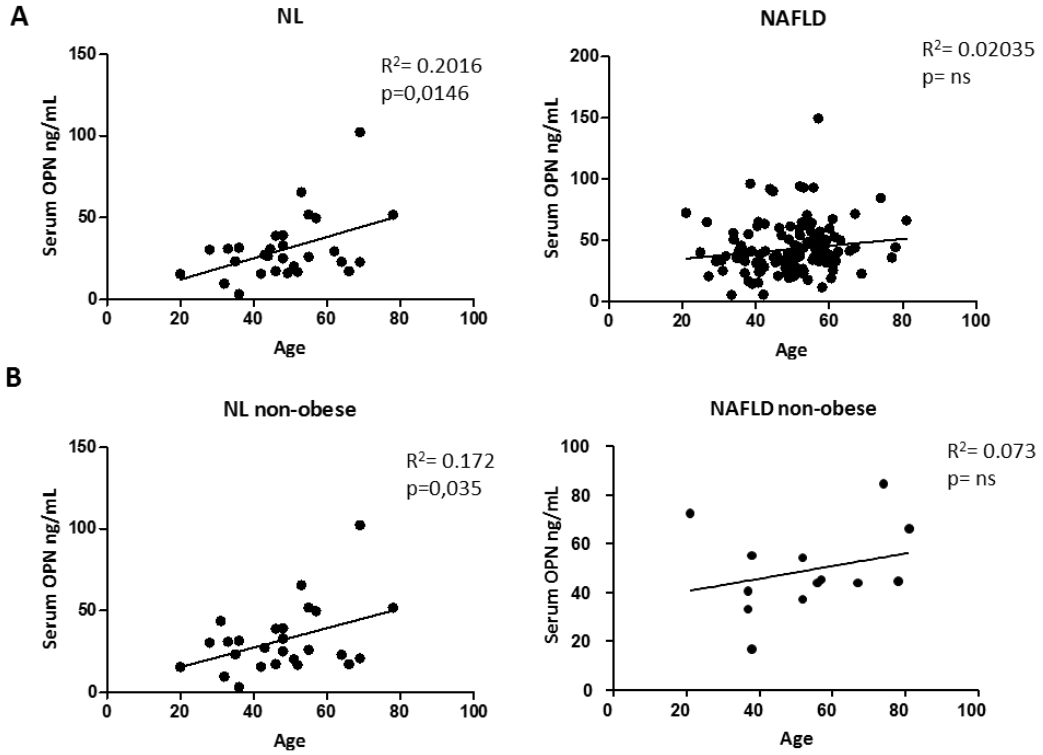

Figure E.8 Serum OPN in NL, NAFLD and non-obese NL and NAFLD patients. (A) Serum samples from normal liver (NL) individuals (n=34), non-alcoholic fatty liver disease (NAFLD) patients (n=129), (B) non-obese NL (n=29) and non-obese NAFLD patients (n=13) were quantified by ELISA to asses circulating OPN levels. Correlation analysis between OPN concentration and age has been performed using the Pearson test.

3.1.2 OPN levels increase in serum and liver during aging in mice

To ascertain whether the observed positive correlation between OPN and age in humans with NL was also observed in mice, we analyzed OPN in serum, for this we used a natural model of aging: male and female wild type (WT) mice ranging from 3 to 20 months-old (m). We measured serum OPN levels and, as observed in humans, we found a positive correlation between age and OPN levels (Fig E.9A). Given the lack of studies performed in female mice, particularly in age-related studies, we analyzed if OPN was increased in serum and liver of natural aged female mice. In this model, 3 m mice represent young mice, 10 m mice represent intermediate-age mice and 20 m mice represent aged mice. We observed that in female mice there was an increase in serum OPN concentration from 3 to 10 m, and that this increase maintained in 20 m mice (Fig E.9B). We also analyzed liver OPN protein expression, and observed a similar result, in which OPN was increased in 10 m mice and levels maintained high at 20 m (Fig E.9C).

Taking all together, we suggest that serum OPN increased with age as a consequence of increased liver secretion. However, if this secretion of OPN is a protective mechanism or makes the liver more vulnerable to liver disease is something we do not know yet.

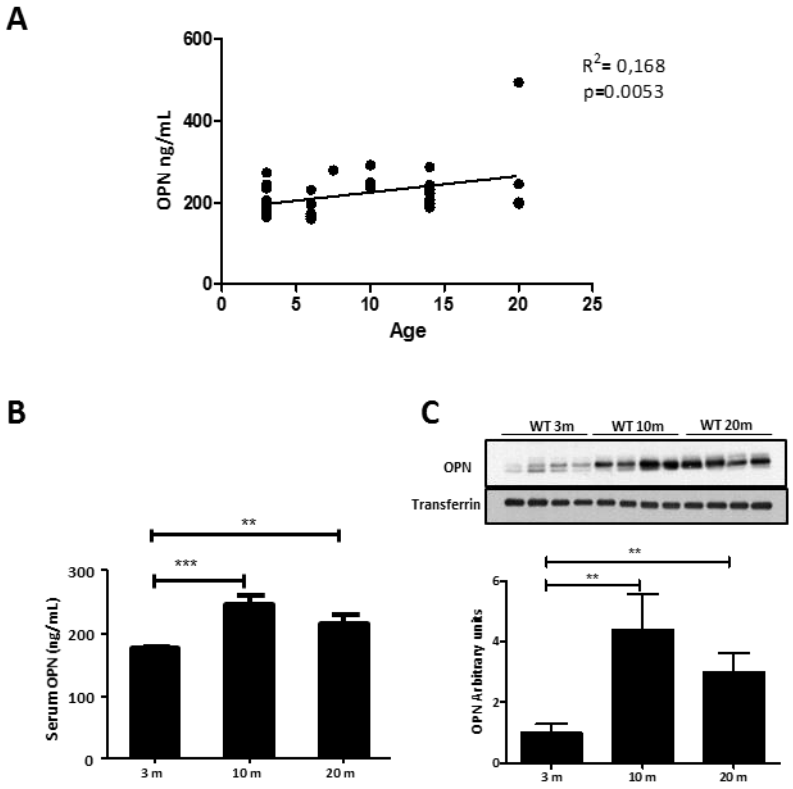

Figure E.9 Circulating and liver OPN levels during aging in a mouse model of aging. (A) Serum OPN levels of 3, 6 10, 14 and 20 month-old (m) wild type (WT) mice was quantified by ELISA. (B) Serum OPN levels of 3, 10 and 20 m female WT mice was quantified by ELISA. Immunoblot analysis of OPN from liver extract was assessed using transferrin as loading control. Values are means ± SEM of n= 3-8. Significant differences are denoted by *p<0.05, **p<0.01 and ***p<0.001 (Student's t test).

3.1.3 Osteopontin expression increases when senescence is induced in the HepG2 cell line

OPN is a cytokine known to be part of the senescence-associated secretory phenotype (SASP). Senescence is one of the hallmarks of aging, and it is primarily a protective mechanism in order to preserve the functionality of the tissue by avoiding the proliferation of damaged cells. Although cellular senesce is part of the aging process, aging is a more complex process. Since the number of senescent cells increases with aging, it has been widely assumed that senescence contributes to aging. In addition, other of the deleterious effects of senescence is that it can paradoxically promote tumorogenesis and cancer, which prevalence is increased with aging.

Given that OPN serum levels show a correlation with age in NL individuals, and 10 and 20 m mice show increased serum and liver OPN levels, we wanted to know if the senescence induction could

induce OPN expression and secretion in HepG2 cells. We induced senescence using two different methods: treating cells with hydrogen peroxide (H_2O_2) and with palbociclib. We checked the induction of senescence using the SA-β-Galactosidase staining, which was positive in both cases. In addition, with both treatments, OPN protein levels and secretion of OPN was induced (Fig E.10), suggesting that OPN might mediate , at least in part, cellular senescence. Besides, the results showed that the senescence induction by palbociclib, which inhibits the cyclin kinase 4/6 (CDK4/6) and thus the Rb protein (pRB) phosphorylation, was reduced when cells were treated with rOPN (Fig E.11). Thus, the effect of palbociclib was reduced when cells were treated with rOPN. This suggest that OPN might be a factor expressed to avoid or restrain senescence.

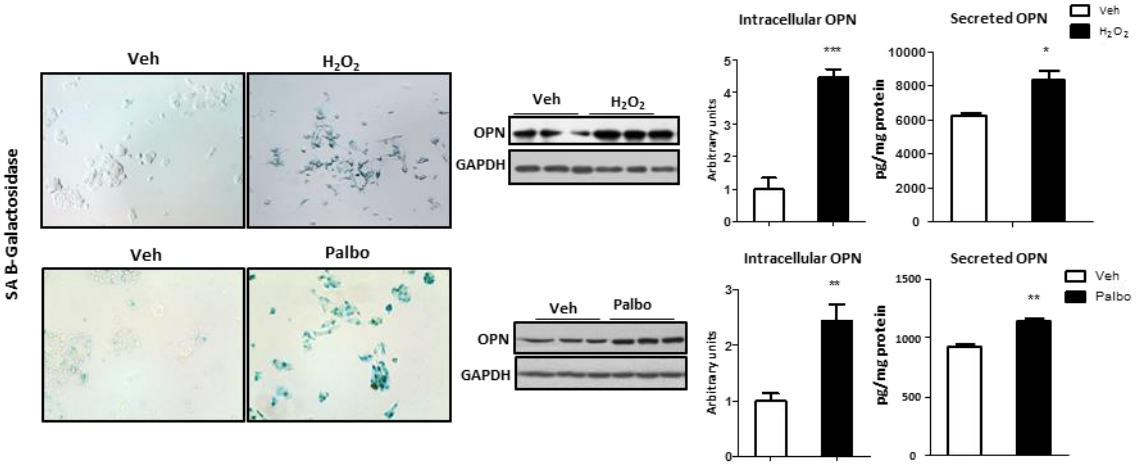

Figure E.10 Senescence induction and OPN protein levels in an in-vitro model. HepG2 cells were treated with hydrogen peroxide (H_2O_2)(700 µM) and Palbociclib (Palbo) (2 µM) or vehicle (Veh). Senescence induction was assessed with the SA-βGalactosidase staining. OPN protein levels from HepG2 cells were measured by immunoblotting using glyceraldehyde -3-phosphate dehydrogenase (GAPDH) as loading control. Secreted OPN in the media was measured by ELISA. Values are means ±SEM of n=4. Significant differences are denoted by *p<0.05, **p<0.01 and ***p<0.001 (Student's t test).

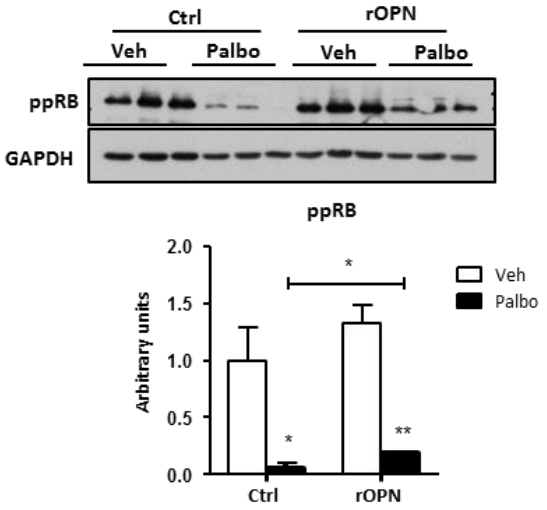

Figure E.11 Recombinant osteopontin (rOPN) reduces palbociclib senescent effect in HegG2 cells. rOPN treated cells (rOPN) and vehicle cells (Veh) were treated with Palbociclib (Palbo) (2µM) to induce senescence or vehicle (Veh). Phosphorylated Rb protein (ppRB) levels were measured by immunoblotting to study palbociclib effect using glyceraldehyde -3-phosphate dehydrogenase (GAPDH) as loading control. Values are means ±SEM of n=4. Significant differences are denoted by *p<0.05, **p<0.01 and ***p<0.001 (Student's t test).

3.2 OPN is plays a role in age-associated hepatosteatosis

3.2.1 Increased liver lipid accumulation is observed in OPN-KO mice during aging

The previous results show that osteopontin is involved in aging, and suggest that it might play a role in the age-associated liver vulnerability to NAFLD progression. Thus, we wanted analyzed if the increased OPN expression during aging is protective or detrimental for the age-associated hepatosteatosis development.

In order to study the role of OPN in the pathogenesis of NAFLD during aging, female WT and OPN-KO mice of 3, 10 and 20 m were used. In these animals, the increase in body weight with aging was similar between genotypes, with a slight increase in body weight in 10 m OPN-KO mice compared to their age-matched WTs (Table E.2). The liver weight increase with age was higher in the 10 m OPN-KO mice compared to their WTs (Table E.2). Serum alanine aminotransferase (ALT) increased as mice aged, but there were no differences between genotypes. Regarding serum lipids, levels of triglycerides (TG) were increased in 10 and 20 m OPN-KO mice compared to their age-matched controls while fatty acids (FA) just increased in 10 m OPN-KO animals. Finally, no changes in serum Chol were found (Table E.2).

Table E.2. Body and serum parameters of WT and OPN-KO female mice.

	3 m		10 m		20 m	
	WT	**KO**	**WT**	**KO**	**WT**	**KO**
Weight (g)	21,43	21,08	24,665$^{\#\#\#}$	26,5 * $^{\#\#\#}$	29,1325$^{\#\#\#}$	30,59$^{\#\#\#}$
LW (g)	0,77	0,74	0,98$^{\#\#}$	1,12* $^{\#\#\#}$	1,2$^{\#\#}$	1,14
ALT (U/L)	17,30**	14,12	18,41	23,61	49,5 $^{\#\#\#}$	46,91$^{\#\#\#}$
Serum TG (mg/dL)	73,620	78,140	43,87$^{\#}$	72,65*	56,611	84,25*
Serum NEFA (mg/dL)	14,69	11,98	11,24	18,52*$^{\#}$	15,44	15,53
Serum Cho (mg/dL)	92,68	98,14	93,21	78,7$^{\#}$	75,63	82,04

Body weight, liver weight (LW), serum alanine aminotransferase (ALT), serum Triglycerides (TG), non-esterified fatty acids (NEFA) and cholesterol (Chol) are represented. Values are means ±SEM of n=4-8. Significant differences are denoted by *p<0.05, **p<0.01 and ***p<0.001 when comparing genotypes of the same age group, and #p<0.05, ##p<0.01 and ###p<0.001 when comparing with previous age group in the same genotype (Student's t test).

Regarding liver lipid concentration, changes along aging were different in WT and OPN-KO mice; while the peak of concentration for all lipids was at 20 m in WT mice, being the concentration similar at 3 and 10 m, in the OPN-KO mice the peak was at 10 m and kept elevated at 20 m. This rise in storage lipid concentration was also observed when analyzing H&E staining (Fig E.12A). The analysis showed a premature increase in TG, CE, FA, DG, PC and FC concentration in 10 m OPN-KO mice compared to their age-matched WTs (Fig E.12B).

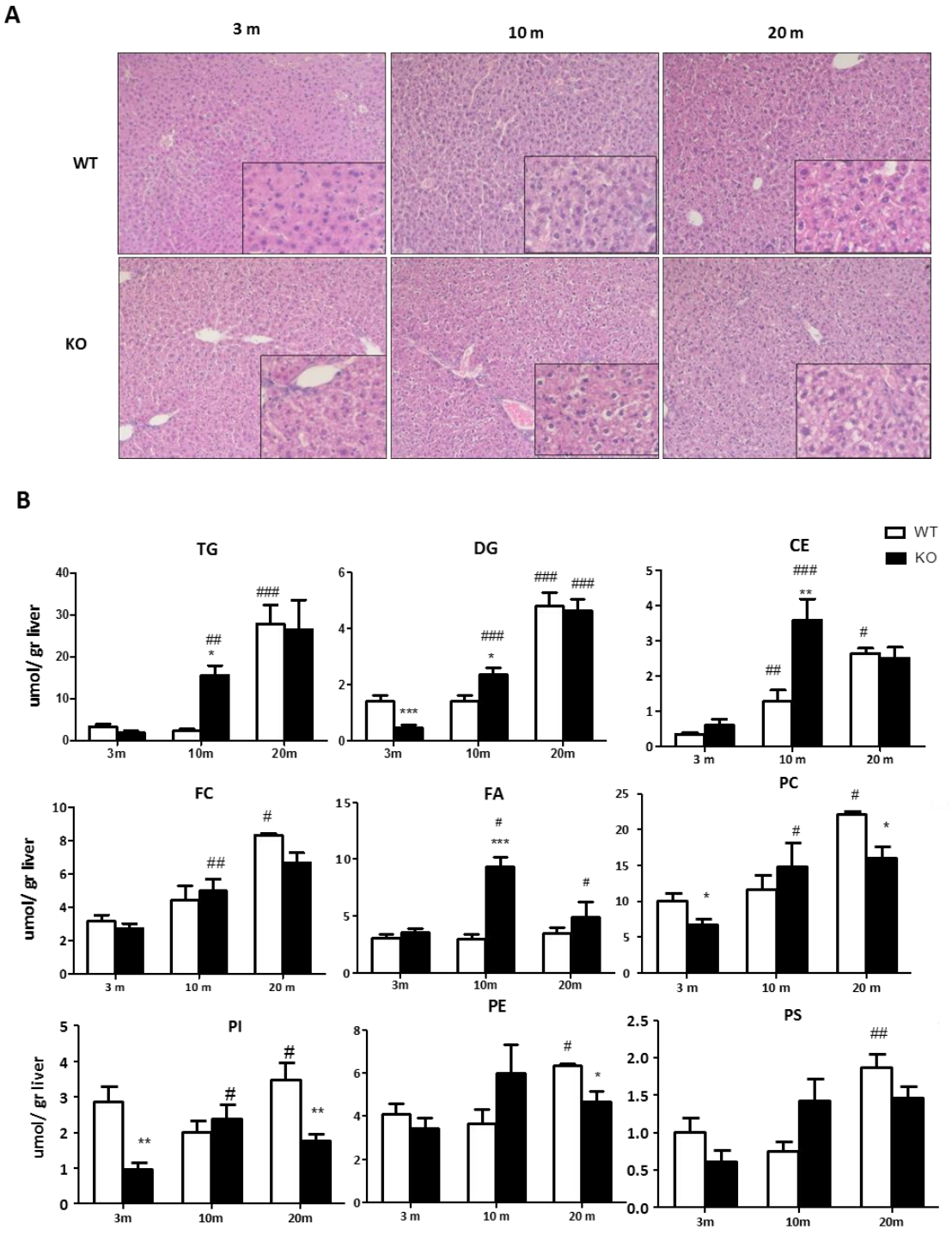

Figure E.12 Liver lipid concentration in OPN-KO and WT mice during aging. (A) H&E staining was performed to study the histology of the liver. Lipids were extracted from liver homogenates and triglycerides (TG), cholesteryl ester (CE), diglycerides (DG), fatty acids (FA), free cholesterol (FC), phosphatidylcholine (PC), phosphatidylethanolamine (PE), phosphatidylserine (PS) and phosphatidylinositol (PI) were separated and quantified. Values are means ±SEM of n=4-8. Significant differences are denoted by *p<0.05, **p<0.01 and ***p<0.001 when comparing genotypes of the same age group, and #p<0.05, ##p<0.01 and ###p<0.001 when comparing with previous age group in the same genotype (Student's t test).

3.2.2 20 month-old OPN-KO mice show increased fibrosis

Next, we analyzed if together with the lipid accumulation there were other markers of NAFLD progression such as fibrosis or inflammation. The Sirius red staining showed that fibrosis was increased in 20 m OPN-KO mice when compared to their age-matched WT or with 10 m OPN-KO mice (Fig E.13A). In contrast, the F4/80, a marker of macrophages and Kupffer cells, showed no changes between WT and OPN-KO mice (Fig E.13B). Taken together, these results show that OPN might be involved in the age-associated hepatosteatosis and its progression to further stages of the liver disease.

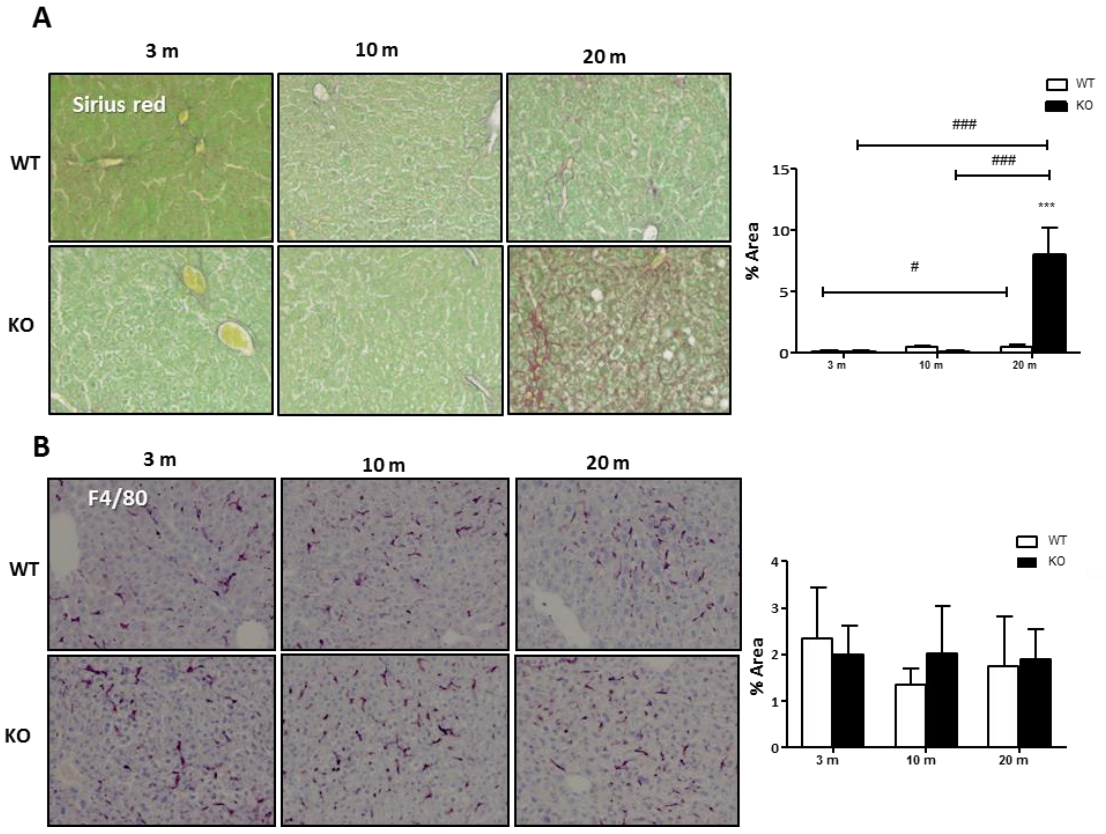

Figure E.13 Liver fibrosis and F4/80 histochemical analysis in OPN-KO and WT mice during aging. (A) Sirius Red and (B) F4/80 stainings were performed to assess fibrosis and inflammation. Values are means ±SEM of n=4-8. Significant differences are denoted by *p<0.05, **p<0.01 and ***p<0.001 when comparing genotypes of the same age group, and #p<0.05, ##p<0.01 and ###p<0.001 when comparing with previous age group in the same genotype (Student's t test).

3.3 Osteopontin deficiency results in several metabolic changes involved in the early disease progression during aging

Metabolic dysregulation is a hallmark for NAFLD development and progression. When the capacity of the liver to handle the excessive energy uptake from metabolic substrates is compromised, the liver starts accumulating lipids and other toxic metabolites. This will induce stress that drives liver damage, fibrogenesis and other harmful effects. Here, we have observed that OPN is required to slow down the development of age-associated hepatosteatosis. We wanted to understand the mechanism involved. For this, 10 m mice were used since it was the age in which deficiency of OPN induced increased lipid accumulation.

3.3.1 Metabolic pathways associated with the liver lipid accumulation in the OPN-KO mice

3.3.1.1 Increased de novo lipogenesis in hepatocytes is associated with the lipid storage in the OPN-KO mice liver

Taking into account that an increased lipogenesis might explain the increased lipid concentration in the liver, we analyzed the de novo lipogenesis (DNL) from acetate in purified hepatocytes from 10 m WT and OPN-KO mice. TG, DG, CE and PL de novo synthesis was increased in 10 m OPN-KO mice hepatocytes (Fig E.14A). In concordance with this, protein levels of the fatty acid synthase (FAS), the enzyme that catalyzes the fatty acid synthesis, was augmented, while no changes were observed in the total or phosphorylated levels of ACC in OPN-KO mice livers (Fig E.14B).

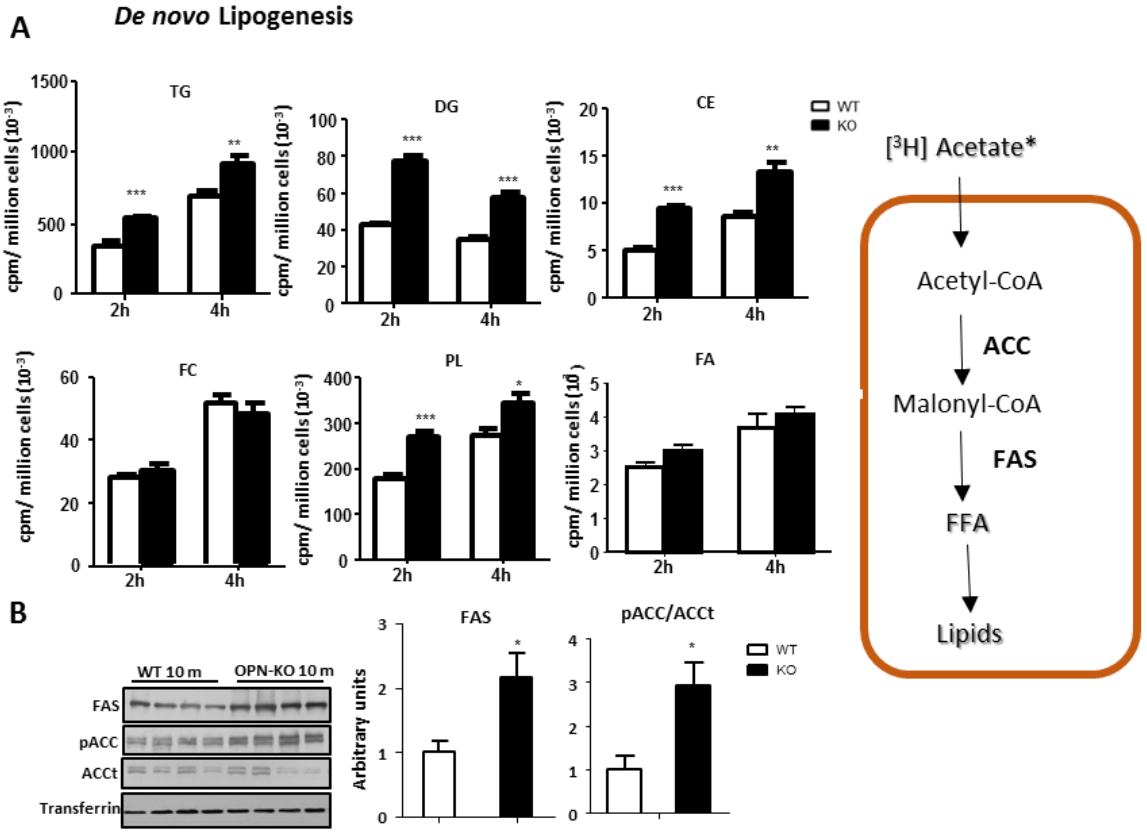

Figure E.14 De novo lipogenesis (DNL) is increased in 10 month-old (m) OPN-KO mice. (A) Hepatocytes isolated from both 10 m WT and OPN-KO mice were cultured in medium with [^{3}H]acetate for 2 and 4 h. Lipids were extracted and radioactivity incorporated into triglycerides (TG), diglycerides (DG), cholesteryl ester (CE), diglycerides (DG), fatty acids (FA), free colesterol (FC), phospholipids (PL) was assesed by liquid scintillation. (B) Fatty acid synthase (FAS) and acetyl-CoA carboxylase (ACCt) and its phosphorylated form (pACC) protein levels were assesed by inmunoblotting using transferrin as loading control. Values are means ±SEM of n=6-8. Significant differences are denoted by *p<0.05, **p<0.01 and ***p<0.001 when comparing 10 m WT and OPN-KO mice (Student's t test).

3.3.1.2 Incorporation of oleate into triglyceride and phospholipids is increased in OPN-KO mice

During esterification FAs are added to glycerol 3-phosphate to finally synthesize TG or PLs; or to Chol for the formation of CE. Thus, the esterification of fatty acids into TG, CE and PLs was studied in purified hepatocytes of 10 m OPN-KO and WT mice. In addition, activity of key enzymes that control esterification and hydrolysis of lipids was analyzed. First, we analyzed the esterification flux in TG and synthetic and hydrolytic enzymes activity. Esterification of oleate into TG was increased in OPN-KO mice (Fig E.15A) even though diglyceride acyltransferase (DGAT) activity, which catalyzes the formation of triglycerides from diglycerides and acyl-CoA, was not changed (Fig E.15B). Regarding hydrolytic enzymes, the only activity that changed was the cytosolic triglyceride hydrolase (TGH), which was increased in 10 m OPN-KO mice (Fig E.15C). However, the microsomal and lysosomal TGH activity maintained unaltered (Fig E.15C). The esterification of oleate into CE remained unchanged

(Fig E.16A), as well as the synthetic and hydrolytic enzyme activities involved in CE metabolism (Fig E.16B, C). Phospholipid metabolism was analyzed too. The oleate esterification was increased for both, PC and PE (Fig E.17A). However, the phosphatidylethanolamine N-methyltransferase (PEMT) activity, in charge of converting phosphatidylethanolamine (PE) to phosphatidylcholine (PC) in the liver, did not change (Fig E.17B).

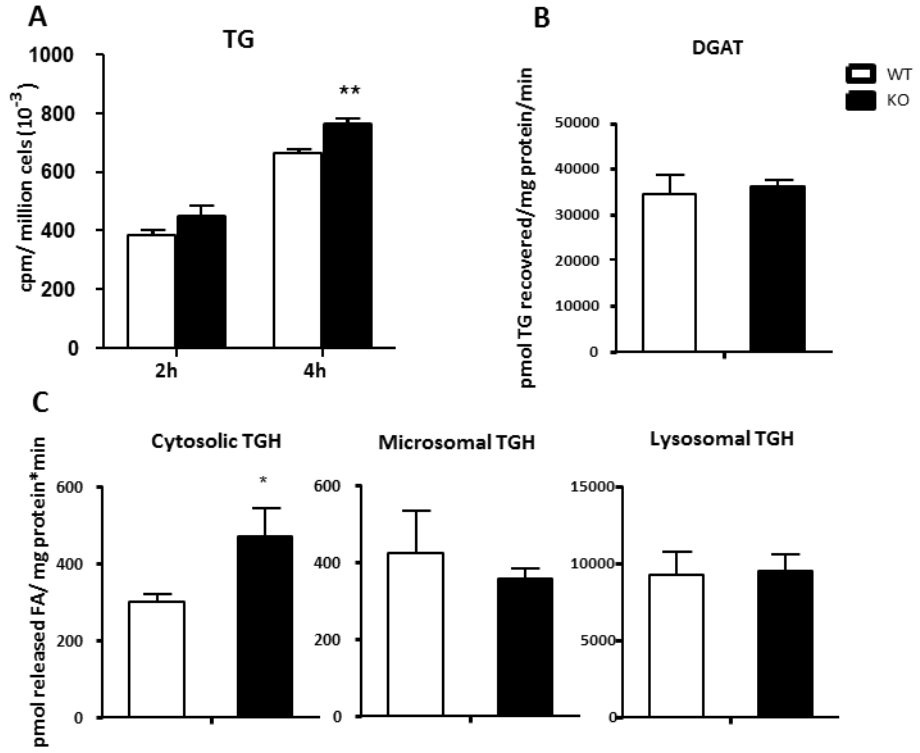

Figure E.15 Oleate esterification and liver enzyme activities in 10 month-old (m) WT and OPN-KO hepatocytes. (A) Oleate esterification in triglyceride (TG), (B) diglyceride acyltransferase (DGAT) and (C) cytosolic, neutral and acid triglyceride lipase (TGH) enzyme activities were determined using radiometric assays. Values are means ±SEM of n=6-8. Significant differences are denoted by *p<0.05, **p<0.01 and ***p<0.001 when comparing 10 m WT and OPN-KO mice (Student's t test).

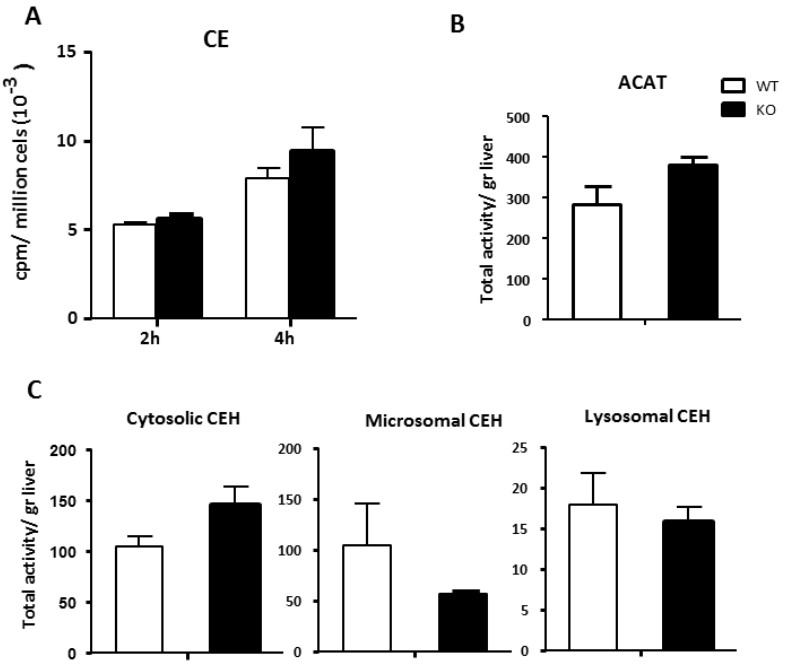

Figure E.16 Oleate esterification and liver enzyme activities in 10 month-old (m) WT and OPN-KO hepatocytes. (A) Oleate esterification in cholesteryl ester (CE), (B) acyl-CoA cholesteryl acyltransferase (ACAT) and (C) cytosolic, neutral and acid cholesteryl ester hydrolase (CEH) activities were determined using radiometric assays. Values are means ±SEM of n=6-8. Significant differences are denoted by *p<0.05, **p<0.01 and ***p<0.001 when comparing 10 m WT and OPN-KO mice (Student's t test).

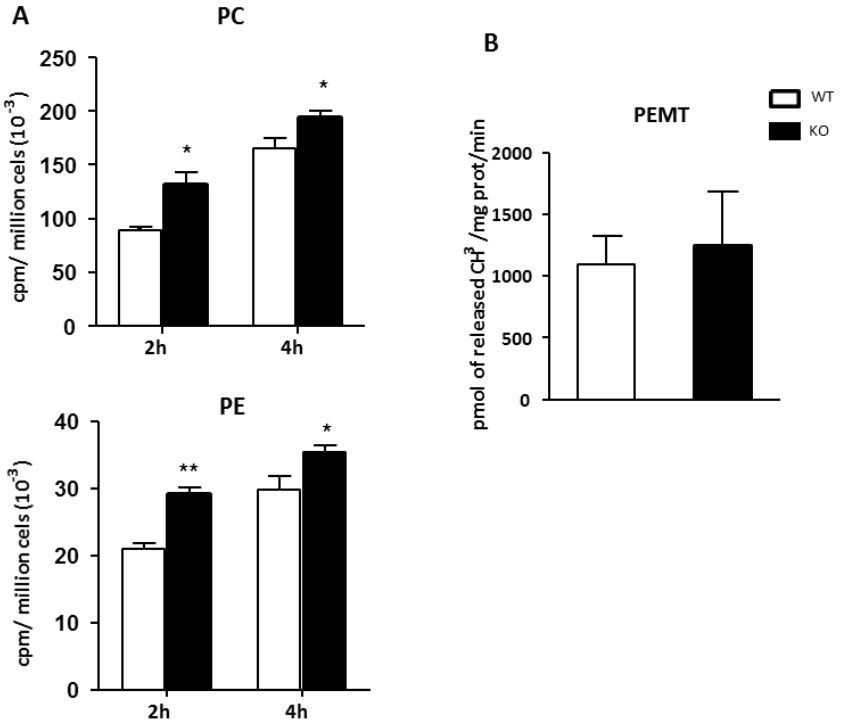

Figure E.17 Oleate esterification and liver enzyme activities in 10 month-old (m) WT and OPN-KO hepatocytes. (A) Oleate esterification in phosphatidylcholine (PC) and in phosphatidylethanolamine (PE) and (B) Phosphatidylethanolamine N-methyltransferase (PEMT) activity was determined using radiometric assays. Values are means ±SEM of n=6-8. Significant differences are denoted by *p<0.05, **p<0.01 and ***p<0.001 when comparing 10 m WT and OPN-KO mice (Student's t test).

3.3.1.3 Fatty acid beta oxidation rate is not altered in 10 month-old OPN-KO mice

The increased cytosolic TGH activity (shown in 3.3.1.2) will provide more FA, that among others, could be catabolized through beta oxidation (β-oxidation). Thus, palmitate β-oxidation was assessed in 10 m mice livers. We analyzed the liver palmitate β-oxidation rate together with the serum ketone bodies (KB), which are a product of β-oxidation and are produced in the mitochondria of liver cells. β-oxidation was not altered, since no changes were found in the acid soluble metabolites (ASM), the CO_2 production (Fig E.18A), or in circulating KB concentration (Fig E.18B). The AMP-activated protein kinase (AMPK) is a sensor of cellular energy status and acts as a metabolic master switch, that when activated, promotes fatty acid oxidation. There were no changes in AMPK phosphorylation (Fig E.18C) as in fatty acid oxidation. Thus, alteration of the β-oxidation was discarded as one of the driving mechanisms for the observed phenotype.

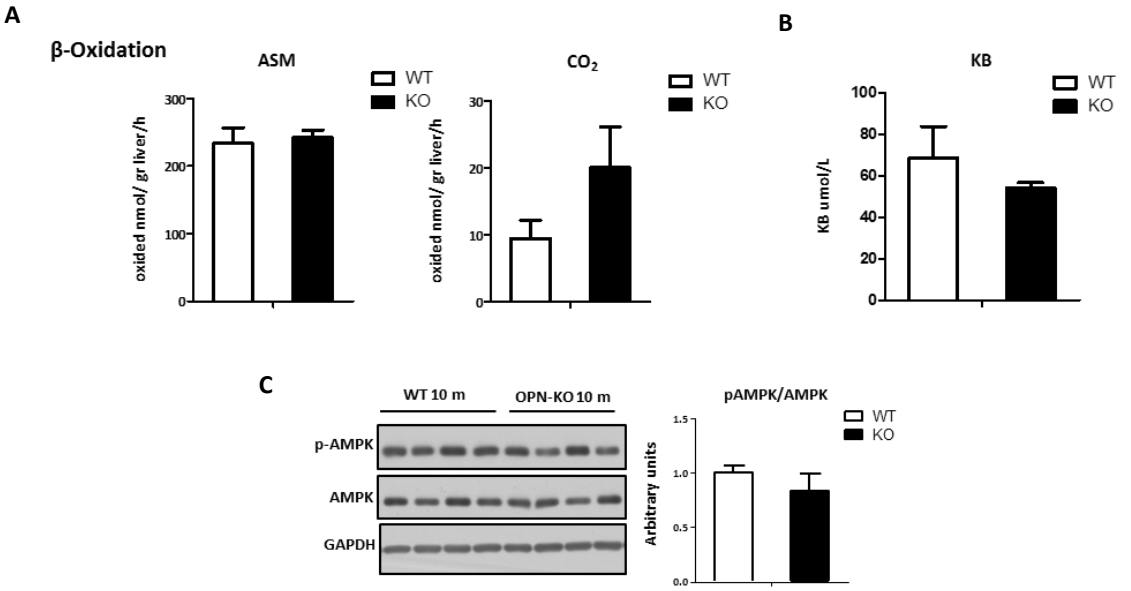

Figure E.18 Beta oxidation is not altered in 10 month-old (m) OPN-KO mice. (A) Fatty acid oxidation assay was performed and the released radioactive acid soluble metabolites (ASM) and CO_2 were quantified. (B) Serum ketone bodies (KB) concentration was quantified. Values are means ±SEM of n= 6. (C) Inmunoblot analysis of phospho/total AMPK phospho/total protein from liver extract were assesed using transferrin as loading control. Values are means ±SEM of n=6-8. Significant differences are denoted by *p<0.05, **p<0.01 and ***p<0.001 when comparing 10 m WT and OPN-KO mice (Student's t test).

3.3.1.4 Several bile acid species and CYP7A1 levels are increased in 10 month-old OPN-KO mice.

We have shown how OPN directly regulates CYP7A1 in hepatocytes via the FAK/AKT signaling pathway, thus, regulating the Chol and BA metabolism. In order to analyze whether this process was altered, we analyzed the liver bile acid composition, and observed in OPN-KO mice an increase of the liver free BA concentration, and a trend towards increase in the total BA concentration (Fig E.19A)

(Table E.3). In concordance with the increased synthesis of BA and our previous results, we also observed an increase of the protein levels of CYP7A1 in the OPN-KO mice (Fig E.19B). This enzyme is in charge of the conversion of Chol into BA and could be regulating Chol concentration in the OPN-KO mice (Nunez-Garcia et al., 2017). As shown earlier, unlike most liver lipids, which are increased in the OPN-KO mice, FC concentration is not increased in 10 m OPN-KO mice when compared to WT mice. Thus, CYP7A1 might be regulating Chol levels by diverting it towards BA synthesis in the OPN-KO mice. In young OPN-KO mice, the FAK/AKT pathway was regulating CYP7A1 levels. Thus, in order to determine whether the implicated signaling pathway for the increased CYP7A1 levels in 10 m mice was indeed FAK/AKT, we analyzed AKT phosphorylation and observed that it was decreased and thus, could be the cause for increased CYP7A1 levels, as observed in younger mice (Fig E.19C).

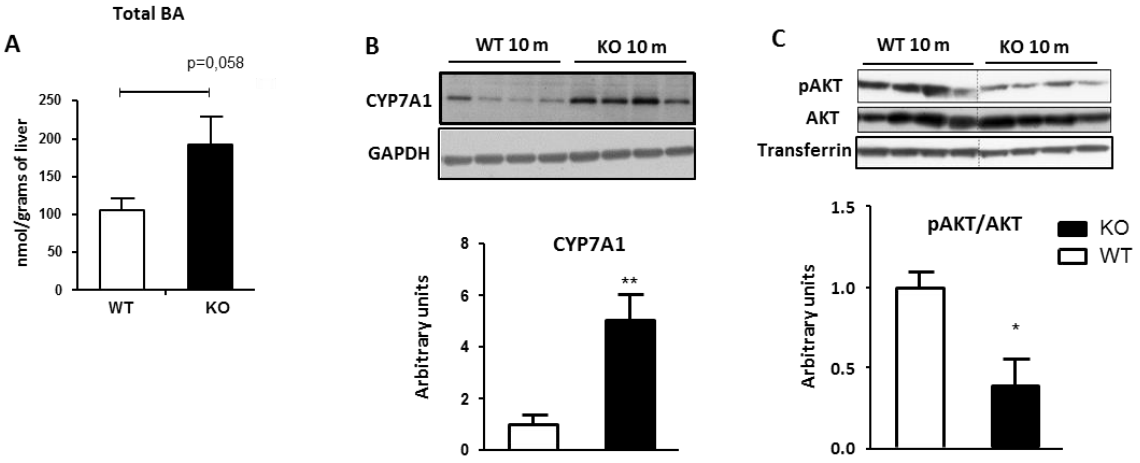

Figure E.19 Liver bile acid concentration and CYP7A1 levels in 10 month-old WT and OPN-KO mice. (A) Total bile acids were quantified. (B) Cholesterol 7 alpha-hydroxylase (CYP7A1) protein levels were assessed by inmunoblotting using GAPDH as loading control (C) Phosphorylated and total AKT protein levels were assessed by inmunoblotting using transferrin as loading control . Values are means ±SEM of n= 4-6. Significant differences are denoted by *p<0.05, **p<0.01 and ***p<0.001 when comparing 10 m WT and OPN-KO mice (Student's t test).

Table E.3 Liver bile acid concentration in OPN-KO and WT mice.

BA (nmol/g tissue)	Species	WT 10m	OPN-KO 10m
Bile Acid	Total	106,19	192,14
Tauroconjugated	Total	102,17	179,85
	TαMC	7,25	11,84
	TβMC	42,31	78,69
	TUDC	3,01	6,648*
	THyoC	0,0156	0,0007
	THyoDC	1,19	0,99
	TCA	38,32	66,32
	TQDCA	4,74	7,23
	TDCA	5,15	7,92
	TLCA	0,18	0,22
	Total	0,10	0,07
Glicoconjugated	GUDC	0,003	0,003
	GC	0,093	0,063
	GQDC	0,001	0,004
	GDC	0,002	0,003
Free	Total	3,93	12,22***
	UDCA	0,60	1,431*
	αMCA	1,23	1,72
	βMCA	0,80	2,11*
	CA	0,98	6,5***
	CDCA	0,21	0,29
	DCA	0,07	0,11
	HDCA	0,00	0,02
	LCA	0,03	0,03

Values are means ± SEM in nmol/gram of liver from 4 animals per group. Significant differences between OPN- KO and WT mice are denoted by *p <0.05. CA, cholic acid; CDCA, chenodeoxycholic acid; DCA, deoxycholic acid; HDCA, hyodeoxycholic acid; LCA, lithocholic acid; UDCA, ursodeoxycholic acid; αMCA, alpha-muricholic acid; βMCA, beta-muricholic acid. All the species starting with T or G correspond to Tauro- or Glyco-conjugated BAs, respectively.

3.3.2 Altered mechanisms related to aging in OPN-KO mice.

3.3.2.1 Lipid accumulation in the OPN-KO mice during aging is associated to increased markers of senescence.

Cellular senescence is a state of irreversible cell-cycle arrest combined with the secretion of proinflammatory cytokines and mitochondrial dysfunction. Senescent cells contribute to age-related tissue degeneration and their accumulation promotes hepatic fat accumulation and steatosis (Ogrodnik et al., 2017). We have shown that OPN might have a role in senescence, and since OPN-KO mice show an early lipid accumulation profile compared to WT mice, we wanted to know whether the OPN-KO mice accumulated more senescent cells. For this, we analyzed the senescence markers p21 and senescence associated β-Galactosidase (SA- β-Galactosidase) in 10 m WT and OPN-KO mice. We observed that both markers were increased in OPN deficient mice (Fig E.20). Because the accumulation of senescent cells promotes steatosis, the increase of senescent cells in the OPN-KO liver could be linked with the observed lipid accumulation.

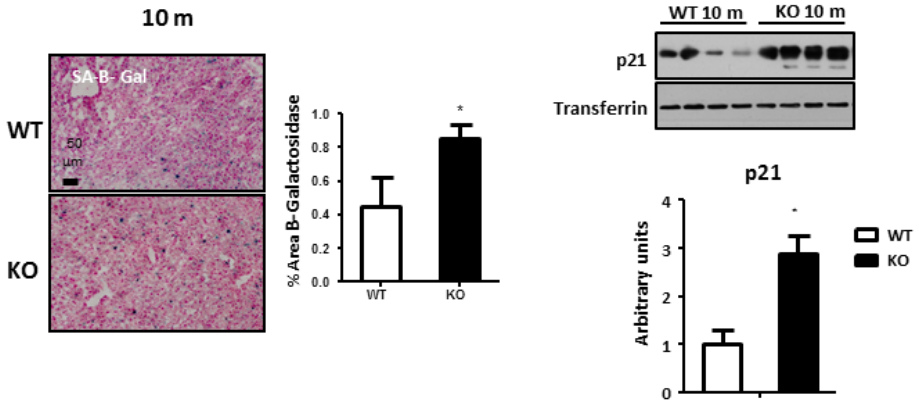

Figure E.20 Senescence markers in 10 month-old (m) mice. Liver SA β-Galactosidase positive area percentage was quantified. Immunoblot analysis of p21 protein from liver extract was assessed using transferrin as loading control. Values are means ±SEM of n=6. Significant differences are denoted by *p<0.05, **p<0.01 and ***p<0.001 when comparing 10 m WT and OPN-KO mice (Student's t test).

3.3.2.2 ER stress is associated to the early senescence and lipid accumulation in OPN-KO mice liver.

Loss of proteostasis is a hallmark of aging. The endoplasmic reticulum (ER) is an important organelle for regulating calcium homeostasis, lipid homeostasis, protein synthesis, and post-translational modifications and trafficking. Many insults can disturb ER homeostasis, which leads to ER stress. This stress and the unfolded protein response (UPR) pathways are involved in lipid metabolism and lipotoxocity. In fact, it can modulate expression levels of key enzymes involved in lipid synthesis or modification (Han & Kaufman, 2016). It is well stablished that lipid accumulation can disturb the endoplasmic reticulum function generating ER stress. If this stress is defective or chronic, there can be an increased transcription of lipogenic genes, and a decrease of fatty acid oxidation genes. Thus, ER stress can increase the accumulation of lipids in hepatocytes, which in turn exacerbates the ER stress increasing the lipid accumulation, generating a vicious cycle. ER stress response has been proposed to play a crucial role in both the development of steatosis and progression to nonalcoholic steatohepatitis (NASH).

We wanted to analyze whether OPN deficiency during aging was linked to ER stress development. When we analyzed ER stress markers in 10 m mice we found that phosphorylation of eIF2a (peIF2a) was increased in OPN-KO mice and the chaperone GRP78 levels were decreased, which can contribute to a worse response to ER stress (Fig E.21A). Several studies have demonstrated that the decrease in chaperone number diminishes the efficacy to deal with unfolded proteins. In addition, the decrease in the number of chaperones is associated with aging, which can be one of the causes of the increase in ER stress with aging. Some studies have shown that forced expression of GRP78

attenuates steatosis by inhibiting sterol regulatory element-binding protein (SREBP-1c) (Kammoun et al., 2009). Thus, the reduced GRP78 levels could increase the steatosis by activation of SREBP-1c, and thus, lipogenic genes. In concordance with this, we showed earlier increased DNL and FAS protein levels, which are regulated by SREBP-1c. Besides, a chronically active ER stress can lead to apoptosis. Thus, in order to know whether the observed ER stress could be causing apoptosis, we analyzed caspase 12 cleavage, which remained unchanged when comparing genotypes. Besides, we analyzed if the ER stress observed at the intermediate age in the OPN-KO mice was also observed in the younger mice, in order to identify if the ER stress was prior to the steatosis and thus, a cause of it. The results showed that any of the changes observed in 10 m mice, were present in 3 m mice (Fig E.21B).

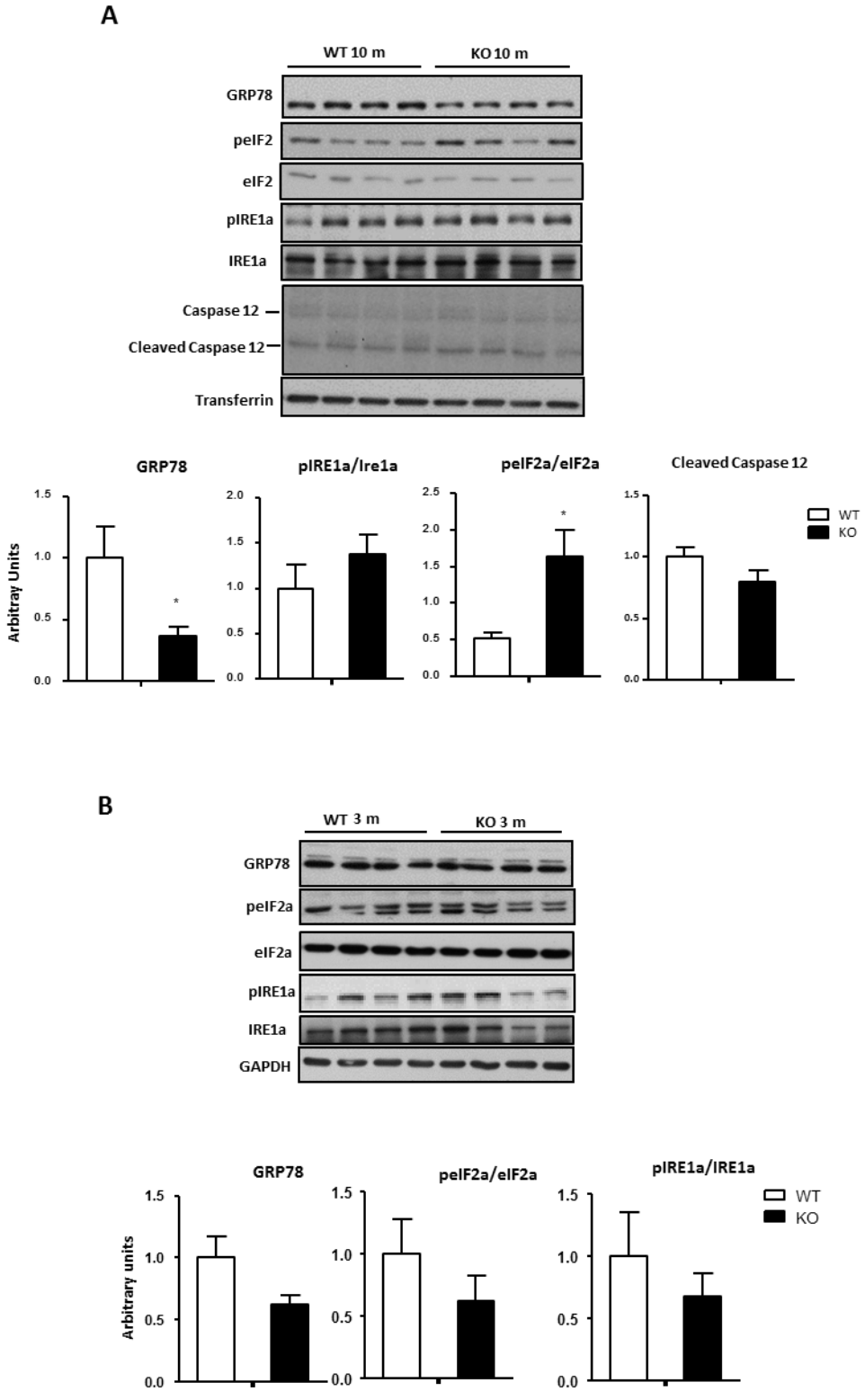

Figure E.21 ER stress markers proteins. (A) Immunoblot analysis of GRP78, total and phosphorylated peIF2a and IRe1a and cleaved caspase 12 protein from liver extract was assessed using transferrin or glyceraldehyde-3-phosphate dehydrogenase (GAPDH) as loading control in 10 month-old (m) and (B) 3 m WT and OPN-KO mice. Values are means ±SEM of n=6-8. Significant differences are denoted by *p<0.05, **p<0.01 and ***p<0.001 when comparing WT and OPN-KO mice (Student's t test).

3.3.2.3 Nutrient sensing is dysregulated in 10 month-old OPN-KO mice.

An altered nutrient sensing is other of the metabolic distinctives of aging. AMPK and mTOR are key metabolic switches. mTOR is part of the TORC1 and 2 complexes which activation is linked to lipogenesis activation. When analyzing this pathway, we observed that not only was not active, but markedly decreased in the 10 m OPN-KO mice (Fig E.22). Therefore, we discarded the activation of this pathway as an explanation for the increased lipogenesis. However, the observed decrease in S6K phosphorylation (Fig E.22) supports the hypothesis that the 10 m OPN-KO mice are dealing with ER stress. Usually under ER stress conditions, the unfolded protein response (UPR) lowers the protein synthesis as a coping mechanism.

Taking together all these results, at 10 m, OPN-KO mice livers exhibit ER stress linked to decreased chaperone levels. This situation could aggravate the pro-lipogenic environment worsening the progression of the liver disease. Therefore, deficiency of OPN induces early lipid accumulation via increased DNL and ER stress; thus, OPN might be necessary to cope with the insults that the organism has to face as it ages.

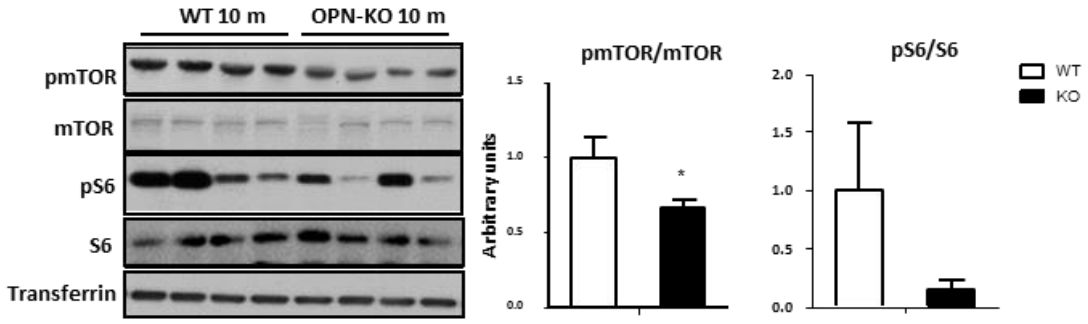

Figure E.22 There is a dysregulated nutrient sensing in the 10 month-old (m) OPN-KO mice. Inmunoblot analysis of total and phosphorylated mTOR and S6 protein from liver extract were assessed using transferrin as loading control. Values are means ±SEM of n=6-8. Significant differences are denoted by *p<0.05, **p<0.01 and ***p<0.001 when comparing WT and OPN-KO mice (Student's t test).

3.4 Osteopontin knockdown in HepG2 cells increases cell vulnerability to senescence by downregulating the ER stress response.

In order to analyze the effect of OPN deficiency in ER stress generation and chaperone levels upon senescence; OPN (SPP1 gene) was silenced in HepG2 cells, which were treated with palbociclib to analyze the effect in senescent cells. In order to simulate a lipid rich environment we treated a group of cells with palmitic acid 200 µM. Knockdown of OPN did not change the levels of GRP78 chaperone (Fig E.23A). However, when treating cells with palbociclib, GRP78 chaperone level decreased in OPN silenced cells (Fig E.23B). Moreover, when OPN was silenced, the decrease in chaperone levels was even greater when senescent cells where challenged with palmitic acid. In this situation, the decrease in the chaperone was 5 times greater when compared with control-silenced cells. In addition, we did not observe the activation of eIF2a pathway in any of these situations, showing that the decrease in the chaperone levels is prior to the activation of this UPR branch (Fig E.23C).

Thus, while the siCtrl group is able in both conditions to deal with the lipid rich environment without fluctuations in their chaperone capacity, the OPN silenced cells are more susceptible to the chaperone decrease and thus to ER stress. Therefore, senescence induction in absence of OPN decreases chaperone levels, and consequently the capacity of the cell to properly respond to ER stressors.

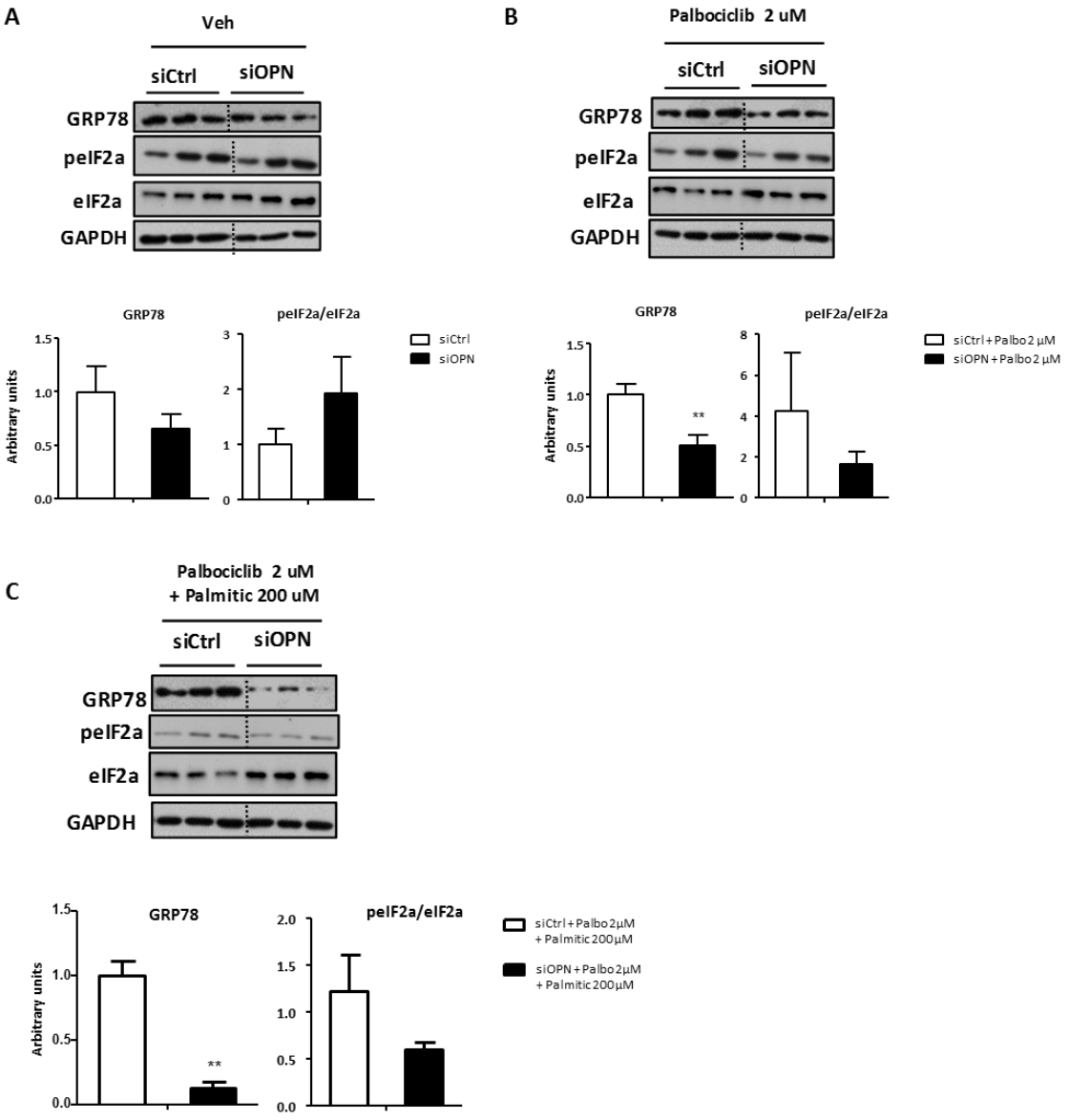

Figure E.23 OPN deficiency in senescent cells decreases GRP78 expression. (A) In HepG2 cells GRP78, phosphorylated eIF2a (peIF2a), and eIF2a protein levels were measured by immunoblotting using glyceraldehyde -3-phosphate dehydrogenase (GAPDH) as loading control were measured in siCtrl and siOPN HepG2 cells, (B) in siCtrl and siOPN HepG2 cells treated with palbociclib (Palbo) for inducing senescence and (C) in siCtrl and siOPN HepG2 cells treated with Palbo and palmitic acid. Values are means ±SEM of n=4. Significant differences are denoted by *p<0.05, **p<0.01 and ***p<0.001 (Student's t test).

3.5 In old mice, high fat diet aggravates the NAFLD progression when OPN is absent.

We have shown that OPN deficiency at 10 m is associated with increased lipid storage, *de novo* lipogenesis and decreased GRP78 levels, also decreased in vitro when silencing OPN and inducing senescence to HepG2 cells. Next, we wanted to analyze the consequences of this phenotype in old mice.

3.5.1 Feeding a high fat diet (HFD) induces an advanced progression of liver disease in 20 month-old OPN-KO mice.

We generated a group of WT aged mice fed a high fat diet (HFD) for 16 weeks prior to the sacrifice at 20 m. We observed that when feeding a HFD the circulating concentration of OPN in 20 m mice was higher than in those fed a chow diet (CD) (Fig E.24). Thus, in order to ascertain if OPN deficiency increased the vulnerability to age-associated NAFLD development, we generated other group of OPN-KO aged mice fed a high fat diet (HFD). We analyzed body parameters and found that the body weight gain in response to the HFD was similar in both genotypes. Serum ALT increased in mice fed a HFD when compared to the CD fed mice in both genotypes but there were no differences between OPN-KO and WT mice (Table E.4). By contrast, serum AST was increased in HFD fed OPN-KO mice compared to their WTs. Serum lipid analysis showed an increase of TG in OPN-KO mice in HFD condition compared to their WTs, which also happened in 10 and 20 m mice (Table E.4).

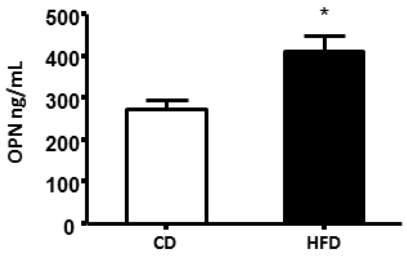

Figure E.24 HFD induces increased circulating OPN levels in 20 month-old (m) mice. Serum OPN of chow diet (CD) and high fat diet (HFD) fed 20 m wild type (WT) mice was quantified by ELISA. Values are means ±SEM of n=4-6. Significant differences are denoted by *p<0.05, **p<0.01 and ***p<0.001 when comparing CD and HFD WT mice (Student's t test).

Table E.4 Body and serum parameters of HFD 20 month-old (m) WT and OPN-KO mice

	20 m HFD	
	WT	**OPN-KO**
Weight (g)	46,33	44,71
LW (g)	1,67	1,38
ALT (U/L)	144,40	165,90
AST (U/L)	55,03	95,14*
Serum TG (mg/dL)	69,516	92,20*
Serum NEFA (mg/dL)	15,93	18,03
Serum Cho (mg/dL)	144,60	171,73

Body weight, liver weight (LW), serum alanine aminotransferase (ALT), aspartate aminotransferase (AST), serum TG, NEFA and Cho are represented. Values are means ±SEM of n=4-6. Significant differences are denoted by *p<0.05, **p<0.01 and ***p<0.001 when comparing 20 m HFD fed WT and OPN-KO mice (Student's t test).

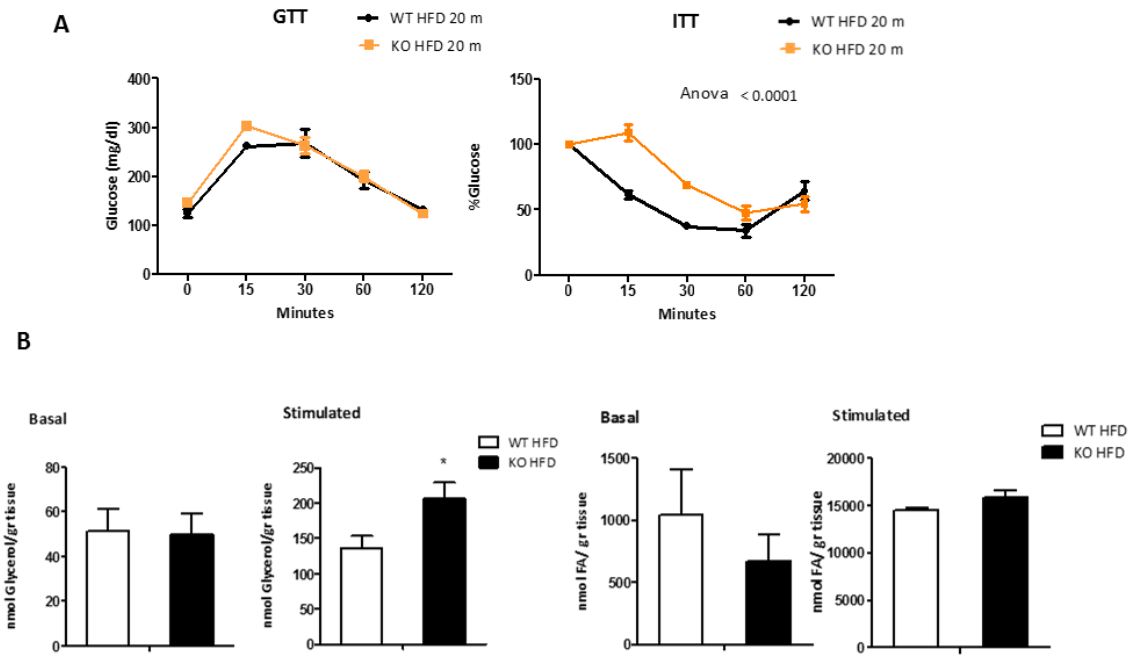

Figure E.25 HFD induces metabolic dysregulation in 20 month-old (m) OPN-KO mice. (A) Glucose (GTT) and insulin tolerance test (ITT) were performed in HFD fed 20 m WT and OPN-KO mice. (B) Lipolysis was measured as the release of glycerol and FFA from WAT pads. Values are means ±SEM of n=4-6. Significant differences are denoted by *p<0.05, **p<0.01 and ***p<0.001 when comparing genotypes (Student's t test). Significant differences in GTT and ITT are denoted by ANOVA test.

While serum FA concentration did not change, serum Chol increased in both genotypes when fed a HFD, but no differences were found between genotypes (Table E.4). ITT analysis in 20 m OPN-KO mice fed a HFD showed that the response to insulin was lower than in WT mice, while the GTT maintained unaltered (Fig E.25A). When stimulating lipolysis in white adipose tissue (WAT), released glycerol was increased in OPN-KO mice, while no changes were found in released FA (Fig E.25B). When liver was analyzed, both HFD fed WT and OPN-KO mice showed the expected increase in hepatic TG (Fig E.26A), while young OPN-KO mice are resistant to hepatosteatosis when fed a HFD (Kiefer et al., 2011; Lancha et al., 2014), in old age this resistance is lost. The evaluation of the liver by an expert histopathologist confirmed the increase in steatosis score in both genotypes when fed a HFD (Fig E.26B). Sirius red staining and the fibrosis score after the trichrome staining (Fig E.26B) showed increased fibrosis in OPN-KO mice compared to their WTs. In terms of inflammation, OPN-KO mice had increased inflammation score compared to their controls (Fig E.26B). In addition, F4/80, a macrophage/ Kupffer marker was higher in HFD fed OPN-KO mice. All together, these results show a worse progression of the disease in the old OPN-KO mice, particularly in the HFD fed group.

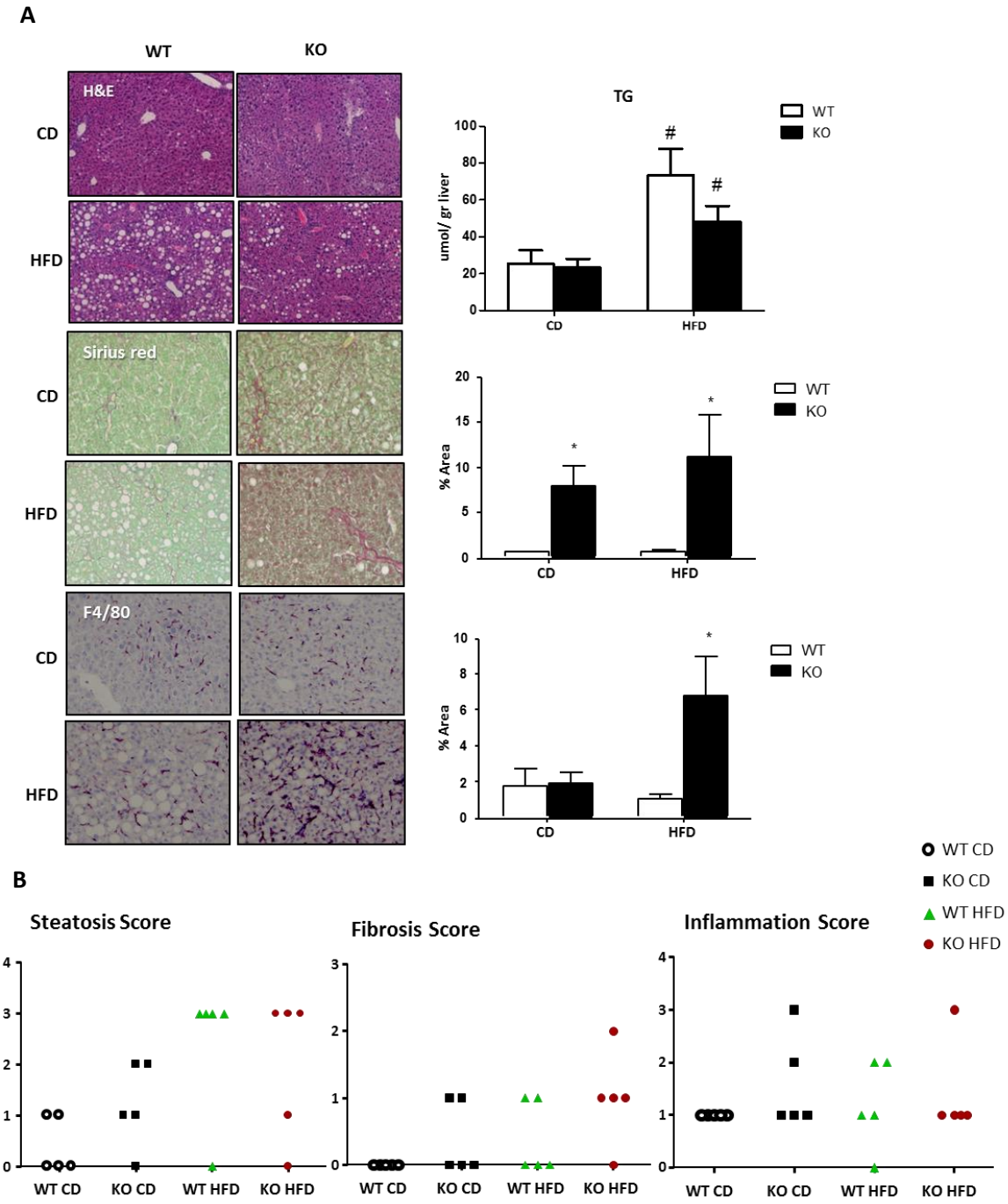

Figure E.26 HFD induces an advanced progression of the disease in 20 month-old (m) OPN-KO mice. (A) H&E, triglycerides (TG) were extracted from liver homogenates and quantified; Sirius Red and F4/80 stainings were performed to assess tissue morphology, fibrosis and inflammation. Values are means ±SEM of n=4-6. Significant differences are denoted by *p<0.05, **p<0.01 and ***p<0.001 when comparing genotypes of the same diet group and #p<0.05, ##p<0.01 and ###p<0.001 when comparing CD and HFD groups of the same genotype (Student's t test). (B) Histopathological study was performed by an expert pathologist. Steatosis, fibrosis and inflammation scores were evaluated. Values are means ±SEM of n=5.

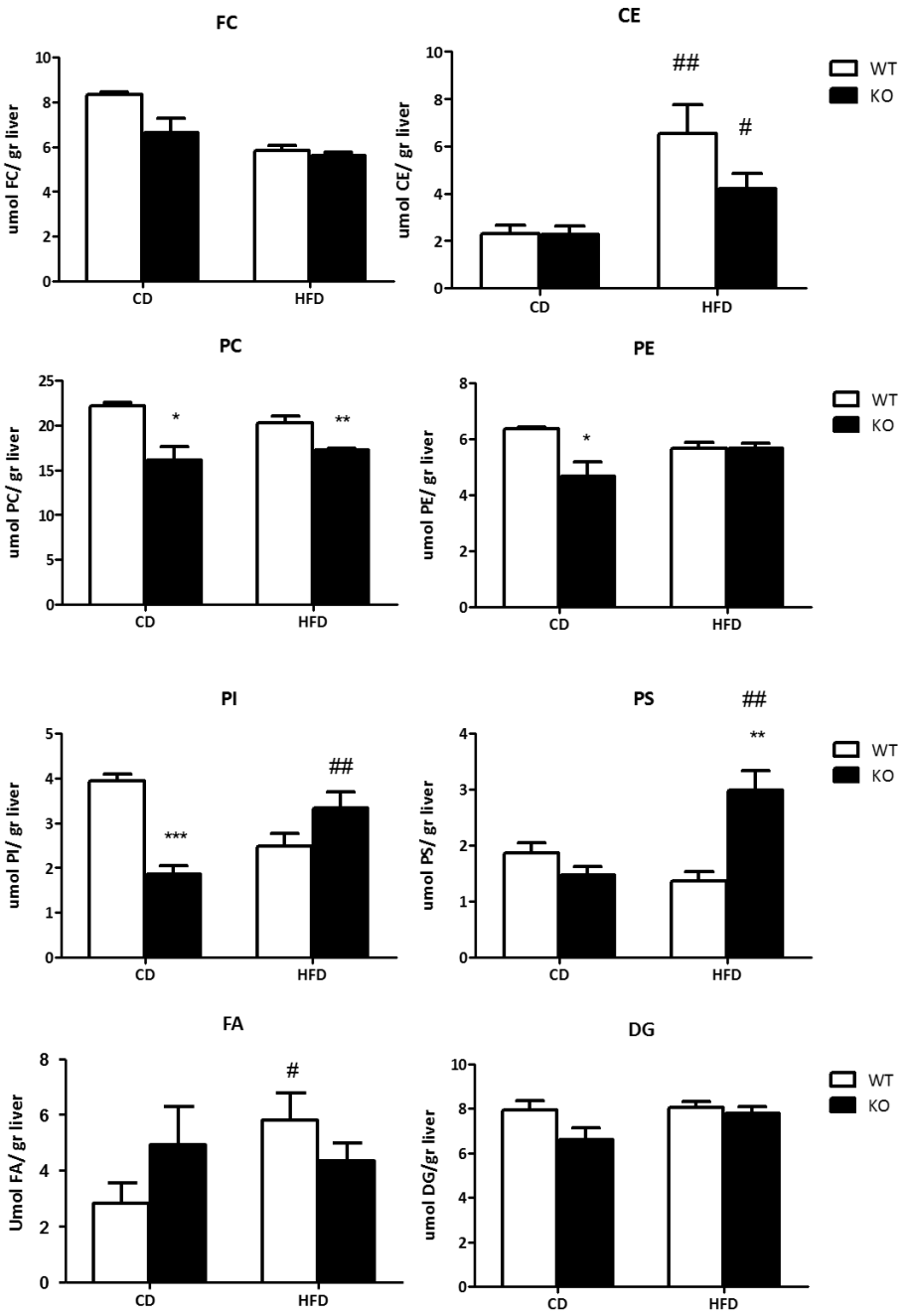

Figure E.27 Liver lipid concentration in 20 month-old (m) mice liver. (A) Lipids were extracted from liver homogenates and free cholesterol (FC), cholesteryl ester (CE), diglycerides (DG), phosphatidylcholine (PC), phosphatidylethanolamine (PE), phosphatidylserine (PS), phosphatidylinositol (PI) and fatty acids (FA) were separated and quantified. Values are means ±SEM of n=4-6. Significant differences are denoted by *p<0.05, **p<0.01 and ***p<0.001 when comparing genotypes of the same diet group and #p<0.05, ##p<0.01 and ###p<0.001 when comparing CD and HFD groups of the same genotype (Student's t test).

Given the observed phenotype, we analyzed the liver lipid profile of 20 m mice. We previously showed (Fig E.27) the liver TG levels, which were increased in HFD fed mice compared with the CD group. CE levels were also increased in HFD fed mice compared to their CD group (Fig E.27). On the

contrary, FC levels did not change in liver. Regarding phospholipids, PC, the most abundant phospholipid was decreased in both CD and HFD OPN-KO mice, whereas the other phospholipids show different profiles. Particularly interesting is the sharp increase in phosphatidylserine (PS) in HFD fed OPN-KO mice.

PS if often related to apoptosis process, and taking into account that 10 m OPN-KO mice show ER stress symptoms and the worsened progression observed at 20 m, we wanted to know if this could lead to liver damage and apoptosis. First, we analyzed protein levels of GRP78 (Fig E.28), which recovered in both CD and HFD OPN-KO mice. Despite this chaperone recovery, gamma-H2AX levels were increased in both CD and HFD OPN-KO mice. In addition, in 20 m HFD fed OPN-KO mice, cleaved caspase 12 was increased compared to the HFD fed WTs. This shows that apoptosis processes and hepatocyte damage are more active in OPN-KO mice than in WT mice. Thus, this reinforces the worsened progression observed in 20 m OPN-KO mice, particularly in the HFD fed group.

Altogether, the results show a worsened progression of the liver disease with aging when OPN is deficient, showing thus, a protective role for OPN in the aging liver. It delays the onset of metabolic alterations and ER stress in liver, preventing liver damage.

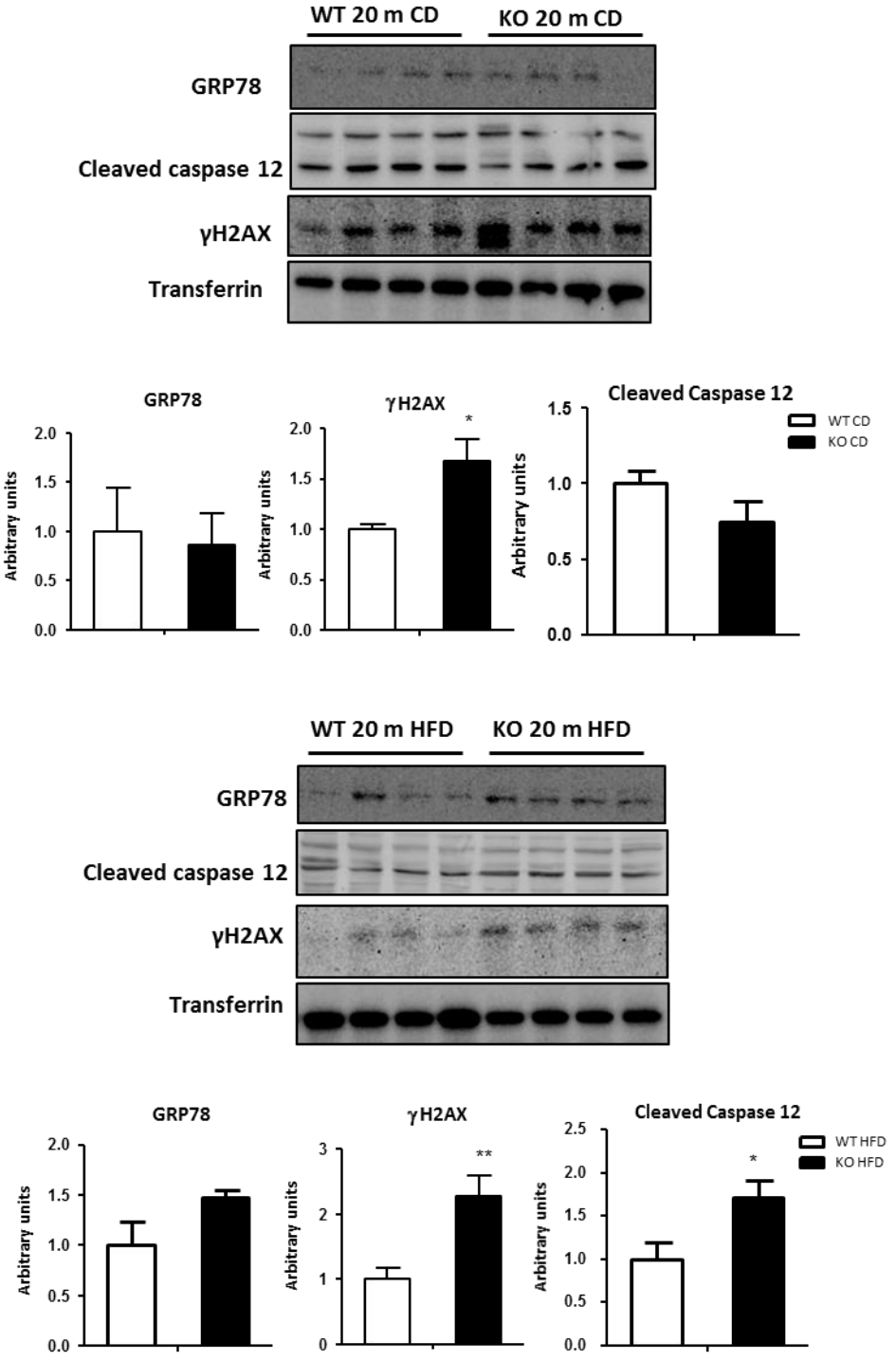

Figure E.28 Damage markers in CD and HFD fed 20 month-old (m) mice liver. Immunoblot analysis of GRP78, Caspase 12 and γH2Ax protein levels from liver extract were assessed using transferrin as loading control in chow diet (CD) and high fat diet (HFD) fed 20 month-old (20 m) mice. Values are means ±SEM of n=4-5. Significant differences are denoted by *p<0.05, **p<0.01 and ***p<0.001 when comparing WT and OPN-KO mice (Student's t test).

3.6 p53 regulates osteopontin expression in liver

3.6.1 Differential hepatic cell line expression of OPN and p53

p53 controls cellular functions and modulates cellular adaptations to stress and is one of the most important tumor suppressor genes. In addition, p53 and other p53 family member, including p63 and p73, controls many metabolic pathways (Napoli & Flores, 2017). Some studies have linked p53 to OPN regulation in fibroblasts (Morimoto, Sasaki, Ishida, Imai, & Tokino, 2002) and in endometrium carcinoma cells (Franco et al., 2017). It has been reported that p53 null mice fed a HFD show increased liver fat content and ER stress markers, and its overexpression improves steatosis and ER stress (Porteiro et al., 2017).

We wanted to analyze whether p53 could regulate OPN expression in liver, for this we analyzed in the Cancer Cell Line Encyclopedia (The Broad Institute of MIT & Harvard) database the mRNA expression of the OPN gene (SPP1) and TP53 gene in several liver cell lines. We observed that the cell line with lower expression of SPP1 was also the cell line with lower expression of TP53 (Fig E.29). While the cell lines that show more expression of p53 have also increased SPP1 expression. This shows that there might be a link between OPN and p53 expression in liver (Fig E.29).

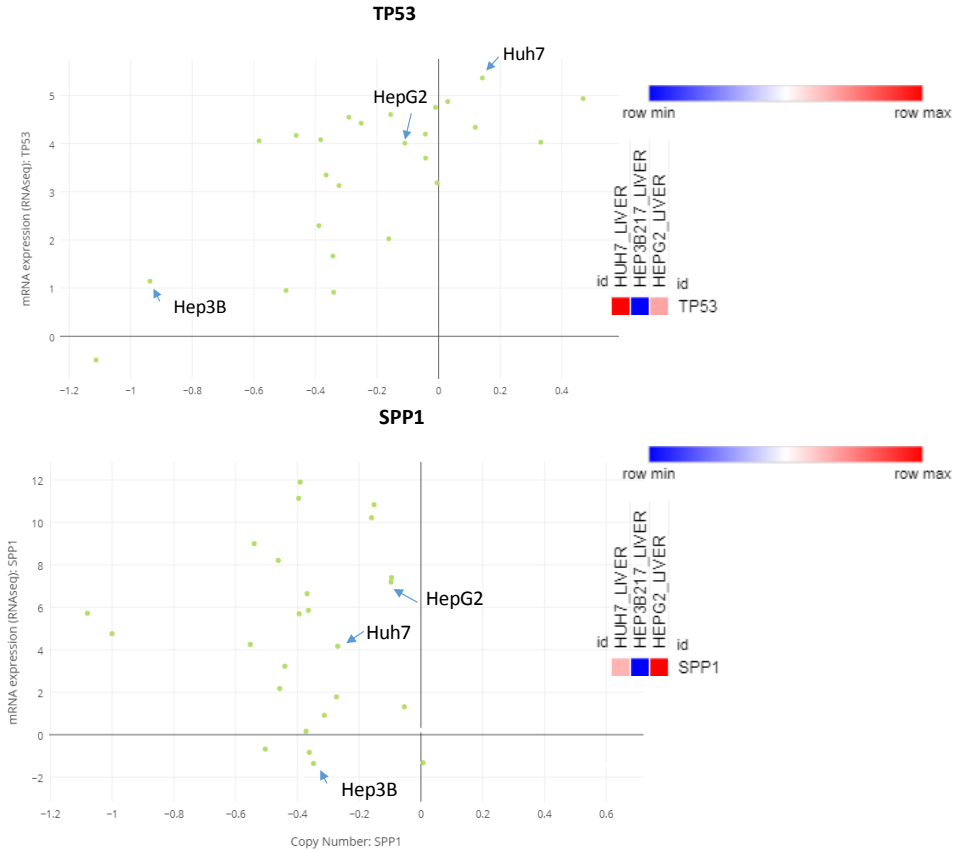

Figure E.29 Differential mRNA expression (RNAseq) of SPP1 and TP53 genes in liver cell lines in liver. SPP1 and TP53 mRNA expression was analyzed in Huh7, Hep3B and HepG2 cell lines. Cancer Cell Line Encyclopedia.

3.6.2 Silencing p53 decreases OPN levels intra and extracellularly

In order to elucidate whether p53 could be regulating OPN, we silenced p53 with a siRNA in HepG2 cells, and observed that OPN levels, both intracellular and secreted were decreased when silencing p53 (Fig E.30A). Interestingly, treating p53-silenced cells with palbocilcib lead to a lower increase of OPN (Fig E.30B) than the increase induced in HepG2 cells (Fig E.30C), showing that p53 might be necessary for the senescence-induced OPN expression. To confirm that p53 could be regulating OPN, we treated Hep3B, that do not express p53, with palbociclib.

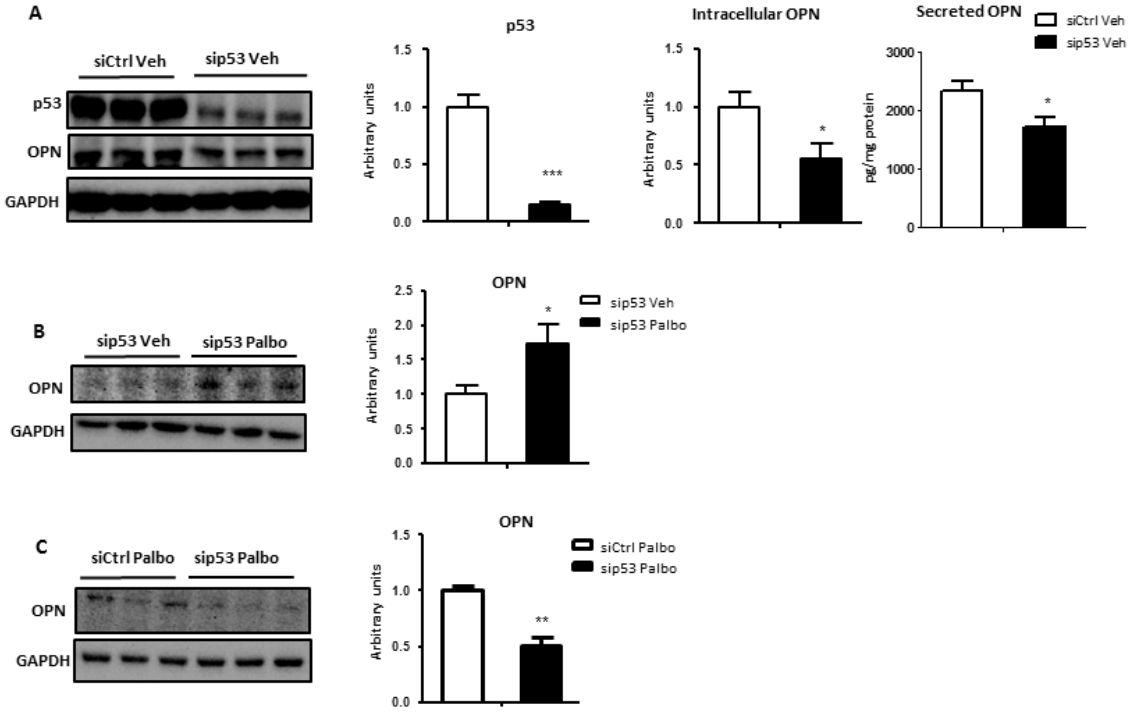

Figure E.30 OPN expression in p53 silenced HepG2 cells. (A) Protein levels of p53 and OPN in siCtrl and sip53 cells were measured by immunoblotting using glyceraldehyde -3-phosphate dehydrogenase (GAPDH) as loading control. Extracellular OPN was measured using an ELISA. (B) Protein levels of OPN were measured in sip53 vehicle (sip53 Veh) and sip53 Palbociclib (sip53 Palbo) treated cells, (C) and in siControl (siCtrl) and sip53 palbocilcib (sip53 Palbo) treated cells. Values are means ±SEM of n=4. Significant differences are denoted by *p<0.05, **p<0.01 and ***p<0.001 (Student's t test).

3.6.3 Palbociclib and H_2O_2 treatment induces the increase in OPN expression and secretion in HepG2 cells, but not in Hep3B cells

We have shown earlier that senescence treatment increases OPN levels in HepG2 cells intra and extracellularly. Hep3B cells, that are p53-null, did not show an increased OPN levels when treated with palbocilcib or H_2O_2 (Fig E.31A). Next, we wanted to analyze whether senescence induction could increase the OPN secretion, because an increased OPN secretion could be one of the causes for the low intracellular OPN expression in Hep3B cells. We observed that HepG2 cells increased OPN secretion to the media when treated with palbociclib or H_2O_2. In contrast, Hep3B cells did not show an increased OPN secretion (Fig E.31B). In fact, OPN secretion levels, even in the vehicle condition were much lower in Hep3B than in HepG2 cells. This result shows that p53 is required for OPN expression under senescent stimuli.

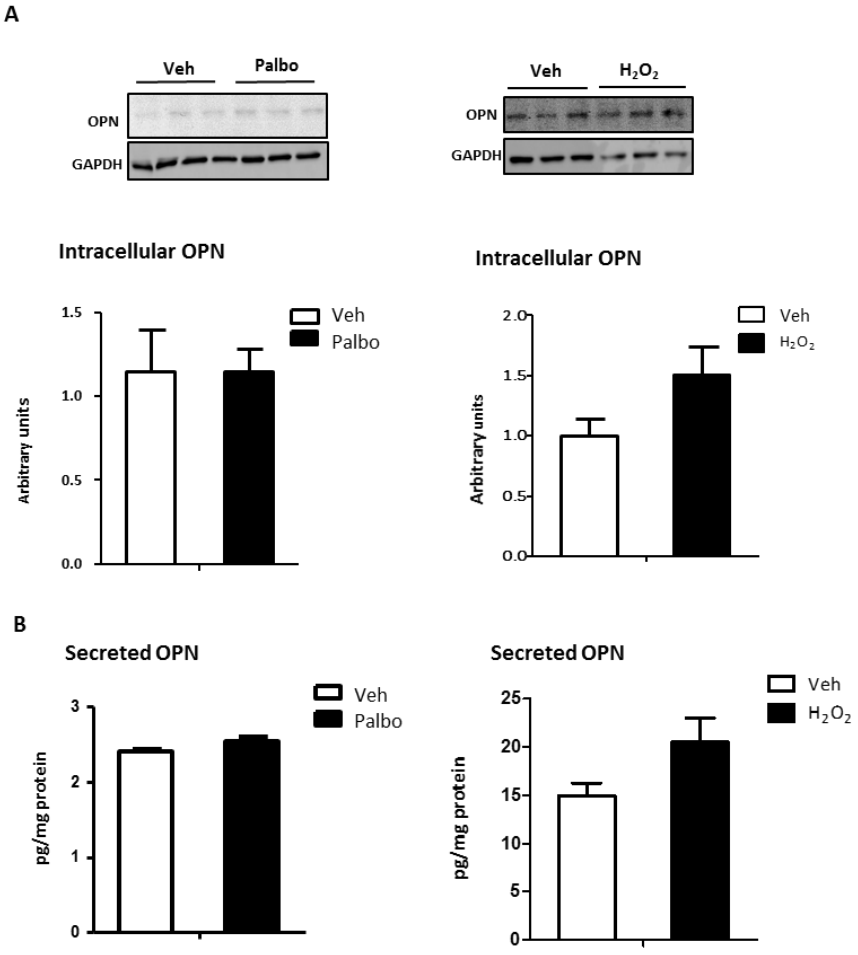

Figure E.31 HepG2, but not Hep3B cells increase OPN protein levels and secretion after palbociclib or H_2O_2 treatment. (A) OPN protein levels from Hep3B cells were measured by immunoblotting using glyceraldehyde -3-phosphate dehydrogenase (GAPDH) as loading control. Values are means ±SEM of n=4. (B) OPN media levels from Hep3B cells treated with either Vehicle (Veh) or Palbociclib (Palbo) or hydrogen peroxide (H_2O_2) were measured by ELISA. Values are means ±SEM of n=4. Significant differences between Veh and Palbo/H_2O_2 treated cells are denoted by *p<0.05, **p<0.01 and ***p<0.001 (Student's t test).

3.6.4 HFD does not induce OPN expression in p53-KO mice

In order to elucidate if p53 is required for OPN expression in vivo we used p53-KO mice and their WT controls. Both groups were fed a CD or a HFD for 4 weeks. Feeding a HFD increased OPN levels in WT mice, as it has been reported before (Bertola et al., 2009); however, p53-KO mice did not show any increase of the OPN liver levels, being the OPN levels low in both CD and HFD (Fig E.32). Hence, showing a role for p53 in OPN expression also in-vivo when feeding a HFD.

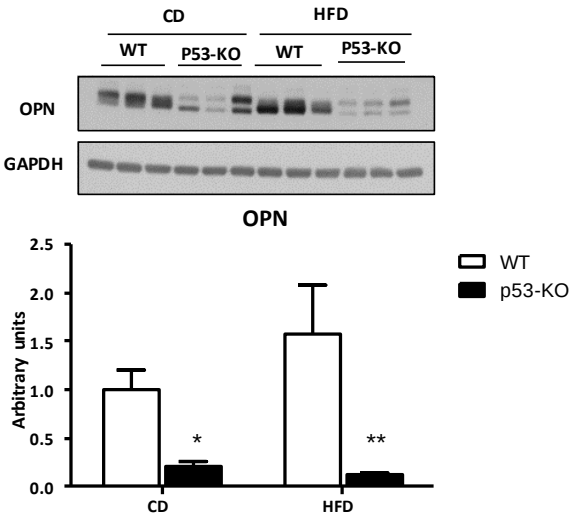

Figure E.32 p53-KO mice do not increase OPN expression when fed a HFD. OPN protein levels from liver homogenates were measured by immunoblotting using glyceraldehyde -3-phosphate dehydrogenase (GAPDH) as loading control. Values are means ±SEM of n=4-6 Significant differences are denoted by *p<0.05, **p<0.01 and ***p<0.001 (Student's t test).

F.DISCUSSION

1. Osteopontin controls biliary metabolism by regulating CYP7A1 levels in liver and hepatocytes.

The liver is the largest and most important metabolic organ in the human body. It has many different functions, including metabolism regulation, detoxification processes and digestion. There has been a rise in the prevalence of nonalcoholic fatty liver disease (NAFLD). NAFLD is an umbrella term that comprises a spectrum of conditions, ranging from hepatic steatosis, to nonalcoholic steatohepatitis (NASH) to fibrosis. NAFLD has a very important metabolic component, it is strongly associated with obesity, insulin resistance, hypertension and dyslipidemia and it has been considered the hepatic manifestation of the metabolic syndrome.

OPN is a multifunctional cytokine that expresses during inflammation and cancer in different tissues (Ramaiah & Rittling, 2007; Zeyda et al., 2011). It plays a role in liver fibrogenesis (Glass et al., 2018) (Syn et al., 2012) and in obesity-related hepatosteatosis (Bertola et al., 2009).

In this work, we provide evidence of a mechanism by which OPN regulates lipid metabolism and conversion of Chol into BA in hepatocytes and liver. As previously mentioned (Nuñez-Garcia el al., 2017), OPN regulates the fate of acetyl-CoA towards cholesterogenesis, and regulates liver PC and FC metabolic cross-talk in mouse liver. These lipids are highly interconnected, both being bile lipids synthesized in the liver. Indeed, PC constitutes 90-95% of bile glycerophospholipids (GPL). Experimental and clinical evidence have linked altered hepatic Chol homeostasis to liver disease (Arguello, Balboa, Arrese, & Zanlungo, 2015). Besides, some BA species are increased in liver of patients with NASH. Thus, the role of extracellular OPN regulating hepatocyte lipid metabolism is of high relevance for liver disease.

On previous work, we found that OPN deficiency led to increased mRNA levels of enzymes involved in the CDP-choline pathway, and to decreased PC content in liver. Here, we propose a mechanism through which extracellular OPN directly modulates biliary metabolism. We previously reported that several factors involved in biliary PC secretion (Abcb4) and nuclear factors that regulate cholesterol 7α-hydroxylase (CYP7A1) expression were upregulated in OPN-KO mice and downregulated in rOPN treated mice. Here we show that protein levels of CYP7A1, in charge of the conversion of FC into BA, were higher in OPN-KO mice than in WT mice, while decreased when WT mice were treated with recombinant OPN (rOPN). We previously found that liver levels of CYP7A1 were slightly decreased in non-obese patients with NAFLD, in whom serum OPN correlates with liver Chol, suggesting that OPN might participate in this regulation of CYP7A1 that could be in charge of the Chol accumulation.

It has been demonstrated previously in HCV-infected hepatocytes that the secreted OPN interacts with integrins and/or CD44 at the cell surface of hepatocytes, among other cell types, thus, inducing a signaling cascade through phosphorylation/activation of FAK and AKT (Iqbal et al., 2014). In addition, several reports have involved AKT (Li, Ma, & Chiang, 2008), in CYP7A1 transcription. Here, we show that OPN, through regulation of the FAK-AKT signaling pathway, modulates CYP7A1 levels in hepatocytes. The specific mechanism involved is still not fully understood and remains to be studied. However, different combinations of integrins that bind to OPN are expressed by hepatocytes (Couvelard et al., 1998; Yokosaki, Tanaka, Higashikawa, Yamashita, & Eboshida, 2005); therefore, we believe that the OPN-integrin interaction leads to the activation of FAK-AKT signaling in mouse hepatocytes, regulating CYP7A1 (Fig F.1), which is the main axis in the cross-talk between PC and Chol metabolism. Thus, controlling biliary PC and Chol secretion, which will influence liver levels of these lipids.

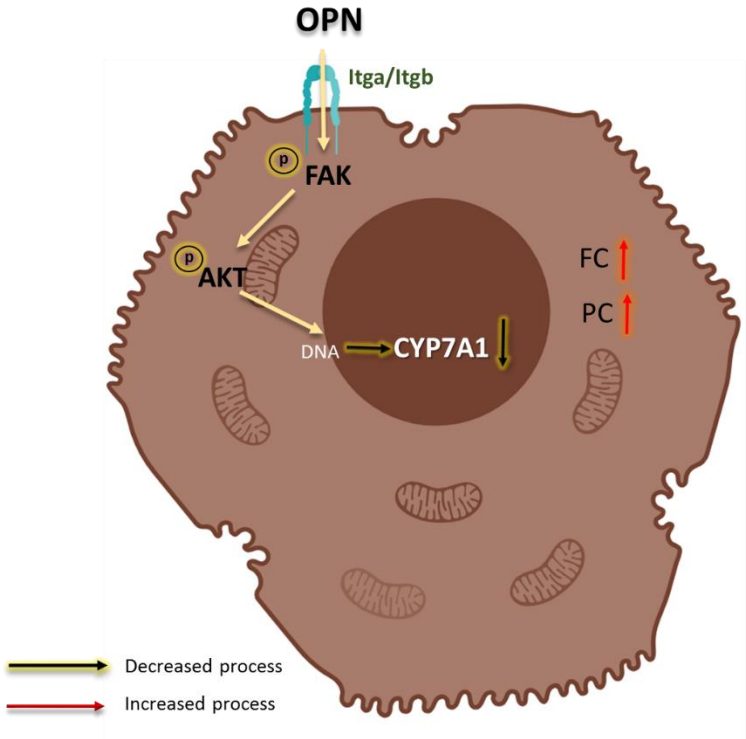

Figure F.1 Proposed model and mechanism of OPN effect in mice hepatocytes regulating CYP7A1 levels.

2. Rewiring of lipid metabolism modulates liver regeneration after partial hepatectomy in OPN-KO mice.

The liver has the capacity for regeneration after cellular damage or surgery resection. During regeneration, liver cells need to acquire sufficient energy and metabolic precursors to support the metabolic demands for rapid proliferation. Thus, a variety of metabolic pathways is switched on. The synthesis of PC, the mayor phospholipid in cellular membranes, is coordinated with the activation of the cell cycle and is an essential step in cell proliferation. Changes in the hepatic PC/PE molar ratio have been linked to impaired liver regeneration (van der Veen, Jelske N et al., 2017). Although hepatic TG content is widely variable and increases during liver regeneration, alterations in either exogenous or endogenous lipid metabolic pathways, demonstrated to promote or diminish hepatic steatosis and influence hepatocyte proliferation (Newberry et al., 2008). Chol is also essential to perform an adequate regeneration, since it is a critical structural component of biological membranes that influences properties such as permeability and fluidity, while also contributing to the modulation of the membrane proteins, protein trafficking, and transmembrane signaling (Delgado-Coello, Briones-Orta, Macías-Silva, & Mas-Oliva, 2011). A growing body of evidence has demonstrated that BAs are important for liver regeneration. The relative BA overload after partial liver resection causes activation of BA receptors in non-parenchymal and parenchymal cells in the liver, thus, providing signals to the regenerative process (van de Laarschot, Liyanne FM, Jansen, Schaap, & Damink, 2016). It is therefore clear, that modulation of lipid metabolism is required to ensure an adequate regeneration after partial hepatectomy (PH). The technique of partial hepatectomy (PH) is widely used to model liver regeneration and cell cycle dynamics in vivo, avoiding the massive necrosis observed in other regeneration models.

We previously showed that OPN regulates the *de novo* lipogenesis in hepatocytes by regulating the fate of acetyl-CoA and modulates glycerolipid and cholesterol metabolism cross-talk (Nunez-Garcia et al., 2017). Therefore, there is a need to understand how OPN affects lipid metabolism during regeneration. On previous studies, we show that there is a substantial increase in the levels of circulating OPN during the first 24 h after PH, occurring at a time when hepatocytes accumulate a significant amount of lipids (mainly TGs), in droplets, in the widely recognized transient regeneration-associated liver steatosis (Tijburg, Nyathi, Meijer, & Geelen, 1991). Evidences suggest that the transient steatosis is likely related to the increased lipogenic activity and the altered lipid fluxes into and out of the hepatocyte (Miyamura et al., 2011). We previously reported that OPN-KO mice are able to regenerate properly, but they show a lipid remodeling when undergoing regeneration (Nuñez-Garcia et al., 2018). Hence, we wanted to analyze which metabolic processes underlie this remodeling that allows an adequate hepatic regeneration.

Previously, we demonstrated that de novo TG synthesis is decreased while the liver TG content maintains unaltered in OPN-KO hepatocytes (Nunez-Garcia et al., 2017). Thus, OPN-KO mice must get TG in another way different from *de novo* synthesis. Here, we demonstrate that OPN-KO mice show enrichment of liver TGs in the most abundant dietary essential FA, the linoleic acid (18:2). Altogether, these results show that the decreased de novo TG synthesis is compensated with dietary FA in OPN-KO mice livers.

During the first 24 h period after PH, the enrichment of TGs in linoleic acid was higher in the WT than in OPN-KO mice, in which beta-oxidation was increased. Altogether, suggesting an increased consumption of dietary fatty acids in the OPN-KO mice. Our findings demonstrated that in OPN-KO mice liver, in which the source of TGs is different, regeneration was not impaired 24 or 48 h after PH. It has also been described that during the first hours (h) of the G1 phase there is an increase in the TG hydrolysis that releases FAs for mitochondrial beta-oxidation (Brasaemle, 2006). Here we observed that in OPN-KO mice there is an increase in beta-oxidation 24 h after PH, which prevents the accumulation of acylcarnitines observed in quiescent livers, and will induce the decrease in acylcarnitines 48 h after PH. This increase in beta-oxidation is coupled with the increase in positive cells for DHE, a marker of ROS. It has been described that the hypoglycaemia that follows PH induces systemic lipolysis which supplies the required FA (Gazit et al., 2010). The loss of body weight that follows the PH is less marked in OPN-KO mice than in WT mice, suggesting that lipolysis of adipose tissue is not the source of FA for the increased beta oxidation. These results are in concordance with the fact that in mice, OPN deletion prevents the development of obesity and hepatosteatosis via impaired adipose tissue functionality (Lancha et al., 2014). Our results suggest that dietary FA will provide the required TG and FA for lipid accumulation and beta-oxidation in OPN-KO mice, allowing a correct regeneration.

The synthesis of PC, the major phospholipid in cellular membranes, is coordinated with the cell cycle activation (Jackowski, 1994). Our results show that liver regeneration is not impaired in OPN-KO mice even when PC content is decreased 24 h post PH. We also found that the decreased *de novo* PC synthesis previously observed is associated reduced liver PC content, but unlike TGs, PC content is not compensated with the dietary essential FA linoleic. Importantly, treatment with atorvastatin, which inhibits cholesterogenesis, induces a new lipidome where PC and DG content increases 24 h after PH. This new metabolic rewiring was associated with improved liver regeneration 24 h after PH, and is consistent with our previous reports of increased *de novo* cholesterogenesis in OPN-KO mice. This study reinforces the role of OPN as a metabolic driver during liver regeneration. However, in this mice model, non-obese with healthy liver, the lack of OPN results in a metabolic remodeling ensuring the success in regeneration 24 and 48 h after partial hepatectomy. OPN is increased in liver diseases and the knockdown of OPN has been proposed as a therapeutical approach. However, through this

study we are not able to know if the lack of OPN will alter liver regeneration in a model of obesity with NAFLD. Liver transplants are increasing due to metabolic disease. Thus, this should be investigated in the future.

In conclusion, the results here support the role of OPN as a liver metabolic driver. OPN regulates multiple metabolic pathways involved in liver regeneration. Treatment with atorvastatin, an inhibitor of *de novo* cholesterogenesis, provides a new metabolic scenario linked to improvement of early regeneration in OPN-KO mice.

3. Osteopontin plays a role in the age-associated NAFLD progression

Osteopontin (OPN) plays a role in the liver lipid metabolism (Nunez-Garcia et al., 2017) (Nuñez-Garcia et al., 2018). Because some of the substantial changes that liver undergoes as it ages are metabolic modifications and liver regeneration decline, we investigated if OPN might regulate liver lipid metabolism during aging. Epidemiological studies have demonstrated that NAFLD is common among the elderly (Bertolotti et al., 2014; Fierbinteanu-Braticevici et al., 2017). Aging is a complex multifunctional process, in which metabolism plays an important role (López-Otín, Blasco, Partridge, Serrano, & Kroemer, 2013; López-Otín, Galluzzi, Freije, Madeo, & Kroemer, 2016). Many aging related diseases, such as diabetes, NAFLD, cardiovascular disease among others, have a metabolic component. In addition, several studies link OPN and aging. However, the available data does not give conclusive results about the role of OPN in the aging process, but its effect seems to be tissue or cell-type dependent. On this study, we show for the first time the involvement of OPN in modulation of liver lipid metabolism during aging.

Here, we show that there is a positive correlation between circulating OPN levels and aging in individuals with normal liver but not in NAFLD patients. In addition, this positive correlation was also observed in WT mice. Thus, showing a possible link between OPN and the liver aging process and disease development. In vitro results showed that OPN expression increased both intra and extracellularly when senescence was induced, which reinforces its role as a senescence associated secretory phenotype (SASP) factor and thus, its involvement in aging related senescence.

It is known that aging affects differently to females and males (Austad & Fischer, 2016). Since most of the studies are performed in male mice, and given that there is a higher complexity in metabolic regulation of females, we focused this study in females. In addition, we decided to use a natural model of aging. It is tempting to study aging using mice with accelerated aging and/or reduced lifespan. However, data obtained from these models should be interpreted carefully. Progeroid mice models might show typical features of aging, but they often exhibit features not seen in normal old mice (Kõks et al., 2016). Consequently, the available mouse models of accelerated aging do not fully represent normal aging in mice. Because of this, and despite the fact that aging research on mice is expensive and time-consuming, we decided to use a natural model of aging in order to obtain reliable data of the aging process.

To elucidate whether the increase of OPN observed during aging was protective or deleterious, we studied the aging process in OPN deficient mice. We observed that mice lacking OPN show a premature lipid accumulation in the liver and increased serum levels of TGs. Interestingly, linked with this, an increase on circulating TG levels is the only serum parameter (apart from transaminases) that

was increased in both obese and non-obese NAFLD patients, compared to their healthy controls. Aging is associated with progressive changes in total and regional fat redistribution, from adipose tissue to other tissues such as the liver, hearth, skeletal muscle and others. These changes have negative health consequences. Indeed, this redistribution increases risk for insulin resistance and cardiovascular disease, and changes in body composition can occur independent of changes in total adiposity, body weight or waist circumference, and represent a phenotype closely associated with increased morbidity and mortality risk (Kuk, Saunders, Davidson, & Ross, 2009). Together with this premature lipid accumulation, old OPN-KO mice show increased liver fibrosis and inflammation (Fig F.2). Surprisingly, OPN is known to be a pro fibrogenic factor and several studies claim that its deficiency avoids fibrosis (Coombes et al., 2015) but there is no previous information of the OPN involvement in fibrosis in old livers. Certainly, aging is the most common cause for the progression of NAFLD. Linked to this, induction of fibrosis by senescent hepatocytes is a way of limiting tissue injury as part of wound healing process. However, accumulation of senescent hepatocytes leads to continuous activation of stellate cells and thereby fibrosis progression (A. Aravinthan et al., 2013; A. D. Aravinthan & Alexander, 2016). The worsened progression observed in old OPN-KO mice, was even more marked when old mice were fed a high fat diet (HFD), since OPN-KO mice fed a HFD mice show more fibrosis together with inflammation, cell damage and apoptosis markers. In addition, they also exhibit higher levels of AST and a mild insulin resistance.

Overall, OPN-KO mice show a worsened progression when compared to their WTs. The early hepatosteatosis observed in 10 m OPN-KO mice leads to a fibrotic and inflammation scenario at 20 m. Thus, we propose that OPN plays a protective role in the aging-associated NAFLD progression, and its deficiency could be detrimental. Supporting the protective role of OPN, other studies have shown a protective role of OPN in alcoholic hepatitis (Lazaro et al., 2015). In addition, it has been reproted that OPN deletion caused greater liver injury and lipid peroxidation, contributing to the pathogenesis and enhancement of alcoholic liver disease in old mice (Magdaleno et al., 2018). Besides, OPN is typically considered an anti-apoptotic factor, and its deficiency could facilitate the occurrence of apoptosis (Iida, Wagatsuma, Hirayama, & Nakase, 2017).

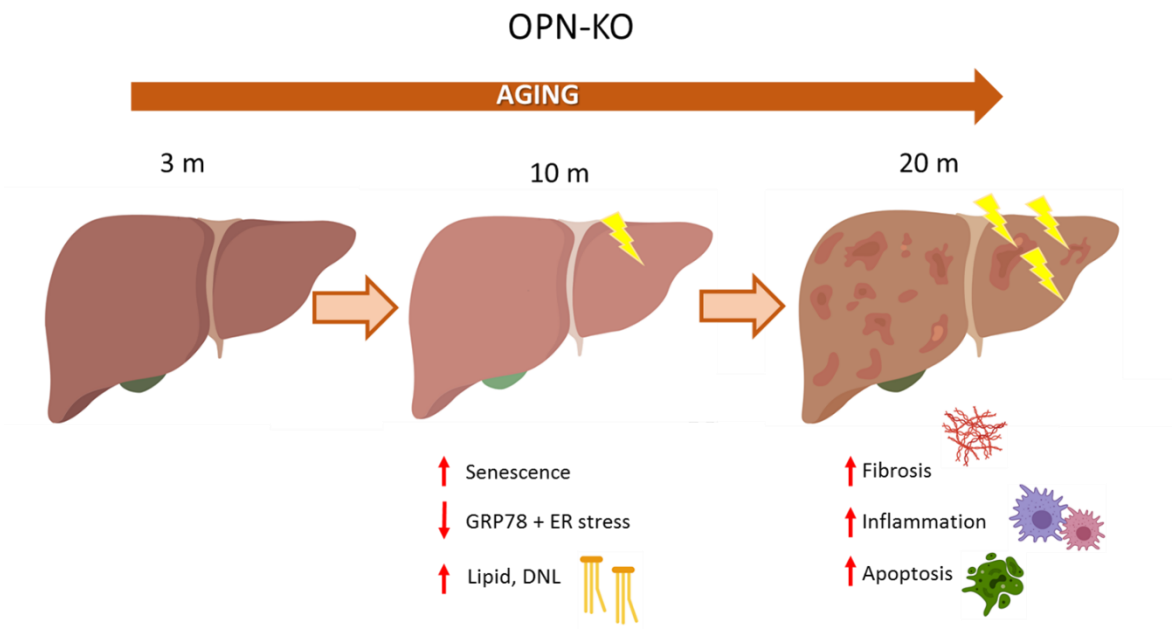

Figure F.2 Schematic representation of the liver progression during aging in OPN-KO mice

Since the previously mentioned premature liver lipid accumulation occurs at 10 m, we took this age point to study the altered underlying mechanism that leads to the observed steatosis and worsened liver disease progression. We show that the *de novo* lipogenesis (DNL) is increased in the OPN-KO mice hepatocytes. Supporting the increased DNL, there is increased esterification of FA to TGs. Several authors have shown that liver DNL increase with aging (Cohen, Horton, & Hobbs, 2011; Sheedfar, Biase, Koonen, & Vinciguerra, 2013). Under physiological conditions, DNL contributes to no more than 5-10% of the hepatic TG content, whereas the contribution increases to more than 25% in NAFLD patients, showing that DNL may be a major determinant for NAFLD development in humans. Age- associated changes in DNL appear to be primarily through changes in systemic mediators such as insulin resistance and changes in GH/IGF axis. Other metabolic alteration linked to aging is the decrease in the FA beta-oxidation, being the mitochondrial dysfunction one of the possible causes (López-Otín et al., 2016). However, in the OPN deficient mice, beta-oxidation remains unaltered. Thus, we determined that increased DNL is one of the causes for the increased lipid storage, and the stored lipid is not consumed in oxidation processes.

Several studies have addressed age-related bile composition alterations (B. Y. Lee et al., 2006; G. Lee, Lee, Hong, Lee, & Jung, 2016). Aging is associated with a reduced bile acid synthesis, possibly related to decreased hepatic expression of hepatocyte nuclear factor-4 and consequently of CYP7A1 (Bertolotti et al., 2007). OPN can decrease CYP7A1 levels (Nunez-Garcia et al., 2017), thus the OPN increase with aging is linked with its decrease. Consequently, 10 m OPN-KO mice show increased expression of CYP7A1 and some increased BA species. The increase in CYP7A1 could be linked to decreased AKT pathway activation. Hepatic degradation to bile acids is the most relevant metabolic

pathway whereby the organism can dispose of excess Chol. Linked to this, liver free cholesterol concentration does not increase when compared to WTs, as happens with other lipids, probably as a consequence of increased flux of Chol to BA. In addition, it has been reported that the ratio 12α-hydroxylated BA/ non-12α-hydroxylated BA increases in NAFLD patients and is associated with lower insulin sensitivity and higher plasma TG (Haeusler, Astiarraga, Camastra, Accili & Ferrannini, 2013). Our BA analysis shows that in 10 m OPN-KO mice this ratio is increased, this is consistent with the high levels of TG observed in this group and also supports the observed worsened progression in the OPN-KO.

Regarding senescence, 10 m OPN-KO mice showed increased percentage of beta galactosidase positive hepatocytes and p21 levels. These markers are known to be increased in hepatocytes upon senescence. The accumulation of senescent hepatocytes can affect the liver function making the liver more prone to disease progression (A. Aravinthan et al., 2013). Linked with this, hepatocyte senescence correlates with severity of NAFLD (Ogrodnik et al., 2017). Interestingly, it has been reported that FAS levels, which are increased in 10 m OPN-KO mice contributing to hepatosteatosis, are upregulated during senescence, and FAS inhibition stops cellular senescence induction (Fafián-Labora et al., 2019). We found that together with the increased senescence markers FAS protein levels were also increased together with de novo lipogenesis. Other hallmark of aging is the dysregulated nutrient sensing (López-Otín et al., 2016). We observed that the mTOR signaling pathway was markedly decreased in mice lacking OPN. Paradoxically, downregulation of mTOR has been associated to longevity in caloric restriction models (DiLoreto & Murphy, 2015; DiLoreto & Murphy,2015; Johnson, Rabinovitch, & Kaeberlein, 2013). Indeed, downregulation of translation upon reduced nutrient availability extend lifespan in many organisms via mTOR signaling in caloric restriction models. However, in our model, the downregulation of this pathway seems to be linked to the attenuation of translation in response to loss of proteostasis, which is another feature of aging. The endoplasmic reticulum (ER) is an important organelle for regulating calcium homeostasis, lipid homeostasis, protein synthesis, and post-translational modifications and trafficking. Many insults can disturb ER homeostasis, which leads to ER stress. The buffering capacity of the proteostasis network decreases with aging. Indeed, aging is directly associated with specific alterations in distinct components of the proteostasis network. Such alterations disrupt the healthy functioning of the cell and may contribute to the emergence of disease (Martínez, Duran-Aniotz, Cabral-Miranda, Vivar, & Hetz, 2017). ER stress can modulate expression levels of key enzymes involved in lipid synthesis or modification (Han & Kaufman, 2016). It is well stablished that lipid accumulation can disturb the ER function generating ER stress. In this work, we show that OPN-KO mice show activation of the PERK branch of the unfolded protein response, which activates when there is ER stress. We also found the decreased chaperone capacity, which is probably involved in this activation. Supporting this, we observed a decrease of phosphorylated S6K that shows a decrease in the protein synthesis as a way

to cope with ER stress when PERK branch of the UPR is activated (Han & Kaufman, 2016). Thus, the decrease in phosphorylation of mTOR and S6K might be a response trying to attenuate ER stress. Interestingly, some studies have shown that OPN can induce s6K and mTOR phosphorylation in breast cancer cells, and therefore might have a role on its activation (Ahmed & Kundu, 2010). Several studies have demonstrated that the decrease in chaperone number diminishes the efficacy to deal with unfolded proteins. In addition, the decrease in the number of chaperones is associated with aging (A. S. Lee et al., 2017) which can be one of the causes of the increased ER stress with aging. Some studies have shown that forced expression of GRP78 attenuates steatosis by inhibiting sterol regulatory element-binding protein (SREBP-1c) (Kammoun et al., 2009). Thus, the reduced GRP78 levels could increase the steatosis by increased activation of SREBP-1c, and thus, lipogenic genes like FAS, which is increased in 10 m OPN-KO mice together with increased lipid accumulation. Severe or prolonged ER stress is associated with the development of degenerative and fibrotic responses in many organs (Kropski & Blackwell, 2018). Thus, in old OPN-KO mice, the prolonged exposure to ER stress could be cause of the observed fibrosis and apoptosis at old age. Paradoxically, at 20 m we did not observe the decreased GRP78 chaperone, but this could be as a consequence of an adaptive response to apoptosis, indeed, GRP78 is known for preventing ER stress-induced cell death by blocking caspase-7 and 12. In the in-vitro model, we observed how silencing OPN with a siRNA decreased GRP78 levels when senescence was induced in HepG2 cells. Some previous studies have suggested the association between OPN with GRP78 in renal tissue in rats (Bhardwaj et al., 2017). In addition, OPN has been linked with other chaperones; e.g. OPN-induced signal transduction involves activation of Hsp90-dependent pathways (Mutrie, Chambers, & Tuck, 2011). Hence, here we observed for the first time, how lack of OPN is associated with reduced GRP78 levels in senescent hepatic cells. We observe that senescence leads to decreased chaperone levels when OPN is deficient. Senescent cells lose the capacity to activate the transcriptional pathways leading to chaperone synthesis, which generates lower levels of chaperone. These low levels in senescent cells is one of the causes for damage accumulation (Ogrodnik, Salmonowicz, & Gladyshev, 2018).

Taking together the mechanisms that are altered in 10 m OPN-KO mice (increased DNL, increased senescence and increased ER stress with low GRP78 levels) apart from being involved in aging, will lead to and increased transcription of lipogenic genes, causing thus, the increased lipid accumulation that with time will progress to further stages of the disease. We propose that OPN is a protein required to properly respond to stressors, and thus upon aging its deficiency makes cells more vulnerable to insults and senescence.

Senescence is one of the key hallmarks of aging. It is a permanent state of cell-cycle arrest in response to different stresses, being thus, a cellular defense mechanism. Senescence happens in several different tissues during different physiological and pathological processes. While senescence

is one of the causative processes of aging and it is responsible of many aging-related disorders, senescent cells can also play a positive role in other processes. For example, it is required for tissue repair and it is an important mechanism for preventing tumorigenesis (Calcinotto et al., 2019). Regarding liver disease, senescence of hepatocytes and other liver cell types is a key feature of chronic liver disease independent of etiology, and plays an important role in the progression of chronic liver disease (A. D. Aravinthan & Alexander, 2016). In our in vitro study, we show that OPN expression increases when treating with senescence-inducing agents and treating cells with rOPN made cells more resistant to senescence. Previous work have described OPN as a SASP factor (Flanagan et al., 2017; Pazolli et al., 2009). Interestingly, integrin beta 3, one of the integrins to which OPN binds, has been found to be a marker and regulator of senescence (Rapisarda et al., 2017). Although senescence-associated cell-cycle exit likely evolved as an anti-tumor mechanism, the SASP contains both anti- and pro-tumorigenic potential (Lau & David, 2019). Thus, identification and characterization of the SASP factors that are pro and those that are anti-tumorigenic depending on the contexts and tissue is crucial. In response to senescence stresses, cells initially trigger survival pathways that prevent damage and promote recovery; however, if the damage persists and becomes unsustainable, cells undergo senescence and senescent cells can accumulate, disrupting the physiological integrity of the tissue. Thus, OPN might be a factor expressed in response to senescent stimuli to prevent cells from becoming senescent. While preventing senescence can be a desirable process in normal aging, in other scenarios can be detrimental.

Indeed, one of the most important features of senescence is that acts as a potent tumor suppressive. Current research indicates that many chemotherapeutic drugs and radiation induce senescence in cancer cells. Senescence-inducing treatments have the advantage of enhancing the efficacy and decreasing the side effects of anticancer therapy. The role of OPN in chemoresistance is currently under investigation, with pre-clinical evidence suggesting that OPN is involved in inducing chemoresistance (Ding et al., 2015; Zhao et al., 2018). As mentioned above, increasing concentration of OPN in the media makes cells more resistant to senescence-inducing agent palbociclib, therefore reinforcing its role in senescence, as an anti-senescent agent. In addition, neutralizing OPN makes cells more vulnerable to senescence inducing agents by impairing ER response to stress. As we explained above, GRP78 levels could be linked to OPN expression, although the mechanism remains to be elucidated. In this context of chemoresistance it has been described that elevated expression of GRP78, has shown to induce chemoresistance and serves as an indicator of poor prognosis in patients (Gifford & Hill, 2018). Thus, in cancer treatment context, OPN could be targeted to improve drug treatment. However, this needs to be further investigated.

In this work we also propose a mechanism by which OPN expression increase in both aging and senescence. p53 is one of the most important tumor suppressor genes. p53 family members control several metabolic and cellular functions, being hepatic lipid metabolism one of them. p53-

KO mice show increased hepatic fat content, and hepatic overexpression of p53 ameliorates hepatic steatosis (Porteiro et al., 2017). Some previous work have shown that OPN is a p53 target in fibroblasts (Morimoto, Sasaki, Ishida, Imai, & Tokino, 2002) and in endometrium carcinoma cells (Franco et al., 2017). Here, we wanted to analyze whether p53 could regulate OPN expression when senescence is induced in cells and in models of HFD induced NAFLD. When analyzing the gene expression of OPN (SPP1 gene) and p53 (TP53) of several hepatic cell lines, we observed that the cell line with the least TP53 expression had also the lower SPP1 expression, implying that there might be a relation between these two proteins. Our results show that silencing p53 with a siRNA diminished OPN protein levels, intra and extracellularly. In the senescence context, p53 expression has shown to be upregulated when inducing senescence to hepatocytes (A. Aravinthan et al., 2014). In vitro, when we treated cells with senescent inducing agents, HepG2 cells increased their OPN levels, both intracellular and secreted, while Hep3B cells, that are p53 null, do not show this increase. Thus, showing that p53 might be necessary for OPN expression under senescent stimuli. In the in-vivo model, it has been reported that p53 null mice fed a HFD show increased liver fat content and ER stress markers, and its overexpression improves steatosis and ER stress (Porteiro et al., 2017). HFD induces OPN expression in liver of WT mice, however, we observed that feeding a HFD to p53-KO mice did not induce the expected increase in OPN, reinforcing the link between p53 and OPN in hepatosteatosis. Altogether, the results show how p53 induces OPN expression in liver when facing senescence and HFD, and suggest that p53-induced OPN might be important for preventing the lipid dysregulation associated to these processes.

With all these evidences, we propose that OPN is involved and has a protective role in liver disease development during aging. Its expression in liver seems to be protective, since its deficiency in aging results in premature senescence, increased lipid accumulation and a worsened ER stress response that leads to a worse progression of the age-associated liver disease. The results suggest that p53 might induce OPN expression in liver and it might mediate a link between cellular senescence and lipid metabolic dysregulation in liver during aging.

G. CONCLUSIONS

CONCLUSIONS

1. Osteopontin (OPN) regulates the cross-talk between cholesterol and PC metabolism through modulation of CYP7A1 levels in hepatocytes. The FAK-AKT signaling pathway is involved in the regulation of CYP7A1 by OPN in liver.

2. OPN modulates metabolic pathways involved in TG and cholesterol metabolism during liver regeneration.

2.1 OPN deficient (OPN-KO) mice show increased fatty acid catabolism when facing regeneration. The increased metabolic demands and the decreased *de novo* synthesis of TG are compensated with dietary fatty acids.

2.2 Inhibition of cholesterogenesis using atorvastatin provides a new metabolic scenario linked to improvement of early regeneration in OPN-KO mice.

3. OPN is required to maintain the whole body metabolic homeostasis during aging.

3.1 OPN is involved in liver aging. Serum OPN positively correlates with age in individuals and animal models with normal liver. In the animal model, the increased OPN levels in serum are linked to increased levels in liver. The induction of senescence in HepG2 cells, through modulation of p53, increases cellular OPN levels and its secretion.

3.2 OPN is regulated to maintain the liver lipid metabolism balance during aging. OPN deficiency in mice makes the liver more vulnerable to age-associated hepatosteatosis, being the underlying mechanism the increased *de novo* lipogenesis linked with induced senescence and an impaired ER stress response due to the GRP78 decreased levels.

3.3 In old HFD-fed mice, deficiency in OPN does not induce body weight changes. However, it induces hypertriglyceridemia and a mild insulin resistance

H. REFERENCES

References

Ahmed, M., & Kundu, G. C. (2010). Osteopontin selectively regulates p70S6K/mTOR phosphorylation leading to NF-κB dependent AP-1-mediated ICAM-1 expression in breast cancer cells. *Molecular Cancer, 9*(1), 1.

Angulo, P. (2002). Nonalcoholic fatty liver disease. *New England Journal of Medicine, 346*(16), 1221-1231.

Aravinthan, A. D., & Alexander, G. J. (2016). Senescence in chronic liver disease: Is the future in aging? *Journal of Hepatology, 65*(4), 825-834.

Aravinthan, A., Scarpini, C., Tachtatzis, P., Verma, S., Penrhyn-Lowe, S., Harvey, R., . . . Alexander, G. (2013). Hepatocyte senescence predicts progression in non-alcohol-related fatty liver disease. *Journal of Hepatology, 58*(3), 549-556.

Aravinthan, A., Shannon, N., Heaney, J., Hoare, M., Marshall, A., & Alexander, G. J. (2014). The senescent hepatocyte gene signature in chronic liver disease. *Experimental Gerontology, 60*, 37-45.

Arguello, G., Balboa, E., Arrese, M., & Zanlungo, S. (2015). Recent insights on the role of cholesterol in non-alcoholic fatty liver disease. *Biochimica Et Biophysica Acta (BBA)-Molecular Basis of Disease, 1852*(9), 1765-1778.

Austad, S. N., & Fischer, K. E. (2016). Sex differences in lifespan. *Cell Metabolism, 23*(6), 1022-1033.

Balch, W. E., Morimoto, R. I., Dillin, A., & Kelly, J. W. (2008). Adapting proteostasis for disease intervention. *Science (New York, N.Y.), 319*(5865), 916-919.

Barzilai, N., Huffman, D. M., Muzumdar, R. H., & Bartke, A. (2012). The critical role of metabolic pathways in aging. *Diabetes, 61*(6), 1315-1322.

Belikov, A. V. (2018). Age-related diseases as vicious cycles. *Ageing Research Reviews,*

Bellahcène, A., Castronovo, V., Ogbureke, K. U., Fisher, L. W., & Fedarko, N. S. (2008). Small integrin-binding ligand N-linked glycoproteins (SIBLINGs): Multifunctional proteins in cancer. *Nature Reviews Cancer, 8*(3), 212.

Berryman, D. E., Christiansen, J. S., Johannsson, G., Thorner, M. O., & Kopchick, J. J. (2008). Role of the GH/IGF-1 axis in lifespan and healthspan: Lessons from animal models. *Growth Hormone & IGF Research, 18*(6), 455-471.

Bertola, A., Deveaux, V., Bonnafous, S., Rousseau, D., Anty, R., Wakkach, A., . . . Gual, P. (2009). Elevated expression of osteopontin may be related to adipose tissue macrophage accumulation and liver steatosis in morbid obesity. *Diabetes, 58*(1), 125-133.

Bertolotti, M., Gabbi, C., Anzivino, C., Crestani, M., Mitro, N., Del Puppo, M., . . . Carulli, L. (2007). Age-related changes in bile acid synthesis and hepatic nuclear receptor expression. *European Journal of Clinical Investigation, 37*(6), 501-508.

Bertolotti, M., Lonardo, A., Mussi, C., Baldelli, E., Pellegrini, E., Ballestri, S., . . . Loria, P. (2014a). Nonalcoholic fatty liver disease and aging: Epidemiology to management. *World Journal of Gastroenterology, 20*(39), 14185-14204.

Bertolotti, M., Lonardo, A., Mussi, C., Baldelli, E., Pellegrini, E., Ballestri, S., . . . Loria, P. (2014b). Nonalcoholic fatty liver disease and aging: Epidemiology to management. *World Journal of Gastroenterology, 20*(39), 14185-14204.

Bhardwaj, R., Bhardwaj, A., Tandon, C., Dhawan, D. K., Bijarnia, R. K., & Kaur, T. (2017). Implication of hyperoxaluria on osteopontin and ER stress mediated apoptosis in renal tissue of rats. *Experimental and Molecular Pathology, 102*(3), 384-390.

Blackburn, E. H., Epel, E. S., & Lin, J. (2015). Human telomere biology: A contributory and interactive factor in aging, disease risks, and protection. *Science, 350*(6265), 1193-1198.

Blackburn, E. H., Greider, C. W., & Szostak, J. W. (2006). Telomeres and telomerase: The path from maize, tetrahymena and yeast to human cancer and aging. *Nature Medicine, 12*(10), 1133.

Bolden, J. E., & Lowe, S. W. (2015). In Mendelsohn J., Gray J. W., Howley P. M., Israel M. A. and Thompson C. B.(Eds.), *15 - cellular senescence*.

Brasaemle, D. L. (2006). Cell biology. A metabolic push to proliferate. *Science (New York, N.Y.), 313*(5793), 1581-1582.

Bratic, A., & Larsson, N. (2013). The role of mitochondria in aging. *The Journal of Clinical Investigation, 123*(3), 951-957.

Bruunsgaard, H., Pedersen, A. N., Schroll, M., Skinhøj, P., & Pedersen, B. (2000). TNF-α, leptin, and lymphocyte function in human aging. *Life Sciences, 67*(22), 2721-2731.

Cabiati, M., Gaggini, M., Cesare, M. M., Caselli, C., De Simone, P., Filipponi, F., . . . Del Ry, S. (2017). Osteopontin in hepatocellular carcinoma: A possible biomarker for diagnosis and follow-up. *Cytokine, 99*, 59-65.

Calcinotto, A., Kohli, J., Zagato, E., Pellegrini, L., Demaria, M., & Alimonti, A. (2019). Cellular senescence: Aging, cancer, and injury. *Physiological Reviews, 99*(2), 1047-1078.

Caputo, S., & Bellone, M. (2018). Osteopontin and the immune system: Another brick in the wall. *Cellular & Molecular Immunology, 15*(4), 405.

Castello, L. M., Raineri, D., Salmi, L., Clemente, N., Vaschetto, R., Quaglia, M., . . . Cantaluppi, V. (2017). Osteopontin at the crossroads of inflammation and tumor progression. *Mediators of Inflammation, 4049098, 22,*

Cleveland, E., Bandy, A., & VanWagner, L. B. (2018). Diagnostic challenges of nonalcoholic fatty liver disease/nonalcoholic steatohepatitis. *Clinical Liver Disease, 11*(4), 98-104.

Cohen, J. C., Horton, J. D., & Hobbs, H. H. (2011). Human fatty liver disease: Old questions and new insights. *Science (New York, N.Y.), 332*(6037), 1519-1523.

Collerton, J., Davies, K., Jagger, C., Kingston, A., Bond, J., Eccles, M. P., . . . Kirkwood, T. B. (2009). Health and disease in 85 year olds: Baseline findings from the newcastle 85+ cohort study. *BMJ (Clinical Research Ed.), 339*, b4904.

Coombes, J. D., Swiderska-Syn, M., Dolle, L., Reid, D., Eksteen, B., Claridge, L., . . . Syn, W. K. (2015). Osteopontin neutralisation abrogates the liver progenitor cell response and fibrogenesis in mice. *Gut, 64*(7), 1120-1131.

Couvelard, A., Bringuier, A., Dauge, M., Nejjari, M., Darai, E., Benifla, J., . . . Scoazec, J. (1998). Expression of integrins during liver organogenesis in humans. *Hepatology, 27*(3), 839-847.

Cristobal, S., Ochoa, B., & Fresnedo, O. (1999). Purification and properties of a cholesteryl ester hydrolase from rat liver microsomes. *Journal of Lipid Research, 40*(4), 715-725.

Cunningham, C. C., & Van Horn, C. G. (2003). Energy availability and alcohol-related liver pathology. *Alcohol Research and Health, 27*, 291-299.

da Costa, J. P., Vitorino, R., Silva, G. M., Vogel, C., Duarte, A. C., & Rocha-Santos, T. (2016). A synopsis on aging—Theories, mechanisms and future prospects*, Ageing Research Reviews, 29, 91-112.*

Delgado-Coello, B., Briones-Orta, M. A., Macías-Silva, M., & Mas-Oliva, J. (2011). Cholesterol: Recapitulation of its active role during liver regeneration. *Liver International, 31*(9), 1271-1284.

Diehl, A. M., & Day, C. (2017). Cause, pathogenesis, and treatment of nonalcoholic steatohepatitis. *New England Journal of Medicine, 377*(21), 2063-2072.

DiLoreto, R., & Murphy, C. T. (2015). The cell biology of aging. *Molecular Biology of the Cell, 26*(25), 4524-4531.

Ding, K., Fan, L., Chen, S., Wang, Y., Yu, H., Sun, Y., . . . Liu, Y. (2015). Overexpression of osteopontin promotes resistance to cisplatin treatment in HCC. *Oncology Reports, 34*(6), 3297-3303.

Ding, W., Yousefi, K., Goncalves, S., Goldstein, B. J., Sabater, A. L., Kloosterboer, A., . . . Shehadeh, L. A. (2018). Osteopontin deficiency ameliorates alport pathology by preventing tubular metabolic deficits. *JCI Insight, 3*(6), 10.1172

Dolinsky, V. W., Douglas, D. N., Lehner, R., & Vance, D. E. (2004). Regulation of the enzymes of hepatic microsomal triacylglycerol lipolysis and re-esterification by the glucocorticoid dexamethasone. *The Biochemical Journal, 378*(Pt 3), 967-974.

Dong, Q., Zhu, X., Dai, C., Zhang, X., Gao, X., Wei, J., . . . Qin, L. (2016). Osteopontin promotes epithelial-mesenchymal transition of hepatocellular carcinoma through regulating vimentin. *Oncotarget, 7*(11), 12997-13012.

Duval, C., Thissen, U., Keshtkar, S., Accart, B., Stienstra, R., Boekschoten, M. V., . . . Muller, M. (2010). Adipose tissue dysfunction signals progression of hepatic steatosis towards nonalcoholic steatohepatitis in C57BL/6 mice. *Diabetes, 59*(12), 3181-3191.

Dyson, J., Jaques, B., Chattopadyhay, D., Lochan, R., Graham, J., Das, D., . . . Cole, M. (2014). Hepatocellular cancer: The impact of obesity, type 2 diabetes and a multidisciplinary team. *Journal of Hepatology, 60*(1), 110-117.

Español–Suñer, R., Carpentier, R., Van Hul, N., Legry, V., Achouri, Y., Cordi, S., . . . Leclercq, I. A. (2012). Liver progenitor cells yield functional hepatocytes in response to chronic liver injury in mice. *Gastroenterology, 143*(6), 1564-1575. e7.

Estes, C., Razavi, H., Loomba, R., Younossi, Z., & Sanyal, A. J. (2018). Modeling the epidemic of nonalcoholic fatty liver disease demonstrates an exponential increase in burden of disease. *Hepatology, 67*(1), 123-133.

Fafián-Labora, J., Carpintero-Fernández, P., Jordan, S. J. D., Shikh-Bahaei, T., Abdullah, S. M., Mahenthiran, M., . . . O'Loghlen, A. (2019). FASN activity is important for the initial stages of the induction of senescence. *Cell Death & Disease, 10*(4), 318.

Fagiolo, U., Cossarizza, A., Scala, E., Fanales-Belasio, E., Ortolani, C., Cozzi, E., . . . Paganelli, R. (1993). Increased cytokine production in mononuclear cells of healthy elderly people. *European Journal of Immunology, 23*(9), 2375-2378.

Fanti, M., Gramignoli, R., Serra, M., Cadoni, E., Strom, S. C., & Marongiu, F. (2017). Differentiation of amniotic epithelial cells into various liver cell types and potential therapeutic applications. *Placenta, 59*, 139-145.

Fausto, N., Campbell, J. S., & Riehle, K. J. (2006). Liver regeneration. *Hepatology, 43*(S1), S45-S53.

Ferramosca, A., & Zara, V. (2014). Modulation of hepatic steatosis by dietary fatty acids. *World Journal of Gastroenterology, 20*(7), 1746-1755.

Ferrucci, L., Giallauria, F., & Guralnik, J. M. (2008). Epidemiology of aging. *Radiologic Clinics of North America, 46*(4), 643-652.

Fierbinteanu-Braticevici, C., Sinescu, C., Moldoveanu, A., Petrisor, A., Diaconu, S., Cretoiu, D., & Braticevici, B. (2017). Nonalcoholic fatty liver disease: One entity, multiple impacts on liver health. *Cell Biology and Toxicology, 33*(1), 5-14.

Flanagan, K. C., Alspach, E., Pazolli, E., Parajuli, S., Ren, Q., Arthur, L. L., . . . Stewart, S. A. (2017). C-myb and C/EBPÎ² regulate OPN and other senescence-associated secretory phenotype factors. *Oncotarget, 9*(1), 21-36.

Fontana, L., Partridge, L., & Longo, V. D. (2010). Extending healthy life span--from yeast to humans. *Science (New York, N.Y.), 328*(5976), 321-326.

Franceschi, C., Garagnani, P., Parini, P., Giuliani, C., & Santoro, A. (2018). Inflammaging: A new immune–metabolic viewpoint for age-related diseases. *Nature Reviews Endocrinology,* 14, 576–590.

Franco, V. F., dos Santos Melo, N., Soares, I. N., Ya-Ting Hsu, Y., Huang, T. H., Araujo, W. M., . . . Gimba, E. R. P. (2017). Osteopontin, p53 and PTEN Isoforms Expression Patterns in Endometrium Carcinoma Cell Lines, *Cancer Research, 77(13).*

Friedman, S. L., Neuschwander-Tetri, B. A., Rinella, M., & Sanyal, A. J. (2018). Mechanisms of NAFLD development and therapeutic strategies. *Nature Medicine, 24, 908–922.*

Gao, X., van der Veen, Jelske N, Hermansson, M., Ordoñez, M., Gomez-Muñoz, A., Vance, D. E., & Jacobs, R. L. (2015). Decreased lipogenesis in white adipose tissue contributes to the resistance to high fat diet-induced obesity in phosphatidylethanolamine N-methyltransferase-deficient mice. *Biochimica Et Biophysica Acta (BBA)-Molecular and Cell Biology of Lipids, 1851*(2), 152-162.

Gazit, V., Weymann, A., Hartman, E., Finck, B. N., Hruz, P. W., Tzekov, A., & Rudnick, D. A. (2010). Liver regeneration is impaired in lipodystrophic fatty liver dystrophy mice. *Hepatology, 52*(6), 2109-2117.

Ge, X., Leung, T., Arriazu, E., Lu, Y., Urtasun, R., Christensen, B., . . . Nieto, N. (2014). Osteopontin binding to lipopolysaccharide lowers tumor necrosis factor-α and prevents early alcohol-induced liver injury in mice. *Hepatology, 59*(4), 1600-1616.

Ge, X., Lu, Y., Leung, T., Sørensen, E. S., & Nieto, N. (2013). Milk osteopontin, a nutritional approach to prevent alcohol-induced liver injury. *American Journal of Physiology-Gastrointestinal and Liver Physiology, 304*(10), G929-G939.

Gifford, J. B., & Hill, R. (2018). GRP78 influences chemoresistance and prognosis in cancer. *Current Drug Targets, 19*(6), 701-708.

Gimba, E. R., Brum, M., & Nestal De Moraes, G. (2019). Full-length osteopontin and its splice variants as modulators of chemoresistance and radioresistance. *International Journal of Oncology, 54*(2), 420-430.

Glass, O., Henao, R., Patel, K., Guy, C. D., Gruss, H. J., Syn, W., . . . Mae Diehl, A. (2018). Serum Interleukin-8, osteopontin, and monocyte chemoattractant protein 1 are associated with hepatic fibrosis in patients with nonalcoholic fatty liver disease. *Hepatology Communications, 2*(11), 1344-1355.

Gómez-Ambrosi, J., Catalán, V., Ramírez, B., Rodríguez, A., Colina, I., Silva, C., . . . Cienfuegos, J. A. (2007). Plasma osteopontin levels and expression in adipose tissue are increased in obesity. *The Journal of Clinical Endocrinology & Metabolism, 92*(9), 3719-3727.

Gong, Z., Tas, E., Yakar, S., & Muzumdar, R. (2017). Hepatic lipid metabolism and non-alcoholic fatty liver disease in aging. *Molecular and Cellular Endocrinology, 455*, 115-130.

González-Rodríguez, Á, Mayoral, R., Agra, N., Valdecantos, M., Pardo, V., Miquilena-Colina, M., . . . Fimia, G. (2014). Impaired autophagic flux is associated with increased endoplasmic reticulum stress during the development of NAFLD. *Cell Death & Disease, 5*(4), e1179.

Gorina, Y., Goulding, M. R., Hoyert, D. L., & Lentzner, H. R. (2006). Trends in causes of death among older persons in the united states. *Aging Trends*, 6.

Guidi, N., Sacma, M., Standker, L., Soller, K., Marka, G., Eiwen, K., . . . Geiger, H. (2017). Osteopontin attenuates aging-associated phenotypes of hematopoietic stem cells. *The EMBO Journal, 36*(7), 840-853.

Haeusler, R. A., Astiarraga, B., Camastra, S., Accili, D., & Ferrannini, E. (2013). Human insulin resistance is associated with increased plasma levels of 12α-hydroxylated bile acids. *Diabetes*, 62(12), 4184-4191.

Han, J., & Kaufman, R. J. (2016). The role of ER stress in lipid metabolism and lipotoxicity. *Journal of Lipid Research, 57*(8), 1329-1338.

Harding, H. P., Novoa, I., Bertolotti, A., Zeng, H., Zhang, Y., Urano, F., . . . Ron, D. (2001). Translational regulation in the cellular response to biosynthetic load on the endoplasmic reticulum. *Cold Spring Harbor Symposia on Quantitative Biology, 66*, 499-508.

Harman, D. (1965). The free radical theory of aging: Effect of age on serum copper levels. *Journal of Gerontology, 20*(2), 151-153.

Henkel, A. S., Anderson, K. A., Dewey, A. M., Kavesh, M. H., & Green, R. M. (2011). A chronic high-cholesterol diet paradoxically suppresses hepatic CYP7A1 expression in FVB/NJ mice. *Journal of Lipid Research, 52*(2), 289-298.

Hirschey, M. D., & Verdin, E. (2010). Measuring fatty acid oxidation in tissue homogenates. *Protocol Exchange.*

Houtkooper, R. H., Argmann, C., Houten, S. M., Cantó, C., Jeninga, E. H., Andreux, P. A., . . . Auwerx, J. (2011). The metabolic footprint of aging in mice. *Scientific Reports, 1*, 134.

Huang, R. H., Quan, Y. J., Chen, J. H., Wang, T. F., Xu, M., Ye, M., . . . Min, Z. J. (2017). Osteopontin promotes cell migration and invasion, and inhibits apoptosis and autophagy in colorectal cancer by activating the p38 MAPK signaling pathway. *Cellular Physiology and Biochemistry : International Journal of Experimental Cellular Physiology, Biochemistry, and Pharmacology, 41*(5), 1851-1864.

Hutcheson, R., & Rocic, P. (2012). The metabolic syndrome, oxidative stress, environment, and cardiovascular disease: The great exploration. *Experimental Diabetes Research, 2012*

Iida, T., Wagatsuma, K., Hirayama, D., & Nakase, H. (2017). Is osteopontin a friend or foe of cell apoptosis in inflammatory gastrointestinal and liver diseases? *International Journal of Molecular Sciences, 19*(1), 7.

Iqbal, J., McRae, S., Mai, T., Banaudha, K., Sarkar-Dutta, M., & Waris, G. (2014). Role of hepatitis C virus induced osteopontin in epithelial to mesenchymal transition, migration and invasion of hepatocytes. *PloS One, 9*(1), e87464.

Issa, D., & Alkhouri, N. (2017). Nonalcoholic fatty liver disease and hepatocellular carcinoma: New insights on presentation and natural history. *Hepatobiliary Surgery and Nutrition, 6*(6), 401.

Jackowski, S. (1994). Coordination of membrane phospholipid synthesis with the cell cycle. *The Journal of Biological Chemistry, 269*(5), 3858-3867.

Jaul, E., & Barron, J. (2017). Age-related diseases and clinical and public health implications for the 85 years old and over population. *Frontiers in Public Health, 5*, 335.

Jia, R., Liang, Y., Chen, R., Liu, G., Wang, H., Tang, M., . . . Wei, H. (2016). Osteopontin facilitates tumor metastasis by regulating epithelial–mesenchymal plasticity. *Cell Death & Disease, 7*(12), e2564.

Johnson, S. C., Rabinovitch, P. S., & Kaeberlein, M. (2013). mTOR is a key modulator of ageing and age-related disease. *Nature, 493*(7432), 338-345.

Kahles, F., Findeisen, H. M., & Bruemmer, D. (2014). Osteopontin: A novel regulator at the cross roads of inflammation, obesity and diabetes. *Molecular Metabolism, 3*(4), 384-393.

Kammoun, H. L., Chabanon, H., Hainault, I., Luquet, S., Magnan, C., Koike, T., . . . Foufelle, F. (2009). GRP78 expression inhibits insulin and ER stress-induced SREBP-1c activation and reduces hepatic steatosis in mice. *The Journal of Clinical Investigation, 119*(5), 1201-1215.

Kiefer, F., Neschen, S., Pfau, B., Legerer, B., Neuhofer, A., Kahle, M., . . . Kenner, L. (2011a). Osteopontin deficiency protects against obesity-induced hepatic steatosis and attenuates glucose production in mice. *Diabetologia, 54*(8), 2132-2142.

Kiefer, F., Neschen, S., Pfau, B., Legerer, B., Neuhofer, A., Kahle, M., . . . Kenner, L. (2011b). Osteopontin deficiency protects against obesity-induced hepatic steatosis and attenuates glucose production in mice. *Diabetologia, 54*(8), 2132-2142.

Klaips, C. L., Jayaraj, G. G., & Hartl, F. U. (2018). Pathways of cellular proteostasis in aging and disease. *The Journal of Cell Biology, 217*(1), 51-63.

Kleiner, D. E., Brunt, E. M., Van Natta, M., Behling, C., Contos, M. J., Cummings, O. W., . . . Sanyal, A. J. (2005). Design and validation of a histological scoring system for nonalcoholic fatty liver disease. *Hepatology, 41*(6), 1313-1321.

Kõks, S., Dogan, S., Tuna, B. G., González-Navarro, H., Potter, P., & Vandenbroucke, R. E. (2016). Mouse models of ageing and their relevance to disease. *Mechanisms on Aging and Development* 160, 41-53.

Kothari, A. N., Arffa, M. L., Chang, V., Blackwell, R. H., Syn, W., Zhang, J., . . . Kuo, P. C. (2016). Osteopontin—a master regulator of epithelial-mesenchymal transition. *Journal of Clinical Medicine, 5*(4), 39.

Kropski, J. A., & Blackwell, T. S. (2018). Endoplasmic reticulum stress in the pathogenesis of fibrotic disease. *The Journal of Clinical Investigation, 128*(1), 64-73.

Kudryavtseva, A. V., Krasnov, G. S., Dmitriev, A. A., Alekseev, B. Y., Kardymon, O. L., Sadritdinova, A. F., . . . Snezhkina, A. V. (2016). Mitochondrial dysfunction and oxidative stress in aging and cancer. *Oncotarget, 7*(29), 44879-44905.

Kuhla, A., Blei, T., Jaster, R., & Vollmar, B. (2011). Aging is associated with a shift of fatty metabolism toward lipogenesis. *Journals of Gerontology Series A: Biomedical Sciences and Medical Sciences, 66*(11), 1192-1200.

Kuk, J. L., Saunders, T. J., Davidson, L. E., & Ross, R. (2009). Age-related changes in total and regional fat distribution. *Ageing Research Reviews, 8*(4), 339-348.

Kumar, A., Sharma, A., Duseja, A., Das, A., Dhiman, R. K., Chawla, Y. K., . . . Bhansali, A. (2013). Patients with nonalcoholic fatty liver disease (NAFLD) have higher oxidative stress in comparison to chronic viral hepatitis. *Journal of Clinical and Experimental Hepatology, 3*(1), 12-18.

Lancha, A., Rodríguez, A., Catalán, V., Becerril, S., Sáinz, N., Ramírez, B., . . . Gómez-Ambrosi, J. (2014). Osteopontin deletion prevents the development of obesity and hepatic steatosis via impaired adipose tissue matrix remodeling and reduced inflammation and fibrosis in adipose tissue and liver in mice. *PloS One, 9*(5), e98398.

Lasry, A., & Ben-Neriah, Y. (2015). Senescence-associated inflammatory responses: Aging and cancer perspectives. *Trends in Immunology, 36*(4), 217-228.

Lau, L., & David, G. (2019). Pro-and anti-tumorigenic functions of the senescence-associated secretory phenotype. *Expert Opinion on Therapeutic Targets,* (just-accepted)

Lazaro, R., Wu, R., Lee, S., Zhu, N., Chen, C., French, S. W., . . . Tsukamoto, H. (2015). Osteopontin deficiency does not prevent but promotes alcoholic neutrophilic hepatitis in mice. *Hepatology, 61*(1), 129-140.

Lee, A. S., Brandhorst, S., Rangel, D. F., Navarrete, G., Cohen, P., Longo, V. D., . . . Dubeau, L. (2017). Effects of prolonged GRP78 haploinsufficiency on organ homeostasis, behavior, cancer and chemotoxic resistance in aged mice. *Scientific Reports, 7*, 40919.

Lee, B. Y., Han, J. A., Im, J. S., Morrone, A., Johung, K., Goodwin, E. C., . . . Hwang, E. S. (2006). Senescence-associated β-galactosidase is lysosomal β-galactosidase. *Aging Cell, 5*(2), 187-195.

Lee, G., Lee, H., Hong, J., Lee, S. H., & Jung, B. H. (2016). Quantitative profiling of bile acids in rat bile using ultrahigh-performance liquid chromatography–orbitrap mass spectrometry: Alteration of the bile acid composition with aging. *Journal of Chromatography B, 1031*, 37-49.

Li, J., García, C. C., Riedt, T., Brandes, M., Szczepanski, S., Brossart, P., . . . Janzen, V. (2018). Murine hematopoietic stem cell reconstitution potential is maintained by osteopontin during aging. *Scientific Reports, 8*(1), 2833.

Li, T., Jahan, A., & Chiang, J. Y. (2006). Bile acids and cytokines inhibit the human cholesterol 7α-hydroxylase gene via the JNK/c-jun pathway in human liver cells. *Hepatology, 43*(6), 1202-1210.

Li, T., Ma, H., & Chiang, J. Y. (2008a). TGFbeta1, TNFalpha, and insulin signaling crosstalk in regulation of the rat cholesterol 7alpha-hydroxylase gene expression. *Journal of Lipid Research, 49*(9), 1981-1989.

Li, T., Ma, H., & Chiang, J. Y. (2008b). TGFbeta1, TNFalpha, and insulin signaling crosstalk in regulation of the rat cholesterol 7alpha-hydroxylase gene expression. *Journal of Lipid Research, 49*(9), 1981-1989.

Liu, G., Fan, X., Tang, M., Chen, R., Wang, H., Jia, R., . . . Yang, Y. (2016). Osteopontin induces autophagy to promote chemo-resistance in human hepatocellular carcinoma cells. *Cancer Letters, 383*(2), 171-182.

Liza, M., Romero, J. R., Chico, Y., Fresnedo, O., & Ochoa, B. (1996). Application of 2-hydroxypropyl-β-cyclodextrin in the assay of acyl-CoA: Cholesterol acyltransferase and neutral and acid cholesterol ester hydrolases. *Lipids, 31*(3), 323-329.

Lomonaco, R., Sunny, N. E., Bril, F., & Cusi, K. (2013). Nonalcoholic fatty liver disease: Current issues and novel treatment approaches. *Drugs, 73*(1), 1-14.

Longo, V. D., Mitteldorf, J., & Skulachev, V. P. (2005). Programmed and altruistic ageing. *Nature Reviews Genetics, 6*, 866.

Loosen, S. H., Roderburg, C., Kauertz, K. L., Pombeiro, I., Leyh, C., Benz, F., . . . Braunschweig, T. (2017). Elevated levels of circulating osteopontin are associated with a poor survival after resection of cholangiocarcinoma. *Journal of Hepatology, 67*(4), 749-757.

López-Otín, C., Blasco, M. A., Partridge, L., Serrano, M., & Kroemer, G. (2013). The hallmarks of aging. *Cell, 153*(6), 1194-1217.

López-Otín, C., Galluzzi, L., Freije, J. M. P., Madeo, F., & Kroemer, G. (2016). Metabolic control of longevity *Cell, 166(4), 802-821.*

Lorena, D., Darby, I. A., Gadeau, A., Leen, L. L. S., Rittling, S., Porto, L. C., . . . Desmoulière, A. (2006). Osteopontin expression in normal and fibrotic liver. altered liver healing in osteopontin-deficient mice. *Journal of Hepatology, 44*(2), 383-390.

Lujambio, A. (2018). Unsplicing senescence. *Science Translational Medicine, 10*(453), eaau7386.

Maeso-Díaz, R., Ortega-Ribera, M., Fernández-Iglesias, A., Hide, D., Muñoz, L., Hessheimer, A. J., . . . Albillos, A. (2018). Effects of aging on liver microcirculatory function and sinusoidal phenotype. *Aging Cell, 17*(6), e12829.

Magdaleno, F., Ge, X., Fey, H., Lu, Y., Gaskell, H., Blajszczak, C. C., . . . Nieto, N. (2018). Osteopontin deletion drives hematopoietic stem cell mobilization to the liver and increases hepatic iron contributing to alcoholic liver disease. *Hepatology Communications, 2*(1), 84-98.

Malaponte, G., Hafsi, S., Polesel, J., Castellano, G., Spessotto, P., Guarneri, C., . . . Libra, M. (2016). Tumor microenvironment in diffuse large B-cell lymphoma: Matrixmetalloproteinases activation is mediated by osteopontin overexpression. *Biochimica Et Biophysica Acta (BBA)-Molecular Cell Research, 1863*(3), 483-489.

Malaquin, N., Martinez, A., & Rodier, F. (2016). Keeping the senescence secretome under control: Molecular reins on the senescence-associated secretory phenotype. *Experimental Gerontology, 82*, 39-49.

Martínez, G., Duran-Aniotz, C., Cabral-Miranda, F., Vivar, J. P., & Hetz, C. (2017). Endoplasmic reticulum proteostasis impairment in aging. *Aging Cell, 16*(4), 615-623.

Matsui, Y., Rittling, S. R., Okamoto, H., Inobe, M., Jia, N., Shimizu, T., . . . Uede, T. (2003). Osteopontin deficiency attenuates atherosclerosis in female apolipoprotein E-deficient mice. *Arteriosclerosis, Thrombosis, and Vascular Biology, 23*(6), 1029-1034. Mazzali, M., Kipari, T., Ophascharoensuk, V., Wesson, J., Johnson, R., & Hughes, J. (2002). Osteopontin—a molecule for all seasons. *Qjm, 95*(1), 3-13.

McHugh, D., & Gil, J. (2018). Senescence and aging: Causes, consequences, and therapeutic avenues. *The Journal of Cell Biology, 217*(1), 65-77.

Mitchell, C., & Willenbring, H. (2008). A reproducible and well-tolerated method for 2/3 partial hepatectomy in mice. *Nature Protocols, 3*(7), 1167.

Miyamura, N., Nakamura, T., Goto-Inoue, N., Zaima, N., Hayasaka, T., Yamasaki, T., . . . Nishina, H. (2011). Imaging mass spectrometry reveals characteristic changes in triglyceride and phospholipid species in regenerating mouse liver. *Biochemical and Biophysical Research Communications, 408*(1), 120-125.

Morimoto, I., Sasaki, Y., Ishida, S., Imai, K., & Tokino, T. (2002). Identification of the osteopontin gene as a direct target of TP53. *Genes, Chromosomes and Cancer, 33*(3), 270-278.

Morinobu, M., Ishijima, M., Rittling, S. R., Tsuji, K., Yamamoto, H., Nifuji, A., . . . Noda, M. (2003). Osteopontin expression in osteoblasts and osteocytes during bone formation under mechanical stress in the calvarial suture in vivo. *Journal of Bone and Mineral Research, 18*(9), 1706-1715.

Munoz-Espin, D., & Serrano, M. (2014). Cellular senescence: From physiology to pathology. *Nature Reviews Molecular Cell Biology, 15*(7), 482.

Musso, G., Paschetta, E., Gambino, R., Cassader, M., & Molinaro, F. (2013). Interactions among bone, liver, and adipose tissue predisposing to diabesity and fatty liver. *Trends in Molecular Medicine, 19*(9), 522-535.

Mutrie, J. C., Chambers, A. F., & Tuck, A. B. (2011). Osteopontin increases breast cancer cell sensitivity to specific signaling pathway inhibitors in preclinical models. *Cancer Biology & Therapy, 12*(8), 680-690.

Nagoshi, S. (2014). Osteopontin: Versatile modulator of liver diseases. *Hepatology Research, 44*(1), 22-30.

Napoli, M., & Flores, E. R. (2017). The p53 family orchestrates the regulation of metabolism: Physiological regulation and implications for cancer therapy. *British Journal of Cancer, 116*(2), 149.

Newberry, E. P., Kennedy, S. M., Xie, Y., Luo, J., Stanley, S. E., Semenkovich, C. F., . . . Davidson, N. O. (2008). Altered hepatic triglyceride content after partial hepatectomy without impaired liver regeneration in multiple murine genetic models. *Hepatology, 48*(4), 1097-1105.

Nuñez-Garcia, M., Gomez-Santos, B., de Urturi, D. S., Mestre, D., Gonzalez-Romero, F., Buque, X., . . . Fresnedo, O. (2018). Atorvastatin provides a new lipidome improving early regeneration after partial hepatectomy in osteopontin deficient mice. *Scientific Reports, 8*(1), 14626.

Nunez-Garcia, M., Gomez-Santos, B., Buque, X., Garcia-Rodriguez, J. L., Romero, M. R., Marin, J. J. G., . . . Aspichueta, P. (2017). Osteopontin regulates the cross-talk between phosphatidylcholine and cholesterol metabolism in mouse liver. *Journal of Lipid Research, 58*(9), 1903-1915.

Nytofte, N. S., Serrano, M. A., Monte, M. J., Gonzalez-Sanchez, E., Tumer, Z., Ladefoged, K., . . . Marin, J. J. (2011). A homozygous nonsense mutation (c.214C->A) in the biliverdin reductase alpha gene

(BLVRA) results in accumulation of biliverdin during episodes of cholestasis. *Journal of Medical Genetics, 48*(4), 219-225.

Ogrodnik, M., Miwa, S., Tchkonia, T., Tiniakos, D., Wilson, C. L., Lahat, A., . . . Anstee, Q. M. (2017). Cellular senescence drives age-dependent hepatic steatosis. *Nature Communications, 8*, 15691.

Ogrodnik, M., Salmonowicz, H., & Gladyshev, V. N. (2018). Integrating cellular senescence with the concept of damage accumulation in aging: Relevance for clearance of senescent cells. *Aging Cell,* , e12841.

Oh, J., Lee, Y. D., & Wagers, A. J. (2014). Stem cell aging: Mechanisms, regulators and therapeutic opportunities. *Nature Medicine, 20*(8), 870.

Olive, J. F., Qin, Y., DeCristo, M. J., Laszewski, T., Greathouse, F., & McAllister, S. S. (2018). Accounting for tumor heterogeneity when using CRISPR-Cas9 for cancer progression and drug sensitivity studies. *PloS One, 13*(6), e0198790.

Paliwal, P., Pishesha, N., Wijaya, D., & Conboy, I. M. (2012). Age dependent increase in the levels of osteopontin inhibits skeletal muscle regeneration. *Aging, 4*(8), 553-566.

Papsdorf, K., & Brunet, A. (2018). Linking lipid metabolism to chromatin regulation in aging. *Trends in Cell Biology, 29(2),97-116.*

Pazolli, E., Luo, X., Brehm, S., Carbery, K., Chung, J. J., Prior, J. L., . . . Stewart, S. A. (2009). Senescent stromal-derived osteopontin promotes preneoplastic cell growth. *Cancer Research, 69*(3), 1230-1239.

Pibiri, M. (2018). Liver regeneration in aged mice*: New insights*. Aging, 10(8), 1801-1824.

Porteiro, B., Fondevila, M. F., Delgado, T. C., Iglesias, C., Imbernon, M., Iruzubieta, P., . . . Nogueiras, R. (2017). Hepatic p63 regulates steatosis via IKKÎ²/ER stress. *Nature Communications, 8*, 15111; 15111-15111.

Ramaiah, S. K., & Rittling, S. (2007). Pathophysiological role of osteopontin in hepatic inflammation, toxicity, and cancer. *Toxicological Sciences, 103*(1), 4-13.

Rando, T., & Chang, H. (2012). Aging, rejuvenation, and epigenetic reprogramming: Resetting the aging clock. *Cell, 148*(1), 46-57.

Rangaswami, H., Bulbule, A., & Kundu, G. C. (2006). Osteopontin: Role in cell signaling and cancer progression. *Trends in Cell Biology, 16*(2), 79-87.

Rao, S. G., & Jackson, J. G. (2016). SASP: Tumor suppressor or promoter? yes! *Trends in Cancer, 2*(11), 676-687.

Rapisarda, V., Borghesan, M., Miguela, V., Encheva, V., Snijders, A. P., Lujambio, A., & O'Loghlen, A. (2017). Integrin beta 3 regulates cellular senescence by activating the TGF-β pathway. *Cell Reports, 18*(10), 2480-2493.

Regev, A., & Schiff, E. R. (2001). Liver disease in the elderly. *Gastroenterology Clinics, 30*(2), 547-563. doi:10.1016/S0889-8553(05)70195-3

Ridgway, N. D., & Vance, D. E. (1992). Phosphatidylethanolamine N-methyltransferase from rat liver. *Methods in enzymology* (pp. 366-374)

Ritschka, B., Storer, M., Mas, A., Heinzmann, F., Ortells, M. C., Morton, J. P., . . . Keyes, W. M. (2017). The senescence-associated secretory phenotype induces cellular plasticity and tissue regeneration. *Genes & Development, 31*(2), 172-183.

Roberts, S. B., & Rosenberg, I. (2006). Nutrition and aging: Changes in the regulation of energy metabolism with aging. *Physiological Reviews, 86*(2), 651-667.

Rosenberg, M., Zugck, C., Nelles, M., Juenger, C., Frank, D., Remppis, A., . . . Frey, N. (2008). Osteopontin, a new prognostic biomarker in patients with chronic heart failure. *Circulation.Heart Failure, 1*(1), 43-49.

Ruiz, J. I., & Ochoa, B. (1997). Quantification in the subnanomolar range of phospholipids and neutral lipids by monodimensional thin-layer chromatography and image analysis. *Journal of Lipid Research, 38*(7), 1482-1489.

Ruzafa, N., Pereiro, X., Aspichueta, P., Araiz, J., & Vecino, E. (2018). The retina of osteopontin deficient mice in aging. *Molecular Neurobiology, 55*(1), 213-221.

Ryaboshapkina, M., & Hammar, M. (2017). Human hepatic gene expression signature of non-alcoholic fatty liver disease progression, a meta-analysis. *Scientific Reports, 7*(1), 12361.

Sahai, A., Malladi, P., Melin-Aldana, H., Green, R. M., & Whitington, P. F. (2004). Upregulation of osteopontin expression is involved in the development of nonalcoholic steatohepatitis in a dietary murine model. *American Journal of Physiology-Gastrointestinal and Liver Physiology, 287*(1), G264-G273.

Salminen, A., Kaarniranta, K., & Kauppinen, A. (2016). Age-related changes in AMPK activation: Role for AMPK phosphatases and inhibitory phosphorylation by upstream signaling pathways. *Ageing Research Reviews, 28*, 15-26.

Santos, A. L., & Lindner, A. B. (2017). Protein posttranslational modifications: Roles in aging and age-related disease. *Oxidative Medicine and Cellular Longevity, 2017*

Sawaki, D., Czibik, G., Pini, M., Ternacle, J., Suffee, N., Mercedes, R., . . . Derumeaux, G. (2018). Visceral adipose tissue drives cardiac aging through modulation of fibroblast senescence by osteopontin production. *Circulation, 138*(8), 809-822.

Schaefer, E. J., Lamon-Fava, S., Cohn, S. D., Schaefer, M. M., Ordovas, J. M., Castelli, W. P., & Wilson, P. W. (1994). Effects of age, gender, and menopausal status on plasma low density lipoprotein cholesterol and apolipoprotein B levels in the framingham offspring study. *Journal of Lipid Research, 35*(5), 779-792.

Schmucker, D. L. (2005). Age-related changes in liver structure and function: Implications for disease? *Experimental Gerontology, 40*(8-9), 650-659.

Schmucker, D. L., & Sanchez, H. (2011). *Liver regeneration and aging: A current perspective. Current Gerontology and Geriatrics Research, 526379, 8.*

Schofield, P. S., Sugden, M. C., Corstorphine, C. G., & Zammit, V. A. (1987). Altered interactions between lipogenesis and fatty acid oxidation in regenerating rat liver. *The Biochemical Journal, 241*(2), 469-474.

Sen, P., Shah, P. P., Nativio, R., & Berger, S. L. (2016). Epigenetic mechanisms of longevity and aging. *Cell, 166*(4), 822-839.

Shang, S., Plymoth, A., Ge, S., Feng, Z., Rosen, H. R., Sangrajrang, S., . . . Beretta, L. (2012). Identification of osteopontin as a novel marker for early hepatocellular carcinoma. *Hepatology, 55*(2), 483-490.

Sheedfar, F., Biase, S. D., Koonen, D., & Vinciguerra, M. (2013). Liver diseases and aging: Friends or foes? *Aging Cell, 12*(6), 950-954.

Shetty, S., Lalor, P. F., & Adams, D. H. (2018). Liver sinusoidal endothelial cells—gatekeepers of hepatic immunity. *Nature Reviews Gastroenterology & Hepatology, 15, 555–567.*

Shi, Z., Wang, B., Chihanga, T., Kennedy, M. A., & Weber, G. F. (2014). Energy metabolism during anchorage-independence. induction by osteopontin-c. *PloS One, 9*(8), e105675.

Shi, R., Guberman, M., & Kirshenbaum, L. A. (2018). Mitochondrial quality control: The role of mitophagy in aging. *Trends in cardiovascular Medicine, 28(4), 246-260.*

Singh, M., Foster, C. R., Dalal, S., & Singh, K. (2010). Osteopontin: Role in extracellular matrix deposition and myocardial remodeling post-MI. *Journal of Molecular and Cellular Cardiology, 48*(3), 538-543.

Slawik, M., & Vidal-Puig, A. J. (2006). Lipotoxicity, overnutrition and energy metabolism in aging. *Ageing Research Reviews, 5*(2), 144-164.

Smedsrød, B., & Pertoft, H. (1985). Preparation of pure hepatocytes and reticuloendothelial cells in high yield from a single rat liver by means of percoll centrifugation and selective adherence. *Journal of Leukocyte Biology, 38*(2), 213-230.

Standal, T., Borset, M., & Sundan, A. (2004). Role of osteopontin in adhesion, migration, cell survival and bone remodeling. *Exp Oncol, 26*(3), 179-184.

Štemberger, C., Matušan-Ilijaš, K., Avirović, M., Bulat-Kardum, L., Ivančić, A., Jonjić, N., & Lučin, K. (2014). Osteopontin is associated with decreased apoptosis and αv integrin expression in lung adenocarcinoma. *Acta Histochemica, 116*(1), 222-229.

Syn, W., Choi, S. S., Liaskou, E., Karaca, G. F., Agboola, K. M., Oo, Y. H., . . . Malladi, P. (2011). Osteopontin is induced by hedgehog pathway activation and promotes fibrosis progression in nonalcoholic steatohepatitis. *Hepatology, 53*(1), 106-115.

Syn, W. K., Agboola, K. M., Swiderska, M., Michelotti, G. A., Liaskou, E., Pang, H., . . . Diehl, A. M. (2012). NKT-associated hedgehog and osteopontin drive fibrogenesis in non-alcoholic fatty liver disease. *Gut, 61*(9), 1323-1329.

Takahashi, Y. (2017). The role of growth hormone and insulin-like growth factor-I in the liver. *International Journal of Molecular Sciences, 18*(7), 1447.

Tardelli, M., Zeyda, K., Moreno-Viedma, V., Wanko, B., Grün, N. G., Staffler, G., . . . Stulnig, T. M. (2016). Osteopontin is a key player for local adipose tissue macrophage proliferation in obesity. *Molecular Metabolism, 5*(11), 1131-1137.

Tijburg, L. B., Nyathi, C. B., Meijer, G. W., & Geelen, M. J. (1991). Biosynthesis and secretion of triacylglycerol in rat liver after partial hepatectomy. *The Biochemical Journal, 277 (Pt 3)*(Pt 3), 723-728.

Timchenko, N. A. (2009). Aging and liver regeneration. Trends in Endocrinology & Metabolism, 20(4), 171-176.

Toth, M., & Tchernof, A. (2000). Lipid metabolism in the elderly. *European Journal of Clinical Nutrition, 54*(S3), S121.

Tovo, C. V., Fernandes, S. A., Buss, C., & de Mattos, A. A. (2017). Sarcopenia and non-alcoholic fatty liver disease: Is there a relationship? A systematic review. *World Journal of Hepatology, 9*(6), 326-332.

Tsuchiya, N., Sawada, Y., Endo, I., Saito, K., Uemura, Y., & Nakatsura, T. (2015). Biomarkers for the early diagnosis of hepatocellular carcinoma. *World Journal of Gastroenterology, 21*(37), 10573-10583.

Uemura, T., Nemoto, A., Liu, Y., Kojima, H., Dong, J., Yabe, T., . . . Tateishi, T. (2001). Osteopontin involvement in bone remodeling and its effects on in vivo osteogenic potential of bone marrow-derived osteoblasts/porous hydroxyapatite constructs. *Materials Science and Engineering: C, 17*(1-2), 33-36.

Urtasun, R., Lopategi, A., George, J., Leung, T., Lu, Y., Wang, X., . . . Nieto, N. (2012). Osteopontin, an oxidant stress sensitive cytokine, up-regulates collagen-I via integrin αVβ3 engagement and PI3K/pAkt/NFκB signaling. *Hepatology, 55*(2), 594-608.

van de Laarschot, Liyanne FM, Jansen, P. L., Schaap, F. G., & Damink, S. W. O. (2016). The role of bile salts in liver regeneration. *Hepatology International, 10*(5), 733-740.

van der Veen, Jelske N, Kennelly, J. P., Wan, S., Vance, J. E., Vance, D. E., & Jacobs, R. L. (2017). The Critical Role of Phosphatidylcholine and Phosphatidylethanolamine Metabolism in Health and Diseas.,*Biochimica et Biophysica Acta (BBA) - Biomembranes, 1859(9), 1558-1572.*

van der Veen, J. N., Kruit, J. K., Havinga, R., Baller, J. F., Chimini, G., Lestavel, S., . . . Kuipers, F. (2005). Reduced cholesterol absorption upon PPARdelta activation coincides with decreased intestinal expression of NPC1L1. *Journal of Lipid Research, 46*(3), 526-534.

Wang, C., Jurk, D., Maddick, M., Nelson, G., Martin-Ruiz, C., & Von Zglinicki, T. (2009). DNA damage response and cellular senescence in tissues of aging mice. *Aging Cell, 8*(3), 311-323.

Wang, J. C., & Bennett, M. (2012). Aging and atherosclerosis: Mechanisms, functional consequences, and potential therapeutics for cellular senescence. *Circulation Research, 111*(2), 245-259.

Wang, M., Chen, F., Li, J., Liu, C., Zhang, H., Xia, Y., . . . Lu, L. (2014). Reversal of hepatocyte senescence after continuous in vivo cell proliferation. *Hepatology, 60*(1), 349-361.

Wang, X., Lopategi, A., Ge, X., Lu, Y., Kitamura, N., Urtasun, R., . . . Nieto, N. (2014). Osteopontin induces ductular reaction contributing to liver fibrosis. *Gut, 63*(11), 1805-1818.

Weber, G. F. (2001). The metastasis gene osteopontin: A candidate target for cancer therapy. *Biochimica Et Biophysica Acta (BBA)-Reviews on Cancer, 1552*(2), 61-85.

Weber, G. F., Lett, G. S., & Haubein, N. C. (2011). Categorical meta-analysis of osteopontin as a clinical cancer marker. *Oncology Reports, 25*(2), 433-441.

Wei, R., Wong, J. P. C., & Kwok, H. F. (2017). Osteopontin -- a promising biomarker for cancer therapy. *Journal of Cancer, 8*(12), 2173-2183.

Weichhart, T. (2018). mTOR as regulator of lifespan, aging, and cellular senescence: A mini-review. *Gerontology, 64*(2), 127-134.

Wen, Y., Jeong, S., Xia, Q., & Kong, X. (2016). Role of osteopontin in liver diseases. *International Journal of Biological Sciences, 12*(9), 1121-1128.

Wiemann, S. U., Satyanarayana, A., Tsahuridu, M., Tillmann, H. L., Zender, L., Klempnauer, J., . . . Manns, M. P. (2002). Hepatocyte telomere shortening and senescence are general markers of human liver cirrhosis. *The FASEB Journal, 16*(9), 935-942.

World Health Organization. (2015). *World report on ageing and health* World Health Organization.

Wu, X. L., Lin, K. J., Bai, A. P., Wang, W. X., Meng, X. K., Su, X. L., . . . Shi, L. (2014). Osteopontin knockdown suppresses the growth and angiogenesis of colon cancer cells. *World Journal of Gastroenterology, 20*(30), 10440-10448.

Wynne, H. A., Cope, L. H., Mutch, E., Rawlins, M. D., Woodhouse, K. W., & James, O. F. (1989). The effect of age upon liver volume and apparent liver blood flow in healthy man. *Hepatology, 9*(2), 297-301.

Yang, L., Wei, L., Zhao, W., Wang, X., Zheng, G., Zheng, M., . . . Zuo, W. (2012). Down-regulation of osteopontin expression by RNA interference affects cell proliferation and chemotherapy sensitivity of breast cancer MDA-MB-231 cells. *Molecular Medicine Reports, 5*(2), 373-376.

Ye, L., Liu, S., Wang, M., Shao, Y., & Ding, M. (2007). High-performance liquid chromatography–tandem mass spectrometry for the analysis of bile acid profiles in serum of women with intrahepatic cholestasis of pregnancy. *Journal of Chromatography B, 860*(1), 10-17.

Yilmaz, Y., & Ozdogan, O. (2009). Liver disease as a risk factor for cognitive decline and dementia: An under-recognized issue. *Hepatology, 49*(2), 698-698.

Yokosaki, Y., Tanaka, K., Higashikawa, F., Yamashita, K., & Eboshida, A. (2005). Distinct structural requirements for binding of the integrins αvβ6, αvβ3, αvβ5, α5β1 and α9β1 to osteopontin. *Matrix Biology, 24*(6), 418-427.

Younossi, Z. M. (2018). Non-alcoholic fatty liver disease—a global public health perspective. *Journal of Hepatology, 70(3),531-544.*

Zeyda, M., Gollinger, K., Todoric, J., Kiefer, F. W., Keck, M., Aszmann, O., . . . Stulnig, T. M. (2011). Osteopontin is an activator of human adipose tissue macrophages and directly affects adipocyte function. *Endocrinology, 152*(6), 2219-2227.

Zhang, C., & Cuervo, A. M. (2008). Restoration of chaperone-mediated autophagy in aging liver improves cellular maintenance and hepatic function. *Nature Medicine, 14*, 959.

Zhang, H., Guo, M., Chen, J. H., Wang, Z., Du, X. F., Liu, P. X., & Li, W. H. (2014). Osteopontin knockdown inhibits alphav,beta3 integrin-induced cell migration and invasion and promotes apoptosis of breast cancer cells by inducing autophagy and inactivating the PI3K/akt/mTOR pathway. *Cellular Physiology and Biochemistry : International Journal of Experimental Cellular Physiology, Biochemistry, and Pharmacology, 33*(4), 991-1002.

Zhao, H., Chen, Q., Alam, A., Cui, J., Suen, K. C., Soo, A. P., . . . Ma, D. (2018a). The role of osteopontin in the progression of solid organ tumour. *Cell Death & Disease, 9*(3), 356.

Zhao, H., Chen, Q., Alam, A., Cui, J., Suen, K. C., Soo, A. P., . . . Ma, D. (2018b). The role of osteopontin in the progression of solid organ tumour. *Cell Death & Disease, 9*(3), 356.

Zheng, W., Liu, Y., Shang, H., Zhang, Y., Ma, D., Hou, N., . . . Pan, L. (2018). Characterization of spontaneously-developed non-alcoholic fatty liver disease in aged rhesus monkeys. *Diabetology & Metabolic Syndrome, 10*(1), 68.

Zhong, H., Hu, S., Yu, B., Jiang, S., Zhang, J., Luo, D., . . . Deng, H. (2017). Apoptosis in the aging liver. *Oncotarget, 8*(60), 102640.

Zhu, C., Ikemoto, T., Utsunomiya, T., Yamada, S., Morine, Y., Imura, S., . . . Shimada, M. (2014). Senescence-related genes possibly responsible for poor liver regeneration after hepatectomy in elderly patients. *Journal of Gastroenterology and Hepatology, 29*(5), 1102-1108.